Technical Report Documentation Page

1. Report No. FHWA/TX-09/0-5444-2	2. Government Accession No.	3. Recipient's Catalog No.
4. Title and Subtitle Assessment and Rehabilitation Methods for Longitudinal Cracks and Joint Separations in Concrete Pavement		5. Report Date October 2008 6. Performing Organization Code
7. Author(s) Megan Stringer, Taylor Crawford, David Fowler, James Jirsa, Moon Won and David Whitney		8. Performing Organization Report No. 0-5444-2
9. Performing Organization Name and Address Center for Transportation Research The University of Texas at Austin 3208 Red River, Suite 200 Austin, TX 78705-2650		10. Work Unit No. (TRAIS) 11. Contract or Grant No. 0-5444
12. Sponsoring Agency Name and Address Texas Department of Transportation Research and Technology Implementation Office P.O. Box 5080 Austin, TX 78763-5080		13. Type of Report and Period Covered Research Report; 9/1/05 – 8/31/08 14. Sponsoring Agency Code

15. Supplementary Notes
Project performed in cooperation with the Texas Department of Transportation and the Federal Highway Administration.

16. Abstract

Researchers surveyed DOTs in the U.S. and searched published literature for effective means of repairing and rehabilitating pavements with longitudinal cracking or longitudinal cracking. These methods included field assessment for determining the severity of the causes of the symptoms and procedures for addressing the issues discovered during the assessment. The methods were evaluated for ease of implementation, cost effectiveness, and durability implications. Results produced an understanding of several of the most popular methods and recommendations for TxDOT's intended implementation. Slot stitching generally proved to be the most effective method for restoring load transfer to joints. Cross stitching is effective for cracks that are still relatively narrow. Details and specifications are included for a section of US 75 near Sherman that exhibited slab faulting and joint separation.

17. Key Words Longitudinal, cracks, joint separation, pavements	18. Distribution Statement No restrictions. This document is available to the public through the National Technical Information Service, Springfield, Virginia 22161; www.ntis.gov.

19. Security Classif. (of report) Unclassified	20. Security Classif. (of this page) Unclassified	21. No. of pages 320	22. Price

Form DOT F 1700.7 (8-72) Reproduction of completed page authorized

Assessment and Rehabilitation Methods for Longitudinal Cracks and Joint Separations in Concrete Pavement

Megan Stringer
Taylor Crawford
David Fowler
James Jirsa
Moon Won
David Whitney

CTR Technical Report:	0-5444-2
Report Date:	October 2008
Project:	0-5444
Project Title:	Assessment and Rehabilitation Methods for Longitudinal Cracks and Joints Separations in Concrete Pavement
Sponsoring Agency:	Texas Department of Transportation
Performing Agency:	Center for Transportation Research at The University of Texas at Austin

Project performed in cooperation with the Texas Department of Transportation and the Federal Highway Administration.

Center for Transportation Research
The University of Texas at Austin
3208 Red River
Austin, TX 78705

www.utexas.edu/research/ctr

Disclaimers

Author's Disclaimer: The contents of this report reflect the views of the authors, who are responsible for the facts and the accuracy of the data presented herein. The contents do not necessarily reflect the official view or policies of the Federal Highway Administration or the Texas Department of Transportation (TxDOT). This report does not constitute a standard, specification, or regulation.

Patent Disclaimer: There was no invention or discovery conceived or first actually reduced to practice in the course of or under this contract, including any art, method, process, machine manufacture, design or composition of matter, or any new useful improvement thereof, or any variety of plant, which is or may be patentable under the patent laws of the United States of America or any foreign country.

Notice: The United States Government and the State of Texas do not endorse products or manufacturers. If trade or manufacturers' names appear herein, it is solely because they are considered essential to the object of this report.

Engineering Disclaimer

NOT INTENDED FOR CONSTRUCTION, BIDDING, OR PERMIT PURPOSES.

Project Engineer: Dr. David W. Fowler
Professional Engineer License State and Number: Texas No. 27859
P. E. Designation: Research Supervisor

Acknowledgments

The research group would like to thank our project director, Dr. Dar Hao Chen, and John Bileou from the Materials and Pavements Section of the Construction Division. They accompanied us and established the formal permissions for us on most of our field trips. We would also like to thank the following TxDOT district contacts whose experience, cooperation and intellectual generosity enabled us to conduct our research more efficiently: Ali Esmaili-Doki from the Paris District, Miles Garrison from the Atlanta District, Lubbock District's Stacey Young, from Childress District's Chris Reed, Dallas District's Abbas Mehdibeigi, El Paso's Tomas Saenz, and Quincy Allen and Charles Gaskin from the Houston District. Many others helped us, too, but working with these people is really what made the project work for TxDOT's long-term interests.

Table of Contents

List of Figures

List of Tables

Chapter 1. Introduction

1.1 Background

The Texas Department of Transportation (TxDOT) has observed longitudinal cracking and longitudinal joint separations on its concrete pavements statewide since the 1970s. This uncontrolled cracking and joint separation at the longitudinal construction joint has often led to further structural deterioration of the pavement. Additional cracking, spalling, and slab faulting has often occurred as well as corrosion of the steel reinforcement and the erosion and pumping of the base layer due to moisture penetration through the cracks and joints. These problems typically reduce the ride quality of the pavement and in severe cases can present safety hazards to motorists.

TxDOT has typically utilized slot-stitching, cross-stitching, and routing and sealing for the repairs but no research has been done to determine the effectiveness of these repairs. This study addresses repair procedures for the existing distressed pavements as well as methods of prevention. Guidelines, recommendations, and specifications for repair and new construction have been developed.

1.2 Scope of Study

The scope of this study includes evaluating current repair practices and methods for monitoring performances, evaluating multiple failure sites in Texas, updating repair methods and designs for tie bars and transverse reinforcement in continually reinforced concrete pavement (CRCP), providing repair and new construction guidelines as well as specifications, and monitoring repairs with an implementation project.

To determine the current state of practice for repairing cracks and joints, a literature review was performed and surveys were distributed to Department of Transportation personnel in Texas and several other states, FHWA representatives, and other industry professionals. The findings are presented in Chapter 2.

Field investigations were conducted on numerous concrete pavements throughout the state. A forensics analysis was utilized to determine the cause(s) of distress and to determine, if present, the effectiveness of repairs. Each field investigation is summarized in Chapter 3.

For each repair method considered, finite element modeling was conducted to examine the relative magnitude of stress that each method introduces to the concrete pavement. Experimental tests were also employed to determine strengths and weaknesses of each method under various loading conditions encountered in the field. Chapter 4 presents the results from these experiments. Dynamic Cone Penetrometer (DCP) tests were performed in numerous districts across the state to determine if there was a direct correlation between DCP readings, or rather subgrade modulus, and the likelihood of longitudinal cracks, joint separations, and faulting. The results are presented in Chapter 4.

Transverse steel and tie bar design methods were investigated and field studies were conducted in the Forth Worth, Rosenberg, and Houston districts. Test results show that current methods of design should be altered. Chapter 5 presents the current methods of design, field studies, and recommendations.

After investigating longitudinal cracking and joint separations throughout the state, a field trial section was selected along US 75 in Sherman, Texas. The intent of this field trial is to

implement slot stitching along the depressed sections along the longitudinal joint. The section would be instrumented and monitored to evaluate the rehabilitation strategy. The section would also be topped with a latex overlay to help with leveling of the section. Chapter 6 presents the findings for an in-depth study of US 75.

Chapter 2. Current State of Practice

Repair methods that are under consideration as part of this research study are briefly described. Key findings from the review of literature and surveys are summarized, as are several concrete pavement repair case studies from other states.

2.1 Description of Repair Methods

Four primary repair methods are considered in this study: (1) cross stitching, (2) slot stitching, (3) stapling, (4) headed bar stitching. Other concrete pavement restoration (CPR) techniques exist, such as full depth repair (FDR), but are generally more expensive and intrusive into the pavement. The focus of this study is on less expensive alternative methods. Each of these is described below.

2.1.1 Cross Stitching

Cross stitching is the most common and easily installed repair method considered in this report. The Texas Department of Transportation has implemented this method on several sections of concrete pavement for longitudinal crack and longitudinal joint repair.

Alternating diagonal holes are drilled into the pavement using an impact drill, with the angle of drilling and distance from the hole to the crack or joint varying by job. Holes are typically cleaned out with compressed air and partially filled with epoxy using a pneumatic injection gun. Three-quarter-inch diameter (#6) deformed bars are then inserted into the holes. Bars are typically spaced 12 to 24 in. apart along the length of the crack or joint. Figures 2.1 and 2.2 and Appendix F contain cross stitching details.

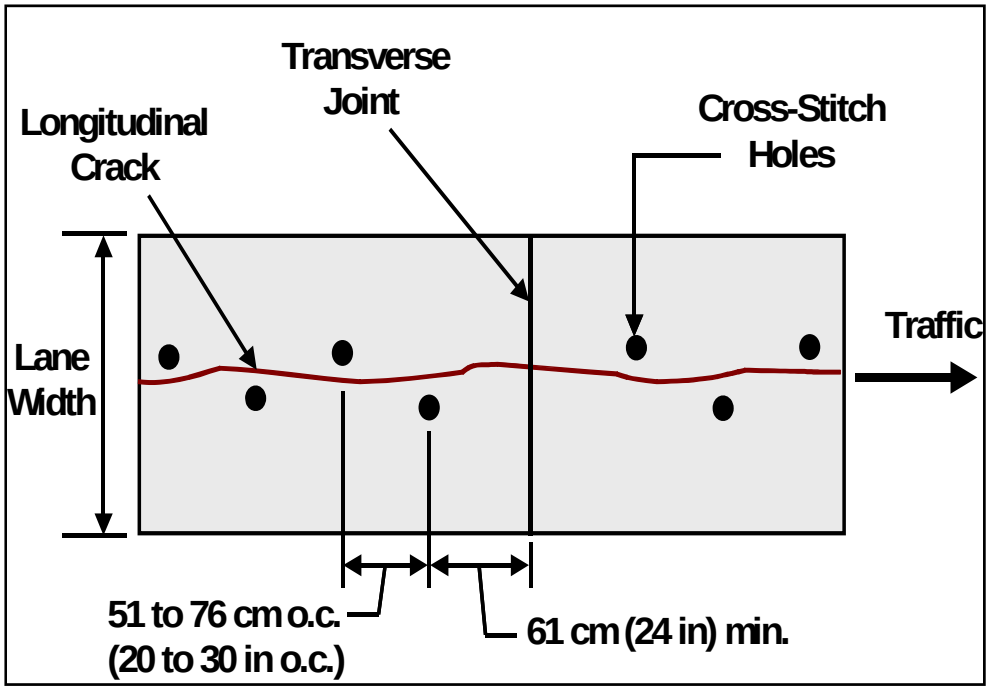

Figure 2.1: Plan View of Cross Stitching Layout (Fowler et al. 2005b)

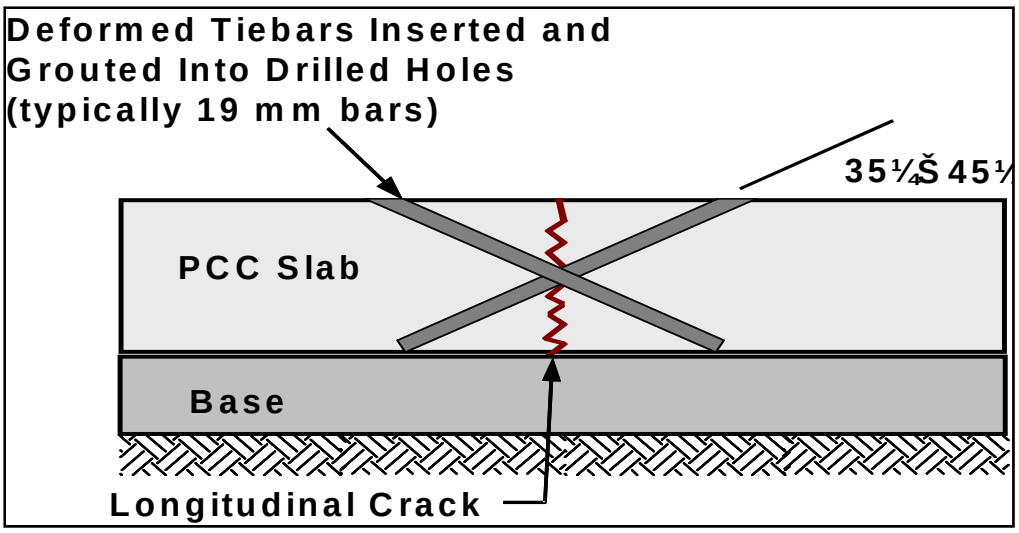

Figure 2.2: Elevation View of Cross Stitching (Fowler et al. 2005b)

2.1.2 Slot Stitching

Slot stitching is similar to the dowel bar retrofit (DBR) technique commonly used to restore load transfer across transverse joints. In slot stitching, slots are saw-cut perpendicular to the joint or crack and chiseled out with a jackhammer to produce a rectangular cavity with a depth approximately equal to one-half the thickness of the pavement slab. Deformed bars are then inserted into the slot and the slots are filled with repair material, (typically a rigid, fast-setting portland cement-based material). DBR provides load transfer across joints, but not horizontal anchorage because smooth, greased dowels are used. Slot stitching provides both load transfer and horizontal anchorage because deformed bars are installed. The goal of slot stitching is to restore the pavement to a pre-distress condition; stitch bar size, spacing, and location within the slab are selected to match the original tie bar design. American Concrete Paving Association (ACPA) gives recommended design details for slot stitching (ACPA 2001), which are shown in Figure 2.3. Bars are placed approximately mid-depth in the slab and are at least 1 in. in diameter.

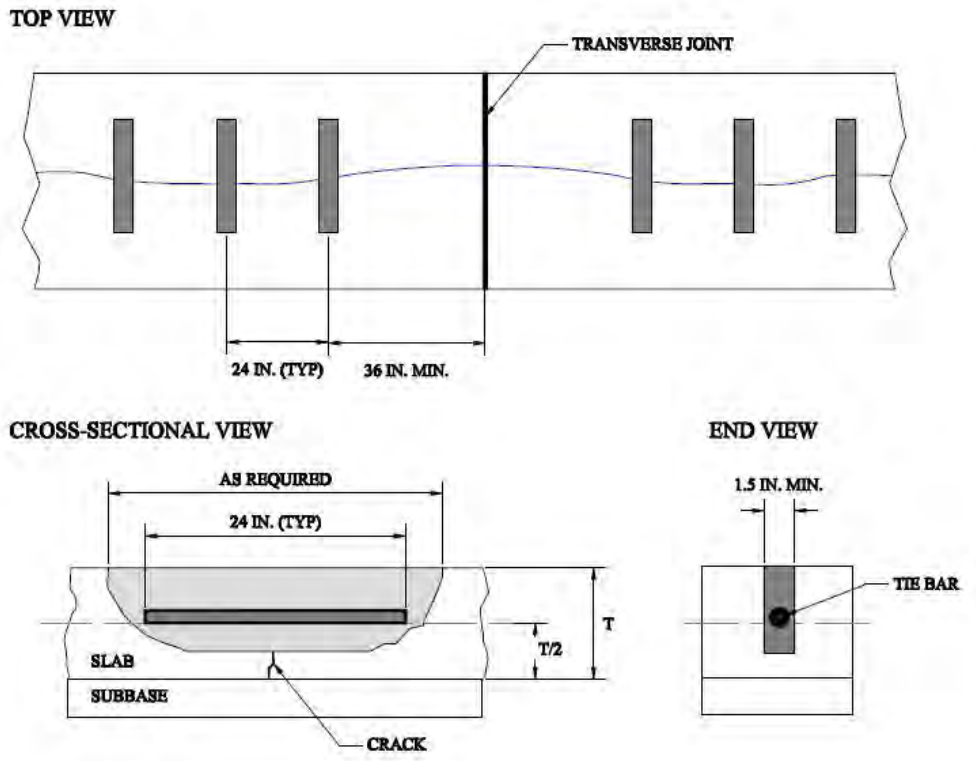

Figure 2.3: Slot Stitching Details (ACPA 2001)

2.1.3 Stapling

Stapling was first introduced to the research team by Mr. Tony Yrigoyen of the Houston District of TxDOT. Mr. Yrigoyen developed the stapling method several years ago to address longitudinal joint separation problems in the Houston District. Pavements showing visible separations were typically continuously reinforced concrete pavements (CRCP) on stabilized base that showed little or no signs of vertical faulting. The stapling repair method was developed to provide positive mechanical anchorage between the separated slabs, but not necessarily to provide load transfer.

Staple slots consist of horizontal slots cut by sawing (much the same technique as described for slot stitching) and vertical holes drilled at the ends of the slots. U-shaped bars ("staples") are inserted into the slots, and the legs anchored into the vertical holes with high-modulus epoxy. The slots and the joint itself are then filled with a low-modulus elastomeric concrete. High modulus material is used for the staple legs to provide positive mechanical anchorage, and low modulus material is used in the slots and the joint to allow the pavement to flex without cracking and spalling the repair material, and to prevent "locking up" the joint so that cracks form elsewhere in the slabs. Bars are typically 1 in. diameter and are spaced 36 in. on center (Figures 2.4 and 2.5).

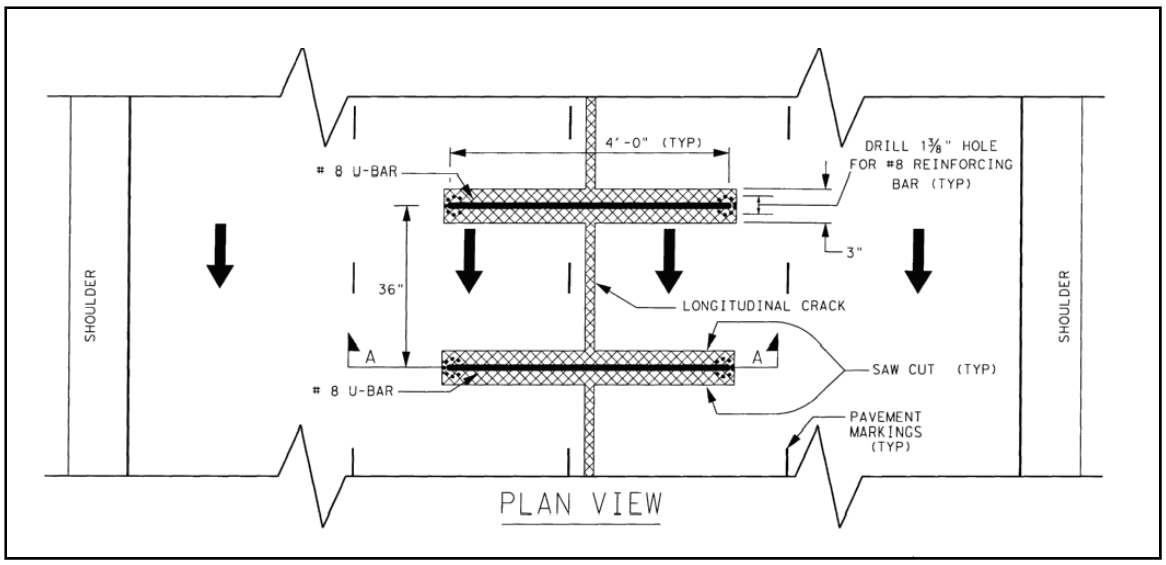

Figure 2.4: Plan View of Stapling Repair (TxDOT 2004c)

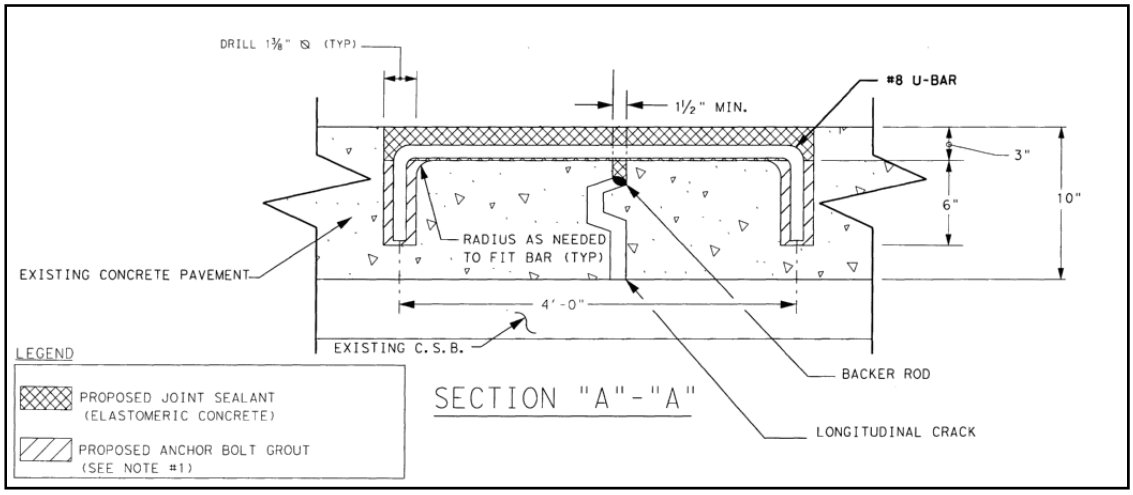

Figure 2.5: Elevation View of Stapling Repair (TxDOT 2004c)

2.1.4 Headed Bar Stitching

The headed bar repair method is a conceptual design that was conceived during the Project 0-5444 kickoff meeting, largely due to input from representatives from Universal Form Clamp. The goal of the design is to provide the load transfer abilities of slot stitching, but with increased resistance to horizontal joint separations. Slots are cut in the same manner as for slot stitching. Holes are drilled at the ends of the slots that are slightly larger than the slot itself. Headed bars are then inserted into the slots, and slots are filled with repair material. Headed bars have increased anchorage capacity over non-headed bars and have been investigated for use in reinforced concrete beam applications when geometric constraints do not provide sufficient anchorage length for conventional bars. For this application, because headed bars were not readily available, a stack of four 1/8-in.-thick flat washers (1/2 in. total) was welded to each end of a #6 bar as heads (Figure 2.6).

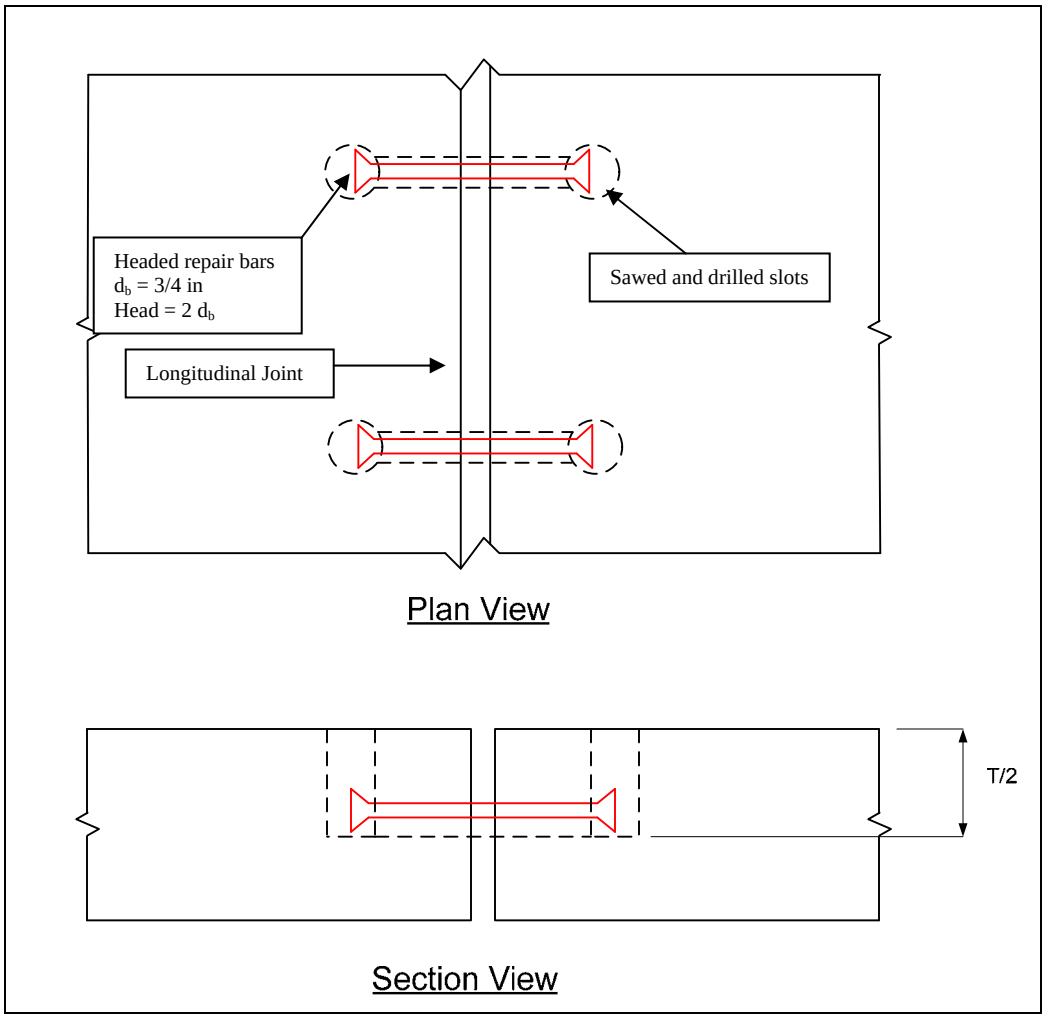

Figure 2.6: Headed Bar Stitching Layout

2.2 Literature Review and Surveys

In order to determine common causes of longitudinal cracking and joint separations and to summarize current repair practices, a review of current literature was conducted. Surveys were also distributed to TxDOT personnel in every district, to pavement engineers in 27 states, and to other experts in government and private industry. Results are summarized by topic.

2.2.1 Causes of Longitudinal Cracking

Surveys and literature indicated the following causes of longitudinal cracking in concrete pavements:

Surveys:

- Base problems (soggy, non-uniform support, inadequate compaction)
- Under-strength concrete
- Late or shallow saw cutting

- Insufficient slab thickness
- Poor concrete consolidation around longitudinal steel
- More than three lanes tied together
- Slab width greater than 15 ft.
- Insufficient base thickness
- Lack of attention to detail during construction (vibrator trails, thin slabs, etc.)

Literature:

- Improper saw cutting (Caltrans 2004a)
- Greater than 50 ft. of pavement (width) tied together (Caltrans 2004a)
- Shallow or late saw cutting (NYSDOT 2005) (ACPA 2000) (Caltrans 2004c and Pierce 2006)
- Bond between slab and base/sub-base increasing effective slab thickness, reducing effective depth of saw cut (ACPA 2000)
- Dry granular base wicking moisture from concrete, causing cracking (ACPA 2000)
- Traffic load fatigue (Pierce 2006)

2.2.2 Causes of Longitudinal Joint Separation

Comparatively, there was significantly less information regarding the causes of longitudinal joint separation than longitudinal cracking. Surveys indicated that joint separation is not a common problem in many states. The following causes were identified:

Surveys:

- Tie bar corrosion or debonding
- Tie bar absence (due to construction error)

Literature:

- Failure of tie bars due to corrosion (NYSDOT 2005)

2.2.3 Repair Recommendations

Much information is available about the repair of concrete pavements. Many sources recommended full depth repair, the most expensive of all possible methods. Because this study is focused on less expensive alternatives to FDR, the summary of literature on repair recommendations will be limited to these methods.

- Surveys indicated cross stitching is an effective repair method for cracks up to one-quarter inch wide. It was not recommended for wide cracks. Number 5 or 6 deformed bars are typically used. Spacing varies, but generally is such that 0.2 sq. in. of steel per foot of repair is present.
- Cross stitching is only suitable for cracks and joints that are in "reasonably good condition" (ACPA 2001). Cross stitching should not be performed on high-severity cracks (NYSDOT 2003) or cracks that are functioning as joints because cracking can be induced elsewhere in the slab (ACPA, 2006).
- Slot stitching has the same limitations as cross stitching, according to ACPA (ACPA, 2001).
- Transverse joint faulting was denoted as "low" for <0.375 in., "medium" for 0.375 to 0.75 in., "high" for >0.75 in. While longitudinal joints are different than transverse joints, this provided a general guideline for the repair of longitudinal cracks (NYSDOT 2005). The Federal Highway Administration's Long Term Pavement Performance (LTPP) program has also shown that load transfer efficiency (LTE) decreases as crack faulting becomes more severe (FHWA 2003).
- Slot stitching longitudinal joints is similar to the dowel bar retrofit (DBR) technique for restoring load transfer across undoweled transverse joints in jointed concrete pavement (JCP). The bars are installed using the same construction method and are generally placed in the same location in the slab. Both techniques are required to provide load transfer across joints. The primary difference between the two methods is that DBR repairs do not prevent joint separation while slot stitching must. Much more research has been conducted on DBR than cross stitching. Because of the similarities in the two methods, many of the observations and recommendations about DBR can be applied to slot stitching. Minnesota uses DBR to establish load transfer across transverse cracks in JCP (MnDOT 2003). The Washington State Department of Transportation recommends that DBR be performed if transverse joint faulting in excess of 0.125 in. is observed (WSDOT 2001).
- Minnesota uses a variation of slot stitching for full-depth repairs of joints. Instead of using deformed bars to prevent slabs from separating, smooth dowel bars are used, installed at skewed angles (Masten 2005).
- The LTPP program also showed that transverse cracks in continuously reinforced concrete pavement (CRCP) do not negatively affect overall long-term pavement performance if they show LTE values greater than 77%. While this study only considered longitudinal cracks, the trend is applicable because there is bi-directional reinforcement (transverse and longitudinal) in CRCP.
- Load transfer restoration should be performed if LTE is less than 50 to 60% (NYSDOT 2002b and Fowler et al. 2005b).
- Repair guidelines for longitudinal cracks given by ACPA were as follows: If the crack is full depth and within 1 ft. of the joint, sawing and sealing of the crack is recommended. If the crack is between 1 and 4.5 ft. from the joint, full depth slab

replacement is recommended. Cross stitching or slot stitching is recommended if the crack is more than 4.5 ft. from the joint (ACPA 2001).

2.2.4 Joint Sealing

Joint sealing may seem a trivial matter, but literature indicated that proper joint sealing techniques and maintenance are some of the most cost-effective ways to ensure long-term performance of the joints (Caltrans 2004c). Poor seals enable moisture to penetrate the crack or joint and erode the base and/or subgrade (NYSDOT 2002b). In addition to causing poor load transfer across joints and cracks, base erosion is a common cause of spalling and corner breaks. Several techniques for sealing joints are summarized below:

- Silicon and pre-formed elastic joint sealers are typically used in New York (NYSDOT 2002a).
- For less severe cracks, Minnesota saw cuts the crack to 0.5 in. wide and 0.625 in. deep (typically). Backer rod is inserted and the crack is filled with silicone or hot pour sealant (MnDOT 2003 and Masten 2005)
- ACPA provides procedures for sawing, cleaning, and sealing cracks in concrete pavements (ACPA 1995). Cracks should be sawed to a width of at least 0.375 in. to allow proper cleaning.
- Silicone, hot pour, and rubberized asphalt sealants were compared in a FHWA study. Silicone and hot pour sealants were found to perform better in warm climates, while rubberized asphalt sealants performed better in cold climates. Silicone sealants have better adhesion to the joint surfaces than hot pour sealants, showing bond failure over time. The life cycle cost for silicone sealants is less than for hot poured sealants (FHWA 2006b and Caltrans 2004a).

2.2.5 Materials

Many high-performance repair materials exist, including alternatives to portland cement concrete and steel reinforcing bar. Many of these materials show great potential for increasing the performance and durability of crack and joint repairs.

- In order to slow corrosion, epoxy coated bars are now widely used in bridge decks in Texas, as well as for dowel bar retrofits in highway pavements. Studies at the University of Texas at Austin have shown that these bars may not perform adequately, primarily due to damage that can occur to the epoxy coating during construction.
- Studies were conducted to determine the potential performance of glass fiber-reinforced polymer (GFRP) dowels. Testing indicated that because they have a lower shear modulus than steel, they were not as efficient in providing load transfer. Larger GFRP bars were required to provide similar performance to steel bars (Eddie et al. 2001).

- FHWA studies show that 1.5-in. dowels are the most effective in resisting faulting on transverse joints, regardless of other design features. This is applicable for the previously mentioned slot stitching method.
- Polymer concrete and epoxy injection have been shown to be effective crack repair methods on bridge decks (Mangum et al. 1986). Bridge decks are similar to CRCP in their reinforcement patterns, so these techniques may be suitable for repairing cracks in CRCP. They are not, however, applicable to unreinforced JCP due to lack of available field and testing data.

2.2.6 Load Transfer Trends

Falling weight deflectometer (FWD) testing is commonly used to determine the load transfer efficiency of a joint or crack. Overall joint performance can be estimated based on LTE and the deflection of certain sensors on the FWD.

A Federal Highway Administration report (FHWA 2003) examined a database of FWD data from several states. Testing was performed on joints and cracks in CRCP and JCP (doweled and non-doweled). Data were examined to determine trends, and the following conclusions resulted:

1. LTE varies significantly with the time of day when the FWD testing is conducted (the same is reported by Caltrans 2004c). Slab curling is thought to be the cause of this phenomenon. Daily variations in LTE of up to 60% were reported.
2. Seasonal variations in LTE can be quite high (differences of up to 50% were reported for jointed pavements). Temperature is thought to be the key factor in this trend.
3. Daily and seasonal variations in LTE are much more pronounced for undoweled pavements than for doweled pavements.
4. Base and subgrade conditions significantly contribute to LTE.
5. CRCP has very high crack LTE; cracks are effectively controlled and punchouts are avoided.
6. Slab faulting is typically associated with low LTE.

- Load transfer is provided by three sources: (1) aggregate interlock, (2) mechanical devices (dowels), and (3) stabilized base. Ideally all three work together (Caltrans 2004c).
- Load transfer efficiency deteriorates over time due to the wearing of crack surfaces, especially in pavements with limestone aggregate (Buch et al. 2000).

2.3 Case Studies

Officials from several states sent information about specific stitching projects in addition to answering survey questions. Case studies are summarized below:

2.3.1 Ontario

Highway 417 was constructed in 2002. Approximately 1700 ft. of longitudinal cracks were identified between 2003 and 2004. Cracks were repaired using cross stitching. Steel bars with 19.5 mm (0.77 in.) diameter were placed at 24 in. spacing, which translates into 0.22 sq. in. of steel per ft. of crack. Repairs have performed well to date (Kazmierowski 2004).

2.3.2 Colorado

Interstate 70 near Agate was constructed in 1999. Approximately 800 ft. of longitudinal cracking was observed in 2001. Cross stitching was performed in 2002 using #5 bars at 18 in. spacing (0.21 sq. in. per ft. of crack)(CDOT 2003).

2.3.3 Washington

Cross stitching was used to repair random longitudinal cracking on JCP in Washington approximately 11 years ago. Number five bars at 20 in. spacing (0.19 sq. in. per ft of crack) were used. Repairs are still performing well (WSDOT 1996).

2.3.4 Kansas

Several successful cross stitching projects have been undertaken in Kansas. Cracks are typically repaired before they reach a width of 1/8 in. Epoxy coated #6 or #8 bars are installed at 24 in. spacing (0.22 and 0.40 sq. in. per ft. of crack, respectively) (KDOT 1990a, 1990b, 2005).

2.3.5 Iowa

Approximately 1.5 miles of PCC pavement were identified as having no tie steel present on the longitudinal construction joint due to contractor error. Slot stitching (also referred to as the “bar and slot” method) was used to repair the joints approximately 17 years ago. Epoxy coated, #5 bars at 30 in. spacing were used. Repairs are still in good condition (Merryman 2005).

Chapter 3. Field Investigations

This chapter describes several field investigations performed as part of this study. The methodology for the investigations is summarized, including descriptions of activities conducted and data collected during each field investigation. Results from each field investigation are described, followed by a summary of key findings and conclusions.

3.1 Methodology

Standard procedures to be used during each field investigation were developed by the research team. Although each location was unique, and field adjustments to the methodology were required on occasion, the general approach was the same in each investigation.

3.1.1 Visual Inspection

Pavements were visually inspected for cracking and spalling, joint separation, slab faulting, corner breaking, elevation irregularities, base and/or subgrade pumping, and other distress. Construction joint and crack widths and slab faulting were measured and recorded. Crack patterns were mapped. Joint filler materials were inspected for integrity and durability. Signs of cracking, spalling, tearing, and other distress of the filler material were noted. Repaired pavement sections were examined to determine the condition of the repairs. Evidence was noted of further joint/crack separation, slab faulting, concrete spalling, etc., after repair. Where possible, the repair bars were visually inspected for signs of section loss and corrosion. Patterns of pavement distress were recorded and compared with field test data in order to determine the cause(s) of distress.

3.1.2 Falling Weight Deflectometer

Falling weight deflectometer (FWD) tests are commonly used to determine the load transfer efficiency (LTE) of joints and cracks and to give a general indication of pavement system integrity. These tests were used in this study to assess the performance of joints and cracks and to determine the potential demand on any future repair methods for each pavement.

Load transfer efficiency measures the portion of a load applied to one side of a crack or joint that is transferred across the crack or joint. For monolithic concrete, the theoretical LTE is 100% (100% of the load is transferred from one sensor to another). Cracks and joints, then, because they do not transfer load as efficiently as monolithic concrete, usually have somewhat lower LTE values.

FWDs used in Texas are typically trailer-mounted (Figure 3.1) and have several accelerometers located on a cradle that is lowered onto the pavement (Figure 3.2 for sensor arrangement). Load is applied to the pavement by dropping weights onto a rubber load plate in contact with the pavement. Sensors are placed on each side of the joint or crack and deflections are calculated using the accelerometers (Figure 3.3 shows the sensor setup in the field). Deflection on the unloaded side of the joint or crack (#4 sensor deflection) is divided by the deflection on the loaded side (#2 sensor deflection) to calculate LTE:

$$LTE = \frac{\Delta_{\#4}}{\Delta_{\#2}} \times 100$$

Figure 3.1: FWD Testing on Longitudinal Joint

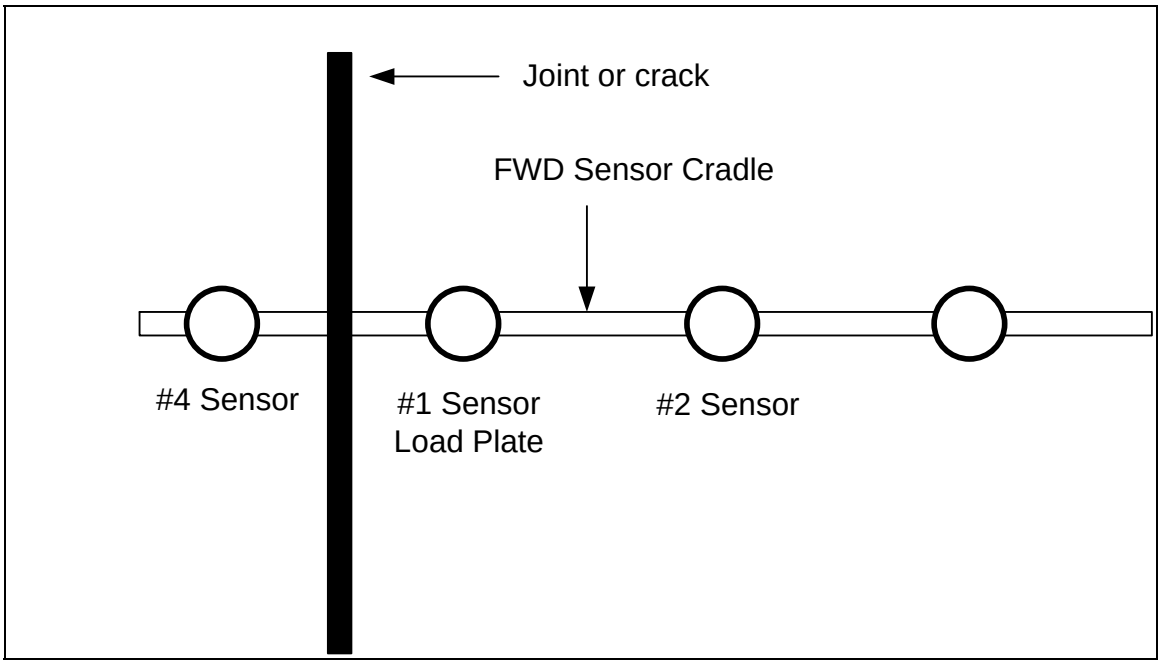

Figure 3.2: FWD Sensor Arrangement

Figure 3.3: FWD Load Plate and Sensors

Falling weight deflectometers typically drop the weights from several heights at the same location, inducing varying magnitudes of load on the pavement. Deflections from loads between 9,000 and 10,000 lbs. are used to calculate LTE.

The number one sensor deflection (at the location of the load plate) is also used to determine overall pavement integrity. Slab stiffness (which is influenced by concrete strength and stiffness, among other things) as well as base and subgrade stiffness can be judged qualitatively by the deflection under the load plate. Pavement systems with stiff concrete, good base and subgrade conditions, and tight joints and/or cracks will have small deflections, while large deflections can be indicative of poor performance in these areas.

Data from the FWD are useful for this study in several ways. First, LTE across separated joints and cracks is used to determine the severity of the distress, and thus whether repairs are needed. The American Concrete Paving Association (ACPA) suggests that repairs need to be implemented if LTE is 60 percent or less (Fowler et al, 2005). Second, the #1 sensor deflection data are used to determine the potential displacement demand on any repair that would be used on the crack or joint. Higher values of #1 sensor deflection indicate a more severe loading condition than for lower deflection values.

3.1.3 Coring

Cores were taken in multiple locations on each pavement, with the exact locations being determined in the field. For longitudinal cracks, several cores were usually taken directly over the crack in order to examine the condition of the crack itself (evidence of weathering, such as polishing of the crack surfaces and deposition of sediment on the crack faces may indicate the relative age of the crack). Pavement thickness and crack widths were also noted. Cores at longitudinal contraction joints were taken to determine if a crack had formed beneath the saw cut as intended, whether the crack extended to the bottom of the slab and through the base, and to measure the width of the crack and saw cut depth.

Cores were taken at longitudinal joints in several locations, including directly over the joint, adjacent to the joint over tie bars, and adjacent to the joint between tie bars. The condition of the joint itself was noted. Tie bars were inspected for signs of corrosion and section loss.

3.1.4 Ground Penetrating Radar

Ground penetrating radar (GPR) was used on several of the field investigations to locate steel bars in the pavement, particularly tie bars and stitch bars. These bar locations were marked and core locations were chosen based on these marks. Early in the study, attempts were made with the GPR to determine if tie bars had experienced section loss. This information was able to be gathered on laboratory specimens, but not in the field. One possible explanation for the discrepancy is that the GPR proved to be very sensitive to moisture. Wet concrete gave very "noisy" results in the lab, and it was not until the slabs had been dry cured for approximately four weeks that bar condition could be determined. Pavements in the field have more moisture present from sources such as residual precipitation and saturated base that may have prevented the GPR from collecting accurate data.

3.1.5 Instrumentation

Field implementation was not part of this portion of the study, so field instrumentation was minimal. One pavement (US 59) was instrumented with gage pins across the longitudinal joints to monitor changes in joint width over time. Measurements were taken at two different times, approximately 14 months apart. Temperature sensors with data logging capability were also installed in the same pavement. However, data were not able to be collected, because traffic caused the sensor leads to shear off.

3.2 US 59 Queen City

3.2.1 Background and Scope of Activities

Approximately 1.572 miles of US Highway 59 from FM 2791 in Queen City to 0.2 miles north of Loop 236 N were investigated on January 24, 2006 and April 5, 2007. The pavement was constructed in 1990 and consists of 14-in. CPCD pavement with non-stabilized density controlled prepared subgrade. Repairs were made in 1997 and 2004 that included slab jacking, installation of pipe underdrain, joint sealing and cleaning, dowel bar retrofit, cross stitching, and diamond grinding. Objectives for the investigation included: (1) obtain a survey of the general condition of the pavement; (2) determine the possible cause(s) of longitudinal joint separation; (3) assess the effectiveness of the cross stitching; (4) install instrumentation that would be monitored over time; (5) begin to formulate a forensics approach to field investigations that would be utilized on several subsequent trips. Activities conducted included:

- Falling Weight Deflectometer (FWD): Unrepaired and cross-stitched longitudinal joints were tested in three primary locations on the longitudinal joint between the shoulder and on the outside lane and the joint between the outside and middle lanes.
- Visual Survey: Measurements of joint and crack widths and slab faulting, presence of spalling, etc. were made.

- Soil Sampling (UT team): Soil samples were taken at various depths at several locations, including at the most severe areas of distress. Qualitative data regarding soil type and presence of lime stabilization were recorded.
- Installation of Crack Width Monitoring Equipment (UT team): Nine sets of recessed stainless steel pins were installed across longitudinal joints in a location of distress that had also been previously cross stitched. Distances between pins were measured during each trip.
- Core Sampling: Three locations were cored, including one over a transverse joint, one mid-slab (uncracked), and one over a transverse crack. Cores were taken in three areas of the worst distress that was observed.
- Installation of Pavement Temperature Monitoring Equipment: Several ibuttons (Dallas Semiconductor) were installed at the top, bottom, and mid-slab in two core holes (located in two of the worst areas of distress) before they were filled.

Figure 3.4 shows the installation of joint width monitoring pins. Short sections of steel rod were placed in holes in the concrete with fast-setting epoxy.

Figure 3.4: Installation of Joint Width Monitoring Pins

3.2.2 Pavement Condition Report

Figure 3.5 gives the layout of the surveyed areas.

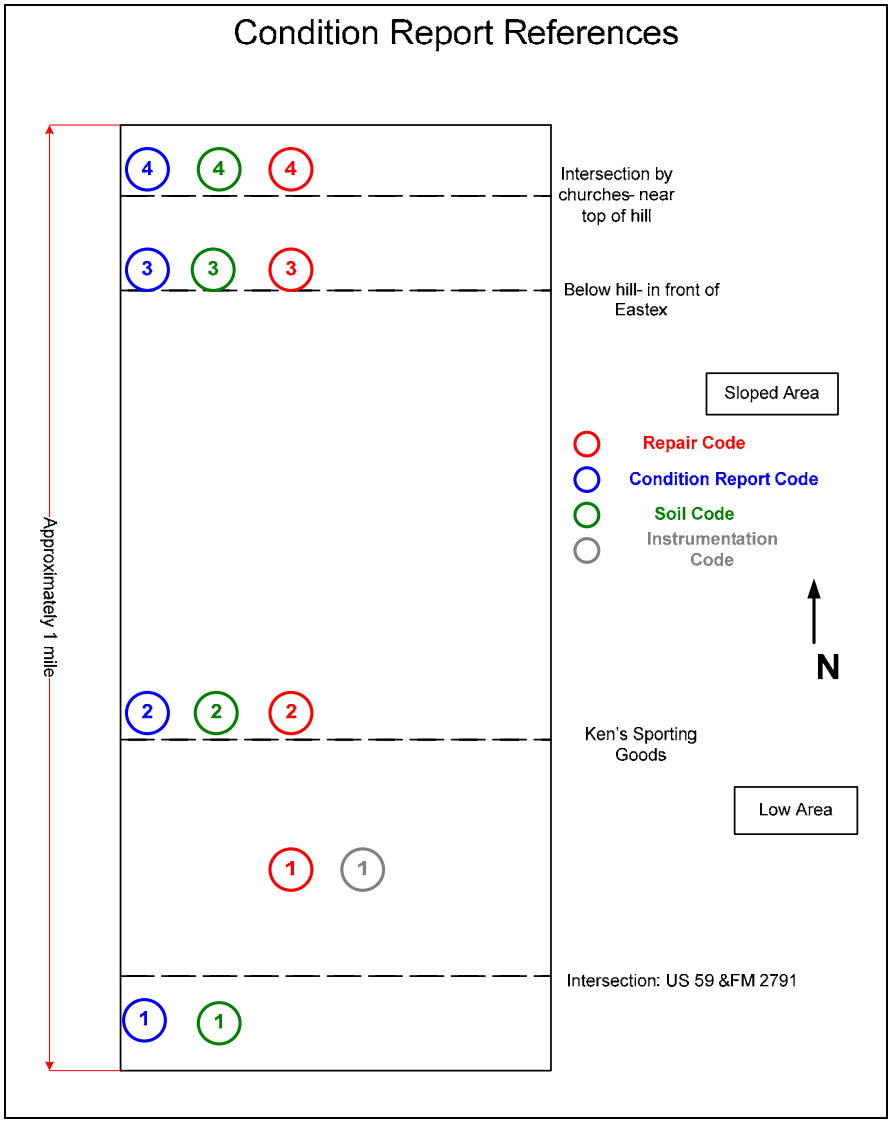

Figure 3.5: Layout of Surveyed Areas

3.2.3 Soil Conditions

Soil samples were taken in several locations. From just below the ground surface to a depth of about three feet, red clay was present. Sandy and silty material was mixed with the clay in some locations. Areas three and four, the sections of pavement with the most distress, had very sticky wet clay just beneath the pavement (sample taken from the core hole #3). Presence of lime could not be detected in the field by UT or TxDOT personnel in any sampling location.

3.2.4 Additional Notes

Core hole #2 was being monitored by the UT team as core hole #3 was being cut. Core hole #3 was higher in elevation and located approximately 50 feet from core hole #2. As core #3 was being cut, researchers observed water (from the coring process) flowing from the #3 hole down the slope, seeping into transverse and longitudinal joints, and filling core hole #2 from beneath the pavement. Water infiltration into core hole #2 was rapid and continuous throughout the cutting of core #3. Evidently, significant voids were present beneath the pavement and the joints were not sealed sufficiently to prevent water seepage. Inspection of the cores taken over cracks and joints confirmed that there has been water infiltration and/or pumping at some time in the past, as aggregates along the cracks and joints were polished smooth and stained a reddish-brown color.

Slabs generally appeared to be in good condition, except for those with edge spalling and cracking as noted above. The only significant transverse crack that was observed is shown in Figure 3.6. No major longitudinal cracks were observed.

Temperature data could not be collected in April 2007 because the temperature sensors were no longer functional or there was a short in the wiring.

Figure 3.6: Transverse Slab Crack in Area Two

3.2.5 Longitudinal Joints

In general, the inside longitudinal joint (shoulder/inside lane joint) showed significant distress. Several 300- to 400-ft. sections of pavement showed longitudinal joint separations of up 51 mm (about 2 inches). Separations of 25 to 40 mm (1 to 1.6 in.) were most common in heavily distressed areas. Isolated faulting across longitudinal joints was also observed, primarily in areas where cross stitching had been previously installed (2004), which indicated that those sections had a history of poor performance. The longitudinal joint between the middle and inside lanes was generally found to be in better condition, with average widths estimated to be 15 to 20 mm (0.6 to 0.8 in.) (measurements could not be taken at all locations due to traffic). Longitudinal joint separation was worse at condition report area three (Figure 3.5) which was higher in

elevation than most of the surrounding soil. In addition to very large longitudinal joint separations and faulting, this area showed significant cracking and spalling of the slabs on the inside of the longitudinal joint, primarily concentrated around the cross stitch bars. Because of the higher elevation of this section, drainage problems typically associated with low-lying areas were ruled out as a cause of the distress. Miles Garrison, the Atlanta District Pavement Engineer, believes that this area might contain an underground spring which could have eroded the subgrade and contributed to shrinking and swelling of the base.

The distance between joint monitoring pins was measured on both trips. Table 3.1 shows the joint width data from both trips. The outside joint grew in width by an average of 0.4 mm, while the middle joint decreased by an average of 0.26 mm over time. The changes indicate at the very least that the roadway crown no longer exists. Further conclusions cannot be drawn because of the limited data set; more frequent measurements leading to a time-history plot of joint movement would be beneficial for TxDOT to pursue in the future. The method used to monitor joint width was very inexpensive and has been utilized by other states (CDOT 2003). The disadvantage is that traffic control is required when measurements are made.

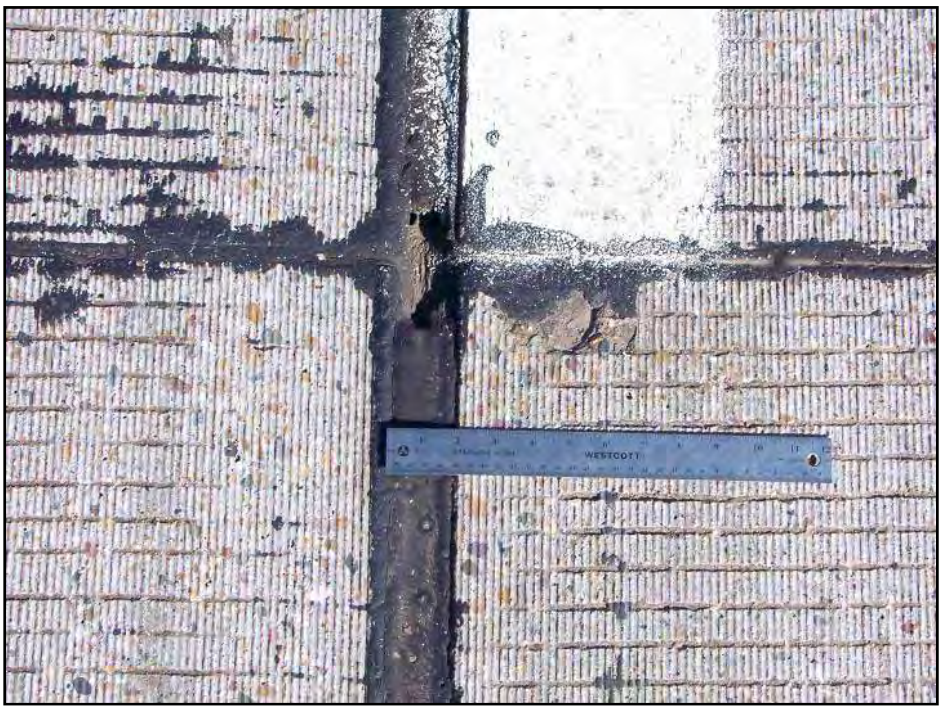

Figure 3.7: 2-Inch Longitudinal Joint Separation

Table 3.1: Joint Width Data

		Joint Width (mm)		
	Location	Jan-06	Apr-07	change (mm)
Outside Joint	1	197.5	198	0.5
	2	201	200.5	-0.5
	3	198.5	199	0.5
	4	196.5	197	0.5
	5	195.5	196.5	1
			AVERAGE	0.4
Middle Joint	6	200	198	-2
	7	198.5	197.5	-1
	8	201	201.5	0.5
	9	199.5	197	-2.5
			AVERAGE	-0.26

Three primary sections of pavement were tested using the FWD. The first section included ten consecutive slabs, the first four being cross stitched and the rest unrepaired. The second section followed this same pattern and was located approximately 200 yards to the north. The third section was located in the area of the worst distress (condition report area three).

Figures 3.8 and 3.9 below show the LTE data for the sections of pavement tested. Average LTE for the unrepaired middle joint was 44% and 34% for the unrepaired outside joint. Cross stitched areas showed LTE values of 52% (middle joint) and 39% (outside joint)

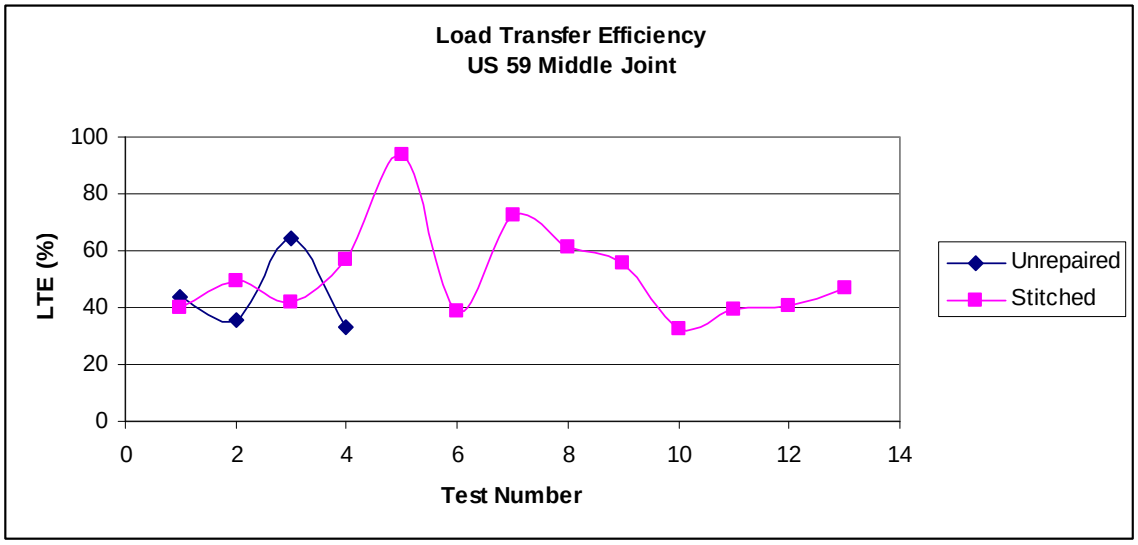

Figure 3.8: LTE of the middle joint

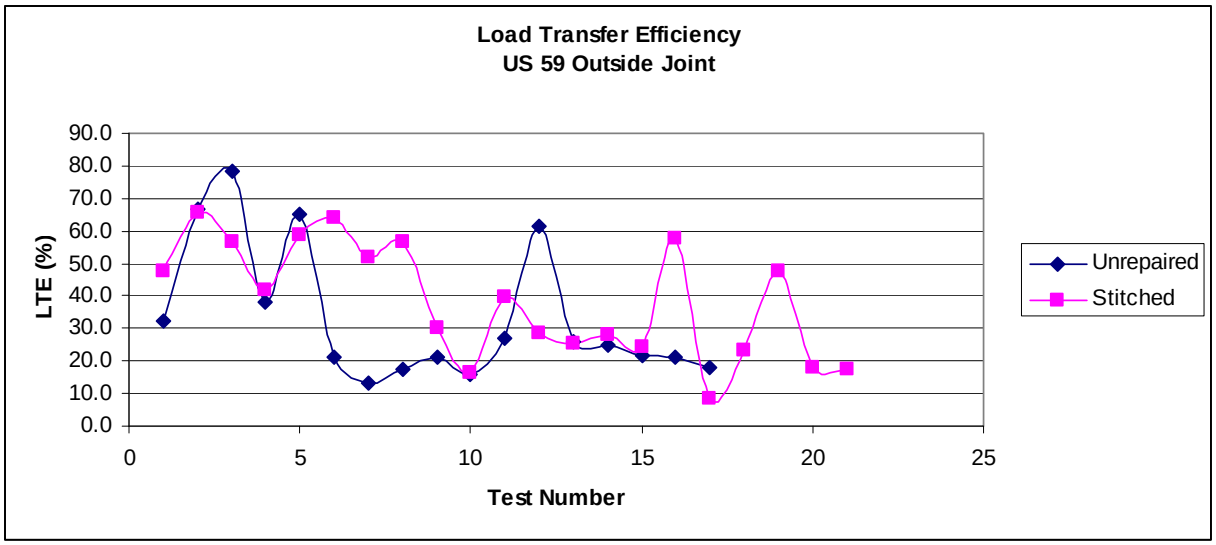

Figure 3.9: LTE of the Outside Joint

The #1 sensor deflection data are shown in Figures 3.10 and 3.11. Average deflection for unrepaired sections was 4.9 mils (outside joint) and 3.9 mils (middle joint). Cross-stitched areas had average deflection values of 4.9 mils (outside joint) and 4.9 mils (middle joint).

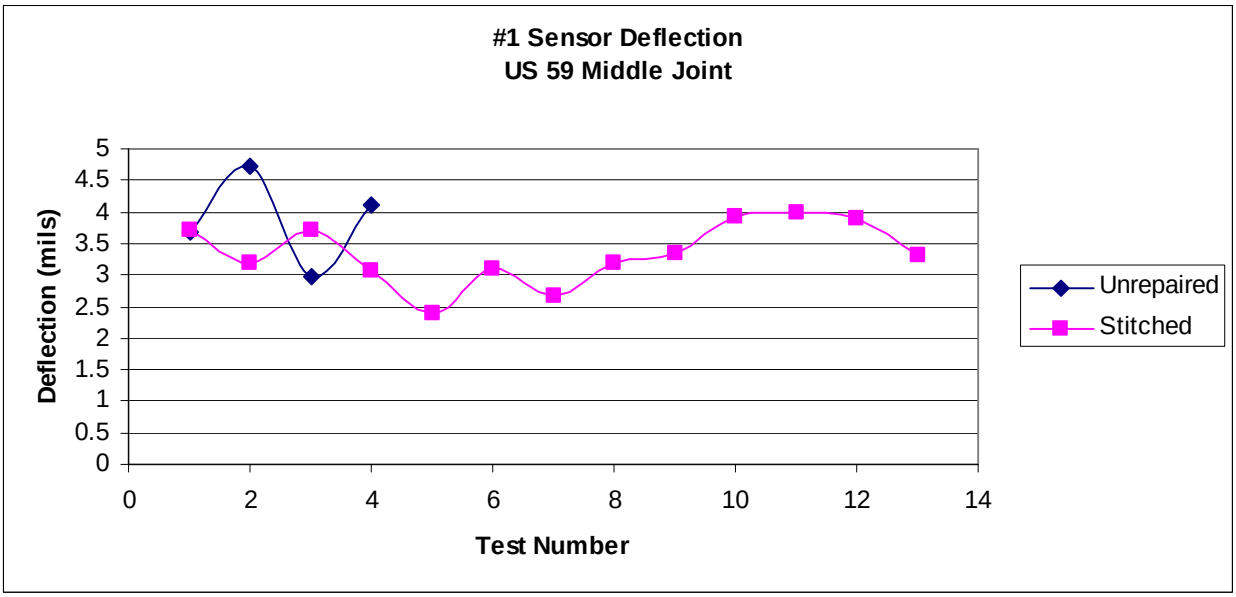

Figure 3.10: #1 Sensor Deflection of Middle Joint

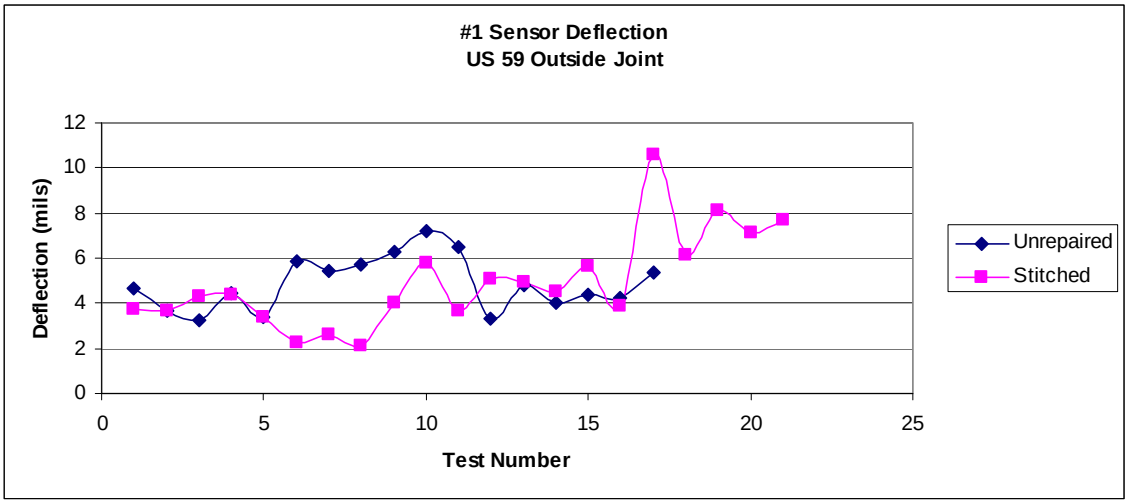

Figure 3.11: #1 Sensor Deflection of Outside Joint

3.2.6 Load Transfer Trends

LTE and Joint Width

Figures 3.12 and 3.13 show the relationship between LTE and joint width. Data from unrepaired slabs do not show any discernable pattern, indicating that LTE does not depend on joint width. Once aggregate interlock is lost (which happens at very small separations for butt joints) load transfer depends primarily on base and subgrade support. For cross stitched areas, there appears to be a correlation between LTE and joint width: as joint width increases, LTE decreases. This behavior makes theoretical sense if the slab is considered to be a cantilever beam. Each cross stitch bar provides some amount of mechanical anchorage between the two slabs it connects. As the distance between the two slabs (i.e., joint width) increases, the moment applied to the stitch bar at the face of each slab increases, thereby increasing the deflection. The overall system becomes less stiff and transfers less load, hence the lower LTE values.

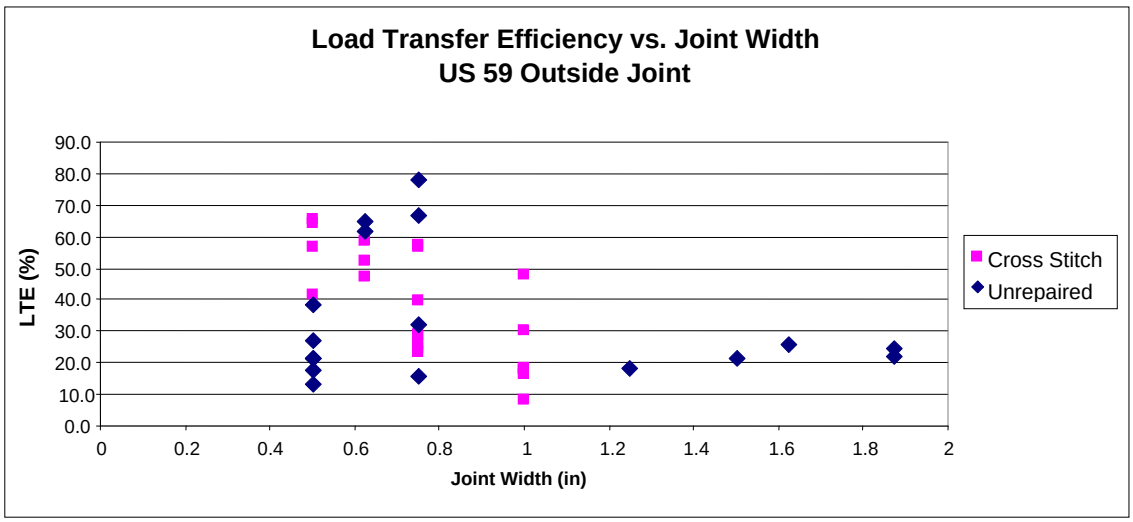

Figure 3.12: LTE vs. Joint Width, Outside Joint

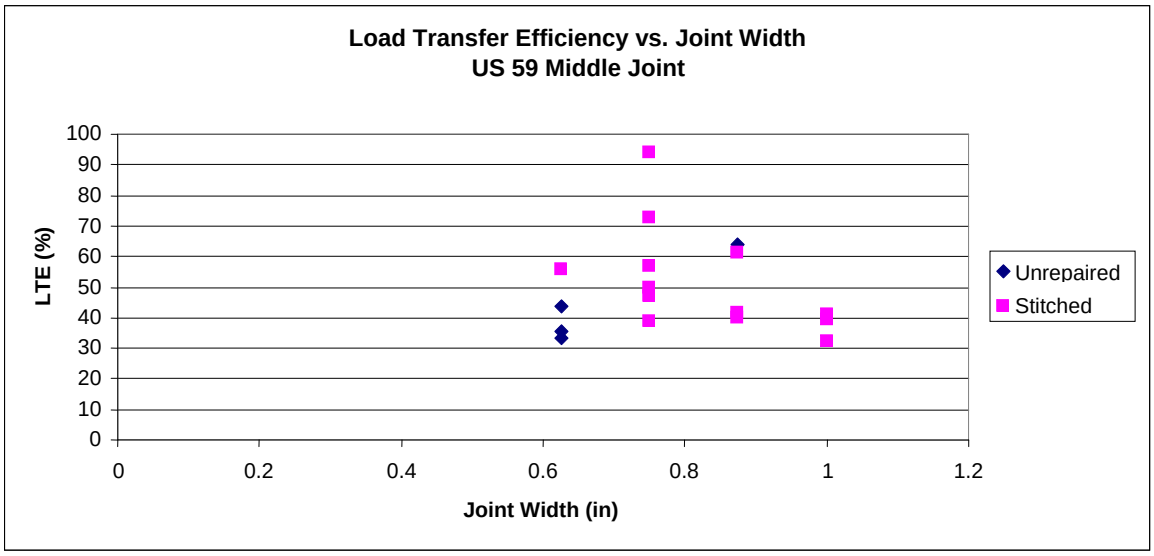

Figure 3.13: LTE vs. Joint Width, Middle Joint

#1 Sensor Deflection and Joint Width

Figures 3.14 and 3.15 show data from the outside and inside joints, respectively. Similar to the LTE case, #1 sensor deflection correlates well with joint width for the cross stitched areas on both joints and poorly on unrepaired areas. Cross stitched areas revealed the expected pattern of deflection increasing with increasing joint width. This is again likely due to the role that bending stiffness of the repair bars plays. The fact that deflection does not depend on joint width is not entirely surprising in this case. Once butt joints have separated, only the base and subgrade provide load transfer, neither contribution of which is dependent on joint width.

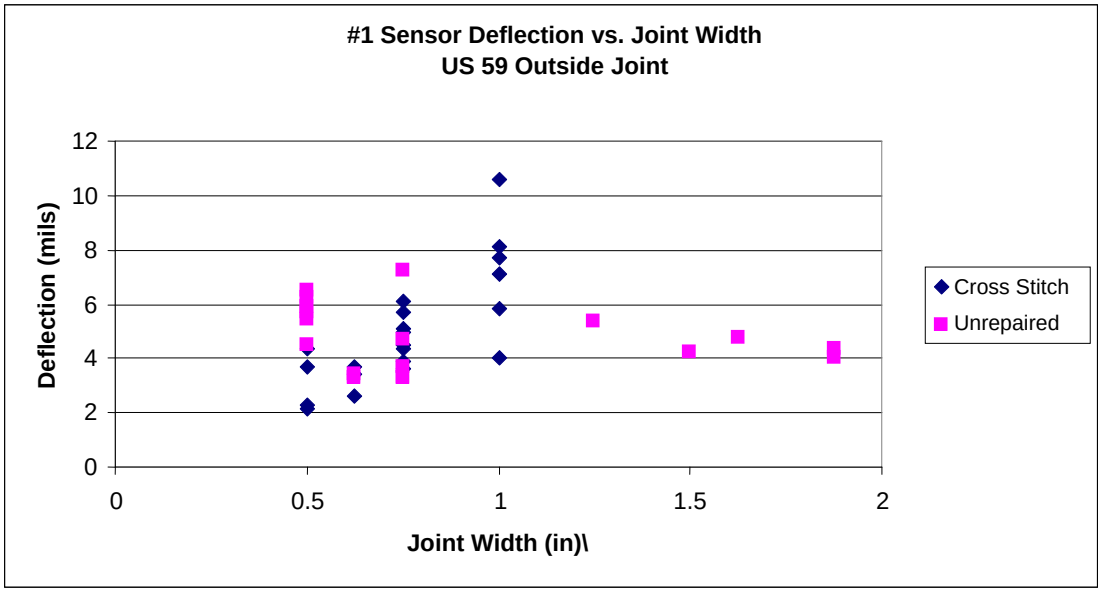

Figure 3.14: Number One Sensor Deflection vs. Joint Width, Outside Joint

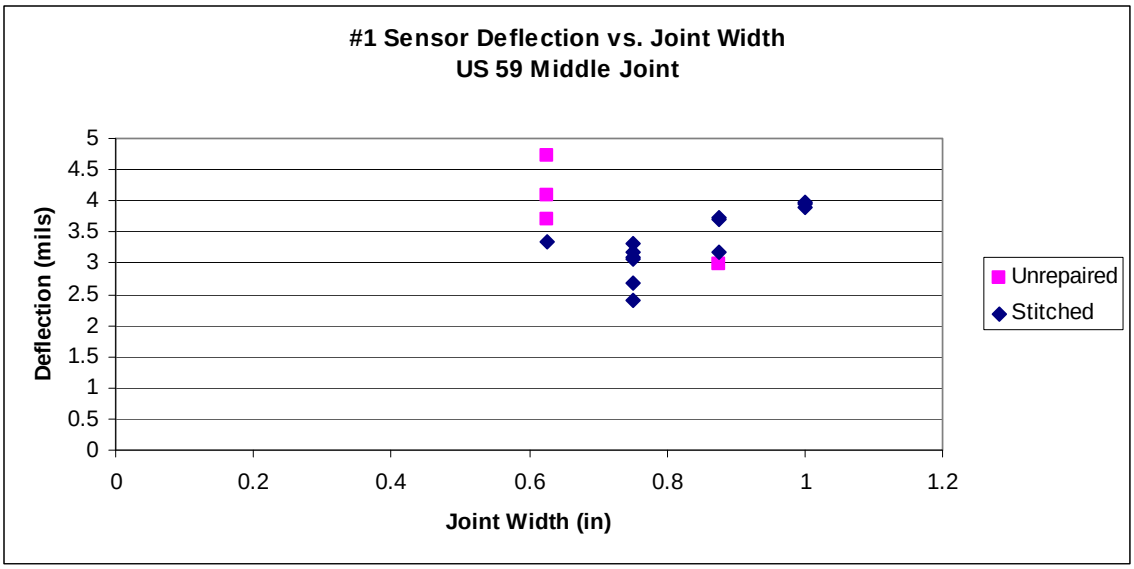

Figure 3.15: Number One Sensor Deflection vs. Joint Width, Middle Joint

LTE and #1 Sensor Deflection

Load transfer efficiency can be correlated to #1 sensor deflection, as Figures 3.16 and 3.17 show. As deflection increases, LTE decreases significantly. This behavior is consistent with the idea that pavements in "poor" condition exhibit not only low LTE, but high #1 sensor deflections as well.

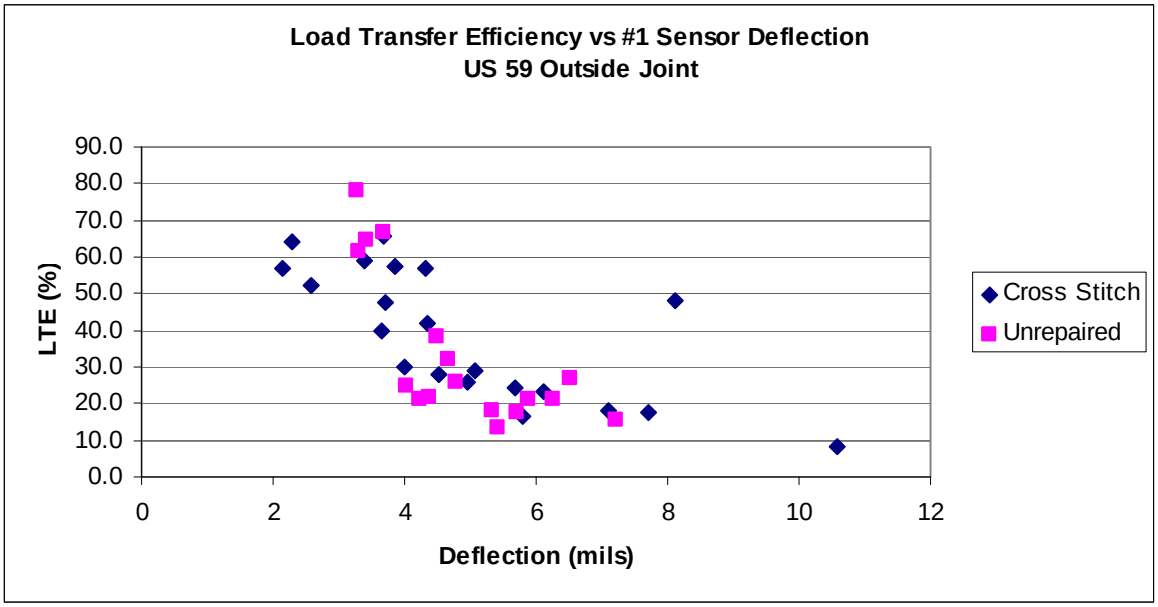

Figure 3.16: LTE vs. #1 Sensor Deflection, Outside Joint

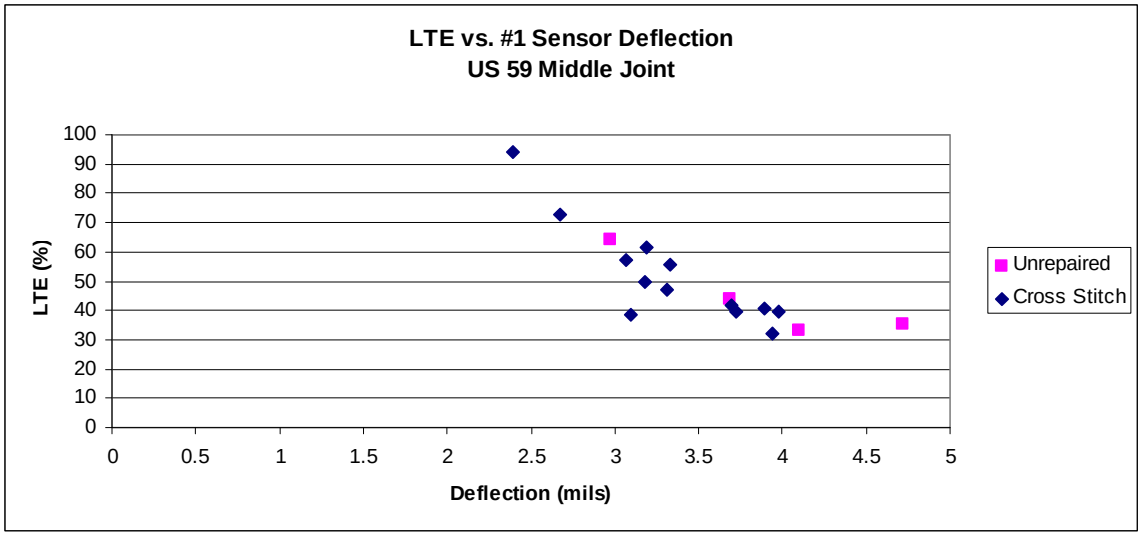

Figure 3.17: LTE vs. Number One Sensor Deflection, Middle Joint

3.2.7 Assessment of Past Repairs

Dowel Bar Retrofit (DBR)

In general, the dowel bar retrofit repairs that were observed appeared to function quite well in preventing slab faulting by providing load transfer across transverse joints. No transverse joint faulting was observed on areas with DBR. Testing was not performed on DBR because it is outside the scope of this study.

Cross Stitching

The effectiveness of cross stitching may be evaluated using several criteria: (1) prevention of further joint separation; (2) restoration of load transfer; (3) increase in pavement integrity (indicated by #1 sensor deflection); (4) increase in joint performance.

With regard to the first criteria, it appears that the cross stitching may have performed well in some cases. Area three, despite its poor physical appearance (Figure 3.18), shows that the cross stitching may have prevented the slabs from drifting farther apart. In areas two and three, cross stitched and unrepaired areas showed smaller differences in average joint width, which indicates that either the mechanism driving joint separation was not very active after cross stitching was installed or that the cross stitched area separated as much as the unrepaired area, making the cross stitching ineffective.

Cross stitching increased LTE in one out of the three areas (Table 3.2). LTE remained virtually the same for the unrepaired versus stitched sections in areas one and three. The reason for the success in area two is uncertain; more consistent construction methods may influence the behavior. Distance from the slab edge to the cross stitch hole and the angle of the hole can strongly influence the strength of the cross stitching. Area three is an example of the poor performance of stitching that is placed too close to the slab edge.

#1 sensor deflections were decreased with cross stitching in area two, and were essentially unchanged in areas one and three.

Table 3.2: FWD Data Averages for US 59

Data Averages - US59 Outside Joint

Area	Repair	Joint width	D1	LTE
1	Cross Stitch	0.59	4.0	52.9
	None	0.65	4.2	50.2
2	Cross Stitch	0.56	2.6	58.0
	None	0.56	5.7	26.0
3	None	1.63	4.6	22.4
	Cross Stitch	0.83	5.3	28.7
	Cross Stitch	0.94	7.3	26.8

Data Averages - US59 Middle Joint

Area	Repair	Joint width	D1	LTE
3	Unrepaired	0.69	3.9	44.1
	Stitched	0.83	3.3	51.5

Figure 3.18: Distressed Stitching in Area Three

After performing literature searches online, reviewing surveys of engineers from TxDOT and other states, and talking with TxDOT engineers and others, it appears that one of the problems with the cross stitching in this area is that it was installed in an already-functioning

joint with severe distress. Some suggest (ACPA 2001, 2006 and NYSDOT 2003) that cross stitching should only be installed if the joint does not have a large separation. In severe cases, full depth repair or other repair techniques were suggested (NYSDOT 2003).

The trends described above indicate that cross stitching performs well in preventing slabs from separating further but fails to significantly increase joint performance, LTE, and D1 in three out of four cases. Based on these observations, cross stitching is more suitable for applications in which joint separations exist, but which still exhibit good joint performance.

Slab Jacking

Areas repaired with this method appeared to have deteriorated significantly. Differential vertical movement (faulting) of the slabs was observed in these sections, which indicates that either the urethane material compressed over time or the soil beneath the urethane experienced continued settlement after the slab jacking repair(s).

3.2.8 Conclusions

1. Longitudinal joint separations were likely caused by a number of factors. Very poor base preparation allowed significant vertical and horizontal movement between slabs. Untied longitudinal joints worsened the problem by not providing mechanical resistance to the joint separation.
2. Cross stitching is not suitable for areas that exhibit low load transfer.
3. Slab jacking does not appear to be an effective method of leveling slabs in areas with soft soil.
4. Base and subgrade conditions greatly affected not only the overall performance of the pavement system, but also had a direct effect on the demand on longitudinal joint repairs.
5. Overall LTE performance was poor in both unrepaired and cross stitched areas.
6. LTE correlated well with #1 sensor deflection for stitched and unrepaired sections; LTE decreased as deflection increased.
7. LTE decreased as joint width increases for stitched areas and does not depend on joint width for unrepaired areas.
8. Mechanical anchorage in the cross stitching method caused the repaired areas to display correlation in the data mentioned in conclusions six, seven, and eight. Without mechanical anchorage, LTE, and D1 were independent of joint width.

3.3 US 290 Houston

3.3.1 Background and Scope of Activities

Hwy 290 in Houston near the Mangum exit contains 10-in-thick CRCP with tied, keyed longitudinal joints constructed on 6 in. cement-stabilized base. Extensive longitudinal joint separations have been observed for many years. Repairs have been made to these pavements on the recommendation of Mr. Tony Yrigoyen (formerly of TxDOT) using the “stapling” method

(see Appendix C for the specification). The intended function of the staples was to prevent further horizontal separation of the longitudinal joints, but not necessarily to provide load transfer. Researchers conducted a field investigation of this location on May 2–3, 2006. Objectives of the investigation included: (1) observe and document the extent of longitudinal cracking and/ or joint separations in the concrete; (2) determine the cause(s) of distress; and (3) evaluate the effectiveness of the stapling method. Activities performed by the research team included:

1. Visual Inspection of Pavement: The following observations were made and documented: occurrence and extent of longitudinal joint separations, condition of stapling repairs (including evidence of further joint separation or slab faulting after the repair), condition of joint filler material, and condition of the concrete around staples.
2. Ground Penetrating Radar (GPR): A GPR unit rented from Exploration Instruments, Inc. (Austin) was used to find the locations of original reinforcing steel and tie bars in the pavement. It was also used to select locations to take cores so that reinforcing steel could be avoided.
3. Falling Weight Deflectometer (FWD): FWD testing was conducted on several sections of pavement across longitudinal joints that had been stapled and also on unrepaired separated joints. Load transfer efficiency is calculated from the FWD data.
4. Coring: Cores were taken from four locations including: (1) one directly over a staple, (2) two on the longitudinal joint that had been sealed with an elastomeric concrete material, and (3) one at mid-slab (control core).

3.3.2 Condition Report

Performance of Stapling Repairs

Longitudinal joints that had been stapled did not generally appear to have suffered any further separation or major faulting. Very limited corner spalling was observed, and concrete around the staple bars was generally in good condition.

All staple bars appeared to be rigidly connected to the pavement as originally installed. No pullouts or bar ruptures were observed. Some exposed bars showed evidence of corrosion, which was confirmed by examining core #1 (Figures 3.19 and 3.20).

Figure 3.19: Staple Corrosion (Core #1)

Figure 3.20: Staple Corrosion

As part of the original repair, epoxy was used to rigidly connect the staple bar legs (vertically) to the concrete (see attached specification), while the horizontal slots and the longitudinal joint itself was filled with an elastomeric concrete manufactured by either SSI or D.S Brown (depending on location). Performance of the rigid epoxy material could not be conclusively evaluated because the material could not be accessed by the research team. The elastomeric material was visible, however, and showed signs of significant deterioration on approximately 5 to 10% of the area investigated. Many areas with deteriorated material were repaired less than two years ago.

Several areas showed extensive cracking and spalling of the joint filler material; both in the staple slots and in the longitudinal joint (Figure 3.21). Non-compressible material had invaded the joint or slot in those areas. Some joints also showed debonding of the joint filler material with the side walls of the joint.

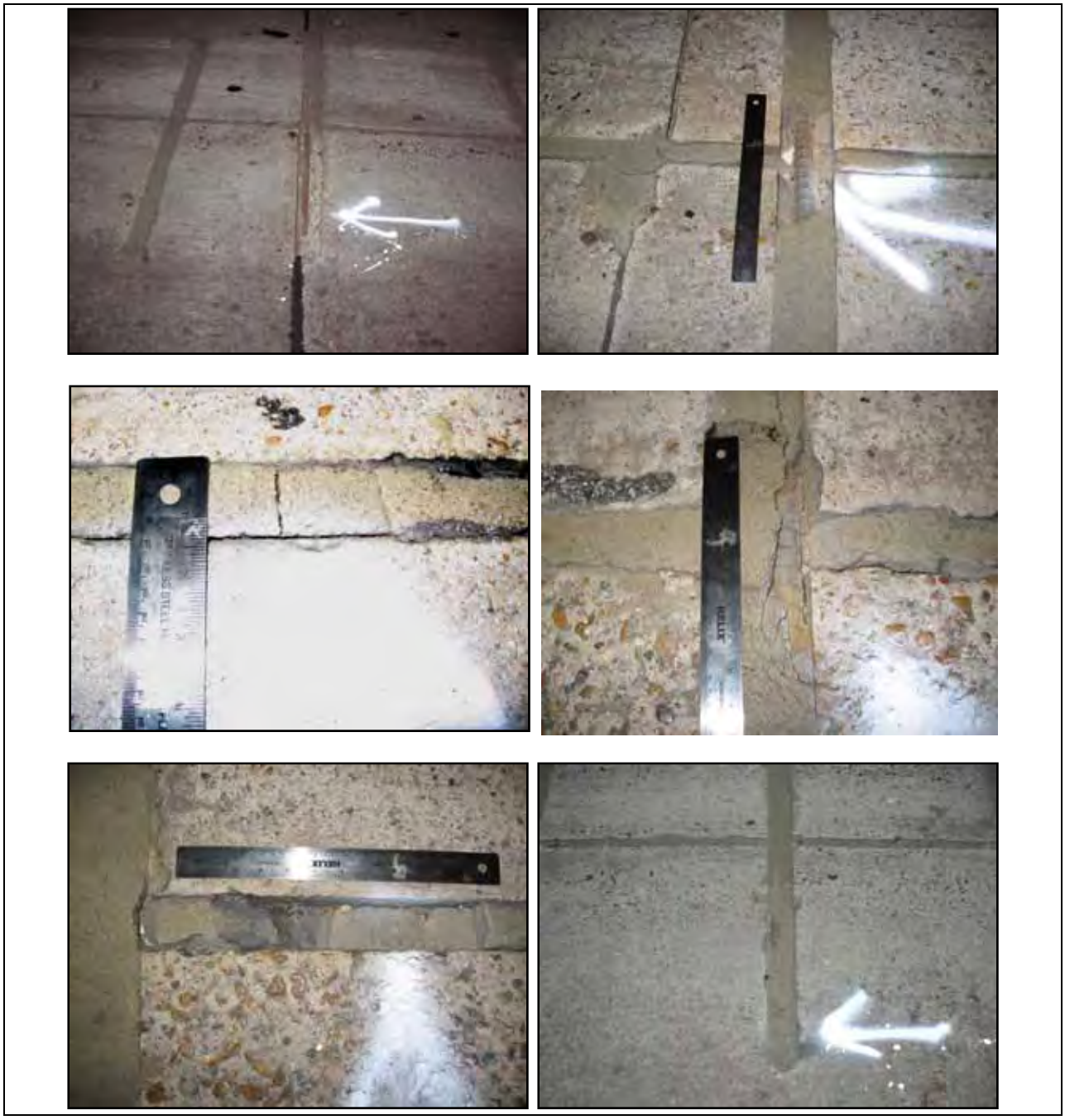

Figure 3.21: Deteriorated Stapling Repair Material

Many problems observed with the joint filler material could have been caused by improper field mixing and placement. Specifically, it appeared that the construction workers underestimated the working time for the material and/or did not use the appropriate material

component proportions. Inconsistencies in the hardness of the material were observed along the length of investigated pavement by subjectively measuring the resistance to a screwdriver pressed into the material. In addition, a recurring pattern was noted; the filler material was in good condition for a certain length, and then progressively deteriorated along the length of the longitudinal joint. This could indicate a situation in which the material had adequate workability and bonded well to the crack surface early in the placement process, then as the material began to harden, bonding ability was lost and wrinkles/folds/seams on the material surface could not meld adequately. Areas filled under these conditions would deteriorate much more rapidly than the surrounding areas (which is consistent with field observations).

Load Transfer Efficiency

FWD testing was performed on only four locations across longitudinal joints due to traffic constraints. Data indicates that the keyed joints contained tie bars at one time (90% load transfer on the unrepaired joint in good condition—see Table 3.3). Load transfer efficiency of the stapled areas was inconclusive due to the small number of tests. More testing is needed, which should include several drops across stapled joints in good condition, stapled joints in poor condition, unstapled joints with little or no separation, and unstapled joints with large separations (1 in. or greater).

Table 3.3: Load Transfer Efficiency

Joint Condition	LTE
Stapled Joint; poor repair condition	57%
Stapled Joint: good repair condition	84%
Unrepaired joint; tight joint	90%
Unrepaired joint: 1" separation	46%

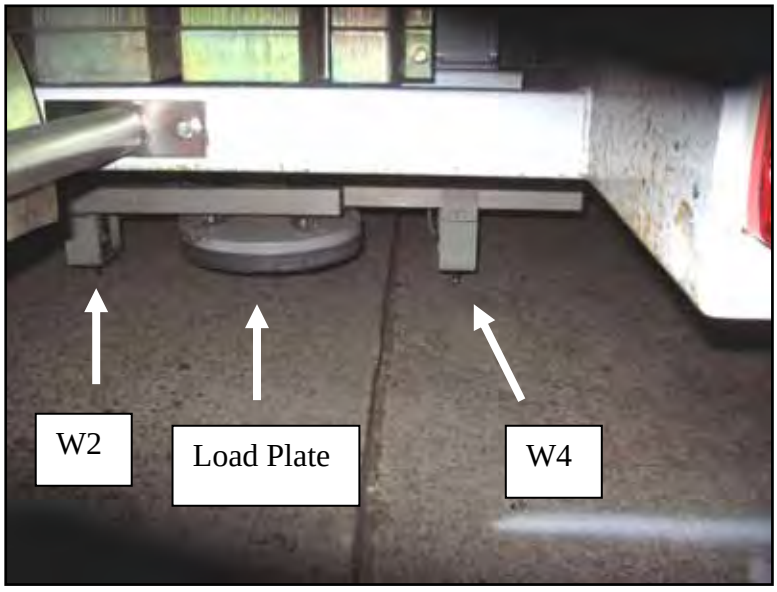

Figure 3.22: FWD Test Setup

Several staples were protruding through the joint filler material (Figure 3.23). It appeared that the staples were not installed with sufficient clear cover above the bar (much less than the 2 in. required by the specification), and the elastomeric material was worn over time by traffic.

Figure 3.23: Protruding Staple Bars

Examination of the cores revealed the absence of backer rod in the longitudinal joint as called for in the stapling specification (Figure 3.24). While not a critical construction error, the backer rod prevents the repair material from intruding into the joint farther than desired. This not only saves money on repair material, but could also cause better performance of the repair material. For low-modulus materials subjected to large strain demands, the effect of Poisson's ratio begins to negatively affect the strain capacity of the material if it is very thick.

Figure 3.24: Absence of Backer Rod in Longitudinal Joint Cores

GPR proved to be a very useful tool during the field investigation. Reinforcing steel was detected at varying depths in the slab, and the equipment was used to select sites to perform coring operations so that slab steel could either be avoided or cored through.

3.3.3 Conclusions

Based upon the observations made on the field investigation, the Center for Transportation Research team came to the following preliminary conclusions regarding the stapling method for repairing separated longitudinal joints:

1. Stapling appeared to perform well for locking slabs together horizontally.
2. Effectiveness of stapling in providing load transfer efficiency across separated longitudinal joints was uncertain.
3. Joint filler material appeared to perform well when properly proportioned, mixed, and placed according to the manufacturer's recommendations.
4. Quality control on slot cutting and joint filler material mixing and placing appeared to be inadequate.

3.4 SH 66 Dallas

3.4.1 Background and Scope of Activities

Construction of 10 in. thick JCP with a 4-in. asphalt stabilized base and 10 in. of lime treated subgrade began in 1996. Longitudinal cracking currently exists in multiple lanes of the eastbound and westbound directions of SH 66 near the intersection with Centerville St. in Dallas, Texas.

Researchers conducted field inspections of approximately one-quarter mile of SH 66 just east of Centerville St. on July 24 and September 13, 2006. Objectives of the field investigation included: (1) Survey and document the extent of longitudinal cracking (2) Determine the cause(s) of such cracking. Activities included:

1. Visual Inspection: Longitudinal cracks were inspected; crack widths and degree of slab faulting were recorded.
2. Falling Weight Deflectometer Testing: FWD testing was performed on several sections of pavement with longitudinal cracking. Load transfer efficiency was calculated for cracks of various widths.
3. Coring: Several cores were taken at the following locations: narrow crack, wide crack, strong slab (no cracking), weak slab (cracking), and through the longitudinal contraction joint adjacent to both cracked and uncracked slabs.

Figure 3.25: Longitudinal Cracking (1)

Figure 3.26: Longitudinal Cracking (2)

3.4.2 Pavement Condition Report

Crack widths from 0.025 to 0.5 in. were measured in the test section. Limited slab faulting of up to 0.25 in. was also observed (Figures 3.27 and 3.28).

Figure 3.27: Narrow Crack

Figure 3.28: Wide Crack with Faulting

Load transfer efficiency of the longitudinal crack and longitudinal contraction joint were measured using the FWD in several locations along the test section. Two data sets were collected: one when the air temperature was approximately 70 deg. F. (pavement temperature was approximately 79.2 deg. F.—see Medina-Chavez et al. 2005, p. 7, eqn. 7) and one at 100 deg. F. (pavement temperature was approximately 107.8 deg. F.). Average LTE for the longitudinal crack was 96% at 70 deg. F. and 87% at 100 deg. F. (See Appendix E for statistical data.) Figures 3.29 and 3.30 show LTE and #1 sensor deflection data taken at the same points along the pavement for the two different temperatures. Figure 3.31 shows LTE data for the contraction joint adjacent to the longitudinal crack for the sake of comparison.

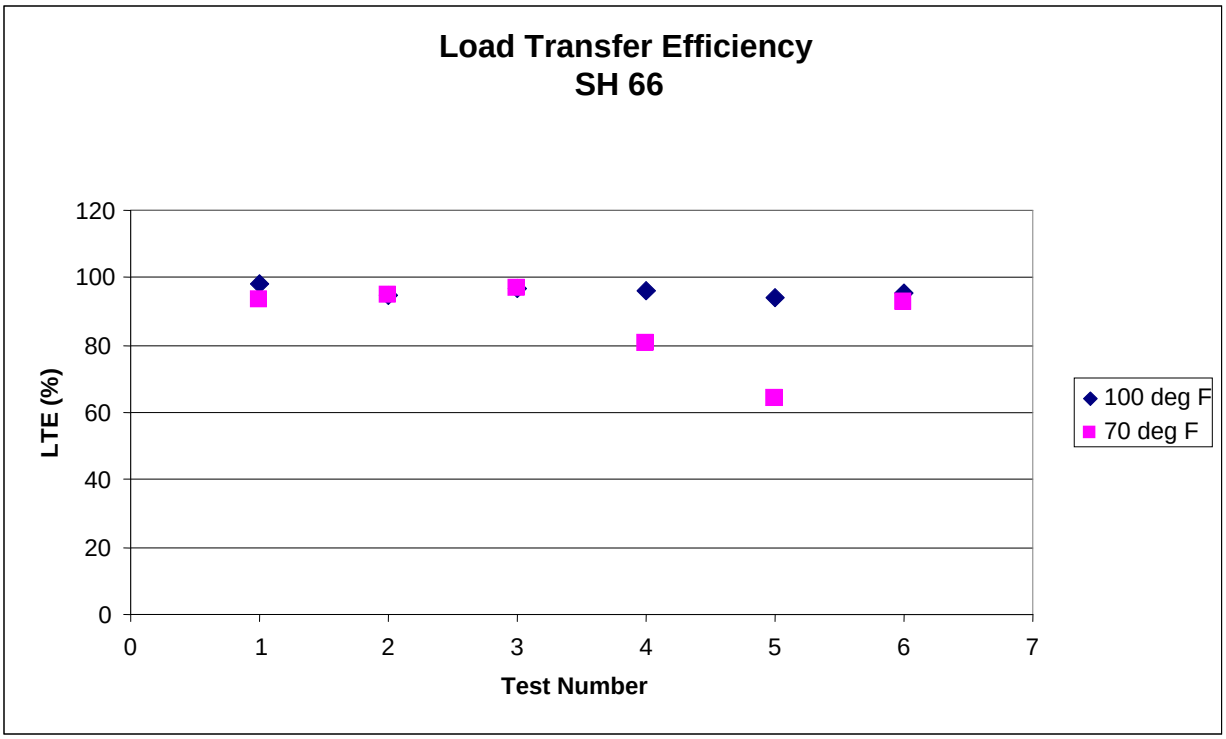

Figure 3.29: Longitudinal Joint LTE

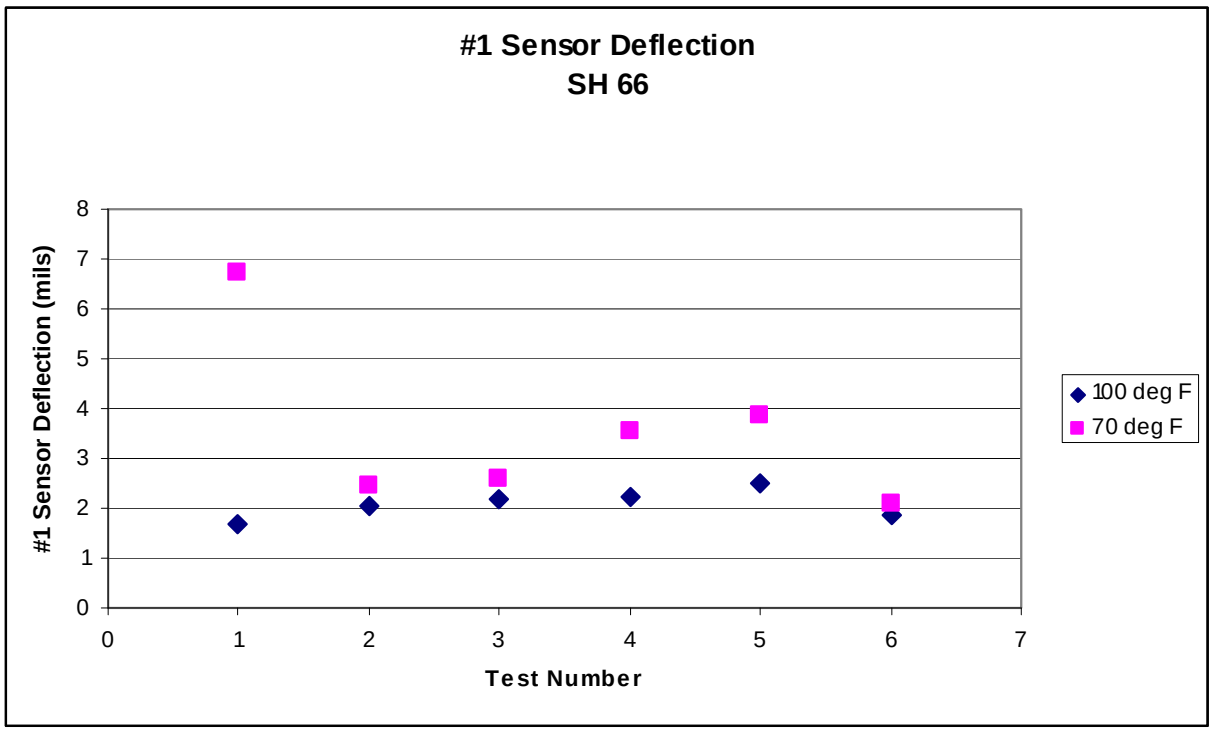

Figure 3.30: Longitudinal Joint #1 Sensor Deflections

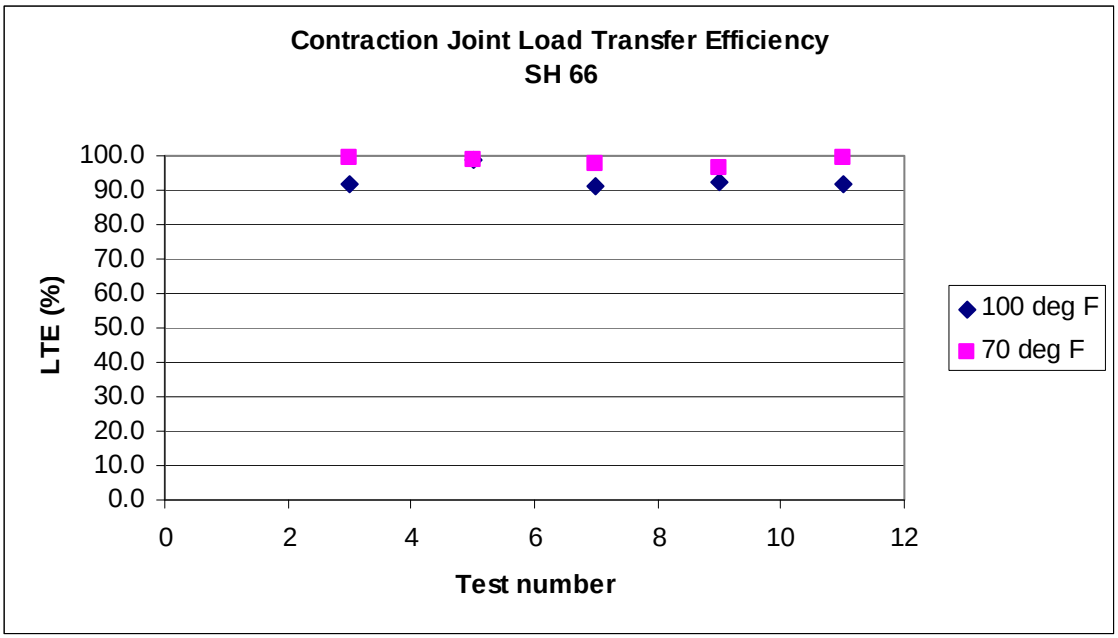

Figure 3.31: LTE for Longitudinal Contraction Joint

Longitudinal cracks generally showed a high degree of load transfer and moderate levels of #1 sensor deflection in the entire range of tested crack widths. Temperature seems to have affected the data mildly in some locations (primarily tests 4 and 5 on Figures 3.29 and 3.30). Temperature appears to not have affected LTE on the longitudinal contraction joint. Because LTE is higher on average for tests at lower temperatures (contrary to expectation), it is likely that the differences were caused by variations in operator procedure and sensor locations on separate field trips. (Different operators ran different FWD machines for the two trips.)

The Federal Highway Administration (FHWA) has reported that LTE is strongly dependent on the time of day that testing occurs as well as the time of year (FHWA, 2003). Temperature variations are responsible for this effect, particularly in cases where aggregate interlock is the primary contributor to LTE. Pavement curling also greatly affects LTE, with early morning tests showing much higher LTE than afternoon tests.

Should the District consider repairing this section of SH 66, additional testing during cooler months would provide a more accurate picture of crack performance and potential demand on any repair method.

3.4.3 Load Transfer Trends

LTE and Crack Width

Data were analyzed to determine trends between load transfer efficiency and crack width and between load transfer efficiency and air temperature. Figure 3.32 shows LTE as a function of crack width for three different data sets. The series labeled “100 deg F” and “70 deg F (1)” represent tests performed on the same section of pavement at two different temperatures (100 and 70 deg. F.), while the series labeled “70 deg F (2)” represent tests performed on a different section (though still in the same general area) at 70 deg. F.

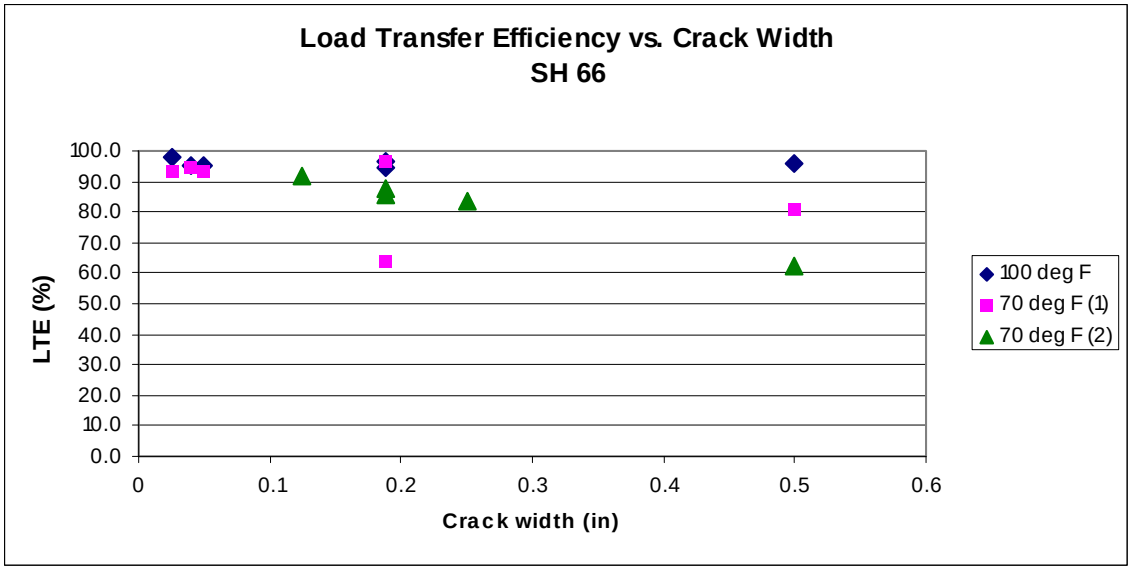

Figure 3.32: LTE vs. Crack Width for Longitudinal Cracking

Load transfer efficiency appears not to have been heavily dependent on crack width for the tests performed at 100 deg. F. Because the cracks that were tested were fairly tight, aggregate interlock was likely contributing to load transfer. Good base conditions also were most likely contributing to load transfer as well, based on the research team's findings on other field investigations. Load transfer did appear to depend on crack width for the tests performed at 70 deg. F. Both sections of pavement that were tested at this temperature showed a trend of decreasing LTE with increasing crack width. The relationship between the two variables was mild, though, and the cracks still exhibited fairly high LTE despite moderate crack widths. Again, aggregate interlock, along with good base and subgrade, are most likely responsible for the high degree of load transfer. Data showed a correlation between LTE and temperature, which is confirmed by findings of the Federal Highway Administration's LTPP program (FHWA 2003). Generally speaking, as the average air temperature increases, the average pavement temperature also increases, and pavement expands according to its coefficient of thermal expansion. At higher temperatures, cracks exhibit a higher degree of load transfer because aggregate interlock plays a greater role than at lower temperatures. Values for cracks and temperatures that mark the threshold between a high degree of aggregate interlock (and thus high LTE) and a low degree have not been established in literature and cannot be determined from the data gathered in this study.

In general, the data showed that for very tight cracks (less than approximately 0.125 in.) temperature did not have an effect on LTE, while it did have an effect on wider cracks. This would seem to indicate that repairing cracks before they separate more than 0.125 in. would increase the likelihood of successful repair because aggregate interlock significantly contributes to the load transfer mechanism.

#1 Sensor Deflection and Crack Width

Figure 3.33 shows the relationship between #1 sensor deflection and crack width. Data from tests at two different temperatures for the same section of pavement are shown.

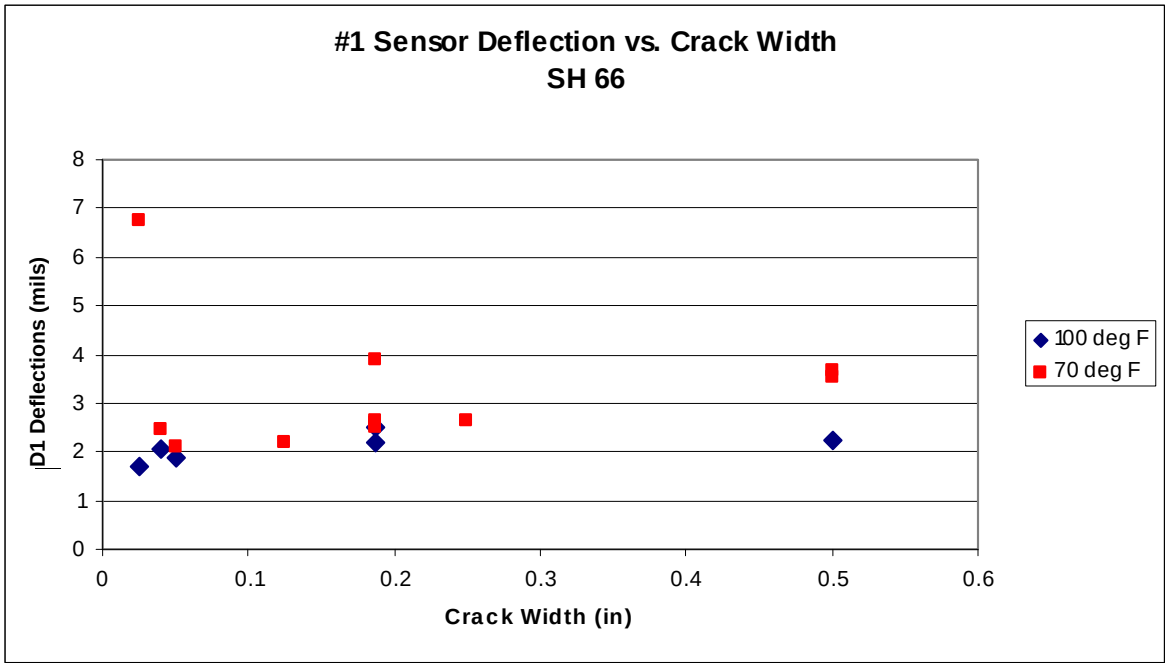

Figure 3.33: #1 Sensor Deflection vs. Crack Width

Data did not indicate a strong correlation between deflection and crack width. Deflection did not vary significantly for different crack widths (only a slight increase in the deflection was seen as crack width increases). The low average deflection indicated that the pavement system is in generally good condition. Base and subgrade were likely robust.

LTE and #1 Sensor Deflection

Load transfer efficiency is compared to #1 sensor deflection in Figure 3.34. Figure 3.35 shows LTE and #1 sensor deflection in the order the data were collected in the field. Data shown are a combination of tests performed on several sections of pavement at the two temperatures mentioned previously.

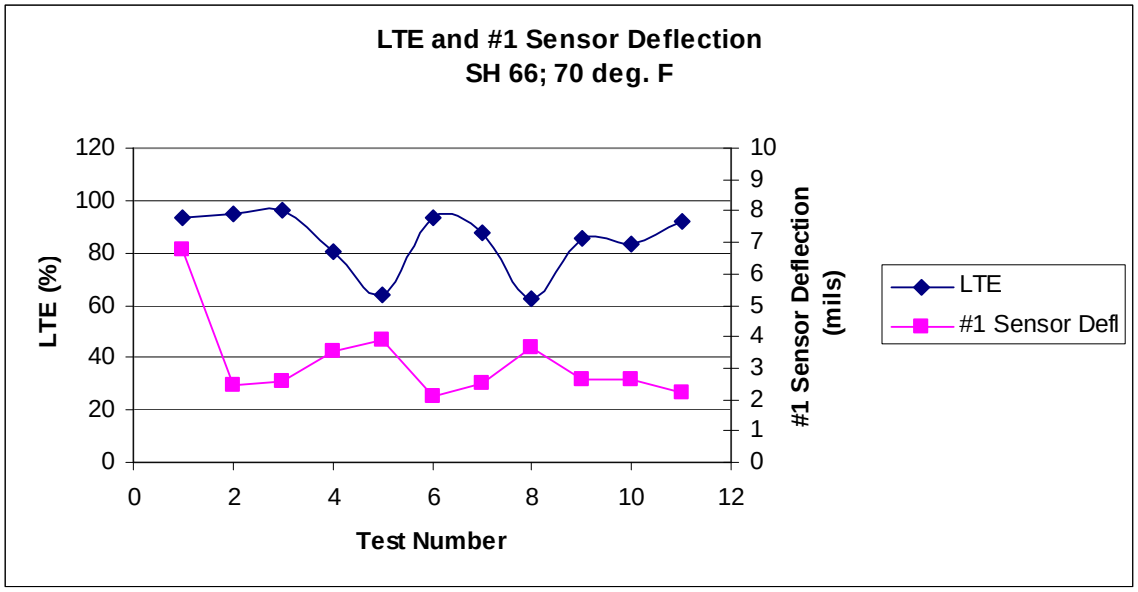

Figure 3.34: LTE and #1 Sensor Deflection

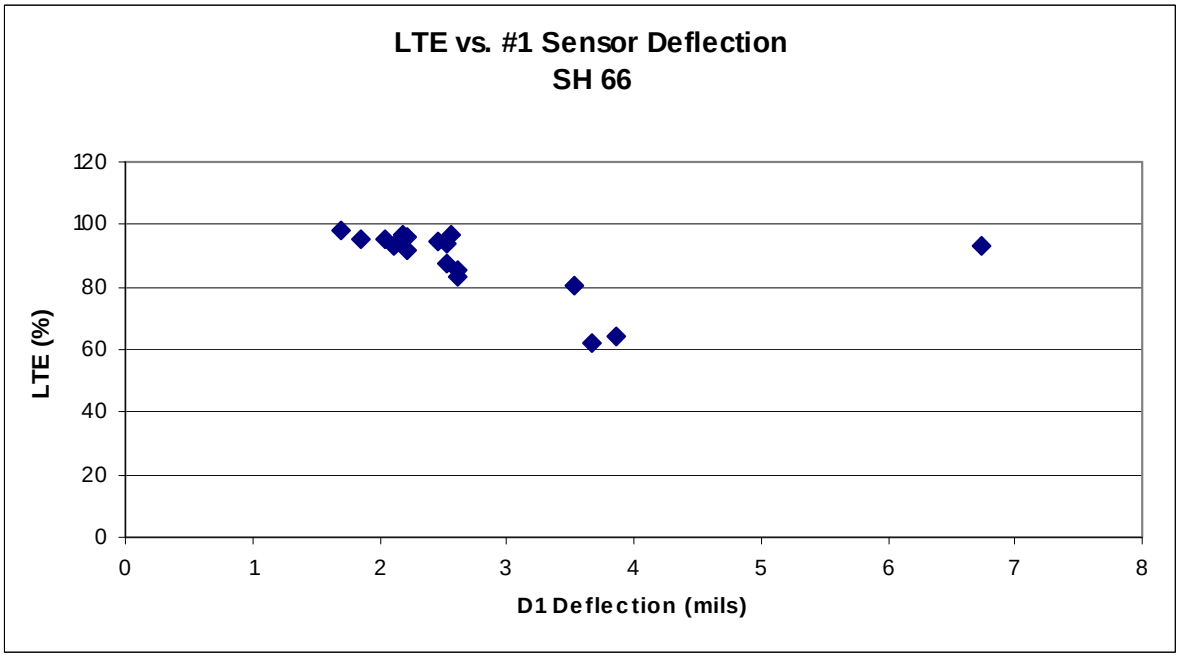

Figure 3.35: LTE vs. #1 Sensor Deflection

Figure 3.34 shows that there was a clear correlation between LTE and #1 sensor deflection. With the exception of the first data point, LTE was inversely proportional to deflection. Data show that (relatively) large deflections correspond to (relatively) low LTE and vice versa.

Figure 3.35 confirms that LTE decreased as deflection increased. As Figure 3.33 demonstrates that deflection was not strongly dependent on crack width, this shows that general

pavement integrity, as indicated by #1 sensor deflection, had a strong impact on LTE of longitudinal cracks.

Cause of Longitudinal Cracking

Cores through the longitudinal contraction joint showed that the likely cause of longitudinal cracking was the shallow (and possibly late) saw cutting of the joint. Figures 3.36 and 3.37 below show cores taken through the joint adjacent to cracked slabs. Figures 3.38 and 3.39 show cores taken through the joint adjacent to an uncracked slab. On average, the crack widths beneath the joint adjacent to the cracked slabs were smaller and did not go through the base, whereas the cracks adjacent to uncracked slabs were wider, showed more evidence of erosion, and had invaded the asphalt stabilized base. In addition, saw cuts were significantly shallower than specified (cuts as shallow as 1.5 in. were observed; T/4, or 2.25 in, is required by the CPCD specification).

In the event that saw cutting operations are begun late or the saw cuts are shallower than specified, excess stresses may accumulate in the pavement due to temperature curling, warping, and drying shrinkage. Before contraction joint cracks are cut, these stresses can accumulate not only at the contraction joint, but elsewhere in the slab. Shallow saw cutting serves to delay the cracking of the contraction joint, which in turn causes higher stress levels than if the contraction joint cracked early per the design. The contraction joint did eventually crack, as is evidenced by the cores. After the contraction joint cracked, longitudinal cracking occurred, probably due to the excess stresses caused by the late cracking of the contraction joint. Carbonation tests were performed on the cores taken over the longitudinal cracks and the contraction joints in order to determine the relative age of the cracks. Test results were inconclusive, but the contraction joints likely cracked before the longitudinal cracking occurred.

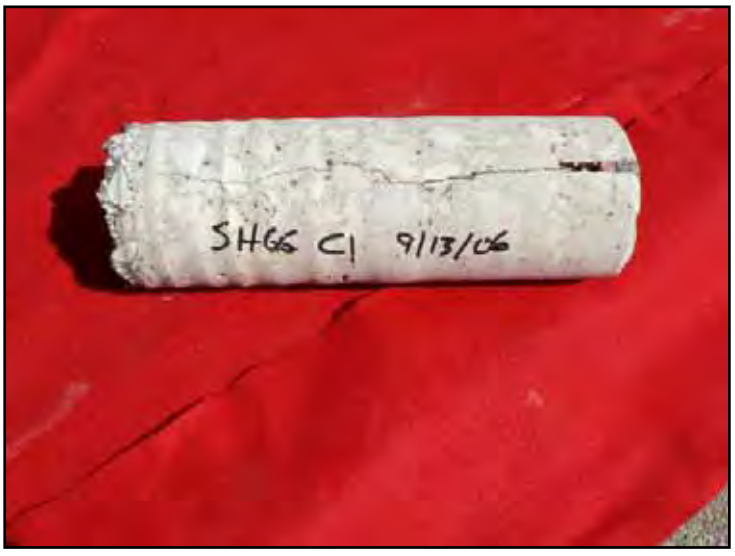

Figure 3.36: Core Through Contraction Joint Adjacent to Cracked Slabs (1)

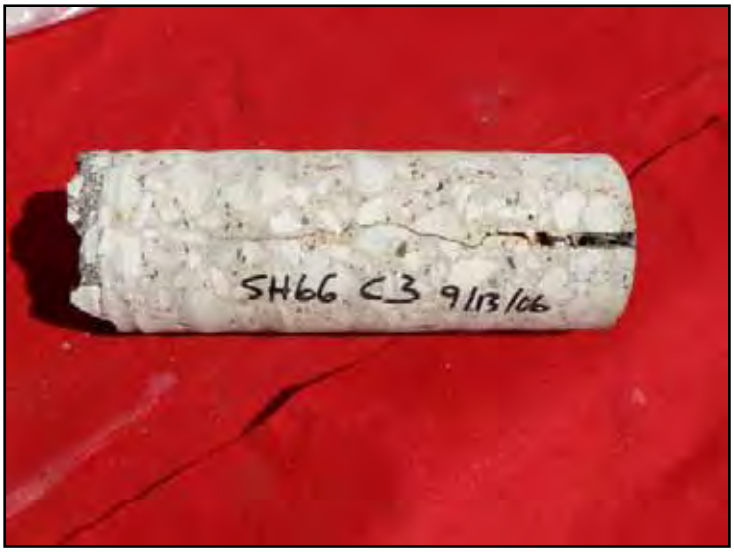

Figure 3.37: Core Through Contraction Joint Adjacent to Cracked Slabs (2)

Figure 3.38: Core Through Contraction Joint Adjacent to Uncracked Slabs (1)

Figure 3.39: Core Through Contraction Joint Adjacent to Uncracked Slabs (2)

3.4.4 Conclusions

1. Longitudinal cracking was most likely caused by shallow and possibly late saw cutting of the longitudinal warping joint.
2. Load transfer efficiency was strongly dependent on overall pavement condition as indicated by #1 sensor deflection
3. Aggregate interlock significantly contributed to LTE for the entire range of crack widths tested (up to 0.5 in.).
4. The #1 sensor deflection was independent of crack width for the tests performed in this field investigation.
5. High LTE values were likely caused by high temperatures and are not an accurate reflection of the average joint performance over time.

3.5 SH 289 Dallas

3.5.1 Background and Scope of Activities

Nine inch thick CPCD with 2-in. thick asphalt stabilized base and lime-treated subgrade was constructed on State Highway 289 in Collin County from SH 121 to FM 720 in 1998. Several sections of pavement in the northbound direction directly north of the intersection with SH 121 have experienced longitudinal cracking ranging from 0.03 to 0.625 in. in width and faulting up to 0.5 in. In November of 2000, approximately 165 ft. of longitudinal cracking was repaired with cross stitching.

Researchers conducted field inspections of approximately one-quarter mile of SH 289 directly north of SH 121 on July 25 and September 13, 2006. Objectives of the field investigation included: (1) surveying and documenting the extent of longitudinal cracking, (2) determining the cause(s) of such cracking, (3) evaluating the effectiveness of cross stitching as a repair method for longitudinal cracking in concrete pavements. Activities included:

1. Visual Inspection: The following observations were made and documented: occurrence and extent of longitudinal cracking, evidence of slab faulting, condition of cross stitch repairs (evidence of cracking or spalling around staple bars, condition of joint filler material).
2. Falling Weight Deflectometer Testing: FWD testing was performed on several sections of pavement with longitudinal cracking. Load transfer efficiency was calculated for cracks of various widths as well as for the cross stitched crack.
3. Coring: Several cores were taken at the following locations: narrow crack, wide crack, strong slab (no cracking), weak slab (cracking), directly over a cross stitch bar, and through the longitudinal contraction joint adjacent to both cracked and uncracked slabs.

Figure 3.40: Longitudinal Cracking (1)

Figure 3.41: Longitudinal Cracking (2)

Figure 3.42: Cross-Stitch Repair (1)

Figure 3.43: Cross Stitch Repair (2)

3.5.2 Pavement Condition Report

SH 289 between FM 720 and SH 121 was upgraded in 1998. Nine-inch thick JCP was constructed, which included multi-piece tie bars across longitudinal joints and dowels across transverse joints. Two-inch thick asphalt concrete (Type B) base and lime treated subgrade exist beneath the pavement.

Crack widths between 0.030 in. and 0.625 in. were measured (Figures 3.44 and 3.45). Isolated slab faulting of up to 0.5 in. was measured (Figure 3.46). Figures 3.51 and 3.52 show cores taken through the cracks. Cores showed that the cracks remained tight beneath the surface of the pavement, and thus had a high degree of aggregate interlock.

Figure 3.44: 0.625 in. Crack

Figure 3.45: 0.030 in. Crack

Figure 3.46: Faulted Crack

Figure 3.47: Core through Longitudinal Crack (1)

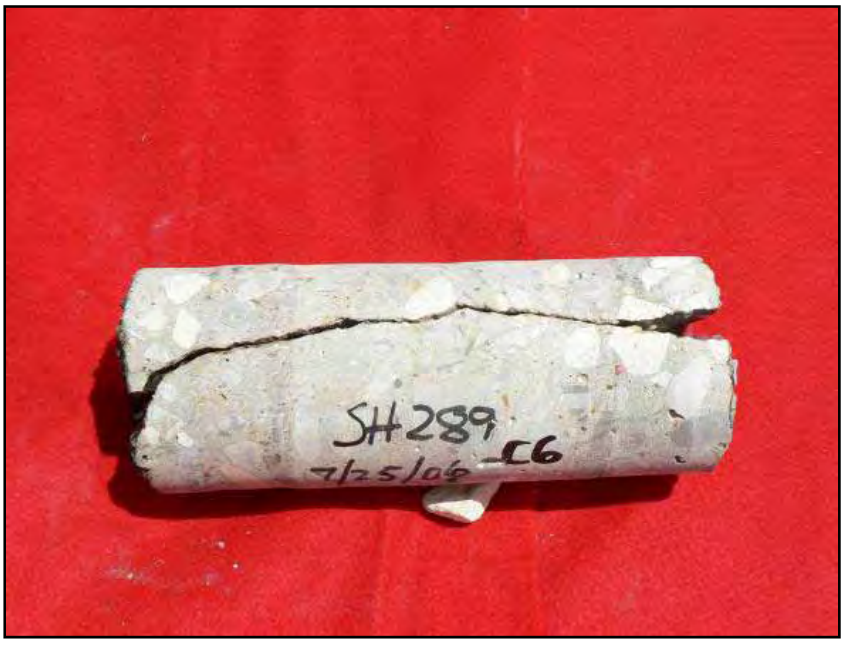

Figure 3.48: Core through Longitudinal Crack (2)

Load Transfer Performance of Longitudinal Crack

Load transfer efficiency was calculated based on FWD measurements for various crack widths on cross stitched areas as well as unrepaired areas. LTE varied from 84% to 100% with an average of 92% for unrepaired cracks and ranged from 88% to 99% with an average of 94% for the cross stitched crack. Number one sensor deflections ranged from 4.7 mils to 10.1 mils with an average of 6.2 mils. See Appendix E for statistical data. Figure 3.49 shows LTE and #1

sensor deflection for each test location in the order they were taken in the field. Data for unrepaired and cross-stitched cracks had similarities in LTE and deflection. Consequently, data were combined to make observations about load transfer trends.

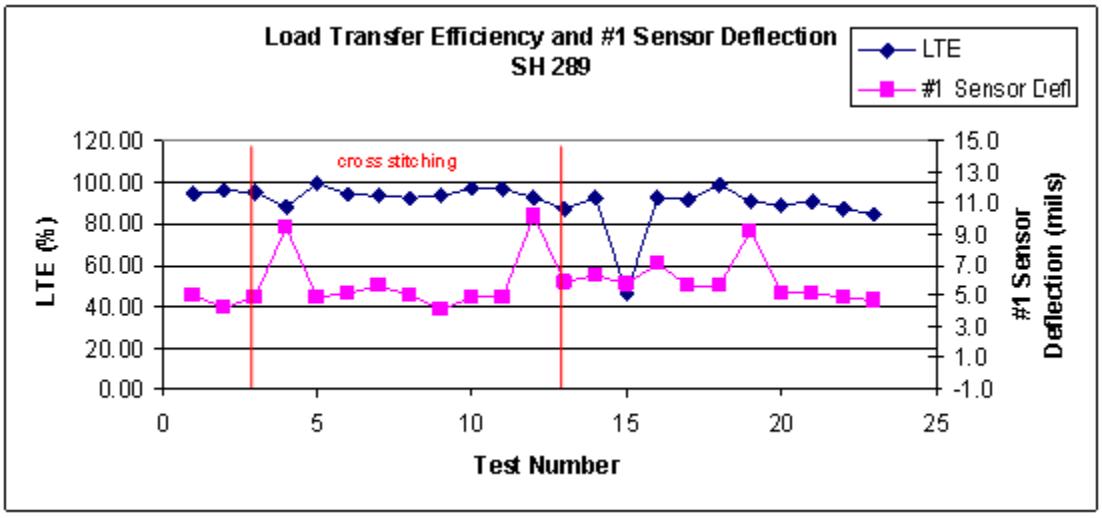

Figure 3.49: LTE and #1 Sensor Deflection

For the unrepaired cracks, the high level of Load Transfer Efficiency (LTE) may indicate two things: first, the base layer was rigid enough to significantly contribute to the load transfer, and second, cracks were tight enough that aggregate interlock was working to provide load transfer. Average air temperature during the time of testing was approximately 95 deg. Fahrenheit. As with SH 66, high temperatures may contribute to the surprisingly high LTE values.

3.5.3 Load Transfer Trends

LTE and Crack Width

LTE did not appear to be dependent upon crack width in this case (Figure 3.50). High levels of load transfer were seen for a wide range of crack widths, which indicates that the cracks were tight enough to engage aggregate interlock. Data seemed to indicate that the aggregate interlock mechanism was fully at work in the range of crack widths tested. What is unclear is whether, as cracks widen until aggregate interlock is no longer engaged, LTE would drop sharply or gradually. Another indication that aggregate interlock was at work was the strong similarity between the data for the unrepaired crack and the cross stitched crack. If aggregate interlock was not at work, then the cross-stitched area would (based on the good visible condition of the repairs) have exhibited higher LTE.

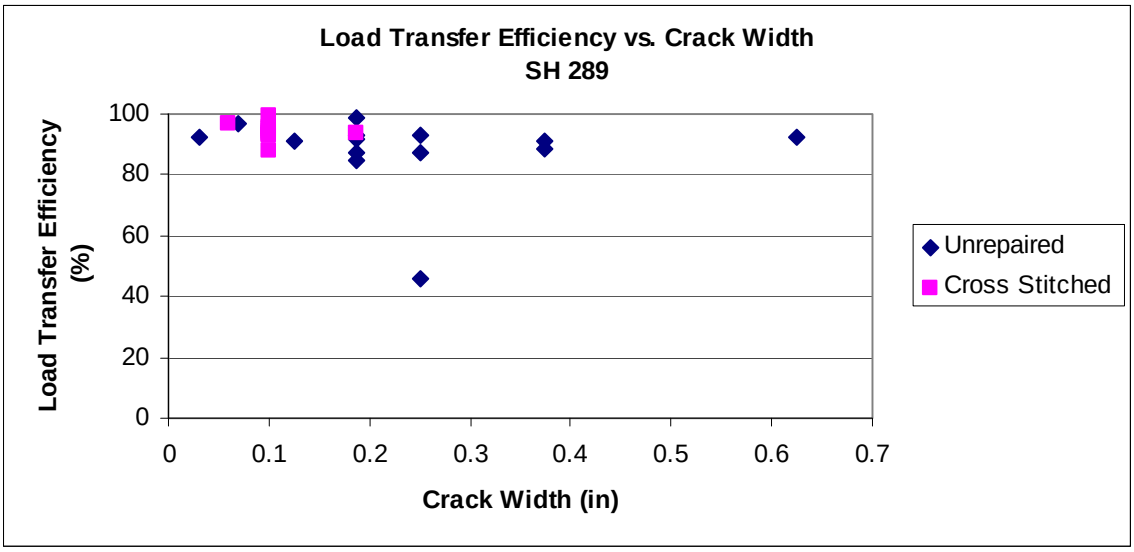

Figure 3.50: LTE vs. Crack Width

#1 Sensor Deflection and Crack Width

Data shown in Figure 3.51 indicate that #1 sensor deflection was not strongly dependent upon crack width for the section of pavement tested. This indicates two things: (1) aggregate interlock was contributing to load transfer for the entire range of crack widths; and (2) base/subgrade conditions were fairly consistent over the test area. If base conditions varied greatly, a corresponding variation in deflections would have been observed. Likewise, if aggregate interlock had disengaged at larger crack widths, an increase in deflection would have been seen.

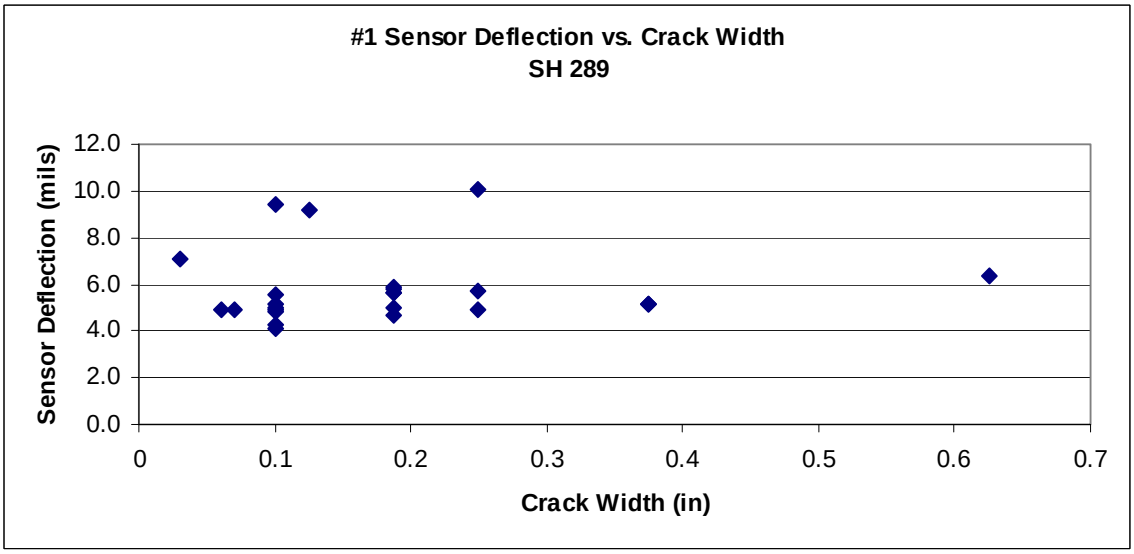

Figure 3.51: #1 Sensor Deflection vs. Crack Width

LTE and #1 Sensor Deflection

Figure 3.52 shows that LTE was not dependent on #1 sensor deflection. With the exception of one point of very low LTE, all the data points showed very high LTE over the entire range of deflection. This would seem to be inconsistent with data from several other field investigations (which showed that LTE decreases with increasing deflection) so the exact reason for the relationship seen on SH 289 is unclear. This may again indicate that aggregate interlock was the primary mechanism providing load transfer. If it was not, then the primary load transfer mechanism would have been the base and subgrade (which #1 sensor deflection indicates) and LTE would have varied with deflection.

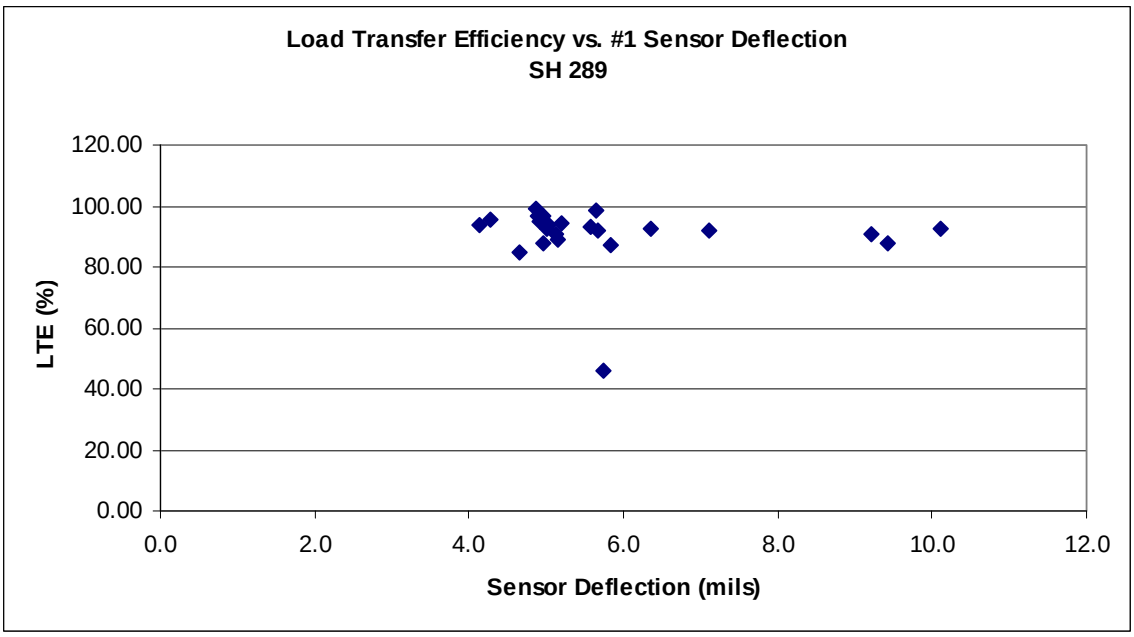

Figure 3.52: LTE vs. #1 Sensor Deflection

Cause of Longitudinal Cracking

Figures 3.54 through 3.56 show cores taken through the contraction joint adjacent to cracked slabs, while Figure 3.57 show cores taken through the same joint but adjacent to uncracked slabs. Due to the highly variable character of the cracks, one single measurement of crack width was not made for each core, but qualitative visual inspection showed that the crack beneath the contraction joint was smaller in areas where the adjacent slabs are uncracked and larger in areas where longitudinal cracking is present. As in the case with the longitudinal cracking on SH 66 (reviewed in previous section), these observations indicate that late and possibly shallow saw cutting delayed formation of cracks beneath the longitudinal contraction joint, thereby increasing the stresses elsewhere in the slab and causing cracking at those locations over time.

Figure 3.53: Longitudinal Warping Joint

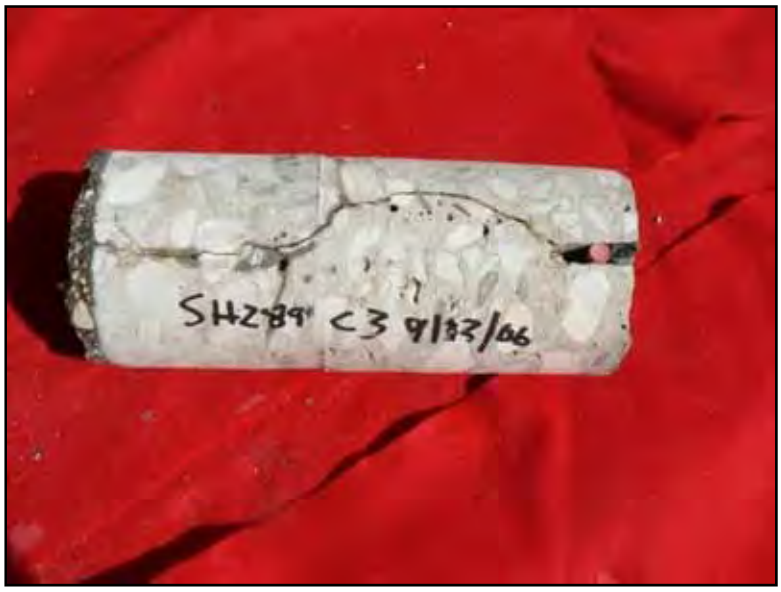

Figure 3.54: Core Through Contraction Joint (1)

Figure 3.55: Core Through Contraction Joint (2)

Figure 3.56: Core Through Contraction Joint (3)

Figure 3.57: Core Through Contraction Joint (4)

Cross Stitching Performance

Cross stitching was installed on approximately 165 consecutive feet of cracked pavement, with stitch bars spaced at 2 ft. The bar holes were filled with rigid epoxy. The stitched crack had been sawed to approximately 0.5 in. and had been filled with a rigid epoxy, possibly the same type used to fill the stitch holes.

Concrete around the stitch bars appeared to be in good condition, with no evidence of cracking or spalling. No evidence of further crack separation or slab faulting was found.

As mentioned above, the cross-stitched area provided a high degree of load transfer. However, it was not significantly different from unrepaired cracks. This indicated that the crack probably exhibited similar load transfer performance to other cracks in the area before it was repaired. The stitching prevented further crack separation, thus maintaining high LTE.

The core taken through one of the stitch bars showed the bar to be in good condition, with no evidence of corrosion (Figure 3.58). Epoxy injected into the stitch hole from the pavement surface appeared to have flowed down the hole and into the crack without filling the hole opposite the crack (Figure 3.59). Figure 3.64 also shows the dry hole with the stitch bar.

After the crack was sawed to a width of approximately 0.5 in., it was filled with what appeared to be a rigid epoxy. Over time, the joint filler material had separated from the sides of the crack in several places, and had begun to crack and spall in others. This indicates that the crack experienced some opening and closing over time, though not enough for non-compressibles to be introduced and the slabs to be jacked apart. In such a case, a rigid epoxy is not a suitable joint filler material. A lower-modulus, more flexible material would be more appropriate; it would effectively seal the crack, thus preventing moisture and non-compressible material from entering the crack. The lower modulus characteristics would enable the crack to move without cracking and spalling the joint filler material.

Figure 3.58: Core Through Cross Stitching (1)

Figure 3.59: Core Through Cross Stitching (2)

3.5.4 Conclusions

1. Cross-stitch repairs were in good condition and showed no visible signs of distress. Effectiveness of stitching to keep crack widths tight and prevent slab faulting was uncertain because the unstitched cracks in the area showed very similar load transfer performance and similar crack widths.
2. Shallow (and possibly late) saw cutting probably delayed the cracking of the longitudinal warping joint, which likely caused excess curling, warping, and drying shrinkage stresses to occur in the middle of the pavement slabs.

Longitudinal cracking may have been caused by the accumulation of these excess stresses.

3. Aggregate interlock appeared to be the primary mechanism by which load is transferred across the cracks.
4. Cracks appeared to be tight enough to engage aggregate interlock in the load transfer mechanism, making LTE independent of crack width for the range of widths tested.
5. Number one sensor deflections were not dependent on crack width.
6. Load transfer efficiency was not dependent on #1 sensor deflection.

3.6 IH 27 Lubbock

3.6.1 Background and Scope of Activities

Researchers conducted a field inspection of approximately one-quarter mile of IH 27 on July 26, 2005. The pavement consists of 10-in. thick CRCP with a 6-in. asphalt base that was constructed on IH 27 north of Lubbock between 1978 and 1981. Approximately one-half mile of pavement on the northbound lanes near Exit 10 has experienced longitudinal joint separations of up to 1.25 in. In 2002 the center construction joint was repaired using a full depth repair technique (FDR).

Objectives of the field investigation included: (1) survey and document the extent of longitudinal joint separations, (2) determine the cause(s) of joint separation, (3) evaluate the effectiveness of FDR as a repair method for longitudinal joint separation in concrete pavements. Activities included:

1. Visual Inspection: The following observations were made and documented: occurrence and extent of longitudinal joint separation, evidence of slab faulting, condition of full depth repair (evidence of spalling, cracking, or joint separation).
2. Falling Weight Deflectometer Testing: FWD testing was performed on several sections of pavement with longitudinal cracking. Load transfer efficiency is calculated for longitudinal cracks and two longitudinal joints, including one repaired section.
3. Coring: Several cores were taken at the following locations: mid-slab (for strength), over crack, over separated longitudinal joint with tie bar, and through full depth repair.
4. Ground Penetration Radar: GPR was used to locate original tie bars and mark location of core to be taken in order to determine condition of the tie bar.

3.6.2 Pavement Condition Report

The following two construction joints were tested with the falling weight deflectometer (FWD) to determine load transfer efficiency (LTE): 1) the joint between outside lane and

shoulder ("shoulder joint"), and (2) the joint between outside and inside lanes ("center joint"). Figure 3.60 shows FWD sensor arrangement and Figure 3.61 gives joint notation.

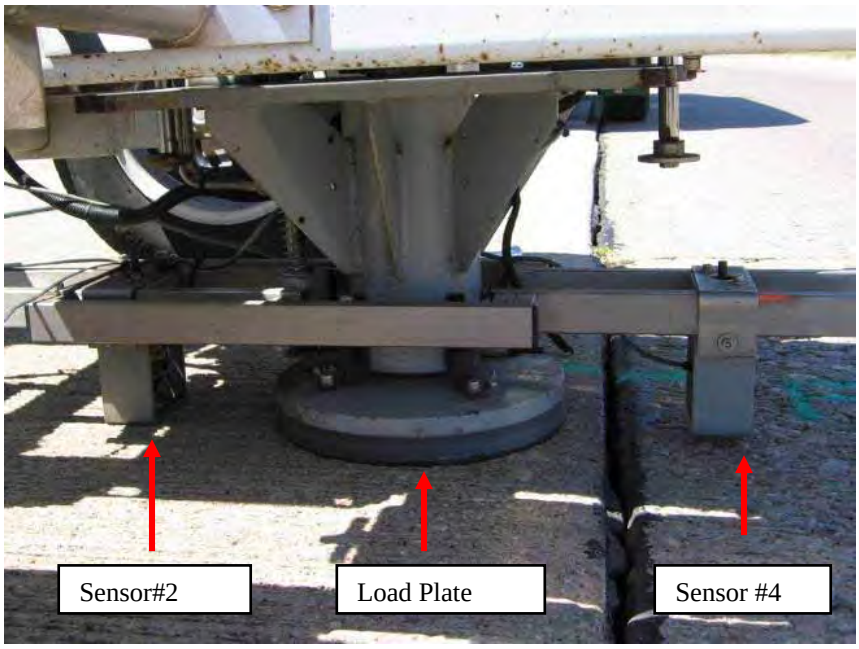

Figure 3.60: FWD Sensor Setup

Figure 3.61: Joint Naming Convention

Load Transfer Performance of Shoulder Joint

Shoulder joint separations between 0.5 in. and 1.25 in. were observed. Average joint width over the area tested was 1.0 in. Slab faulting of up to 0.25 in. was observed. Load transfer

efficiency varied from 41 to 76%, with an average of 58%. Number one sensor deflections averaged 6.7 mils (Figure 3.62).

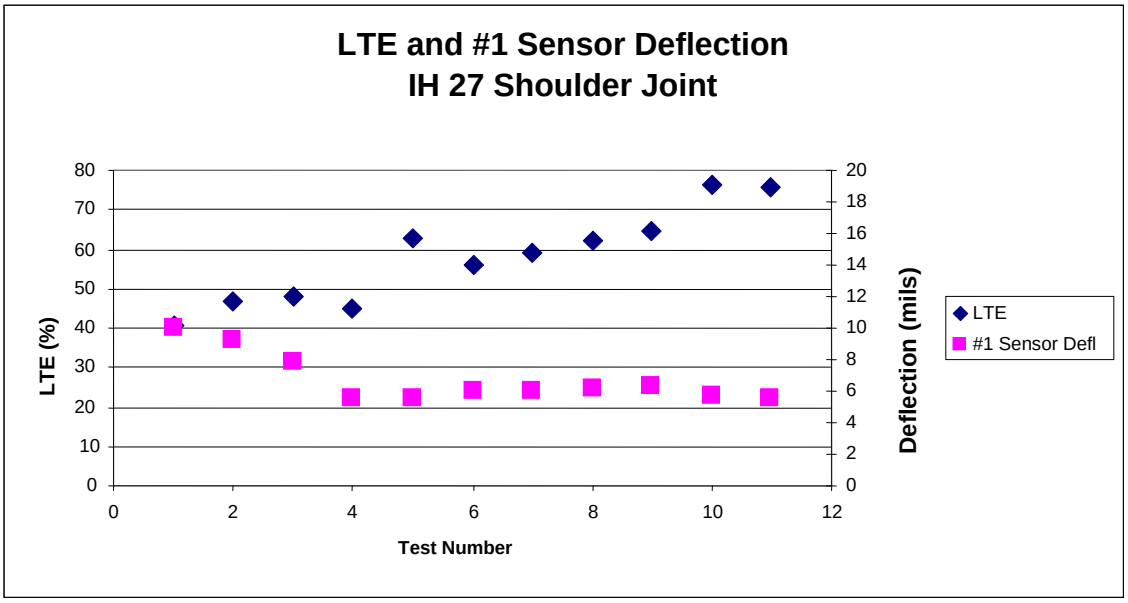

Figure 3.62: LTE and #1 Sensor Deflection (Shoulder Joint)

Data showed a progressive increase in LTE and decrease in #1 sensor deflection throughout the test. At the location of the first test, the joint was approximately 4 to 6 ft. from the edge of the pavement. At the location of the last test, the joint was about 12 ft. from the edge. Figure 3.63 (from Won 2006b) summarizes #1 sensor deflection data taken at different distances from the longitudinal free edge of another pavement. Deflections generally decreased as the test was moved farther from the pavement free edge. The shape of the curve was unique to the pavement tested, and was influenced by the overall stiffness of the pavement, base and subgrade conditions, etc. The general tendency applies, however.

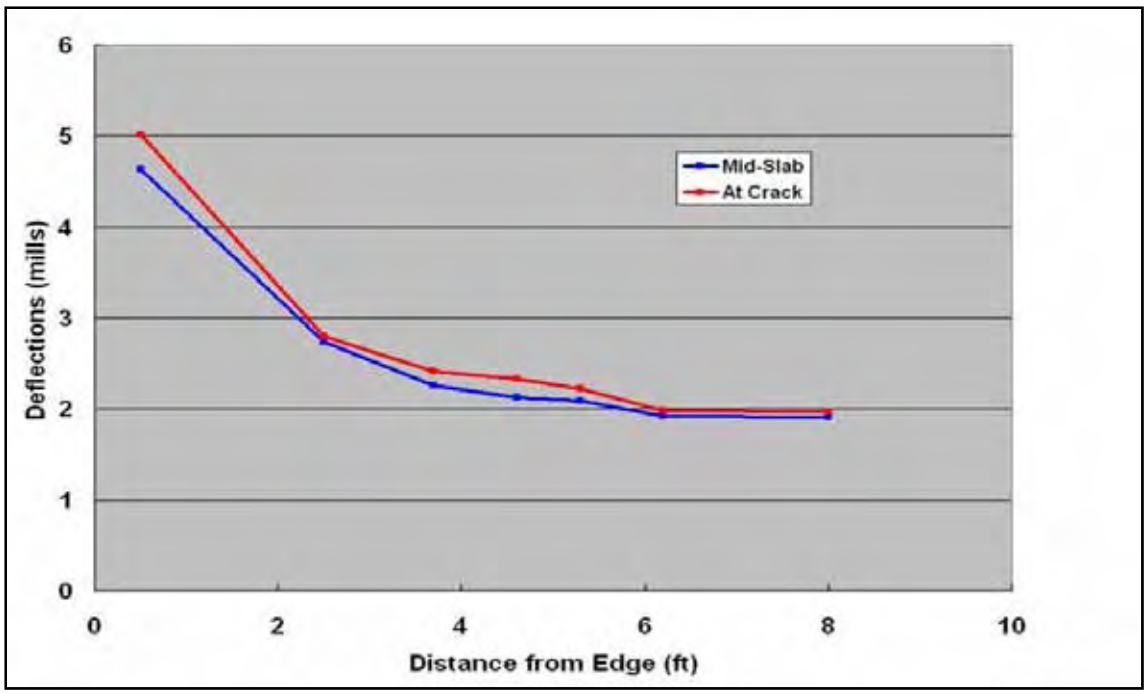

Figure 3.63: #1 Sensor Deflection vs. Edge Distance (Won, 2006b)

#1 Sensor Deflection and Joint Width

Figure 3.64 shows a general trend of a decrease in #1 sensor deflection as joint width decreased. This seems to be inconsistent with not only theoretical behavior but also with results from other field investigations. However, the three points with the highest deflection corresponded to the first three tests where the joint was the closest to the pavement free edge. Because of the data given in Figure 3.63 and in the preceding paragraph, the data in Figure 3.64 are not reliable because the deflections for the first three tests are artificially high.

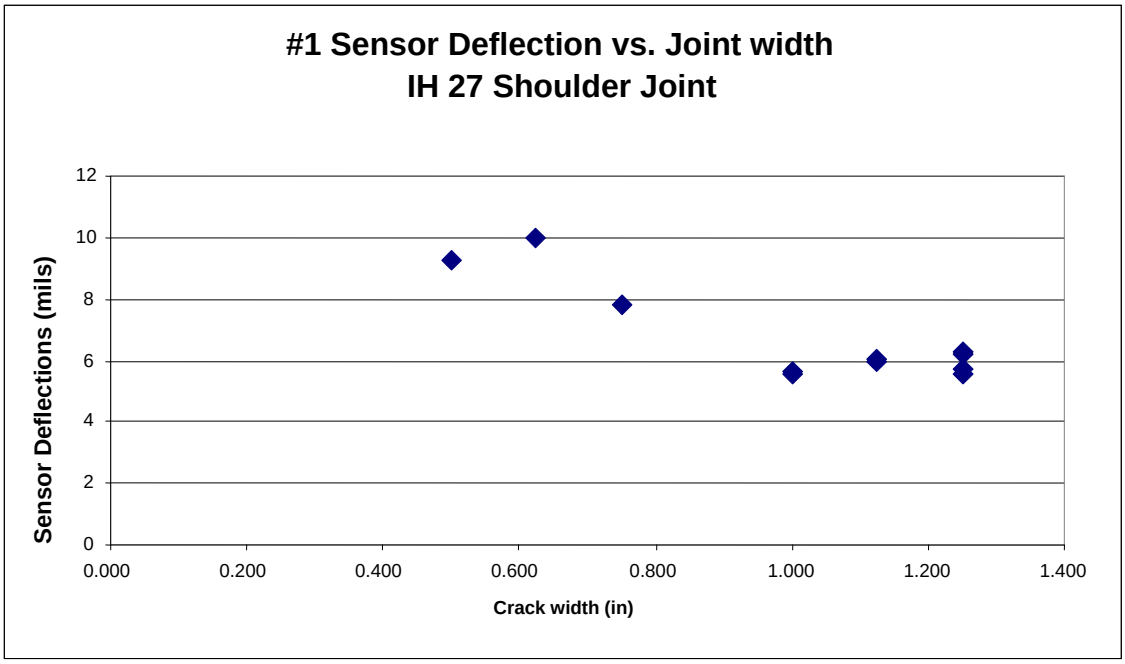

Figure 3.64: #1 Sensor Deflection vs. Joint Width (Shoulder Joint)

Load Transfer Performance of Center Joint

Center joint separations between 0.75 in. and 1.25 in. were observed, with an average joint width of 1.0 in. Slab faulting up to 0.5 in. was observed. Load Transfer Efficiency varied from 46 to 77%, with an average of 71%. Number one sensor deflections averaged 5.5 mils.

FWD testing was also performed on a portion of the center joint that had been repaired using full depth repair (FDR) method. Average LTE was 92% and #1 sensor deflections averaged 3.7 mils.

Longitudinal cracking was also observed on several sections of pavement, with cracks ranging from 15 to 40 ft. in length and 0.010 and 0.030 in. in width. Average LTE for longitudinal cracks was 97%.

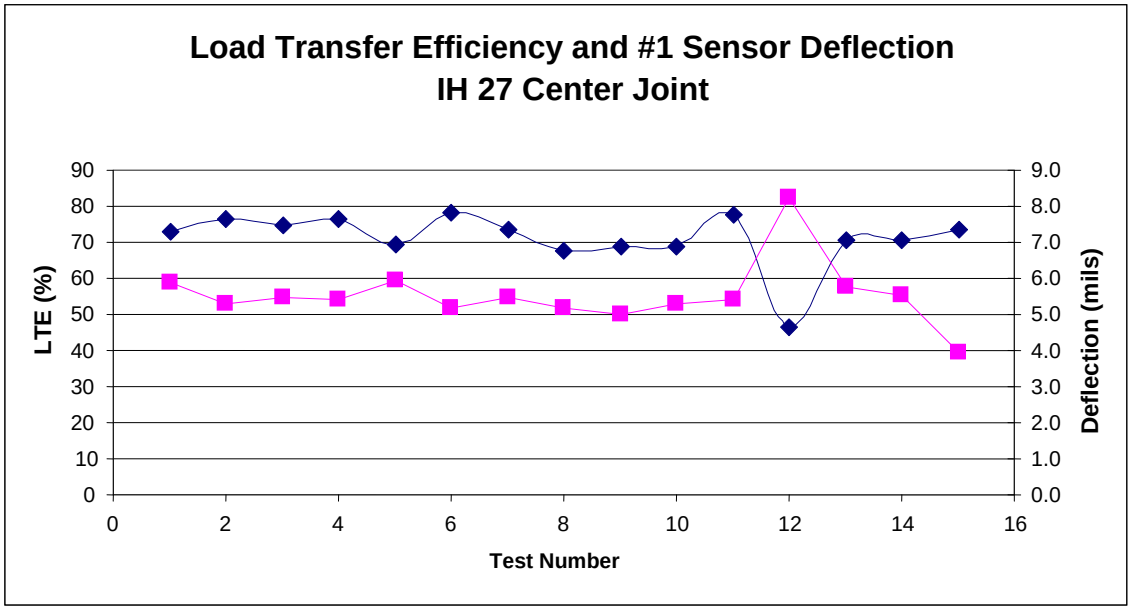

Figure 3.65: LTE and #1 Sensor Deflection (Center Joint)

Figure 3.65 shows the LTE and #1 sensor deflection for all the FWD tests along the (unrepaired) center joint. Data show a consistent pattern in which higher LTE corresponds to lower deflection and lower LTE to higher deflection.

FWD tests on the center joint gave more consistent LTE results than for the shoulder joint. Average LTE was 71%, which was higher than expected for such a large joint separation. Despite the high temperature during the tests (over 100 deg. F), aggregate interlock appeared not to have contributed to LTE because of the large separation distance. For example, during one of the visual inspections, a chisel was dropped in the joint, and it fell unobstructed through the joint to the base. The higher-than-expected LTE for the center joint may be due to the role of the base and in the load transfer mechanism. LTE for the repaired joint was 92% on average, 21% higher than the adjacent unrepaired sections. Longitudinal cracks showed a high degree of load transfer, most likely due to aggregate interlock, the presence of mat steel, and good base and subgrade conditions.

3.6.3 Load Transfer Trends

LTE and Joint Width

Figure 3.66 shows that there was little correlation between LTE and joint width for the section of pavement tested. This was not surprising, as the joint had separated to the point that little or no aggregate interlock could be engaged to provide load transfer. Consequently, other mechanisms not reliant upon joint width provided the load transfer. In other words, once the joint separated to the point that no aggregate interlock was present, further separations did not reduce LTE. The high value of LTE was suspicious, though, because of the lack of aggregate interlock across the joint. One contributing factor might be that the FWD sensor array (as it was used for this series of tests) can give artificially high LTE values (see Appendix A for more detail). In addition, the base and subgrade could have been contributing more to the LTE than originally thought possible. Temperature is not thought to have affected LTE on this section of IH 27,

given the large joint separations. Cracks and tighter joints may be sensitive to temperature because aggregate interlock can play a primary role in the load transfer mechanism, but the joint widths observed on IH 27 were so large they likely would not be affected by even very large temperature changes.

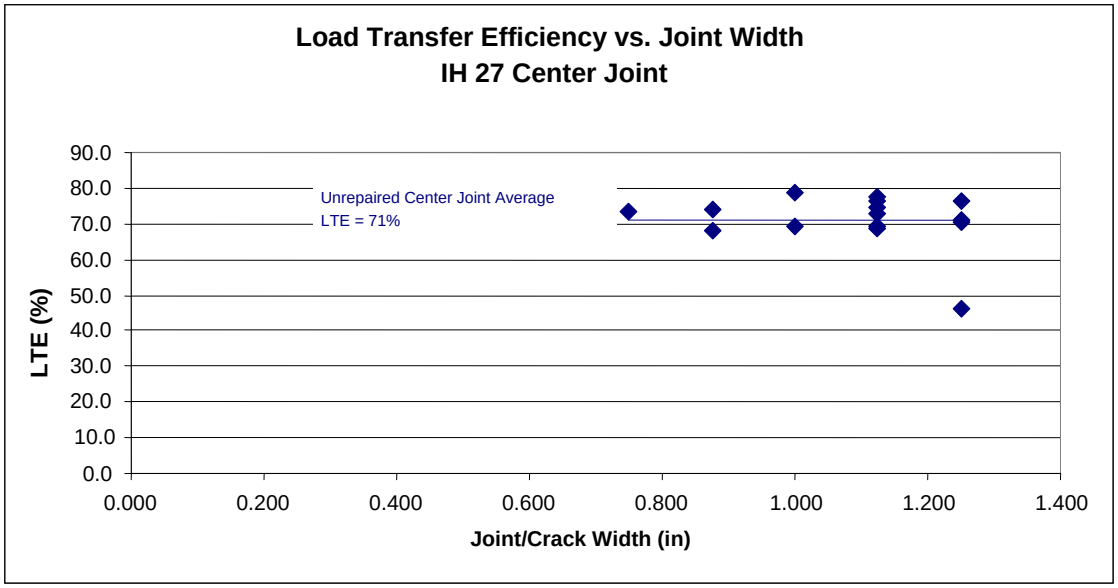

Figure 3.66: LTE vs. Joint Width (Center Joint)

LTE and #1 Sensor Deflection

Figure 3.67 shows that a good correlation between LTE and #1 sensor deflection was hard to determine. With the exception of one point, all the data were clustered within a tight range of deflection values. In other field investigations, where more representative data were available, the general trend was for LTE to decrease with increasing sensor deflection. Because sensor deflection is a measure of general pavement integrity (which depends on, among other things, condition of base and subgrade), LTE is also dependent on the same.

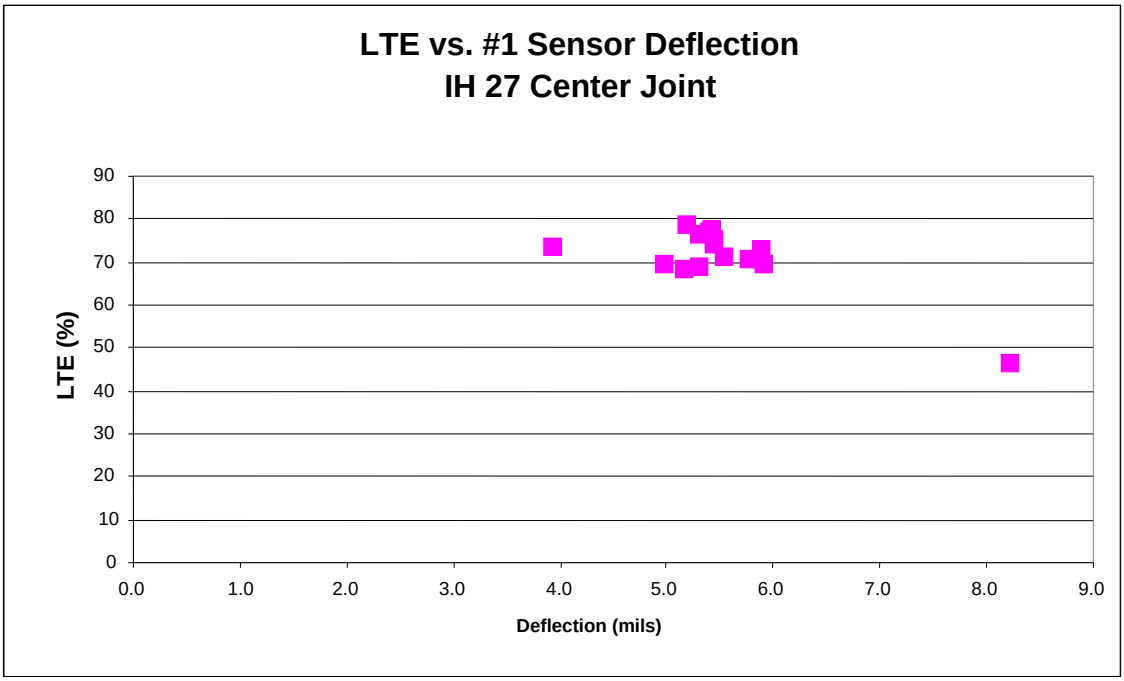

Figure 3.67: LTE vs. #1 Sensor Deflection (Center Joint)

#1 Sensor Deflection and Joint Width

Sensor deflection increased with increasing joint width, as evidenced by data shown in Figure 3.68.

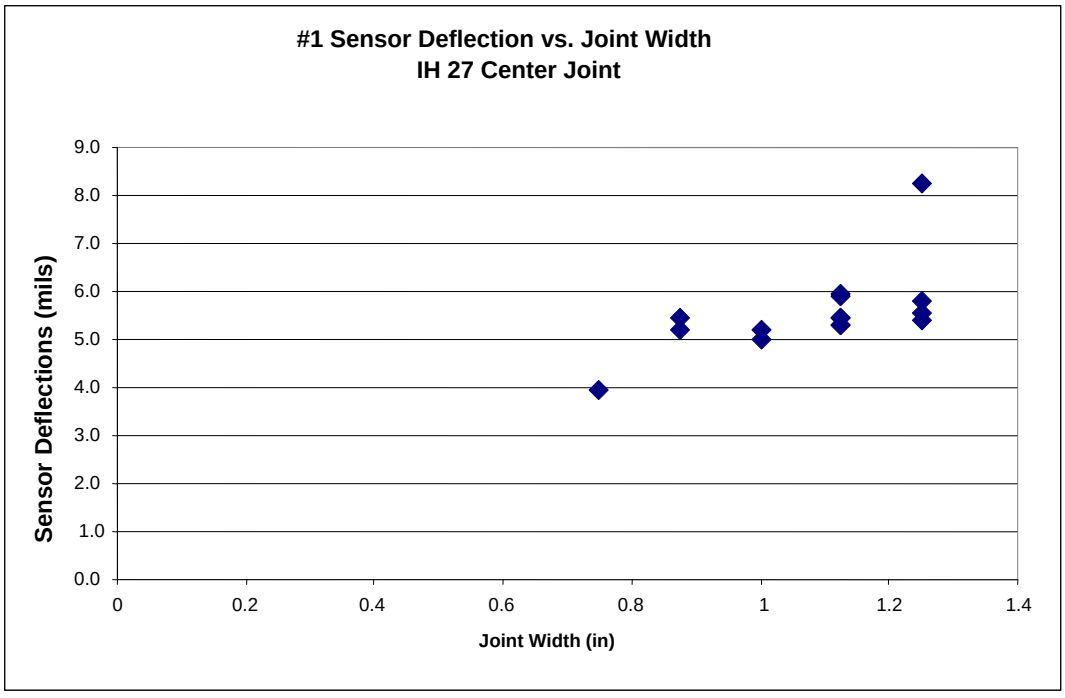

Figure 3.68: #1 Sensor Deflection vs. Joint Width (Center Joint)

Effectiveness of FDR

Full-depth repairs appeared to have beneficially affected the performance of the longitudinal joint. The FDR reduced average #1 sensor deflections by 33% (1.8 mils). Table 3.4 shows a summary of the averaged data and Figures 3.69 and 3.70 show the LTE and #1 sensor deflections for the individual tests, respectively.

Table 3.4: Effectiveness of FDR

	LTE	#1 Sensor Deflection (mils)
Unrepaired	71%	5.5
FDR	92%	3.7

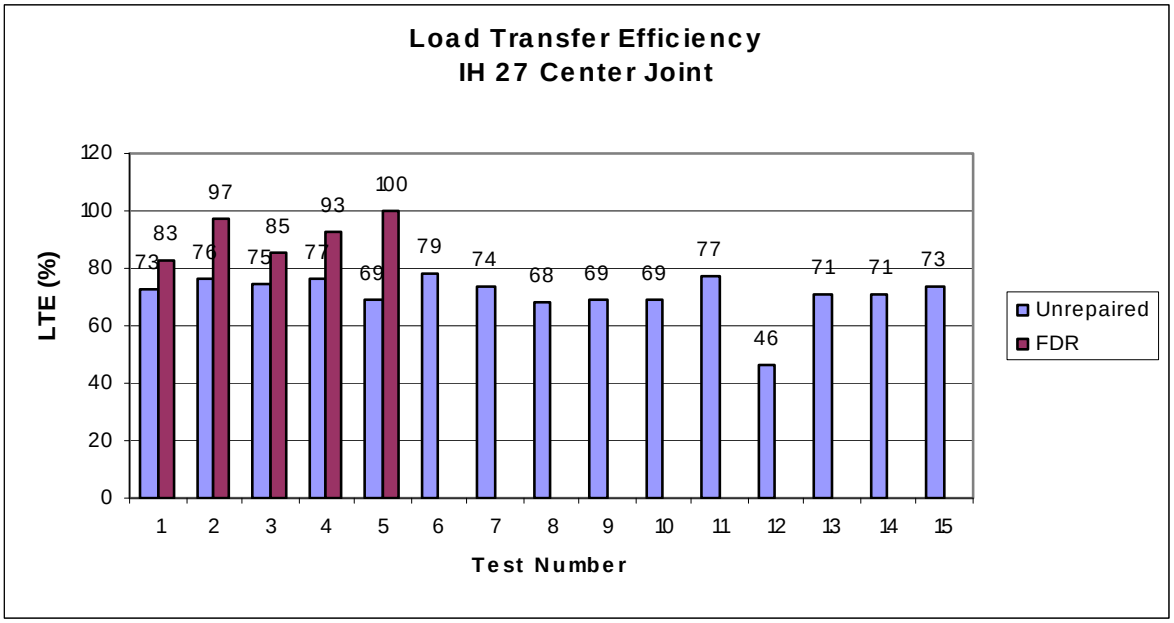

Figure 3.69: LTE for FDR and Unrepaired Sections

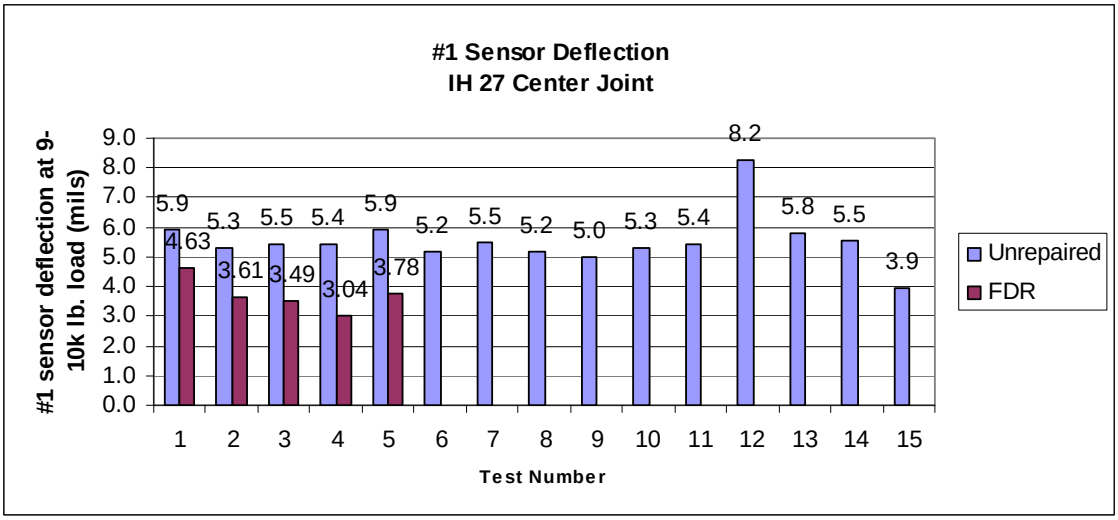

Figure 3.70: #1 Sensor Deflections for FDR and Unrepaired Sections

Condition of Tie Bars

GPR was used to locate one of the steel tie bars that originally spanned the center longitudinal construction joint. One core was then taken at the tie bar to determine its condition. Figures 3.72 through 3.74 below illustrate the tie bar condition.

Figure 3.71: GPR Operation

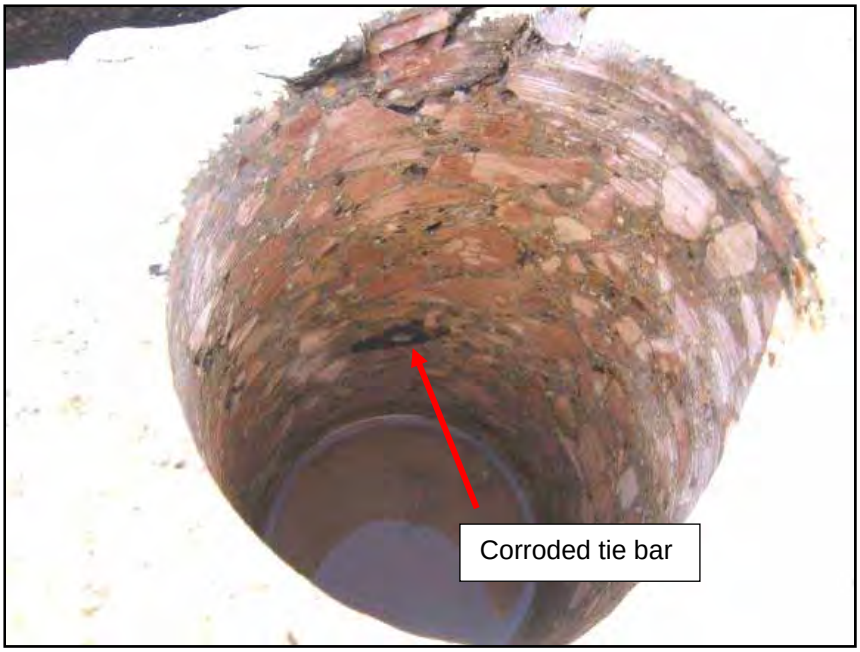

Figure 3.72: Core Hole Over Tie Bar

Figure 3.73: Core (Side Farthest from Joint)

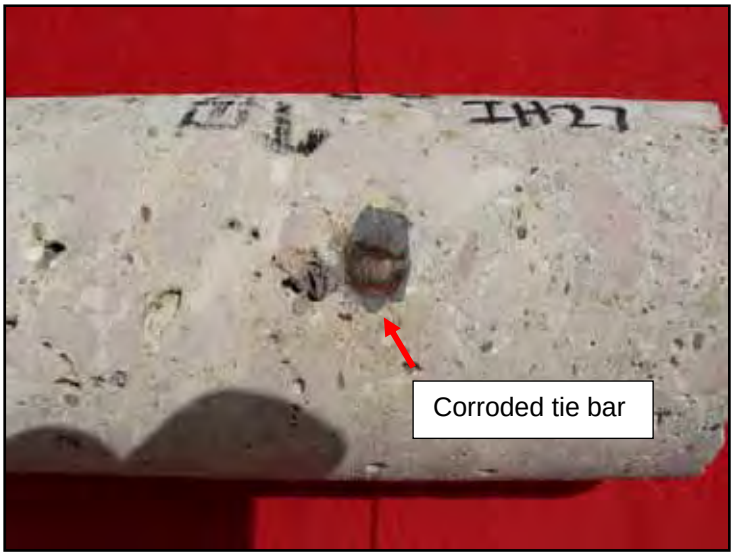

Figure 3.74: Core (Side Closest to Joint)

Figure 3.72 shows the core hole at the tie bar, directly adjacent to the separated longitudinal construction joint. At the face of the construction joint, the bar was completely corroded (no steel was present). At the face of the core hole nearest the joint, the tie bar was approximately 50 percent corroded. At the inside face of the core itself (Figure 3.72), the bar was approximately 30 percent corroded. At the outside face of the core (Figure 3.73), the bar was not corroded at all. Thus it appeared that the corrosion was concentrated within a few inches of the joint. Tie bar corrosion likely contributed to joint separation. However, it is not certain that tie bar corrosion was the initial factor that caused separation. Excess strain on the steel tie bars due to thermally-induced stresses in the pavement could have caused the joint to open, allowing air and moisture to penetrate into the joint, and initiating the corrosion. Conversely, worn joint sealant may have allowed air and water to penetrate and begin corrosion, as the (relatively) smooth faces of the construction joint offer little physical resistance to such penetration. In either case, tie bar corrosion would have contributed to joint separation.

Condition of Full Depth Repair

Approximately 50 ft. of repaired joint was inspected. No cracking, spalling, joint separation or slab faulting was observed. One core was taken through the repaired area (shown in Figure 3.75 below).

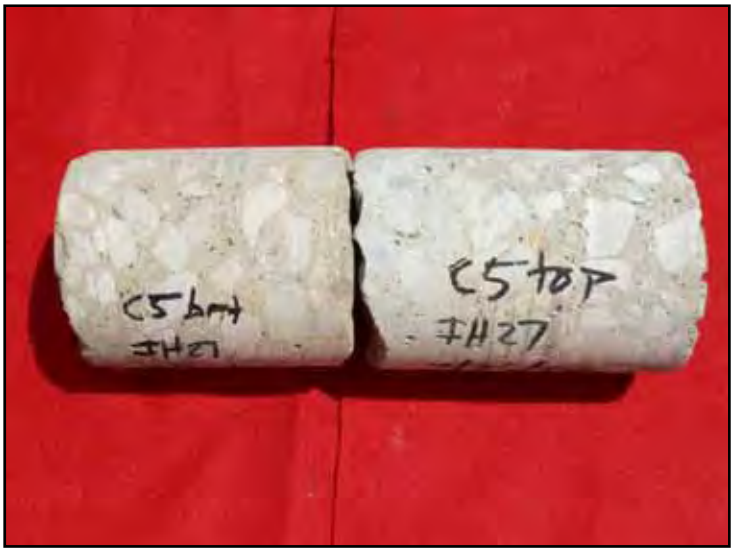

Figure 3.75: Core Through Full Depth Repair

At a depth slightly below mid-slab, a weathered crack could be seen in the core. Other than this crack, the repair appeared to be in good condition, with no visible external distress.

3.6.4 Conclusions

1. Longitudinal joint separations were likely caused by dynamic loading effects from traffic and corrosion of tie bars.
2. Data indicate that for the range of joint widths tested, load transfer efficiency did not significantly depend on the joint width. LTE may have decreased with increasing #1 sensor deflections. Deflections increased with increasing joint width.
3. Full depth repair on center construction joint appeared to have been effective in restoring load transfer efficiency. Durability appeared to be very good after five years of service.

3.7 IH 10 El Paso

3.7.1 Background and Scope of Activities

IH 10 in El Paso and surrounding areas was most likely constructed in the 1960's. Records of the exact construction date were not able to be located. Pavement in the sections that were investigated consisted of eight in. thick CRCP with untied, keyed longitudinal joints and cement stabilized base.

Researchers conducted field inspections of approximately two miles of the westbound and eastbound lanes of IH 10 near Exit 22B on December 5-6, 2006. The purpose of the field investigation was to determine the cause(s) of the joint separation and to provide data to TxDOT regarding the overall pavement integrity so that TxDOT may decide whether to repair or re-pave the Interstate. Activities included:

1. Visual Inspection: Longitudinal joints widths were measured; differential vertical movement between slabs (faulting) was measured.
2. Falling Weight Deflectometer Testing: FWD testing was performed at approximately 44 locations in the westbound direction and approximately 31 locations in the eastbound direction.
3. Ground Penetrating Radar: GPR was used to locate tie bars, longitudinal, and transverse bars. Locations for coring were also selected using the GPR.
4. Coring: Coring operations were conducted in several areas within the investigated area. Cores were taken next to the longitudinal construction joint to determine the type of joint, location, size, and condition of rebar and tie bars.

3.7.2 Pavement Condition Report

Longitudinal joint separations of varying widths were observed on both eastbound and westbound lanes. The outside joint (between the outside and middle slabs) had the most severe separations. Joint separations between one-half inch and 2 in. were observed. Minimal faulting was observed; slabs were mostly level. Very little longitudinal cracking was observed, with most occurrences found very near the outside longitudinal joint (less than three inches away) and running parallel to it. Transverse cracking present was not abnormal for CRCP pavement.

Cause of Longitudinal Joint Separations

Observation of the pavement slope revealed a pattern in the width of longitudinal joints; in areas where the pavement sloped downward from the concrete traffic barrier (CTB) toward the shoulder, joint separations were larger than in areas where the pavement sloped from the shoulder towards the CTB (Figure 3.76).

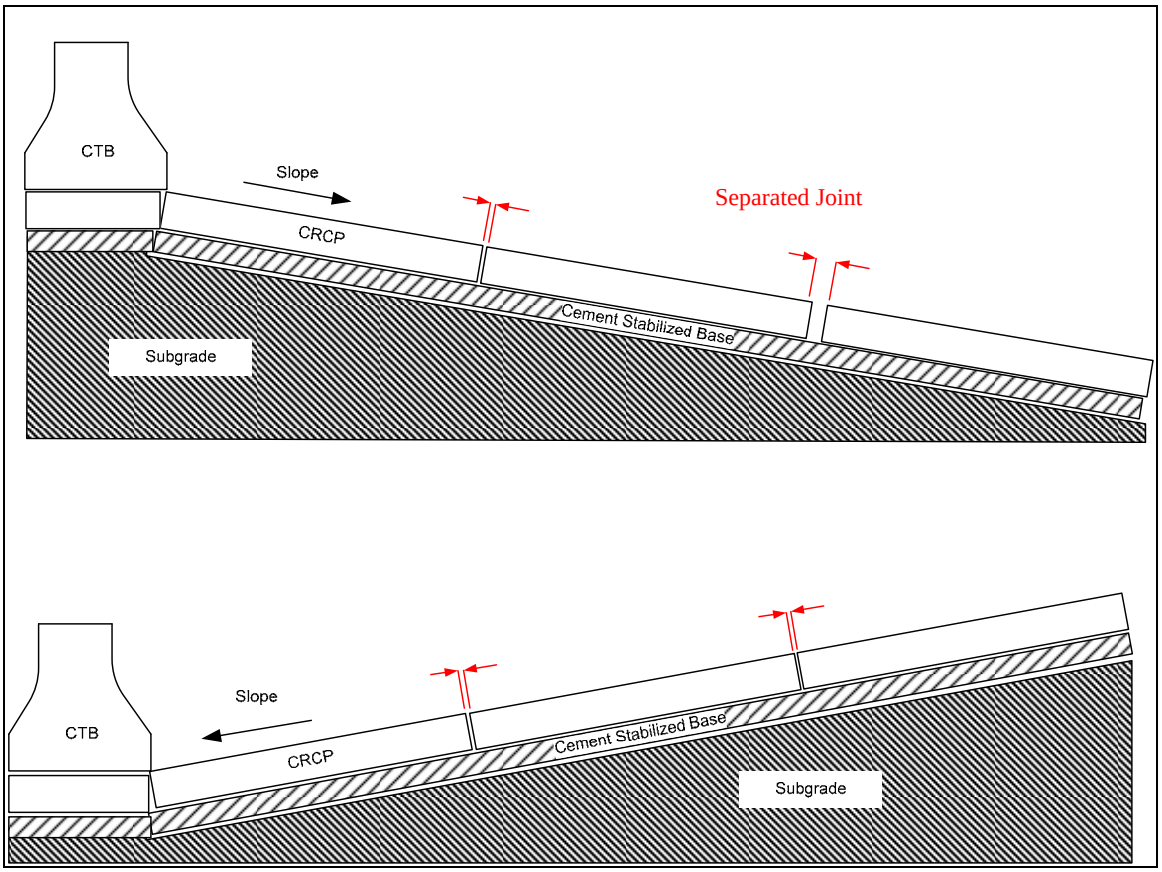

Figure 3.76: Effect of Pavement Slope on Joint Separation

During the course of the investigation, discussions with TxDOT maintenance personnel produced some clues as to the cause of the longitudinal joint separations. Evidently the CTBs have been known to "creep" across the pavement in this area due to the dynamic loading (vibration) of large trucks. This loading condition could be the cause of longitudinal joint separations as well. For sections that slope outward (as in the top diagram in Figure 3.76), vibration would tend to reduce the friction between the pavement and the subgrade, allowing the slabs to move downhill. Gravitational and dynamic forces could contribute to this movement. For sections sloping inward (as in the bottom diagram in Figure 3.76) the dynamic loading would not cause the same joint separation because gravitational forces tend to push the slabs inward toward the CTB. This theory is consistent with field observations.

Another factor contributing to joint separation was the lack of tie bars across the joint. Cores showed that the pavement was constructed with untied, keyed joints Figures 3.79 and 3.80. GPR was used to locate the transverse steel (see Figure 3.78 for a picture of the GPR screen), then cores were taken directly adjacent to the joint at the location of the transverse steel (Figure 3.77) as well as over the joint itself in the same location. The purpose of taking cores at these locations was to determine if tie bars had been used and had completely corroded (as seen in other field investigations) or if tie bars were not used.

Figure 3.77: Coring Operation

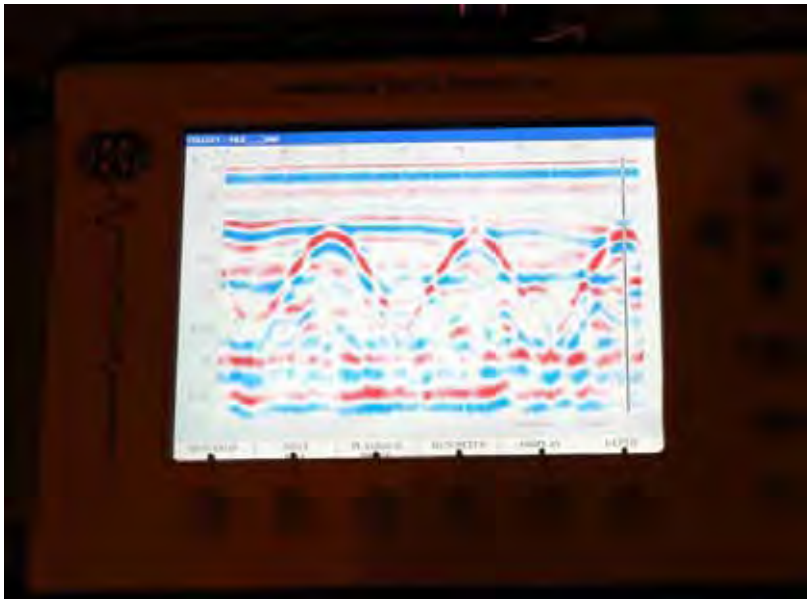

Figure 3.78: GPR Screen

Figures 3.81 through 3.83 show the keyed joint with no evidence of tie bars. Figure 3.83 shows one of the cores taken through the longitudinal joint. The key could clearly be seen, but no evidence of a tie bar existed.

Figure 3.79: Core hole through joint (1)

Figure 3.80: Core Hole Through Joint (2)

Figure 3.81: Core Through Joint (1)

Figure 3.82: Core Through Joint (2)

Figure 3.83: Core Through Joint (3)

Load Transfer Performance of Longitudinal Joints

FWD testing was performed slightly differently than other field investigations. Data from past trips indicated that the existing sensor arrangement may give artificially high values for LTE. Equipment was fabricated by TxDOT that allowed the sensors to be arranged in such a way as to produce more accurate test results. Figure 3.84 shows the new sensor arrangement on the FWD machine used for testing on IH 10. Figures 3.85 and 3.86 show diagrams of the old and new sensor arrangements. Appendix A contains a full explanation of the rationale behind the development and implementation of the new sensor arrangement.

Figure 3.84: Modified FWD Setup

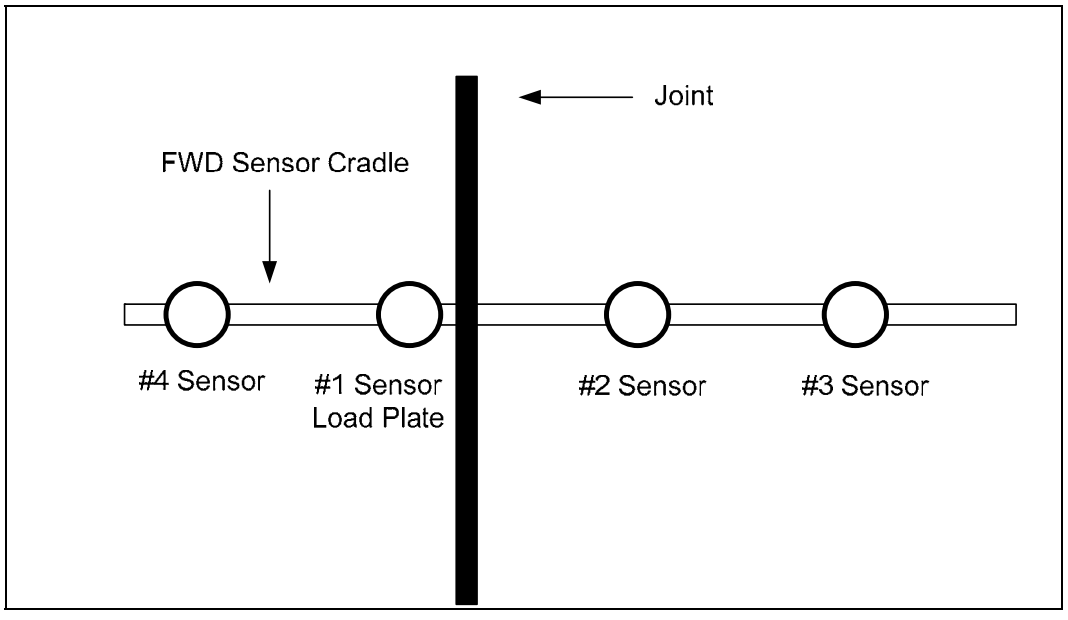

Figure 3.85: Conventional FWD Sensor Arrangement

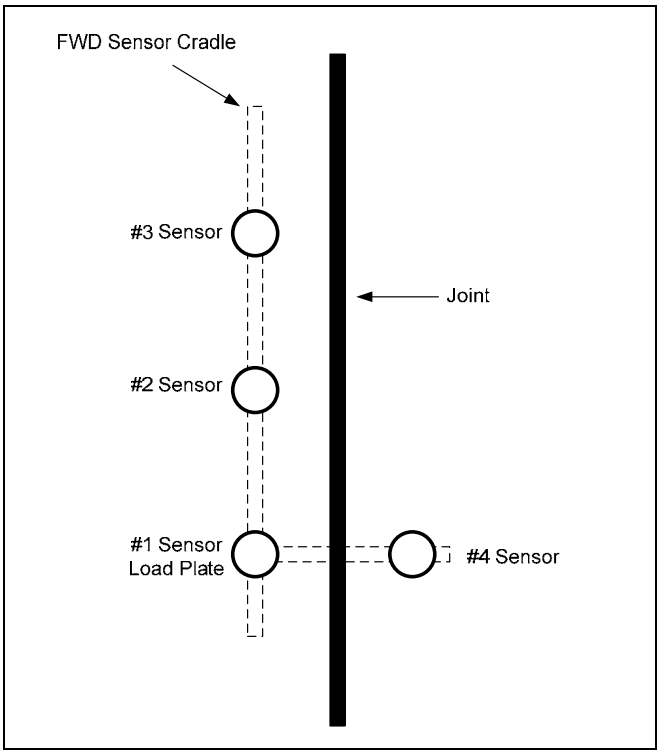

Figure 3.86: Modified FWD Sensor Arrangement

Figures 3.87and 3.88 show the LTE along the tested longitudinal joints. Load transfer efficiency varied greatly along the pavement, with eastbound lanes showing LTE between 10 and 90 percent and the westbound lanes between 9 and 109 percent. Overall pavement integrity, as measured by the #1 sensor deflections at a load of 9,000 lbs. (nominal), is shown in Figures 3.89 and 3.90. The westbound joint had an average #1 sensor deflection of 12.8 mils, while the joint in the eastbound direction had an average of 4.2 mils.

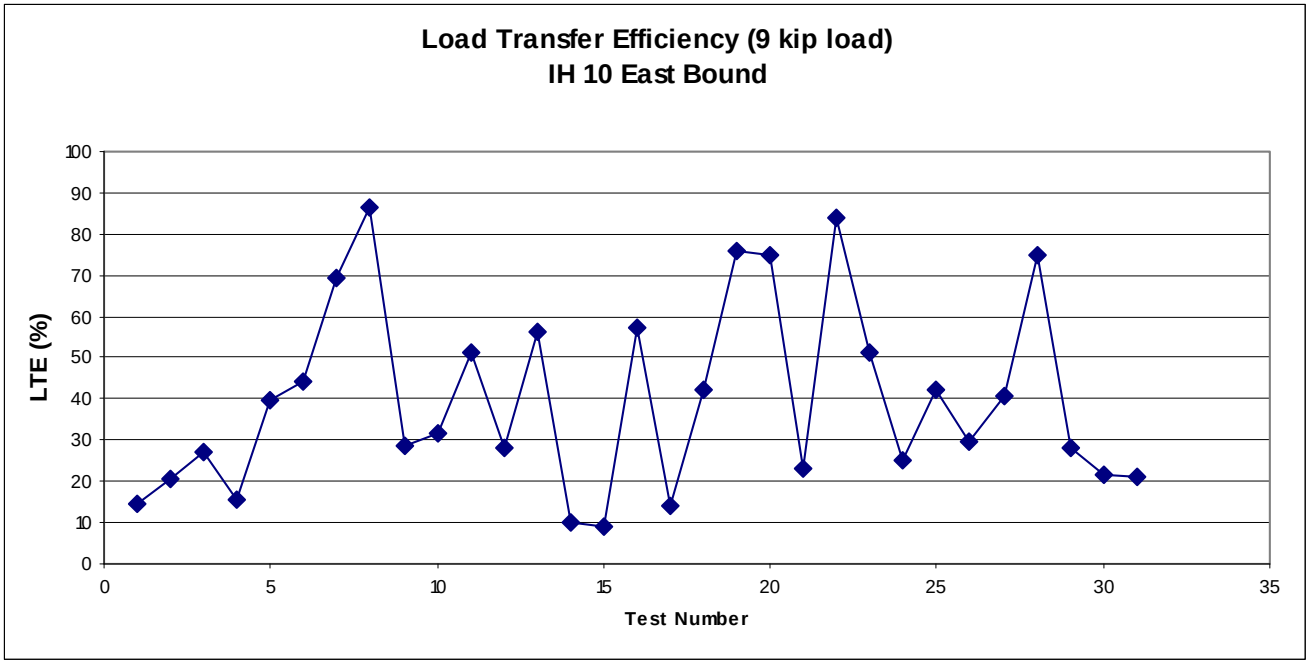

Figure 3.87: Load Transfer Efficiency (Eastbound)

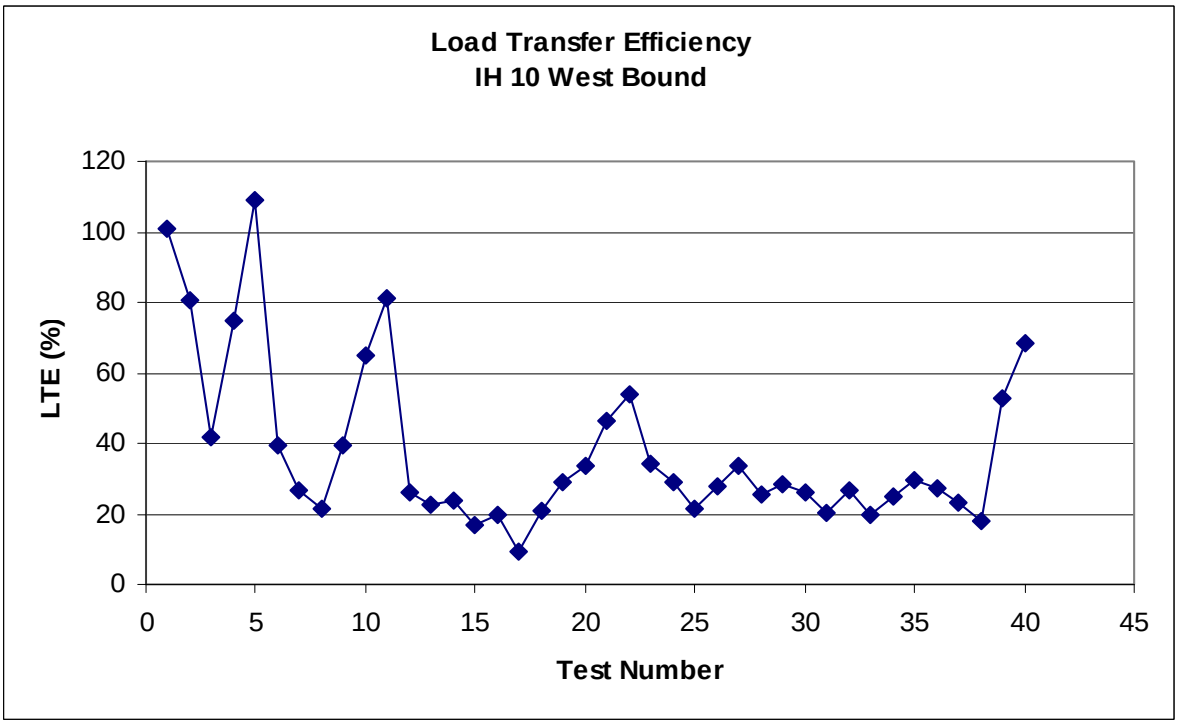

Figure 3.88: Load Transfer Efficiency (Westbound)

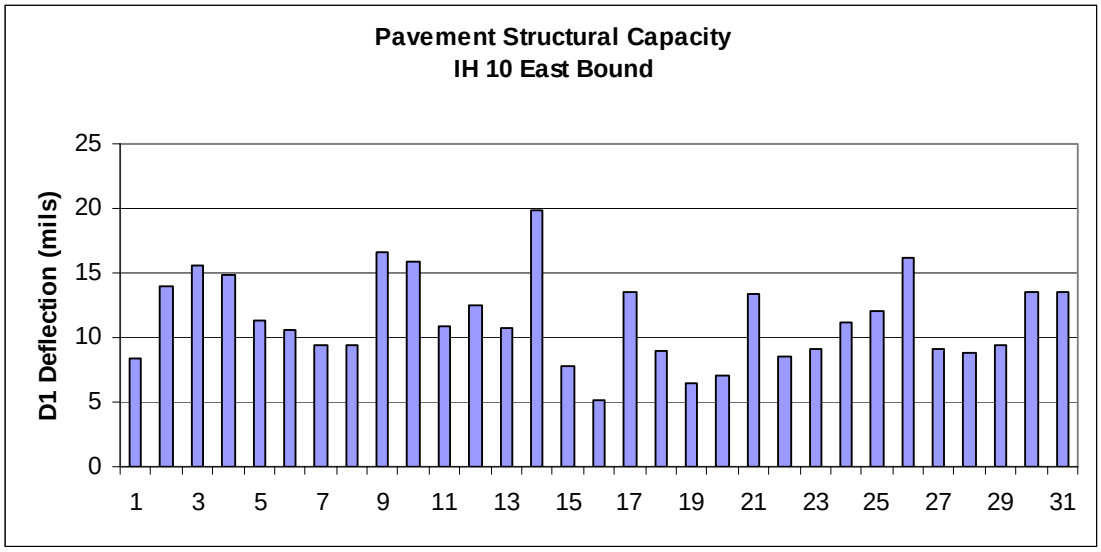

Figure 3.89: #1 Sensor Deflections (Eastbound)

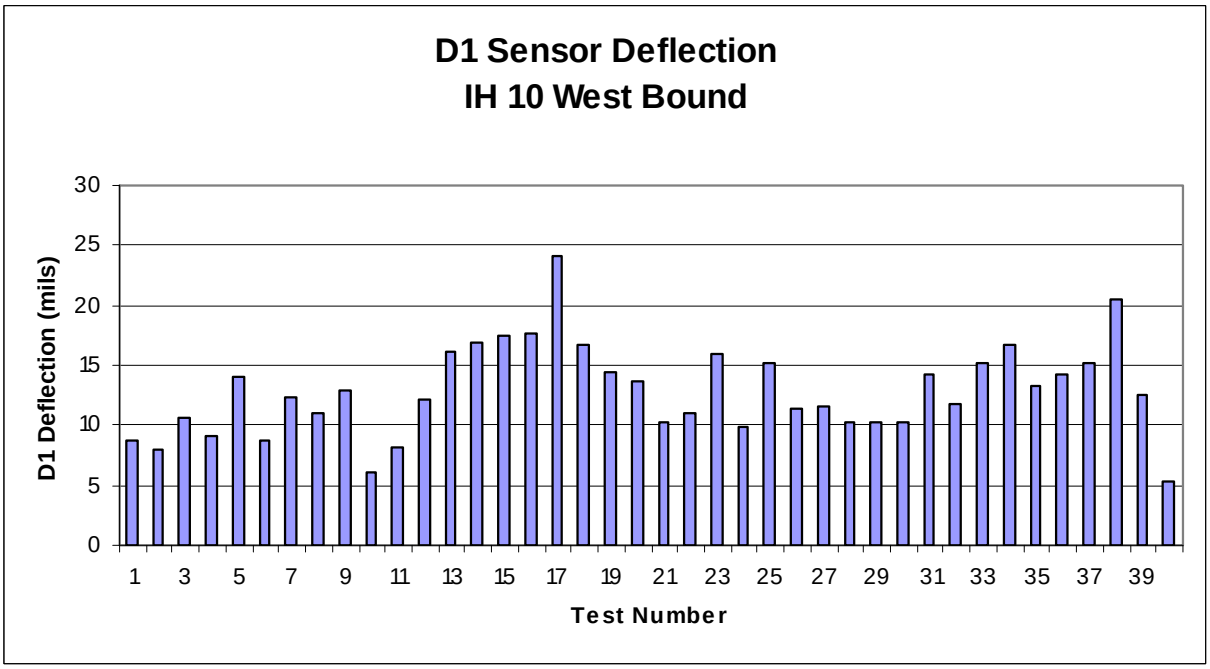

Figure 3.90: #1 Sensor Deflection (Westbound)

3.7.3 Load Transfer Trends

LTE and Joint Width

Figures 3.91 and 3.92 show the relationship between LTE and joint width for the eastbound and westbound lanes of IH 10, respectively. Though there was some (expected) scatter in the data, the general trend was that LTE decreased with increasing joint width. This is intuitively correct; the wider the joint, the less aggregate interlock occurs, and the less load is

transferred across the joint (lower LTE). For this particular pavement, because the longitudinal joints were keyed, higher LTE could be developed compared to pavements with untied smooth (butt) joints (up to the point where the keys no longer engaged).

Figure 3.91: LTE vs. Joint Width (Eastbound)

Figure 3.92: LTE vs. Joint Width (Westbound)

#1 Sensor Deflection and Joint Width

Figures 3.93 and 3.94 show the relationship between #1 sensor deflection and joint width. Data did not show a clear and consistent pattern, which led to the conclusion that #1 sensor deflection depended on more than just the joint width. This is consistent with statements in the preceding paragraph. For example, two different sections of the same type of pavement might have a 1-in. separated longitudinal joint, but have different #1 sensor deflections because one is a very stiff pavement with thick, asphalt-stabilized base and well-compacted subgrade and the other is thinner, more flexible pavement with no base and very soft subgrade.

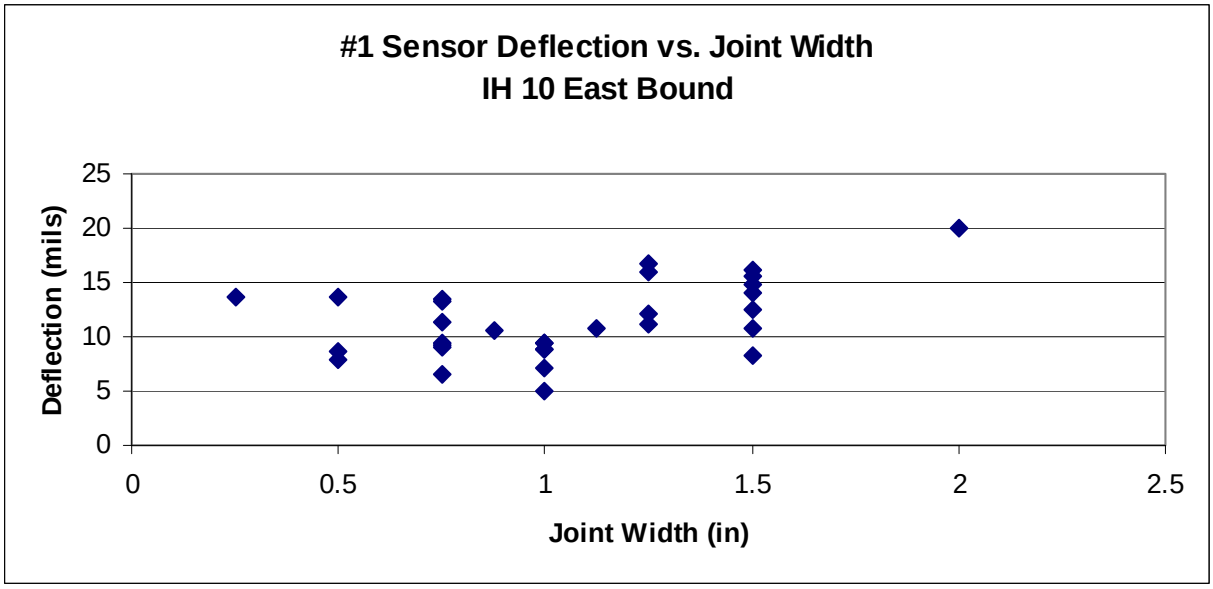

Figure 3.93: #1 Sensor Deflection vs. Joint Width (Eastbound)

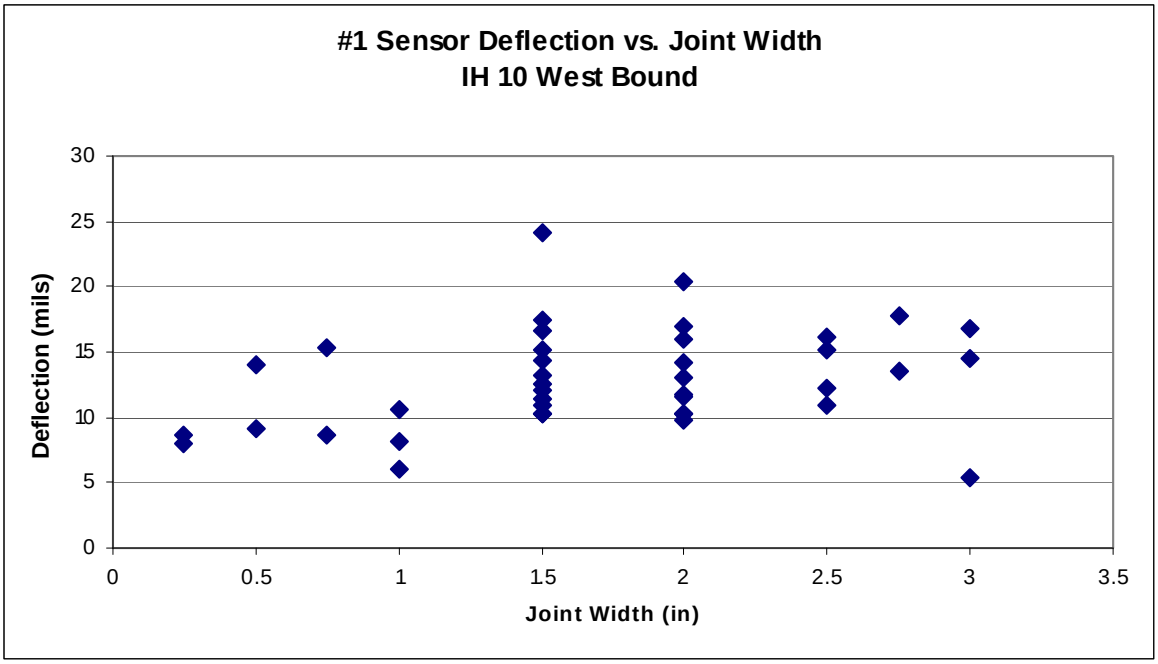

Figure 3.94: #1 Sensor Deflection vs. Joint Width (Westbound)

LTE and #1 Sensor Deflection

Figures 3.95 and 3.96 show the relationship between LTE and #1 sensor deflection. Recall that the #1 sensor was located at the load plate. As deflection of the #1 sensor increases, LTE decreases (arguably, exponentially). This behavior makes theoretical sense. Number one sensor deflection is a function of several parameters, including base and subgrade conditions, LTE across the longitudinal joint (if the load plate is dropped near a joint), and pavement strength and stiffness (which is dependent on pavement thickness, amount of steel, concrete strength and stiffness, etc.). This indicates an overall trend of higher LTE for pavement systems that are stiffer.

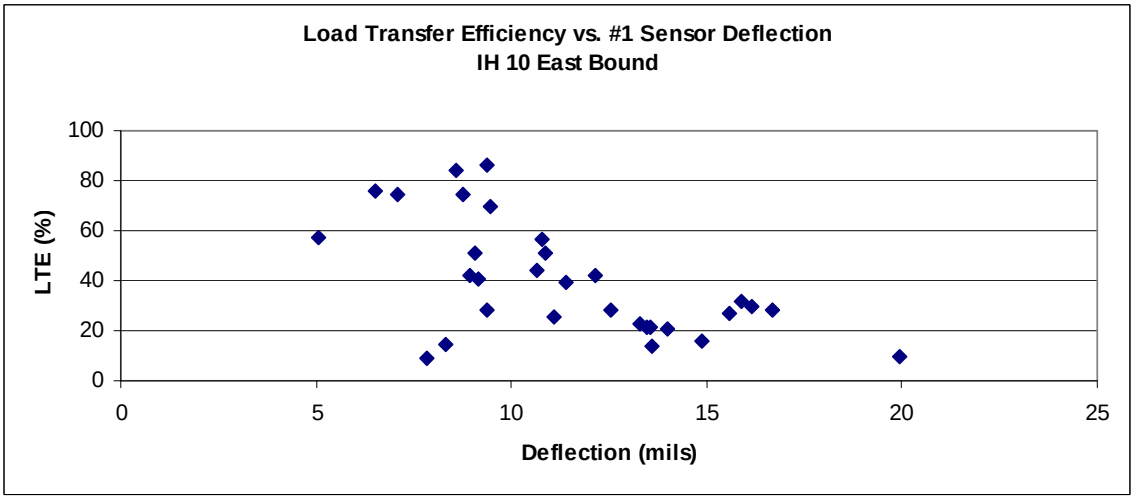

Figure 3.95: LTE vs. #1 Sensor Deflection (Eastbound)

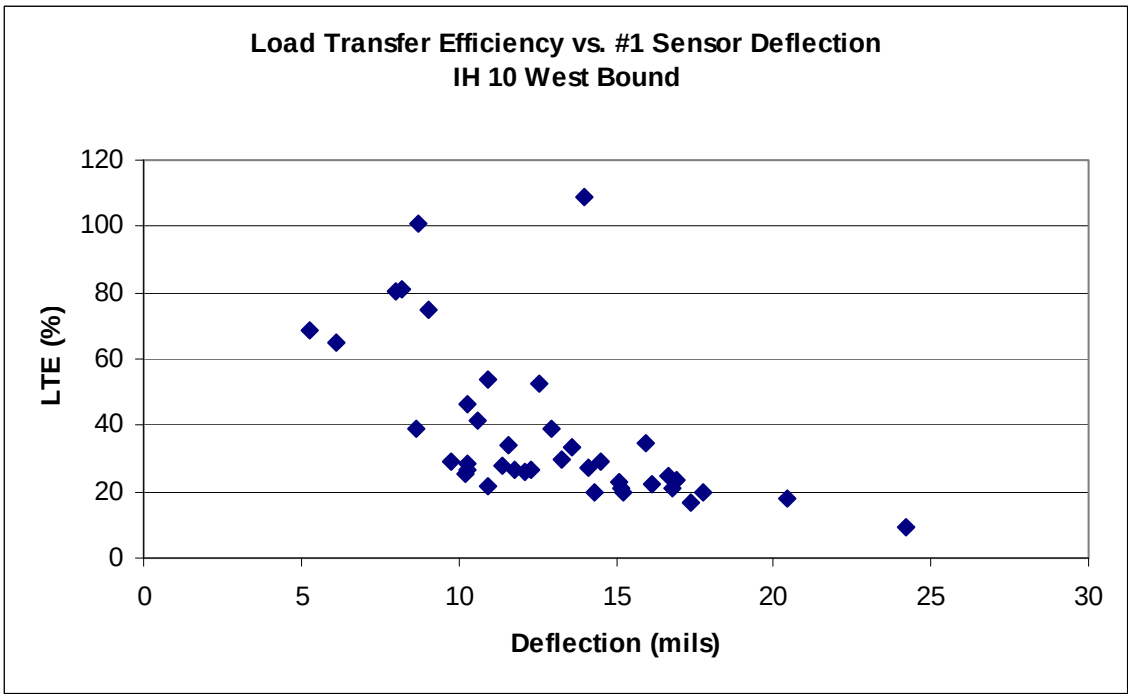

Figure 3.96: LTE vs. #1 Sensor Deflection (Westbound)

3.7.4 Conclusions

1. Dynamic loading due to traffic (particularly from large trucks) in areas where the pavement is sloped towards the shoulder was most likely the mechanism causing longitudinal joint separations. Untied joints contributed to the problem because they offered no resistance to these driving forces.
2. Load transfer efficiency decreased as joint widths increased in both eastbound and westbound lanes.
3. Number one sensor deflection was not exclusively dependent on joint width. Base and subgrade conditions, as well as general pavement stiffness, influenced these values.
4. Load transfer efficiency was dependent on #1 sensor deflection and therefore also on base and subgrade conditions and general pavement stiffness.

3.8 Summary of key findings

Key findings from the field investigations are presented here. Trends in data that can be employed in the repair decision making process are summarized.

3.8.1 Causes of Longitudinal Joint Separations

Longitudinal joint separations were likely caused by a combination of three phenomena: (1) dynamic loading from heavy truck traffic; (2) tie bar corrosion; and (3) poor joint sealing. Dynamic loading from heavy truck traffic is likely the mechanism creating the force that tends to

drive slabs apart and create longitudinal joint separations. Corrosion reduces the strength of the tie bars, and in some cases causes section loss which further increases the stress in the remaining steel. Because strain in steel (and therefore displacement of the joint) is directly proportional to stress in the steel, further joint separation occurs as corrosion progresses, until the tie bars rupture completely. Poor joint sealing contributes to corrosion of the tie bars. Moisture invades the joint as the sealant breaks down, and the unprotected steel easily corrodes.

3.8.2 Causes of Longitudinal Cracking

Longitudinal cracking on the pavements investigated as part of this study were likely caused by shallow and possibly late saw cutting of the longitudinal contraction joint. Contraction joints are an integral part of the design of JCP pavements. Curling and warping stresses due to temperature variations between the top and bottom surfaces of the concrete pavement cause cracking. Contraction joints introduce stress risers in specific locations by reducing the thickness of the pavement. Cracks are forced to propagate through steel bars so that the two pieces of pavement do not drift apart after the crack forms. Without contraction joints, cracks would occur in relatively random locations and potentially in areas where no reinforcement exists. If the contraction joints are not sawed soon after initial setting (before the concrete gains enough strength to begin cracking), cracks will form elsewhere in the pavement. Likewise, if the joints are not cut deep enough, stress may not be concentrated enough to induce a crack in that location. Stress builds elsewhere in the slab and cracks form at those locations first. This is what is believed to have caused the cracking on SH 66 and SH 289.

Literature review and surveys revealed that longitudinal cracking can occur for a host of reasons (Chapter 2). In order to determine the cause of cracking for a specific pavement, a forensic investigation must be performed in that location.

3.8.3 Load Transfer Efficiency and Crack/Joint Width

Figure 3.97 shows data from all field investigations in which longitudinal joints were tested. Results show that there was a general trend for LTE to decrease as joints widened. Data from pavements with some sort of mechanical anchorage (tie or stitch bars or keyed joints) between slabs showed a much stronger correlation than untied pavements or tied pavements with ruptured or corroded tie bars. Longitudinal cracks showed no correlation between LTE and crack width, most likely because the high temperatures and small crack widths worked to provide excellent LTE across the entire range of crack widths (Figure 3.98).

Joints with smaller separations showed significant data scatter, which indicates that joint width alone is not a sufficient indicator of load transfer efficiency and is not a reliable predictor of the need for joint repair. For example, pavements showing 1 in. joint separations may have a LTE range between 30% and 80%. Repair guidelines, then, cannot be solely based on joint or crack width.

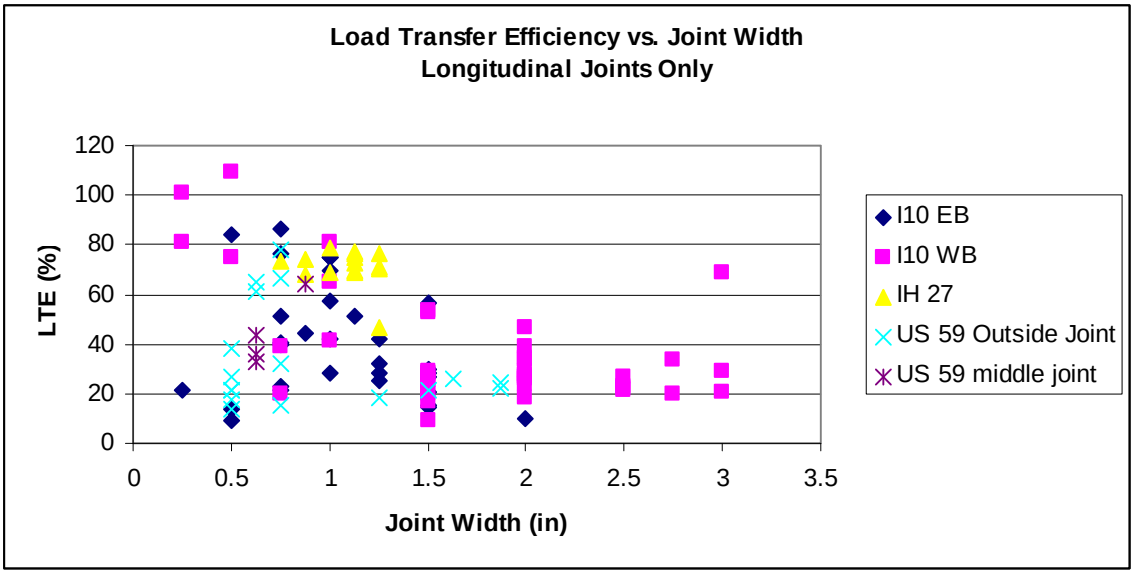

Figure 3.97: LTE vs. Joint Width

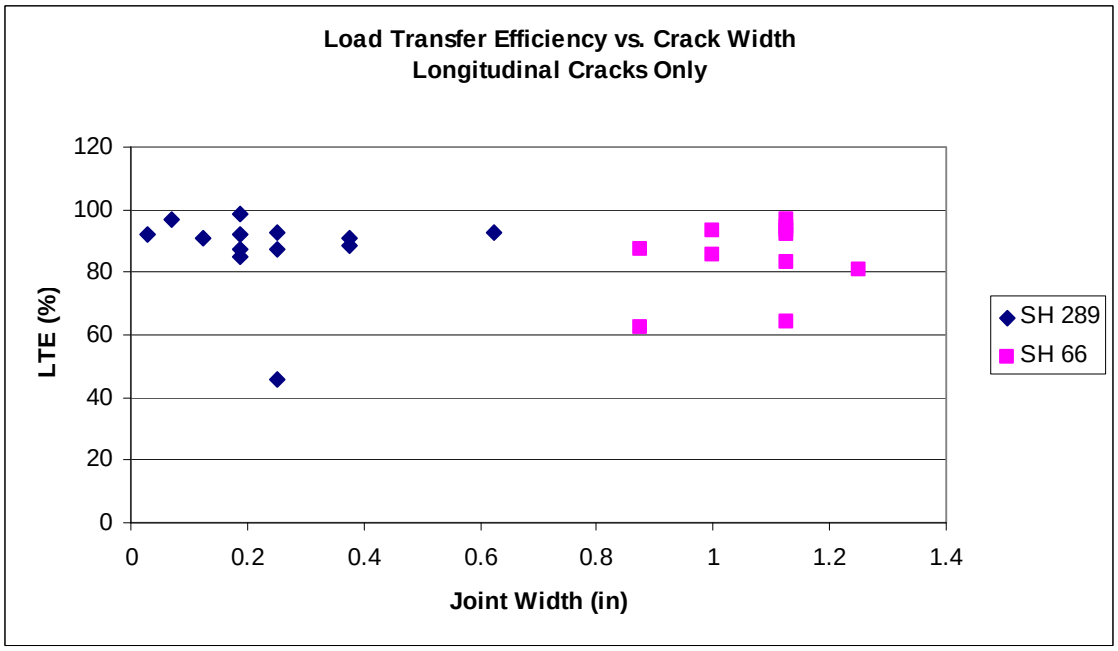

Figure 3.98: LTE vs. Crack Width

3.8.4 #1 Sensor Deflection and Crack/Joint Width

Data from unrepaired longitudinal joints and cracks are shown in Figures 3.99 and 3.100, respectively. Although one pavement (IH 10 westbound) showed a mild correlation, most pavements showed #1 sensor deflection to be independent of crack/joint width. Recall that stitched areas showed that deflection increases with increasing joint width due to the mechanics at work in the repair.

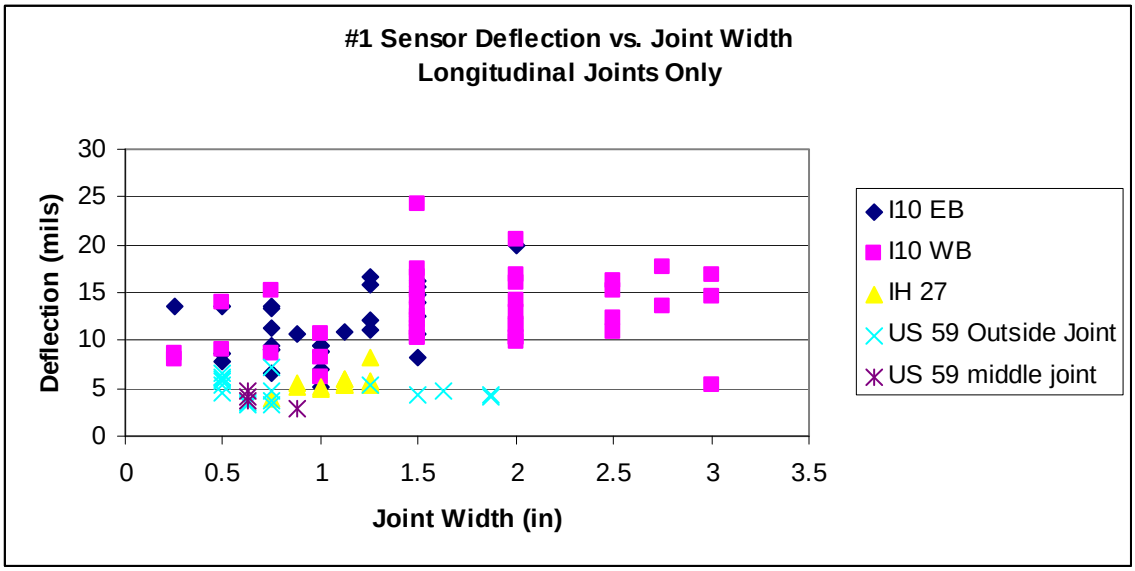

Figure 3.99: #1 Sensor Deflection vs. Joint Width for Joints

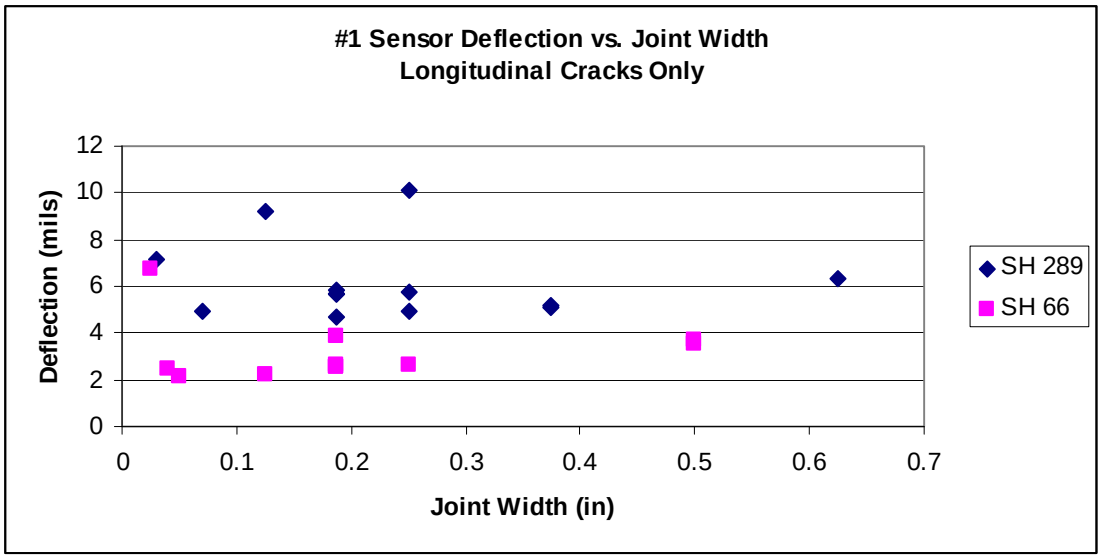

Figure 3.100: #1 Sensor Deflection vs. Joint Width for Cracks

3.8.5 Load Transfer Efficiency and #1 Sensor Deflection

Figures 3.101 and 3.102 show longitudinal joint and crack data from each field investigation. Longitudinal joints revealed a general trend of decreasing LTE with increasing #1 sensor deflection. This shows that load transfer efficiency of longitudinal joints deteriorates as the general performance and structural capacity of the pavement system deteriorates. In practical terms, this means that the cost of repairing a pavement increases as overall pavement quality worsens. Poor pavement structural capacity means lower LTE, which in turn creates higher demand on any repair method. Higher demand will require a more robust repair; this usually means that bars will need to be installed deeper in the pavement, a higher quality repair material

will be necessary, and more steel per length of crack/joint will be needed. All these aspects of the repair increase costs significantly. The most efficient and cost-effective approach to pavement repair would be to run tests as soon as the distress is identified and to repair it as soon as possible before overall pavement system performance deteriorates.

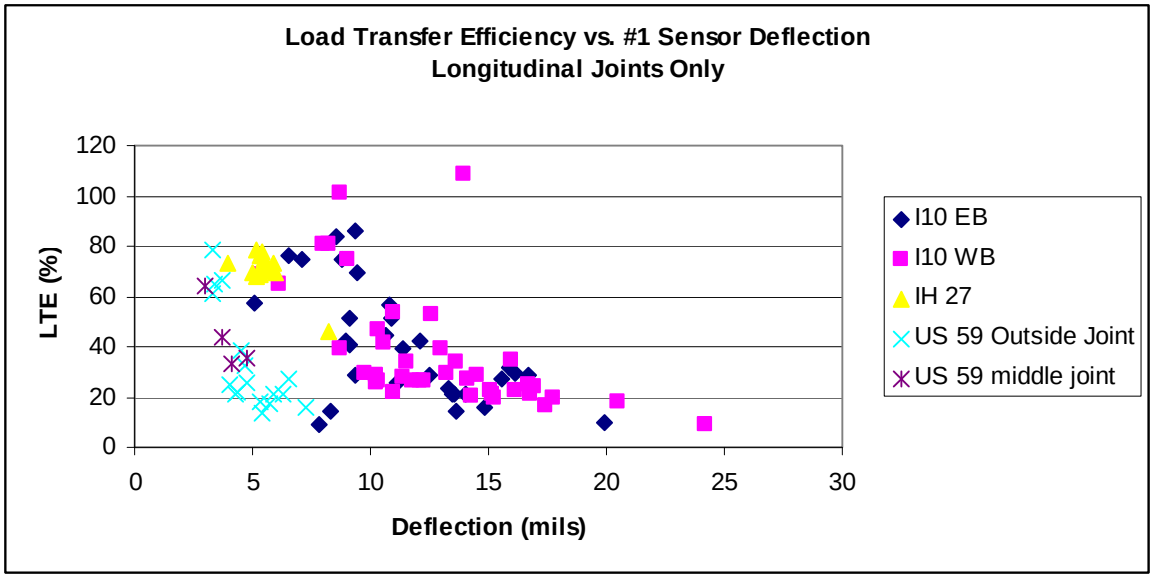

Figure 3.101: LTE vs. #1 Sensor Deflection for Joints

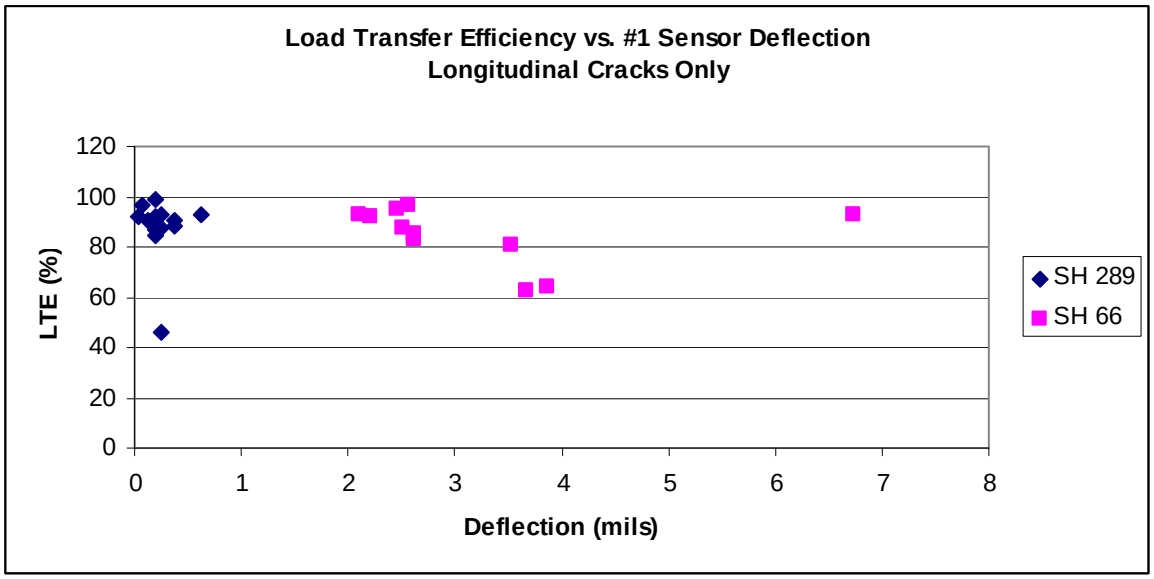

Figure 3.102: LTE vs. #1 Sensor Deflection for Cracks

3.8.6 Base Type and Joint/Crack Performance

Base type and condition certainly affect the overall performance of joints and cracks, but may not strongly affect LTE. Conclusions regarding the magnitude of the contribution of the base and subgrade to LTE and deflection are difficult to determine because each pavement has

unique properties. IH 27 (asphalt stabilized base in good condition) and IH 10 (cement stabilized base in poor condition) data showed higher average LTE and lower average deflection. Stronger base conditions on IH 27 likely contributed to the better joint performance. US 59 showed results that were puzzling at first glance. The joint performance of that pavement, which had no base and was resting on a subgrade of high-PI clay, showed joint performance similar to IH 27. It would appear that US 59 would have had significantly poorer joint performance given its base conditions, but that was not the case. The explanation may lie in the pavement thickness. US 59 has 14 in. thick pavement whereas IH 27 is 10 in. thick. The pavement on US 59 was significantly stiffer due to the higher thickness, which reduced the magnitude of #1 sensor deflection in FWD tests.

Additional field tests on varied pavement types would be required to draw more accurate conclusions about this subject.

3.8.7 Joint Repair Materials

Field investigations showed that longitudinal joints are typically filled with a low modulus caulk or tar. In most instances, these materials were in poor condition. Such materials deteriorate over time, becoming brittle and developing holes and cracks. This allows moisture to invade the joint and corrode the steel tie bars, which have no protective coating. Investing in high quality repair materials that will remain flexible over time and effectively seal joints and cracks is an important part of any repair strategy.

3.8.8 Repair Guidelines Approach

Guidelines cannot be solely based on joint/crack width, #1 sensor deflection, or LTE. Consulting only one of these parameters in exclusion of the others will result in inaccurate assessments of joint or crack performance and potential demands on repair methods. Joint/crack performance and repair demand depend on both LTE and D1, therefore repair guidelines must take into account both.

One of the goals of developing the repair guidelines was to provide TxDOT with suggestions regarding the most cost-effective approach to repairing distressed longitudinal joints and cracks. Part of this mandate included not only evaluating the costs of the repair methods themselves, but the cost of the repair process. If repair decisions are made based solely on the lowest initial cost, the result may be higher long-term costs if the strengths of the repair do not match the demand induced by the joint or crack. One crucial aspect of the repair process that drives cost is the timing of the repairs. Data generally indicate that joint/crack performance tends to deteriorate rapidly as the joint/crack width increases. Repair costs increase as the demand on joints/cracks becomes more severe, so the most economical approach is to repair pavements as soon and appropriately as possible.

Chapter 4. Research Program

4.1 Finite Element Modeling

Analytical finite element modeling (FEM) was conducted by Dr. Seongcheol Choi of the Center for Transportation Research (CTR) under the supervision of Dr. Moon Won to determine the elastic distribution of stress in concrete for three repair methods under consideration for inclusion in repair guidelines. Results from the modeling are presented (Won 2006a), followed by preliminary conclusions about the potential applications of each repair method.

4.1.1 Scope

Three repair methods were considered in the modeling: (1) cross stitching, (2) slot stitching, and (3) stapling. Because finite element modeling was not in the original scope of the project, the loading condition was limited to the most severe condition a repair might experience in the field. Each repair model was subjected to shear-type loading by a simulated truck wheel next to the joint. The maximum principle tensile stress in the concrete was calculated for each model.

4.1.2 Assumptions

The following assumptions were inherent to the FEM analysis:

- FEM software: Dyana
- Two-dimensional elastic analysis (a unit depth in the direction of traffic was assumed)
- 12-ft.-wide slabs with 0.5-in. longitudinal joint separation
- No aggregate interlock across the joint
- Wheel loading only (no environmental effects)
- Load: 9 k single wheel at edge of joint; 90 psi tire pressure
- Concrete pavement: 12 in. thick, modulus of elasticity = 5×10^6 psi, Poisson's ratio = 0.15
- Steel areas were taken from TxDOT specifications and adjusted to account for different bar spacing for each method in order to obtain the same bar area per unit length of joint (0.33 sq. in. per ft. of joint).
- Steel reinforcement: modulus of elasticity =29×10^6 psi, Poisson's ratio = 0.3
- Uniform subgrade support (no voids underneath the slabs).
- Subgrade reaction modulus = 200 psi/in.

The demand on the repair methods under the assumed loading condition is dominated by shear, although some flexural demand is present due to the gap between the slabs.

4.1.3 Analysis of Results

Cross Stitch

Because cross stitch bars are oriented in an alternating fashion in the field (see Appendix F) two models were created: one in which the load is applied on the same slab in which the cross stitch bar is inserted (Case "R") and one in which the load is applied on the slab opposite the inserted bar (Case "L").

Cross stitching Case "L" gave a maximum principle tensile stress in the concrete of 300 psi. In Figure 4.1, the model and distribution of stresses are shown. Cross stitching Case "R" yielded a maximum principle stress in the concrete of approximately 140 psi. Figure 4.2 illustrates the model.

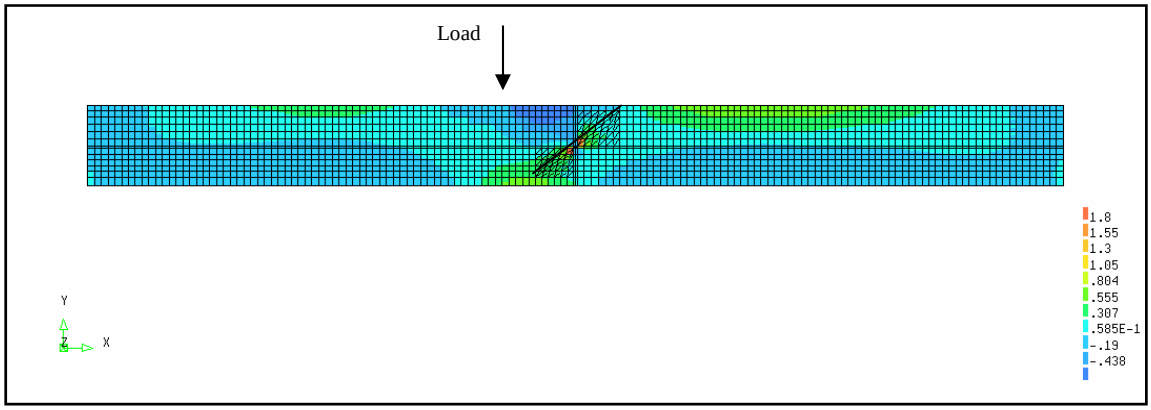

Figure 4.1: Stress Contours for Cross Stitching Model (Case "L")

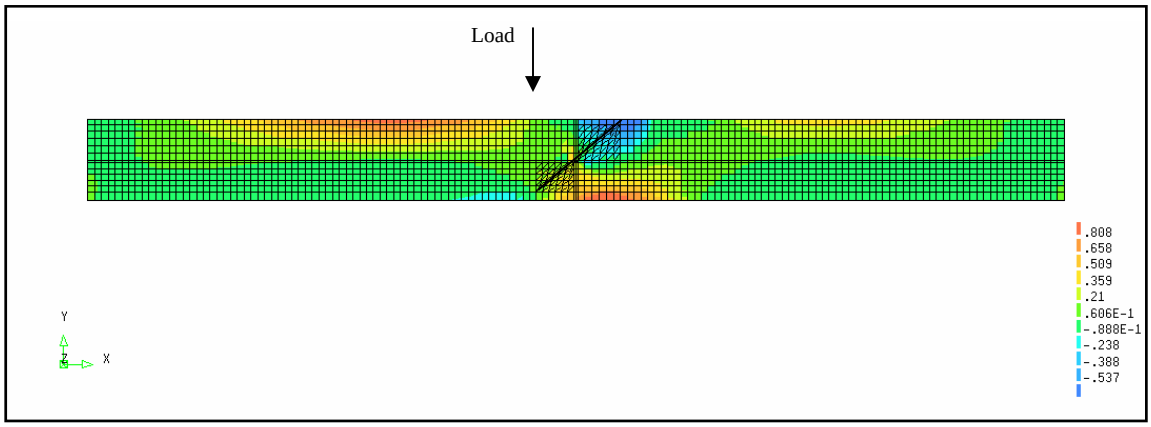

Figure 4.2: Stress Contours for Cross Stitching Model (Case "R")

Slot Stitch

Slot stitching gave a maximum stress of approximately 130 psi (Figure 4.3).

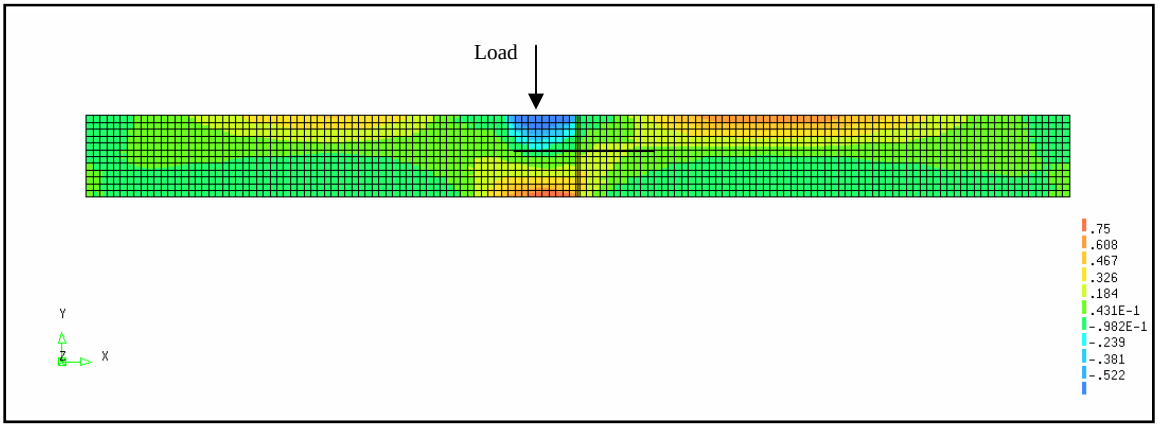

Figure 4.3: Stress Contours for Slot Stitching

Staple

Stapling showed a maximum stress of approximately 150 psi (Figure 4.4).

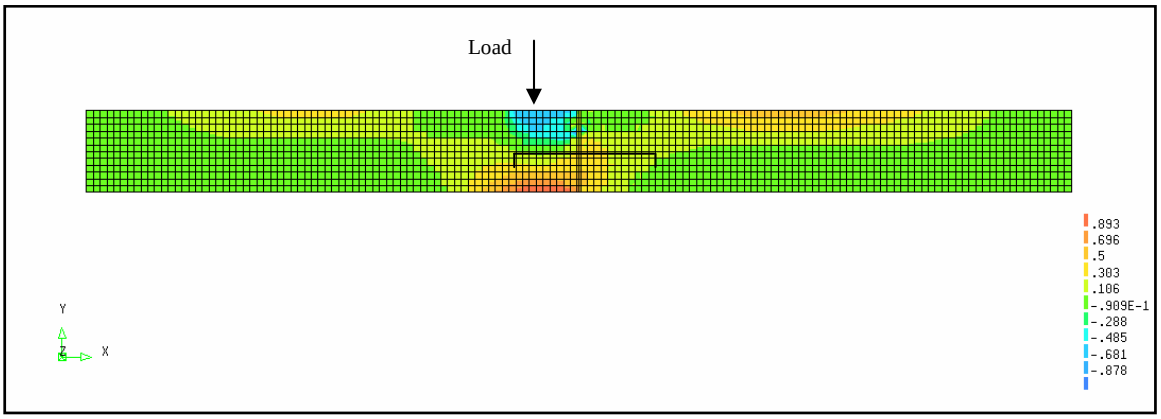

Figure 4.4: Stress Contours for Stapling

Analysis of Results

In Figure 4.5, the results from the modeling are summarized. Because both load cases for cross stitching are present in the field, the worst case governs. As a truck wheel rolls along a joint that is cross stitched, the load will be transferred across the joint by several bars (the proportion of load sharing between the alternating stitch bars is an indeterminate structural analysis problem and is outside the scope of this study). Case “L” stress can be thought of as an upper bound solution, and Case “R” as a lower bound solution. The worst condition would be a wheel directly over a bar that Case “L” simulates, in which case the stress in the concrete would approach the 300 psi level. The least demanding condition would be when the wheel is directly over a bar of opposite orientation (Case “R”). Stress would approach the lower bound value of

140 psi in that case. Because the cross stitching is being evaluated from a global rather than local basis, the upper bound stress of 300 psi will be used for comparison with other repair methods.

Cross stitching showed the highest stress, followed by stapling. Slot stitching showed the lowest stress of the three repair methods.

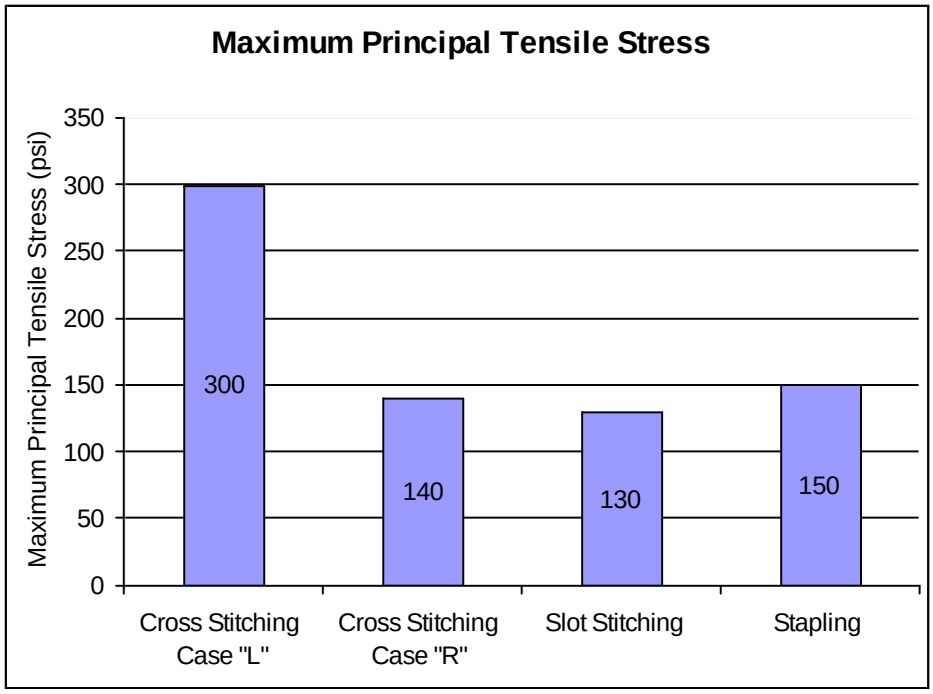

Figure 4.5: Maximum Stress Values for Each Repair

The stress value for slot stitching (as opposed to the other two methods) is likely the most accurate reflection of what the repair would experience in the field. Repair materials used to fill the slots are typically rigid grouts, often portland cement-based, and have similar properties to concrete. Stapling, on the other hand, typically has a low-modulus elastomeric concrete in the slots. This difference would need to be accounted for when predicting ultimate failure loads of the repair. Because of this difference in repair materials, stapling would likely fail at a lower load than predicted by the FEM results, because the model assumed the slots to be filled with concrete.

4.1.4 Conclusion

Results indicate that for the shear-type loading simulated in the analysis, slot stitching likely would perform best in the field. Cross stitching would likely perform worst. Stapling would likely perform similarly to stapling.

4.2 Experimental Program

4.2.1 Scope

Field investigations revealed the need to develop repair methods for two types of distress commonly found in the field: (1) separation of longitudinal construction joints, and (2)

longitudinal cracking. Field investigations also underscored that each potential repair site is different; the construction date could fall anywhere in a 40-year life span, during which time vastly different pavement design and construction methods were used. Site conditions of a pavement vary, including subgrade type, type and thickness of base and sub-base, weather patterns, severity of loading conditions, etc. Because of the highly variable nature of each site, a single repair method cannot be specified for state-wide use in all situations. Forensic investigations must be performed to determine the mechanism behind pavement distress, to identify the primary type of loading to which the repair might be subjected, and to select the repair method that has demonstrated the best performance for the loading case in question.

Four repair techniques were developed and/or selected for investigation as part of this project: (1) slot stitching, (2) cross stitching, (3) stapling, and (4) headed bar stitching. Two specimens of each of the first three methods were constructed. Specimens were subjected to shear and bending type loads, which closely simulate vehicular loading under field conditions. One specimen was constructed using the fourth method, and tested in direct tension.

The goal of laboratory testing was to determine the relative strengths and weaknesses of each pavement repair method for loading conditions commonly found in the field. Results from lab testing were combined with field observations in order to develop a system by which repair methods could be recommended for implementation in the field.

4.2.2 Testing Methods

Description of Test Specimens

Seven specimens were cast to simulate continuously reinforced concrete pavement (CRCP) with a 1.5-in. longitudinal joint separation. (This measurement of joint separation was frequently observed in the field.) Longitudinal and transverse steel ratios were selected from TxDOT CRCP(1)-03 detail. Longitudinal reinforcement consisted of #6 grade 60 rebar. The space between the edge of the longitudinal joint and the first bar was four inches, with subsequent spaces of six inches. Transverse steel consisted of a single #6 bar on each side of the specimen. Longitudinal steel was held in place by metal chairs and transverse bars were tied to the bottom of the longitudinal bars. See Figure 4.6 for typical reinforcement layout. The centroid of the transverse bars was at approximately mid-depth of the slab (centroid of bars at 5.75 inches for most specimens). Bars were placed in the forms prior to concrete placement. Polystyrene was placed in the forms to create the joint separation and the voids to be used to house displacement sensors. Concrete conforming to TxDOT's Type P specifications was placed in the forms and wet cured with plastic sheeting. After the concrete had cured, the polystyrene was dissolved with acetone. The surfaces of the slots were sand blasted to remove the polystyrene residue and to roughen the surfaces to increase the ability of the repair material to bond to them. At the time of placing, the slump was 1.5 inches and air content was 3.5 percent. Appendix I includes the material strengths for each test.

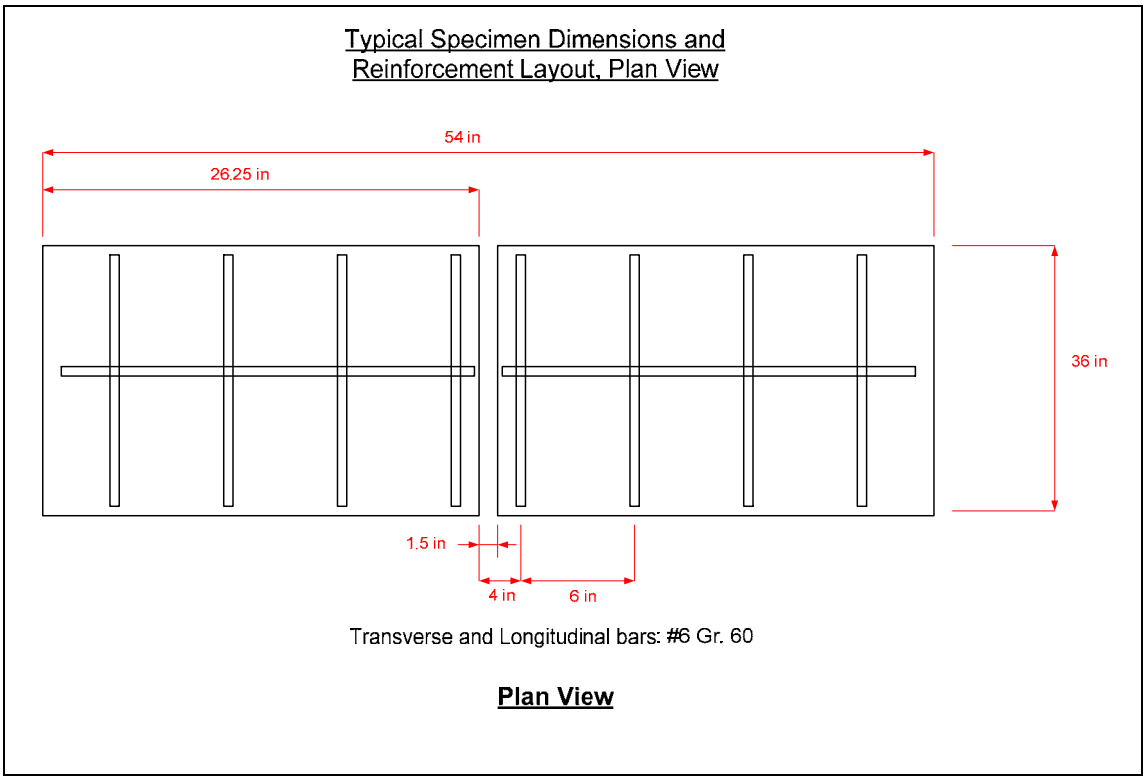

Figure 4.6: Typical Specimen Dimensions and Reinforcement Layout

Cross Stitch

Two specimens were cast, one to be tested in shear loading (hereafter referred to as "shear" specimen), and the other in combined shear loading and bending (referred to as "bending" or "flexure" specimen because bending demand dominates over shear). For the shear specimen, no instrumentation was installed prior to concrete placement. The bending specimen contained one vibrating wire jointmeter at the bottom of the form that spanned the simulated construction joint. Polystyrene was used to create an additional void at the top of the specimen, directly above the other jointmeter, wherein another jointmeter was placed after sandblasting operations described above were complete.

Two one-inch diameter holes were drilled into each specimen after the concrete had hardened sufficiently (compressive strength was at least 4,000 psi) using an impact drill. Holes were placed approximately 7 in. from the edge of the simulated construction joint, and drilled at an angle of approximately 28 degrees. (TxDOT usually drills holes at a steeper angle, but 28 degrees was used in order to avoid the reinforcement in the adjacent slab when drilling.) In the field, a steeper angle can be used for unreinforced slabs. Otherwise, the location of rebar would need to be determined and the angle of drilling chosen prior to commencing repair operations. Stitch holes were cleaned by scrubbing with a wire brush and flushing with compressed air.

Eighteen-inch-long stitch bars were instrumented with electrical resistance strain gages. Stitch holes were partially filled with Redhead G-5 Anchor Bolt Epoxy. Bars were inserted into the holes, leaving approximately two inches of clear distance between the tops of the bars and the surface of the concrete. Epoxy was inserted into the top of the holes to produce a surface flush with the concrete. The top jointmeter was inserted into the small slot and the slot was filled with Sikaquick 2500 quick-setting repair mortar. The specimen during construction is shown in

Figures 4.7 through 4.9. Figures 4.10 and 4.11 show the location of stitch bars and sensors in the specimens. Figure 4.12 shows one of the specimens after casting.

Figure 4.7: Cross Stitch Shear Specimen Before Casting

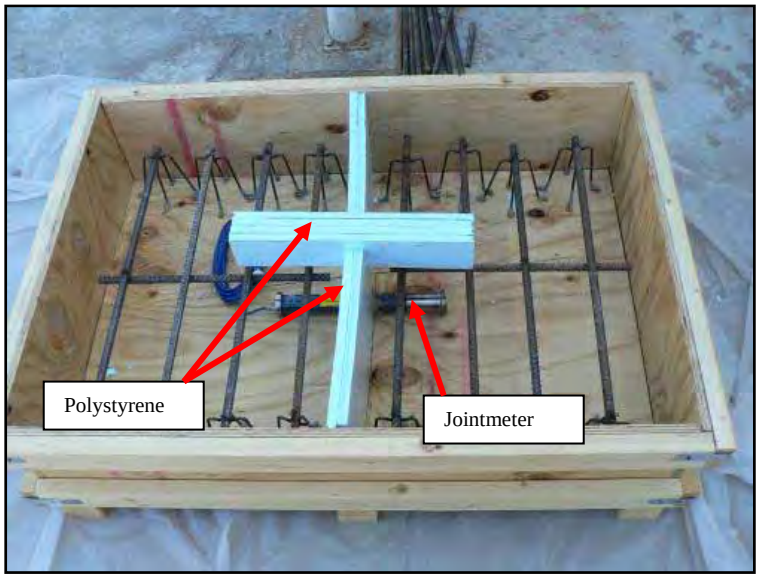

Figure 4.8: Cross Stitch Flexure Specimen Before Casting

Figure 4.9: Cross Stitch Shear (Top) and Flexure (Bottom) Specimens

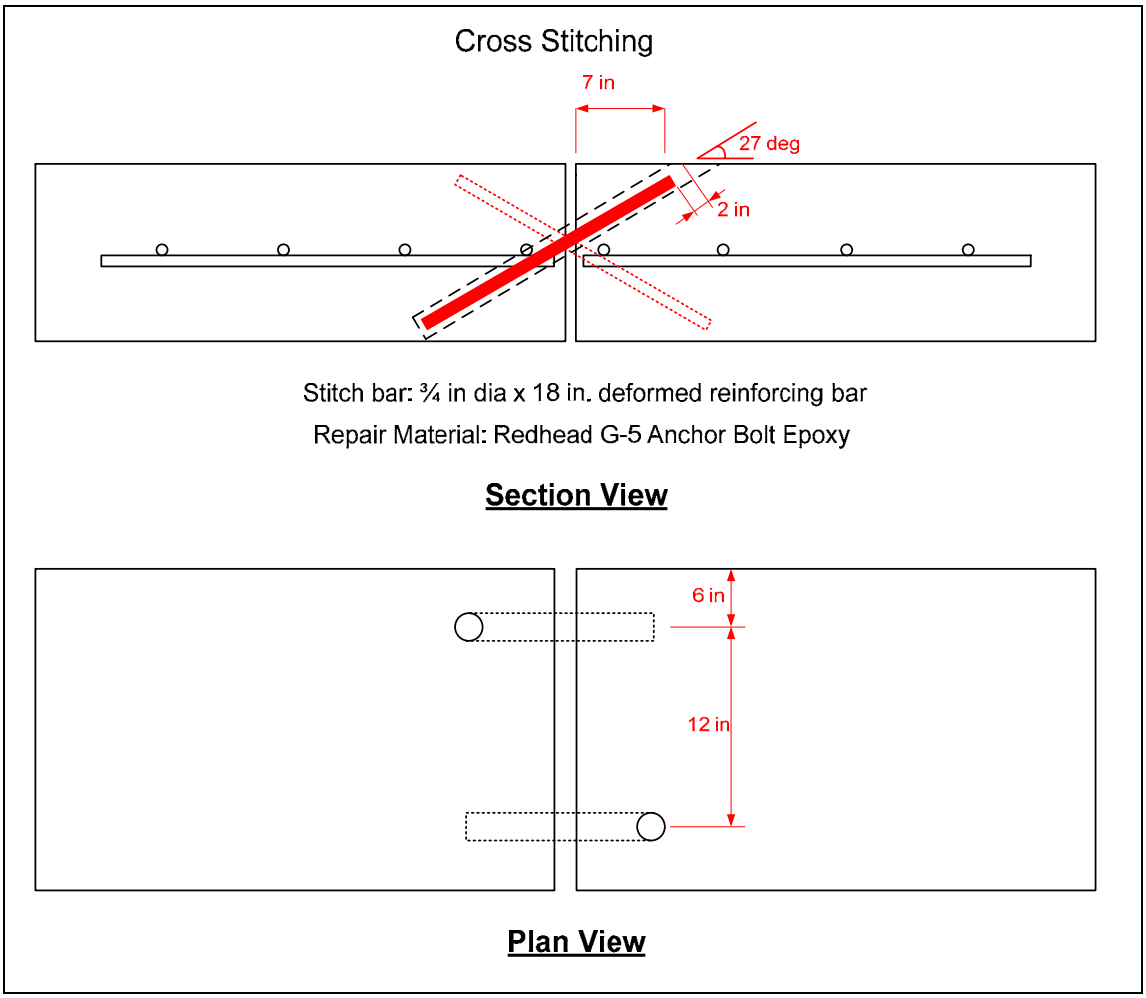

Figure 4.10: Cross Stitch Specimen Repair Bar Diagram

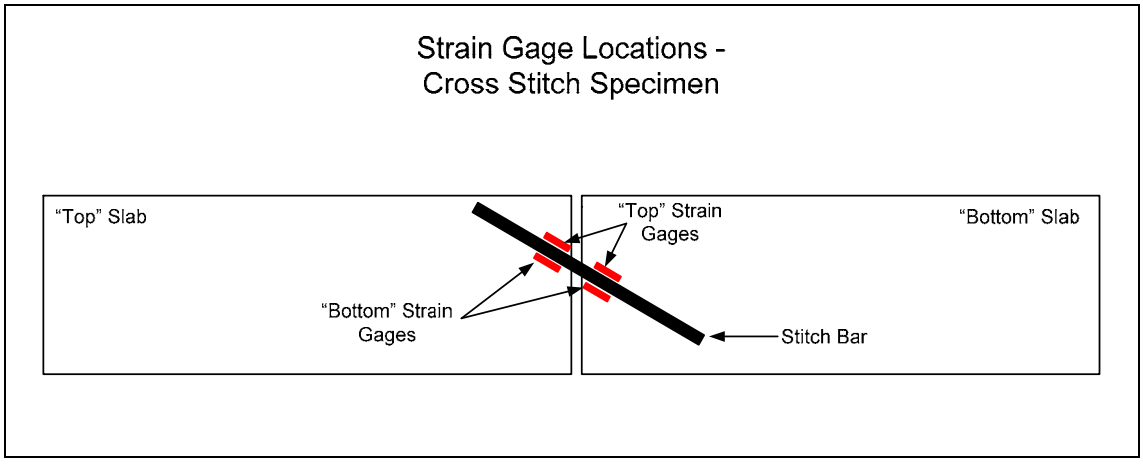

Figure 4.11: Strain Gage Locations on Cross Stitch Specimens

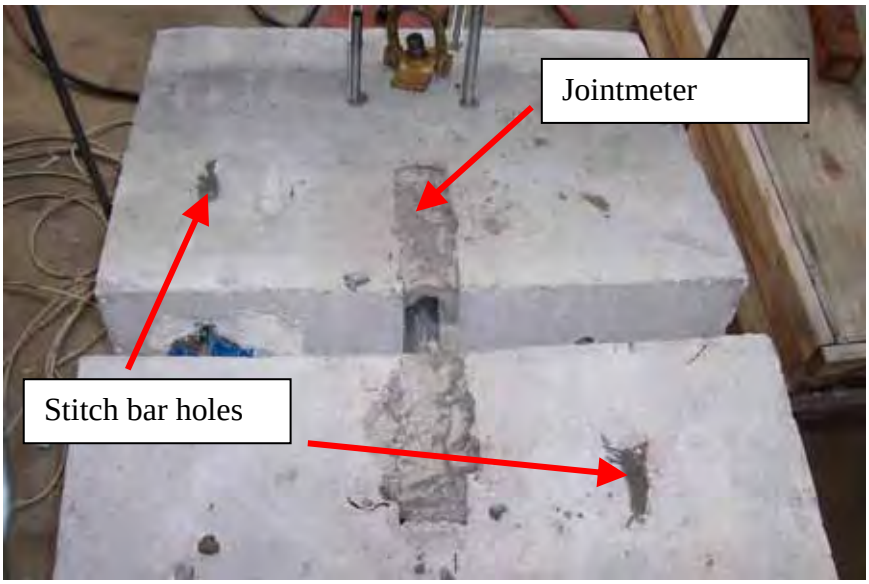

Figure 4.12: Cross Stitch Specimen

Slot Stitch

Two slot stitching specimens were constructed, one for shear loading and one for bending. Longitudinal and transverse bars were placed in the same arrangement as in the cross stitch specimens. Field conditions were simulated as closely as possible for this testing, but the equipment used for saw cutting was too large, expensive, and time consuming to be used for the lab specimens. Jointmeters were installed in the flexure specimen as in the cross stitching specimen, and an additional void was formed to house a vibrating wire tiltmeter. Slot stitch bars consisted of 46 in. long, three-quarter inch diameter Gr. 60 rebar fitted with a combination of vibrating wire and electrical resistance strain gages. Bars were placed flush with the bottom of the slots, and slots were filled with Sikaquick 2500 quick-setting repair mortar. Repair material was wet-cured with burlap and plastic sheeting for three days. The top jointmeter was also installed at this time using Sikaquick 2500 (Figures 4.13 through 4.17).

Figure 4.13: Slot Stitch Shear Specimen Before Casting

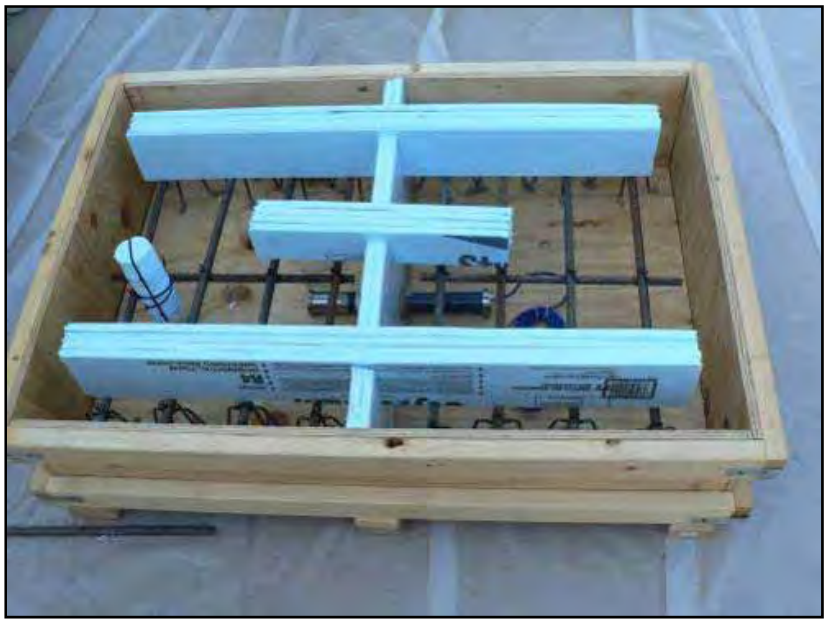

Figure 4.14: Slot Stitch Flexure Specimen Before Casting

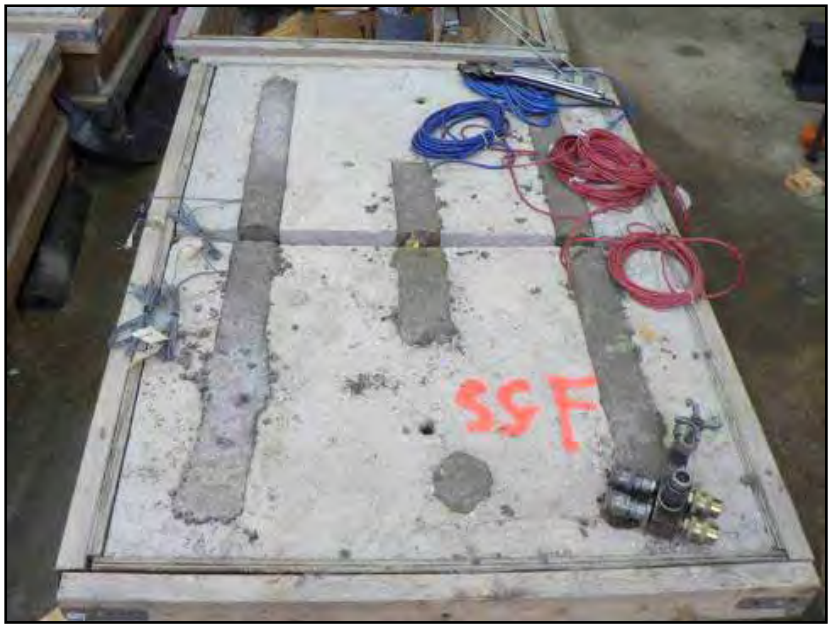

Figure 4.15: Slot Stitch Flexure Specimen After Casting

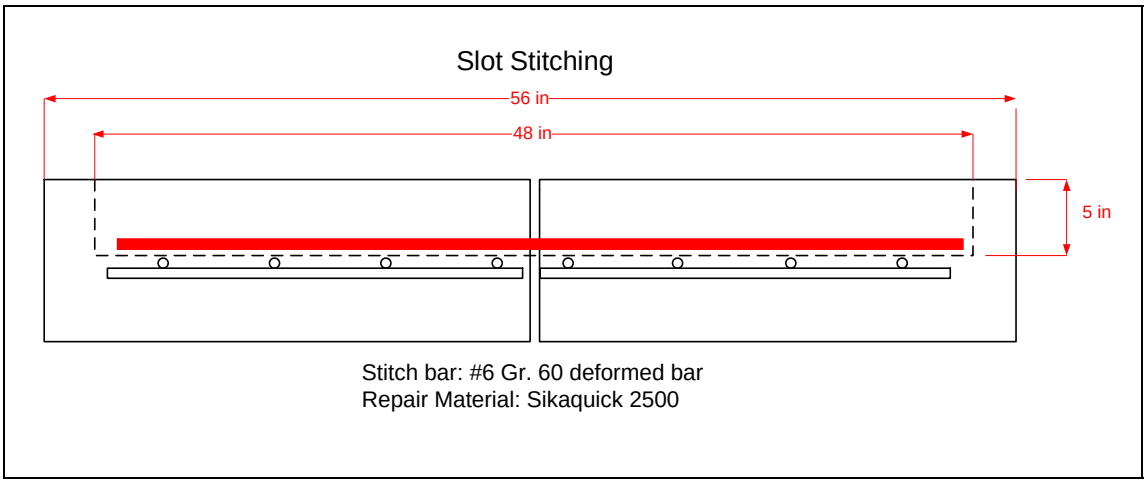

Figure 4.16: Slot Stitch Repair Bar Diagram

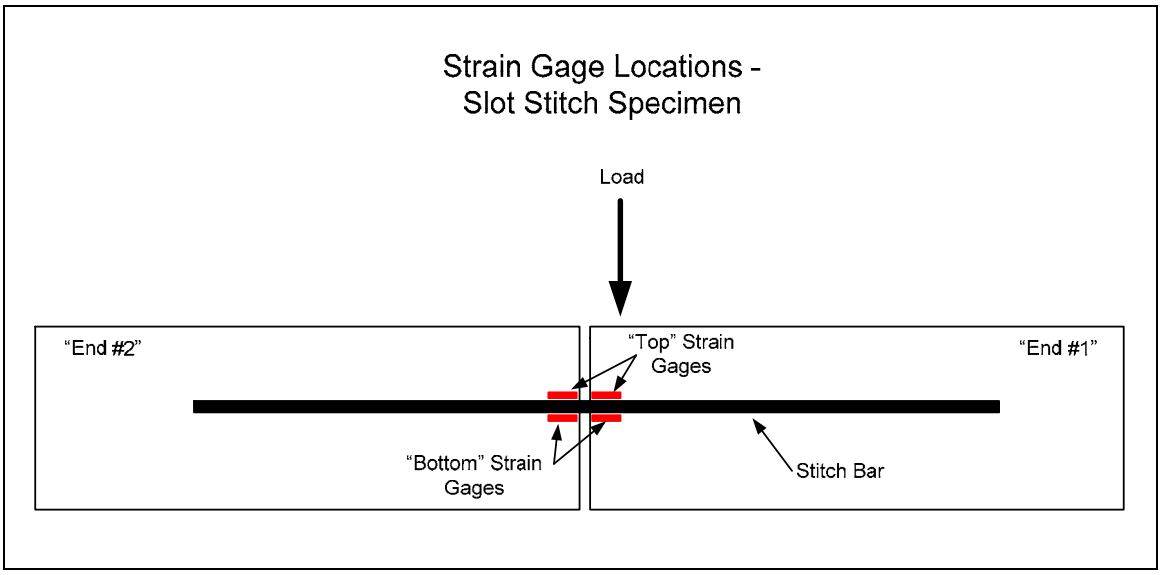

Figure 4.17: Strain Gage Locations on Slot Stitch Specimens

Staple

Two staple specimens were constructed, one for shear testing and one for flexural testing. Longitudinal and transverse reinforcement ratios and arrangements matched those of the slot stitch and cross stitch specimens. Staple bars were fabricated from straight pieces of #6 Gr. 60 rebar by bending with a vise and heating the bar with a cutting torch. Bends did not conform to ACI specifications (required radius is 3 in.), due to geometric constraints. Field investigations showed that larger-radius bends prevented bars from fitting flush against the bottom of the slots, thereby reducing the amount of clear cover to the pavement surface. One location in Houston showed bars protruding through the surface of the repair material.

Staple bars used in the lab testing were instrumented with a combination of vibrating wire and electrical resistance strain gages. After concrete placement, clearing of slots, and sandblasting, bars were installed in the specimens. Staple legs were anchored into the vertical slots with Sikadur 35 High-Mod LV Epoxy. Approximately twenty-four hours after pouring the epoxy, the slots were filled with SSI Flexpatch. Repair material cured for approximately 14 days in controlled conditions (approximately 70 deg. F.; not exposed to water) before the first test (Figures 4.18 through 4.22).

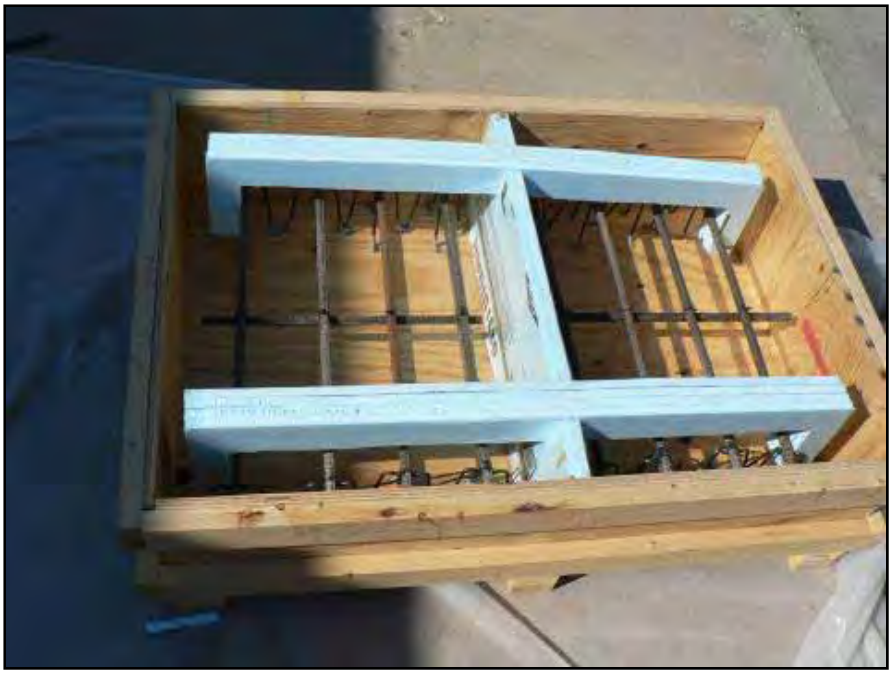

Figure 4.18: Staple Shear Specimen Before Casting

Figure 4.19: Staple Flexure Specimen Before Casting

Figure 4.20: Staple Flexure Specimen After Casting

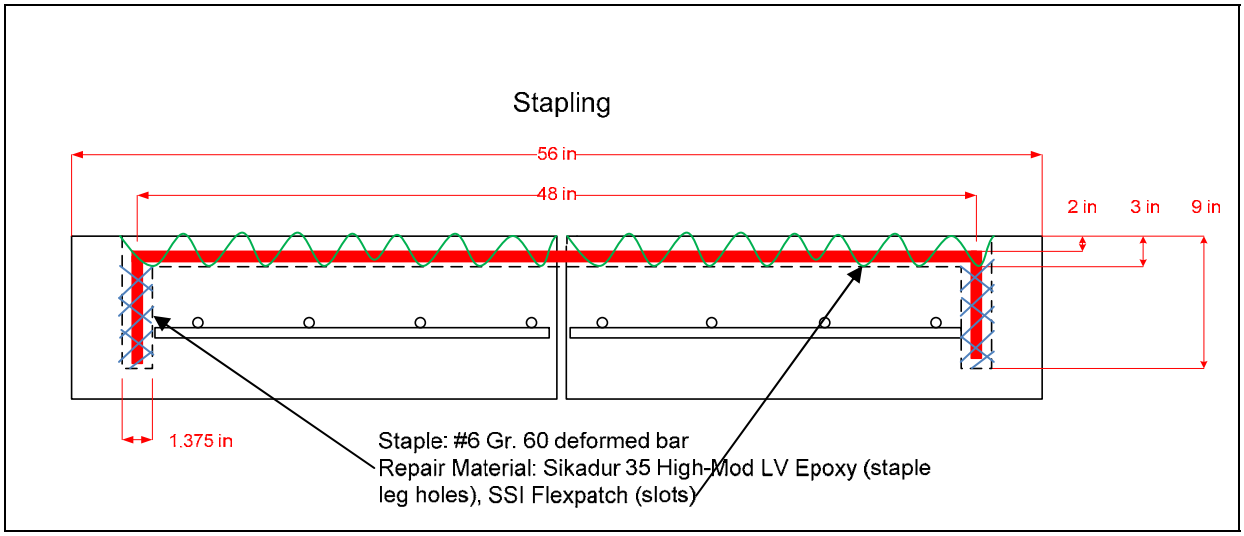

Figure 4.21: Staple Specimen Repair Bar Diagram

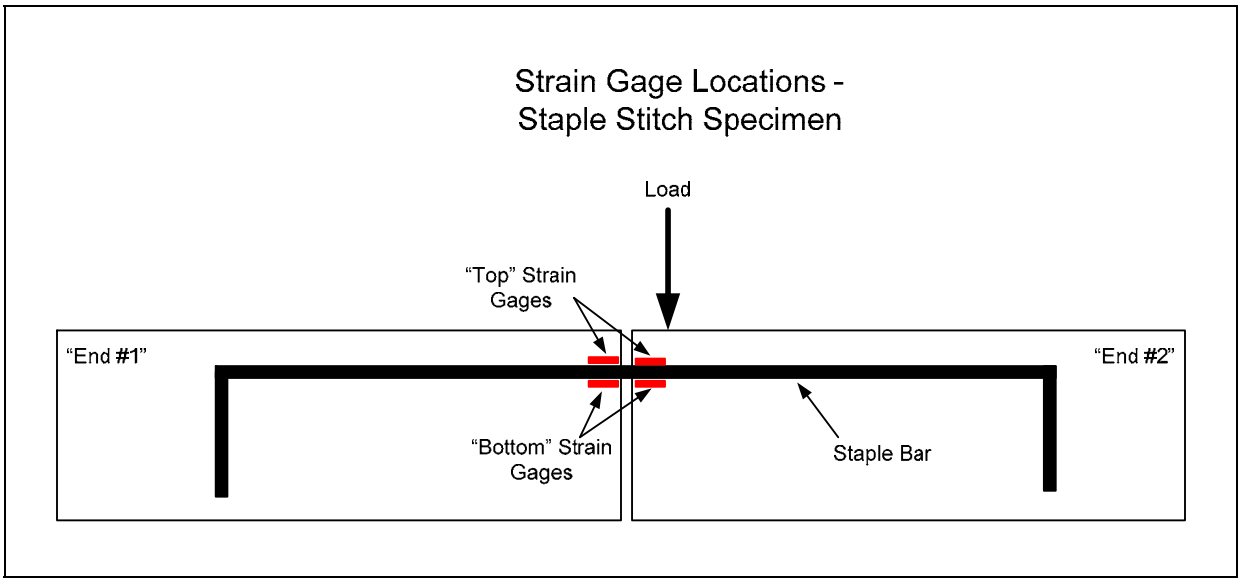

Figure 4.22: Strain Gage Locations on Staple Specimen

Headed bar

The headed bar specimen was the first to be cast, and changes were made to the typical specimen dimensions afterwards. The specimen contained only one repair bar instead of two, and was 18 in. wide and 14 in. thick. The slot for the bar was cut one inch deeper than the other specimens, but the heads on the bar raised its height in the slab, which put it very close to the same level as the slot stitch bars.

The headed bar specimen was tested to determine whether adding heads would improve the performance relative to a conventional non-headed reinforcing bar. Heads were attached to a #6 Grade 60 deformed bar by welding four 1/8 in. thick, 1.5 in. diameter flat washers to each end of the bar. The bar was placed in the concrete and the slot was filled with Sikaquick 2500. No sensors were installed on the bar (Figures 4.23 and 4.24).

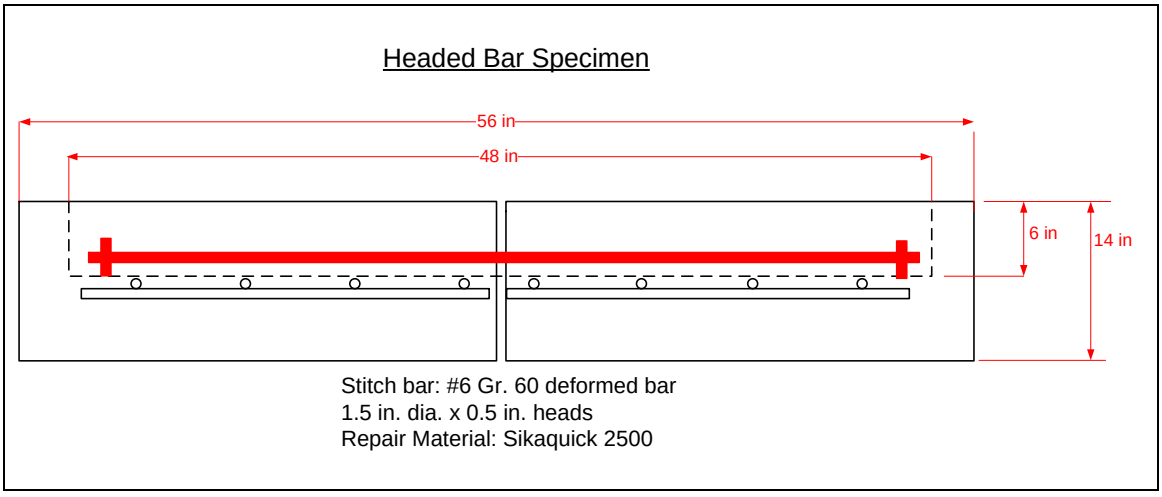

Figure 4.23: Headed Bar Specimen

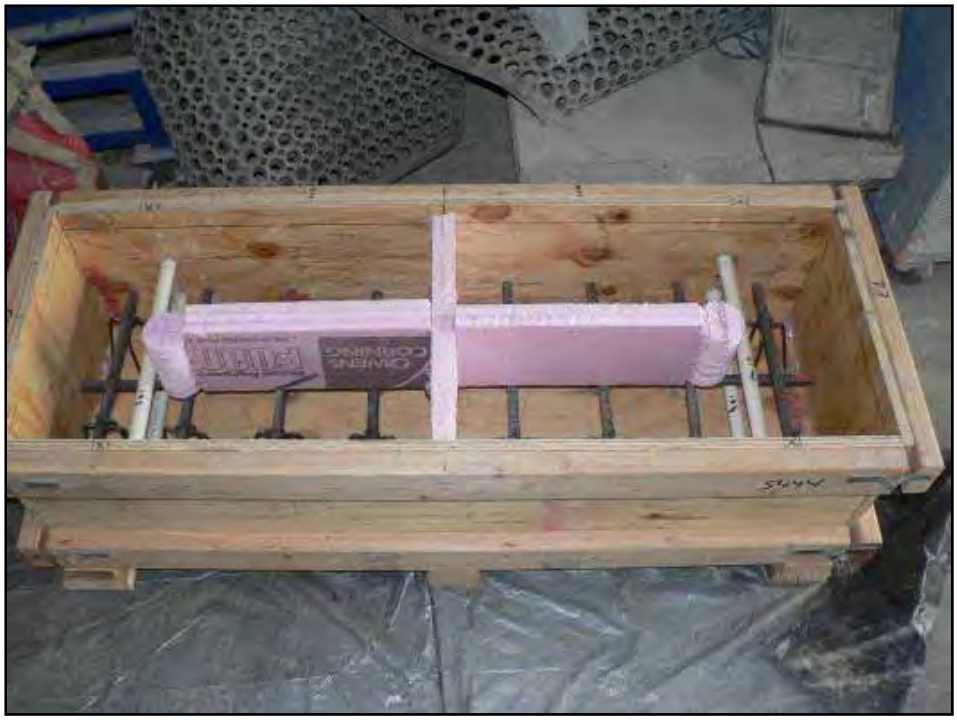

Figure 4.24: Headed Bar Specimen Before Casting

Loading Conditions

A reaction frame was fabricated at Ferguson Structural Engineering Laboratory which utilized an existing strong floor to provide reaction against loads. A series of steel beams was used to carry the load from the ram to tension rods connected to the strong floor.

Shear Test

The shear test was designed to simulate a truck edge- loading condition: the most severe shear condition for repair bars and the surrounding concrete occurs when a truck wheel is driven very near the edge of one slab (next to the longitudinal construction joint). The loading condition can be thought of in terms of a simple beam statics problem; the closer to one support the load is placed, the higher the reaction at that support. In the case of a pavement, the repair at the longitudinal construction joint can be thought of as synonymous with the simple beam support. In reality, the support conditions are more accurately described by a uniform distributed support, but the simplifying principle is still valid.

For shear tests, the side of the specimen subjected to direct loading by the hydraulic ram is referred to as the “loaded” side while the side not subjected to direct loading is referred to as the “non-loaded” side. Specimens were elevated from the floor using concrete blocks. Neoprene bearing pads were used to approximate base/subgrade support in the field. Bearing pads totaling four inches in thickness were used to support the non-loaded sides of the specimens. Figures 4.25 through 4.27 show the test setup.

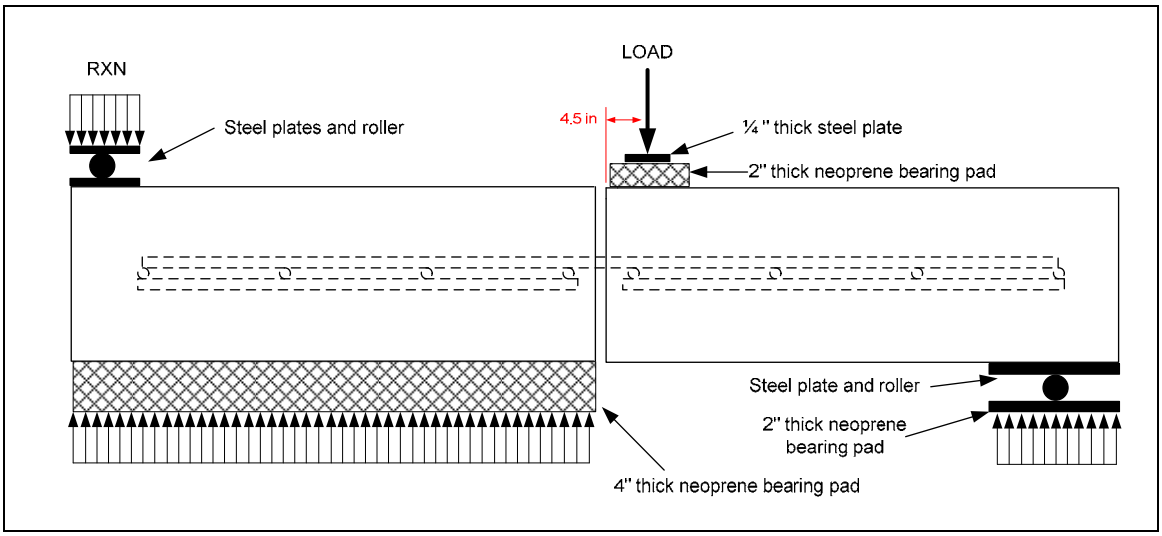

Figure 4.25: Shear Loading Test Setup

Figure 4.26: Shear Loading Test Frame (Side View)

Figure 4.27: Shear Loading Test Frame (Front View)

Flexure Test

The flexure test was developed to simulate the rise and fall of pavement edges in areas with soil that is known to shrink and swell. Soil near the middle of a pavement is usually saturated, but the moisture content of soil near the pavement edges fluctuates to a much higher degree as weather changes. Swelling and shrinking of the soil due to changes in moisture content may cause the pavement edges to rise and sink, thus introducing a flexural loading condition. The flexural test was designed to simulate this behavior. Figure 4.28 shows the test setup.

Improperly sealed joints often accumulate dirt, rocks, and other material that clog the joint and obstruct its movement. This material is not rigid, but offers some resistance to joint closure; hence it will be referred to as "semi-compressible material." A wood 2 x 2 was wedged in the joint flush with the bottom of the slab to simulate the semi-compressible material. The load was applied by a hydraulic ram in the middle of the specimen, 6.25 in. from the edge.

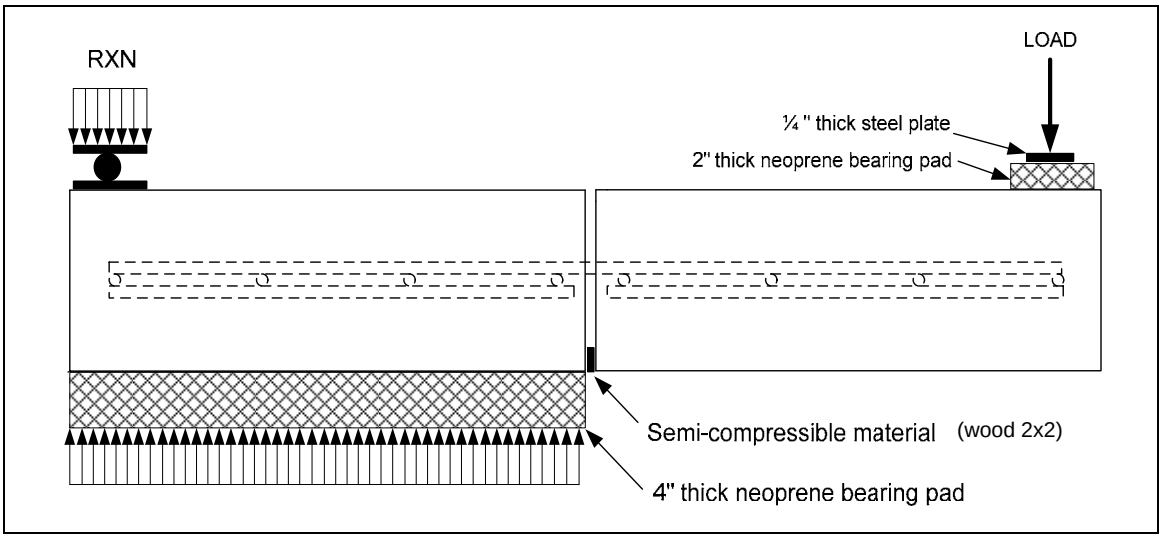

Figure 4.28: Flexure Loading Test Setup

Tension Test

The purpose of the tension test was to create a loading condition that separated the longitudinal joint without introducing shear or flexure into the specimen. The headed bar stitching was the only method tested; the primary purpose was to qualitatively observe the failure mechanism created by a headed bar.

One hydraulic jack was placed on each side of the specimen. Loads were applied to the specimen by attaching steel angle brackets to each side with threaded rods running through the specimen via plastic ducts cast into the specimen (Figures 4.29 and 4.30).

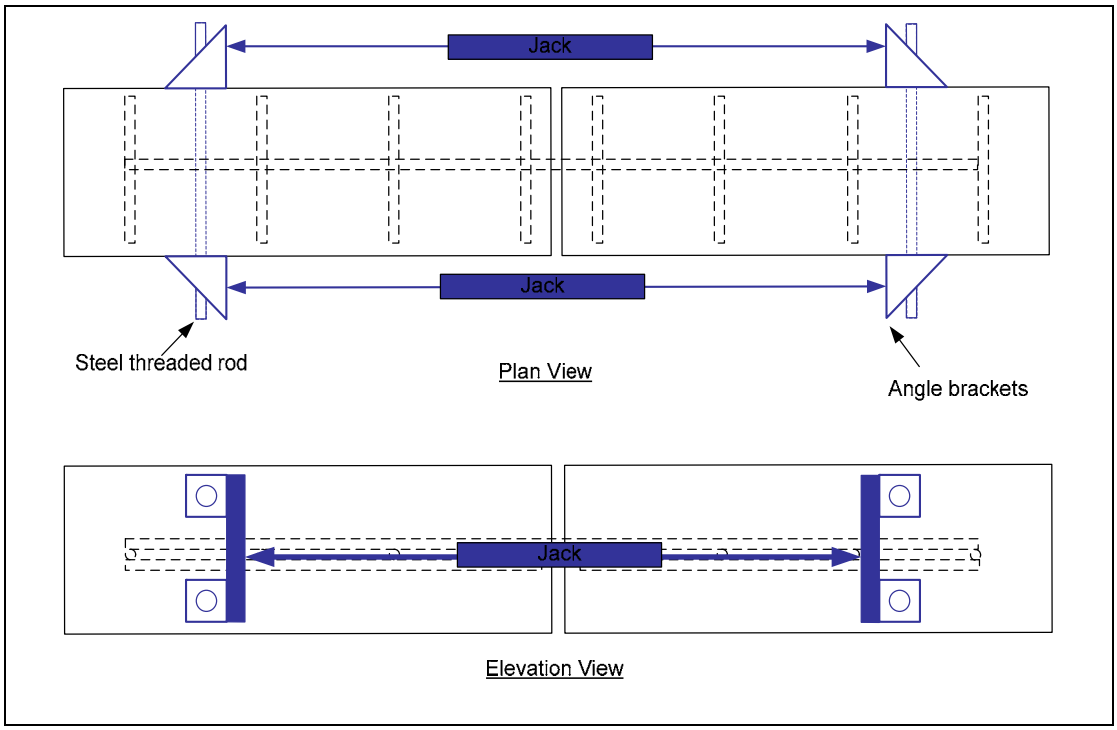

Figure 4.29: Tension Test Setup

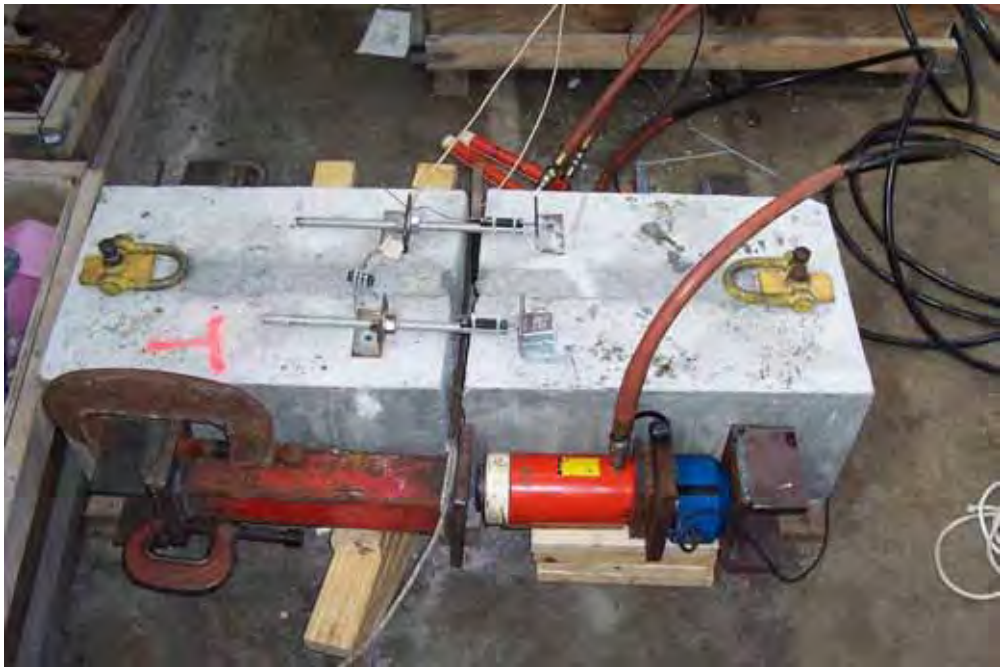

Figure 4.30: Headed Bar Specimen Before Loading

4.2.3 Test Results

Shear Tests

References to specimen sides are in accordance with the following convention: “left side” refers to the left hand side of the loaded portion of the specimen if one were standing behind the non-loaded portion looking toward the loaded portion.

Cross Stitch

Note that the shear test theoretically produced symmetric loading conditions with regard to the steel bars in the slot stitch and staple specimens. In other words, the two bars were the same distance away from the load, had the same amount of concrete cover, and were both oriented symmetrically in the vertical and horizontal planes. Because of the geometric symmetry, the bars had the same stiffness, which resulted in an even distribution of load between the two bars. The cross stitch specimen, on the other hand, had an asymmetric loading condition: the two bars were oriented oppositely in the vertical plane (as they are installed in the field). One bar was in compression and the other in tension. The load-deflection behavior observed during the test led to the following hypothesis by the research team: The bar in compression, due to the relatively flat angle of inclination, acted primarily as a bending member, which is much less stiff than a bar in compression. As a result, the tension bar took a larger portion of the load. Load-deflection behavior was determined by a combination of the independent results of the two bars if they were loaded on their own. The net result is believed to be more heavily influenced by the behavior of the tension bar. Behavior of the specimen during testing and the post-processed load-deflection data support this assertion.

The cross stitching specimen showed roughly linear behavior up to the point where the tension bar pulled out of the concrete hole (Figure 4.31). Two failure mechanisms could have led to this pullout: (1) bond failure of the epoxy itself and/or (2) failure of the epoxy-concrete interface. Examination of the specimen after the test did not reveal which of these mechanisms caused the failure. At the point of pullout, a dramatic drop in load was observed, along with a corresponding increase in deflection. Load carrying capacity did not completely diminish, however, due to the presence of the compression bar.

As the specimen was loaded further, the stiffness was similar to that shown at the beginning of the test. At approximately 11.8k, the stiffness decreased significantly until the termination of the test. The initial stiffening of the specimen after the failure of the tension bar is thought to be due to the fact that the load was transferred to the compression bar, and the geometry of the specimen at that point prevented significant bending from occurring in the bar. As the test progressed, the compression bar began to rotate, inducing more bending than compression in the bar, which caused the system stiffness to decrease. The test was terminated at 22.6 k because the large amounts of deflection of the specimen introduced unsafe geometry between the loading ram, loading beam, and the specimen. Figures 4.32 and 4.33 contain photographs of the specimen during testing. Maximum load was 22.6 k.

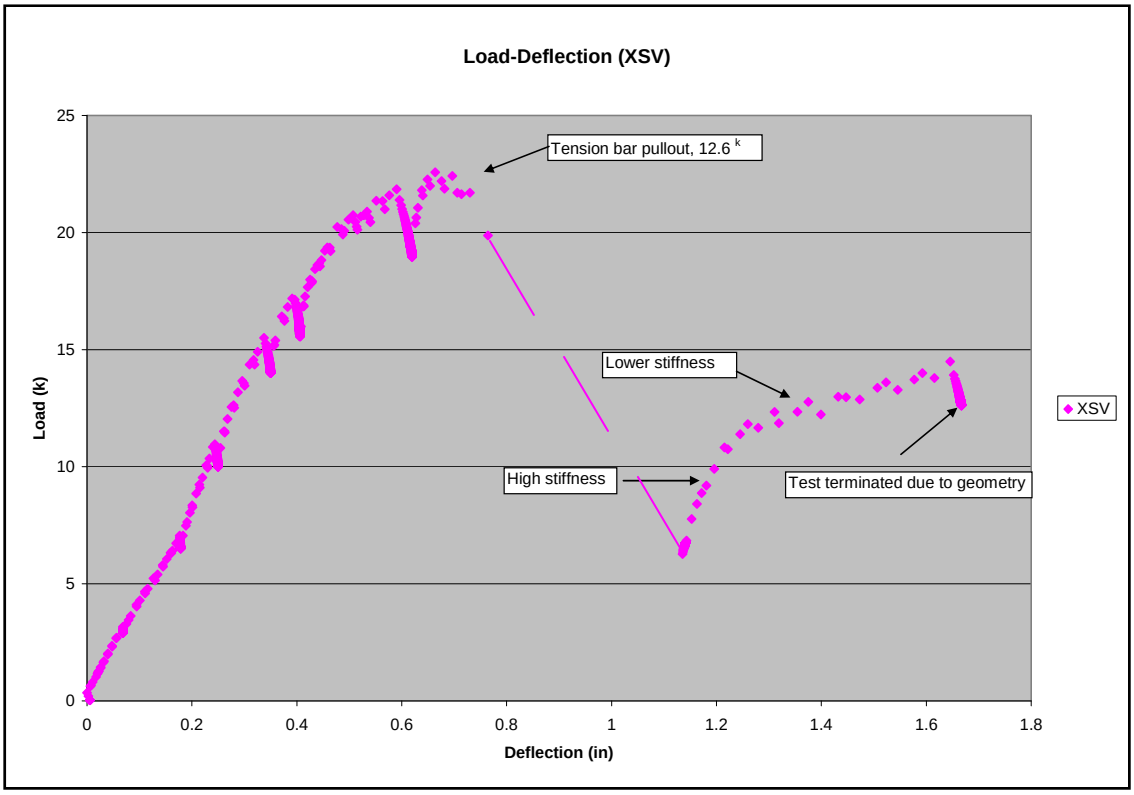

Figure 4.31: Load-Deflection Graph for Cross Stitch Shear Test

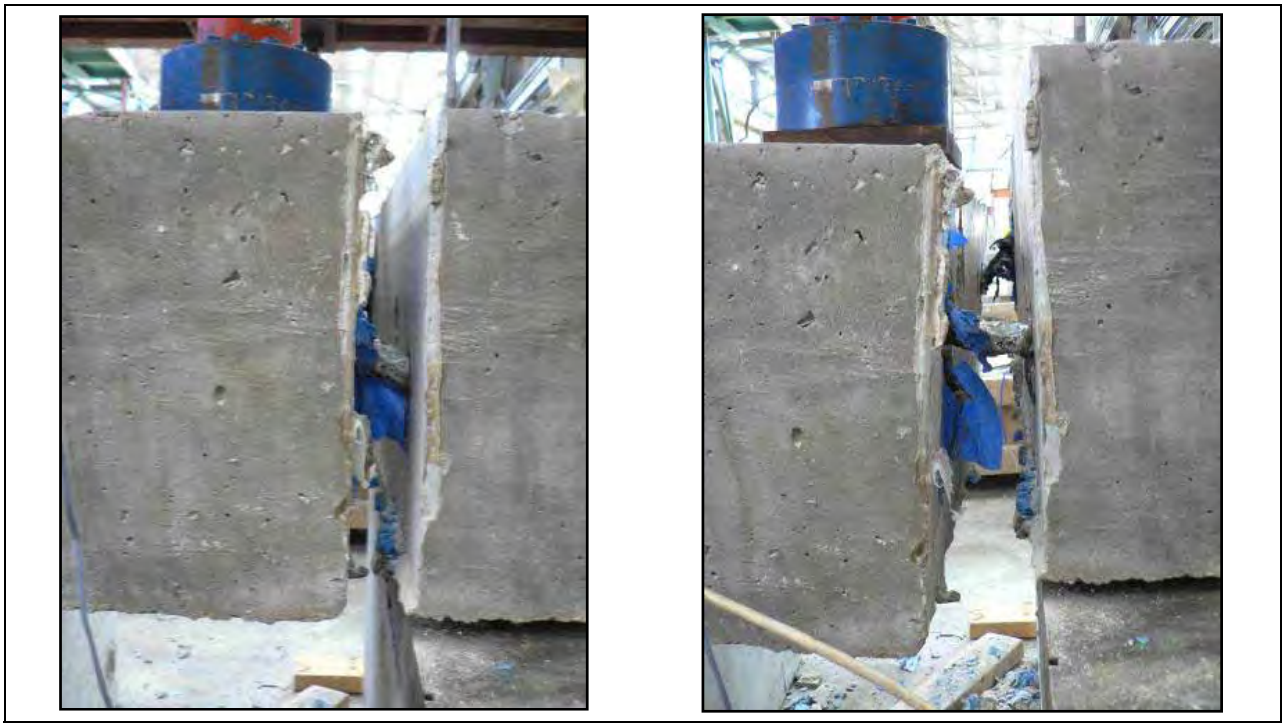

Figure 4.32: Cross Stitch Specimen Before (L) and After (R) Shear Test

Figure 4.33: Cross Stitch Specimen at Failure Under Shear Load

Staple

The staple specimen showed linear behavior up to a load of approximately 5.2 k (Figure 4.34). Strain gage data showed that the behavior of the specimen mirrored the behavior of the steel bars (Figure 4.35)[1]. Nonlinear behavior dominated from load values of 5.2 k to 6.7 k. Failure of the repair material on the left side of the specimen occurred at 6.7 k (Figure 4.36). After this failure, the load carrying capability of the specimen was reduced, and the load dropped to approximately 6 k, at which time the repair material on the right side of the specimen failed (Figure 4.37). Load cell readings dropped rapidly, and a corresponding increase in deflection was observed. The specimen resisted a load of approximately 4.4 k while undergoing large deflection. The test was terminated at a load of 4.4 k and a deflection of approximately 1.5 inches. At this point, the specimen could have been loaded further due to the presence of intact repair material behind the failed portions of material. The test was terminated, though, because further testing would have introduced unsafe geometry into the loading setup.

Figure 4.36 through 4.39 show the failure of the repair material on the left and right sides of the specimen. As can be seen from Figure 4.39, the left side of the specimen failed due to the repair material losing bond with the walls of the slots cut in the concrete. The right side of the specimen failed due to the repair material itself failing in shear. This is evidenced by the diagonal shear surfaces (“shear cone”) propagating through the repair material. Maximum Load was 6.7 k.

[1] The slope of the load-deflection curve of the specimen (Figure 5.29) from a load of 0 k to approximately 5.2 k closely follows the shape of the load-strain graph of the bars (Figure 5.30). The behavior of the specimen during this load increment was governed the bending of the bars because gages at the top and bottom of a bar indicate strain of opposite sense or bending. Strain gages show that significant deformation of the specimen occurred due to the formation of plastic hinges in the bars at the faces of the concrete adjacent to the 1.5 inch joint. Data showed that these hinges began to form when the steel reached a strain of approximately 0.002, which is very close to the theoretical yield strain for grade 60 rebar. At approximately 6.7 k, the repair material began to fail, and deformation of the repair material began to govern the behavior of the specimen.

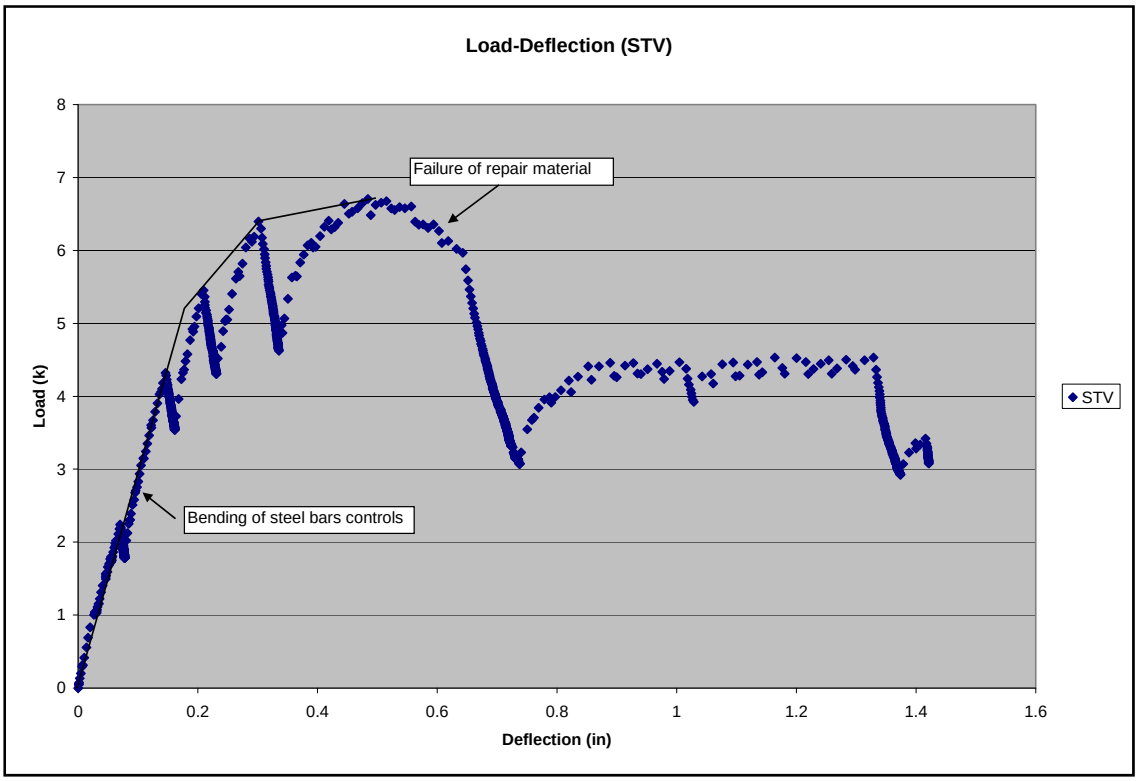

Figure 4.34: Load-Deflection Graph for Staple Specimen Shear Test

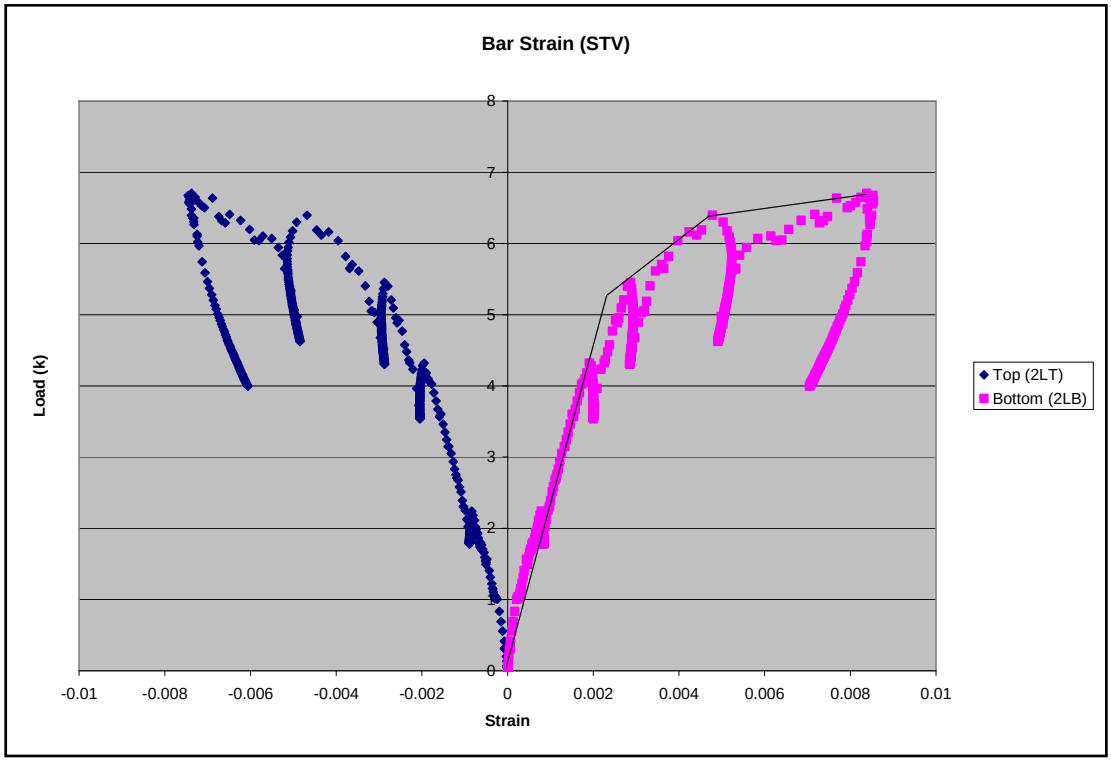

Figure 4.35: Strain Gage Data for One Staple Bar During Shear Test

Figure 4.36: Repair Material Failure (Left Side)

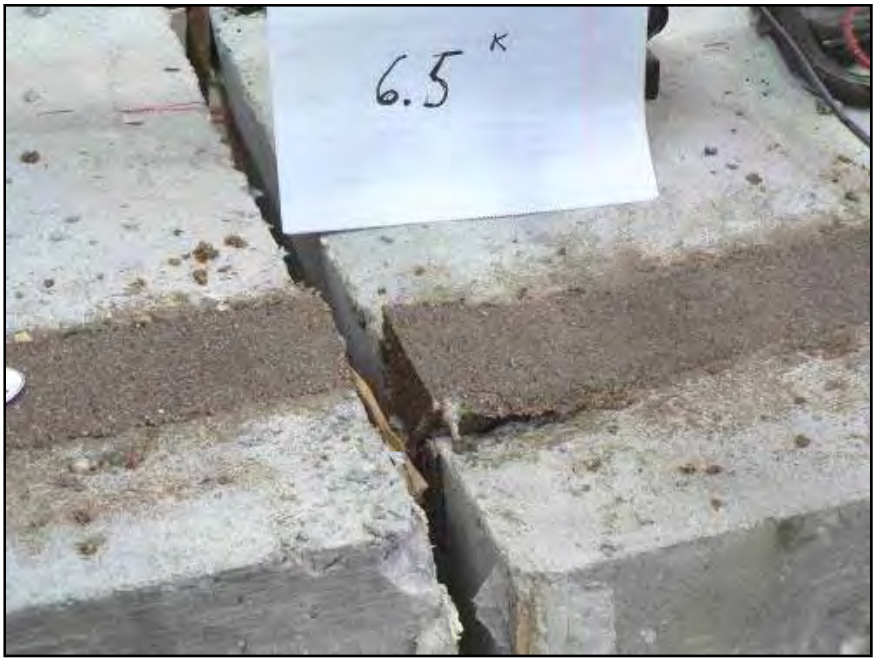

Figure 4.37: Repair Material Failure (Right Side)

Figure 4.38: Cross-section View of Staple Specimen After Testing

Figure 4.39: Left (L) and Right (R) Staple Bars After Testing

Slot Stitch

The staple specimen showed linear behavior up to a load of approximately 10 k, at which point the concrete near the edge of the specimen around the left bar began to spall. Visible cracking was observed at that point. A reduction in stiffness of the specimen occurred after initial cracking, as can be observed by the decrease in slope of the load-deflection curve (Figure 4.40). Loading approached 12 k when spalling occurred around the right repair bar. Load carrying capacity decreased at that point, and the load dropped to approximately 8.1 k. The specimen still resisted load after spalling around both bars, and the test was continued until additional spalling occurred around the left bar. At that point the load dropped to about 10 k, and then loading continued. The test was terminated at a load of 11 k due to the large rotation of the loaded side of the specimen.

Figure 4.41 shows slot stitch specimen at end of shear test, with Figure 4.42 showing the left side of the specimen after the end of the test. The pieces of loose concrete were removed to show the failure surface. The failure surface on the left side began directly beneath the repair bar in the repair material, and propagated through the interface between the repair material and the concrete. The failure surface revealed a combination of shear and tension failure of the concrete. Bond strength between the repair material and the concrete was high enough to prevent de-bonding. The failure surface on the right side was similar in nature to that of the left side, but much smaller (Figure 4.43). Maximum load was 12.0 k.

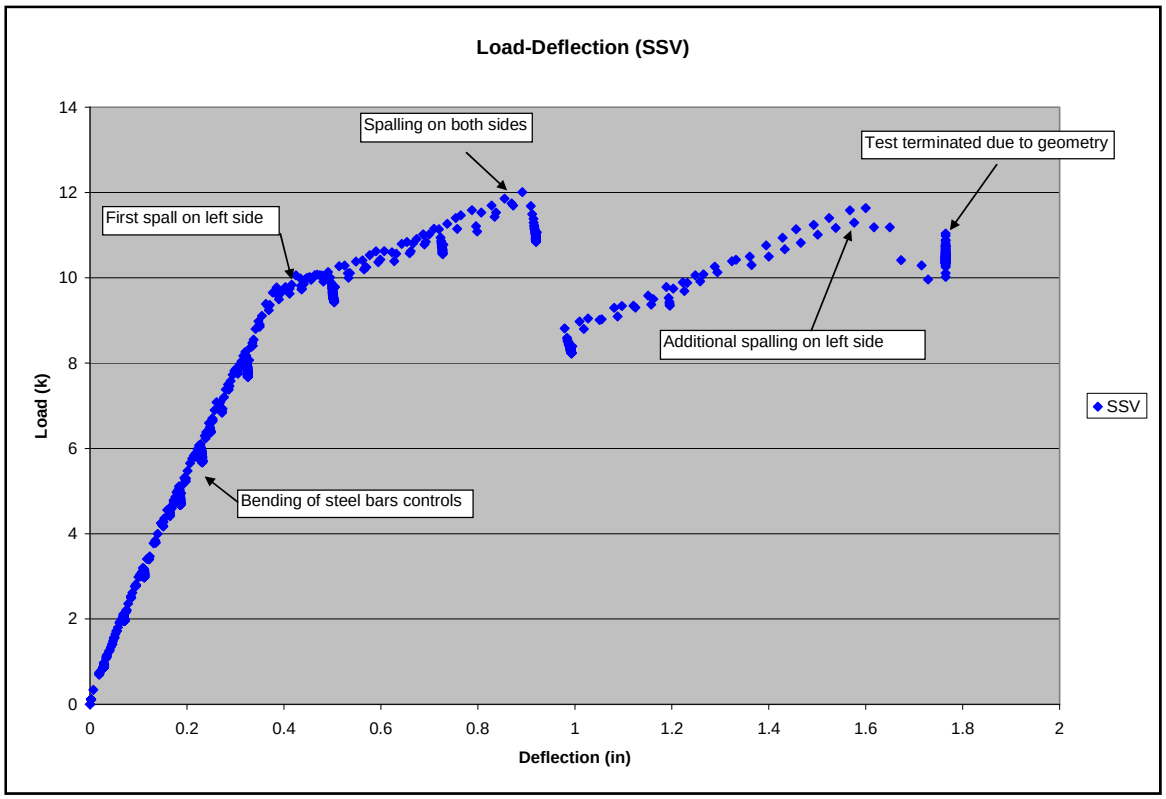

Figure 4.40: Load-Deflection Graph for Slot Stitch Shear Test

Figure 4.41: Slot Stitch Specimen at End of Shear Test

Figure 4.42: Left Side of Slot Stitch Specimen at End of Test

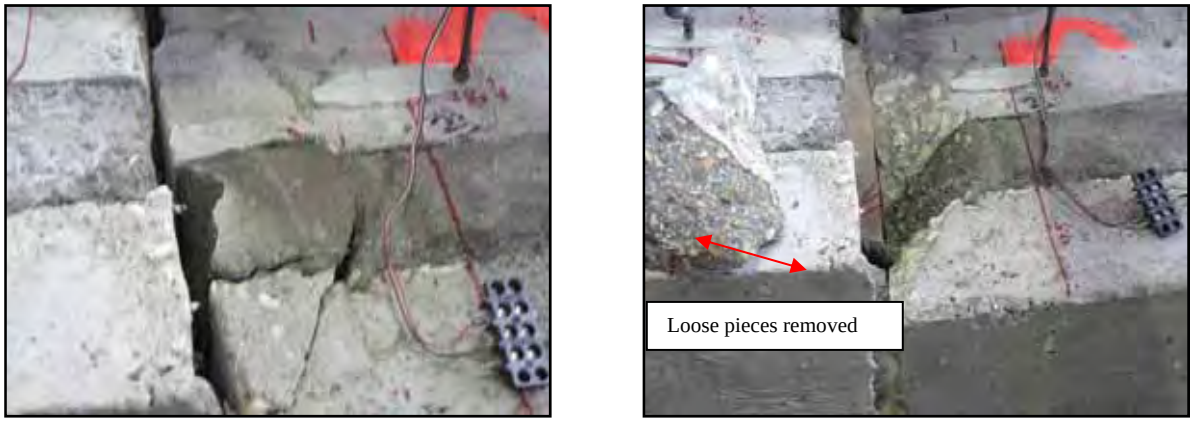

Figure 4.43: Right Side of Slot Stitch Specimen at End of Test

Flexure Tests

Cross Stitch

The cross stitch specimen carried a maximum load of 3 k. The test was terminated when the deflection at the load point reached approximately 4.5 in. because of unsafe geometry of the setup caused by the large deflection. See Figures 4.44 and 4.45 for photographs of the specimen during testing. Figure 5.42 shows the load-displacement behavior of the specimen, with a slight modification to the load parameter. Because the three repair methods had stitch bars set at different levels beneath the concrete surface, the resisting moment created by the tension force in the bars and the compression force of the wood block varies from specimen to specimen. The driving moment created by the load ("M") is divided by the internal resisting moment arm between the compression and tension forces ("d") and plotted against the deflection at the ram. The value M/d represents the theoretical force in the bars for slot stitching and stapling as those bars were oriented horizontally. For the cross stitching specimen, the couple force is not equal to the bar force because the bars are inclined and are subjected to bending as well as tension.

A malfunction in the data acquisition system prevented data for the first few load steps from being recovered. One data point for the peak load is known, and the shape of the load curve was estimated for the missing data points[2].

Figure 4.44: Cross Stitch Specimen at End of Test

[2] All other tests show that the three repair methods have similar slopes of the load-deflection curve up to a certain load level. The slope of the curve for the cross stitching specimen is assumed to be the same as the other two specimens up to a couple force of approximately 6.5 k. A softening of the curve is assumed to occur around the point of maximum load, followed by a downward slope towards the data where the acquisition system began to function properly.

Figure 4.45: Left Cross Stitch Bar at End of Test

Note: the spalling on the face of the concrete where the bar entered the specimen as seen in Figure 4.46 was not due to testing, but occurred during installation of the stitch bars during hammer drilling of the holes. The bar shown is loaded primarily in flexure, as can be seen from its curvature.

Figure 4.46: Right Cross Stitch Bar at End of Test

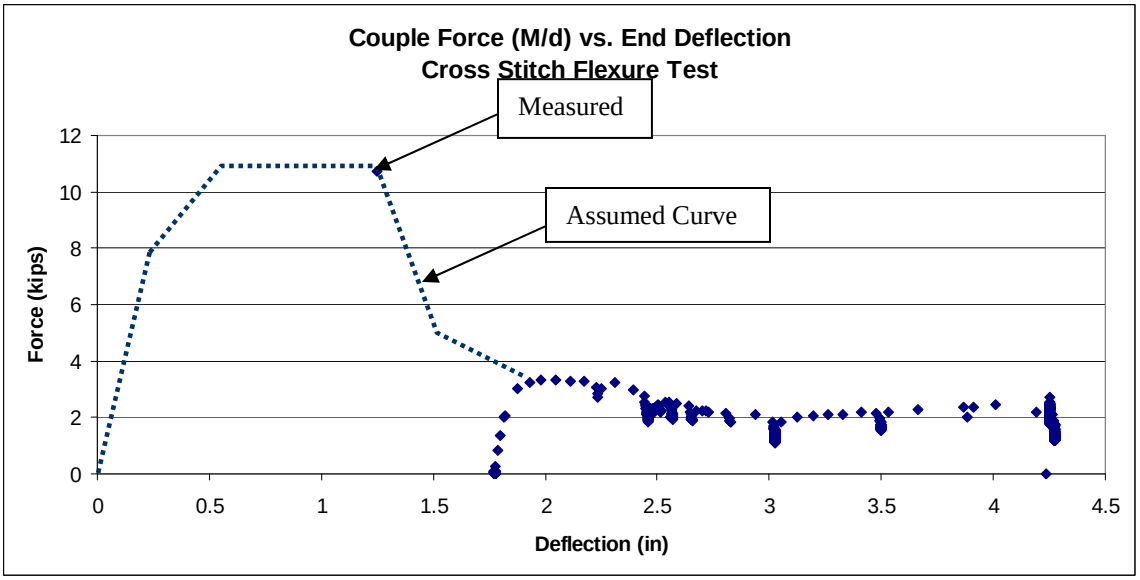

Figure 4.47: Couple Force vs. End Deflection for Cross Stitch Flexure Test

Strain gage data suggested that the bars yielded prior to the beginning of proper function of the data acquisition system. None of the gages were still reading when the data collection began, and at least two of the gages had visibly detached from the bars due to shearing of the wires by large deflections.

Staple

Figures 4.48 and 4.49 below show the staple specimen at the termination of testing. The specimen never actually "failed"; no cracks or spalls in the repair material or concrete were observed and the specimen continued to carry increasing load at the end of the test. The test was terminated because the large amount of deflection of the loaded side of the specimen introduced unsafe geometry into the testing frame. Field repairs would likely never experience such deflections, so to continue the test would have been superfluous.

Figure 4.48: Staple Specimen at End of Flexure Test (1)

Figure 4.49: Staple Specimen at End of Flexure Test (2)

Figure 4.49 shows the top of the staple specimen at the end of testing. No obvious distress was observed in the repair materials. Material used to fill the jointmeter slot spalled and began to break off at large deflections. See Figure 4.50 for load-deflection behavior of the specimen.

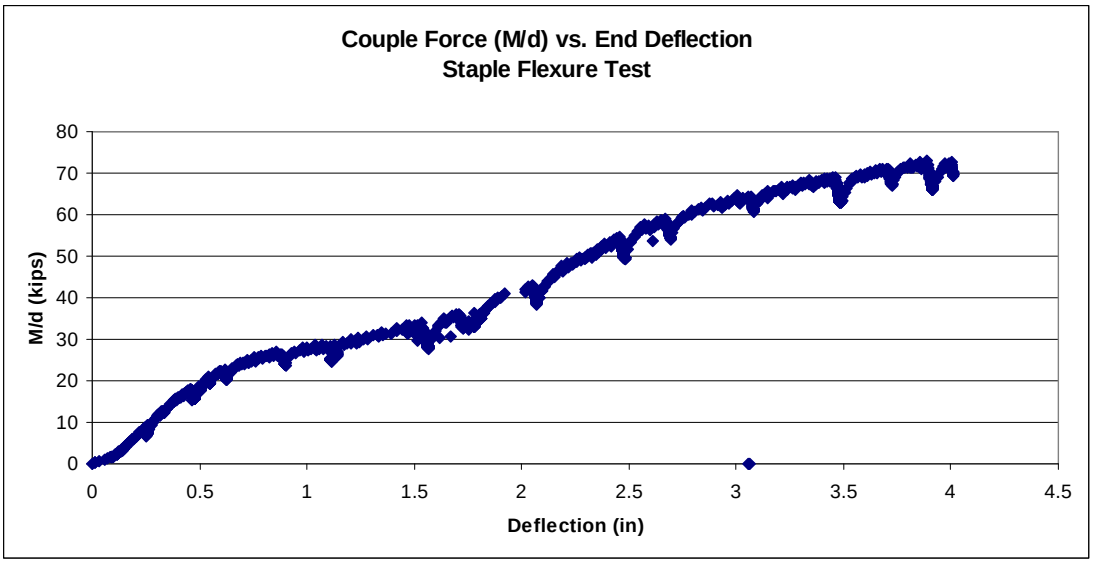

Figure 4.50: Couple Force vs. End Deflection for Staple Flexure Test

The specimen showed a "softening" of the force-deflection curve at around 20 k, then stiffened around 30 k. From 30k until the end of the test, roughly linear behavior was seen. The cause of the softening of the specimen at from 20 to 30 k was likely the top of the staple bars yielding in tension. Figure 4.51 shows strain measurements from the bars at several load levels. Gauges on the top side of each staple bar reached yield at an applied load of 12 k at gage 2RT and 7 k at gage 2LT. The 7 k load corresponded to a couple force (M/d) of about 20 k, and the 12 k load corresponded to a couple force of approximately 30k. This showed that in the range of M/d of 20 to 30 k, tension yielding occurred on the tops of both stitch bars, which is consistent with softening of the M/d – deflection curve in that region.

The staple specimen performed very well, showing very high flexural strength. The SSI repair material did not deteriorate, and anchoring the staple legs with epoxy appeared to significantly contribute to the flexural strength of the specimen by rigidly fixing the ends of the bars.

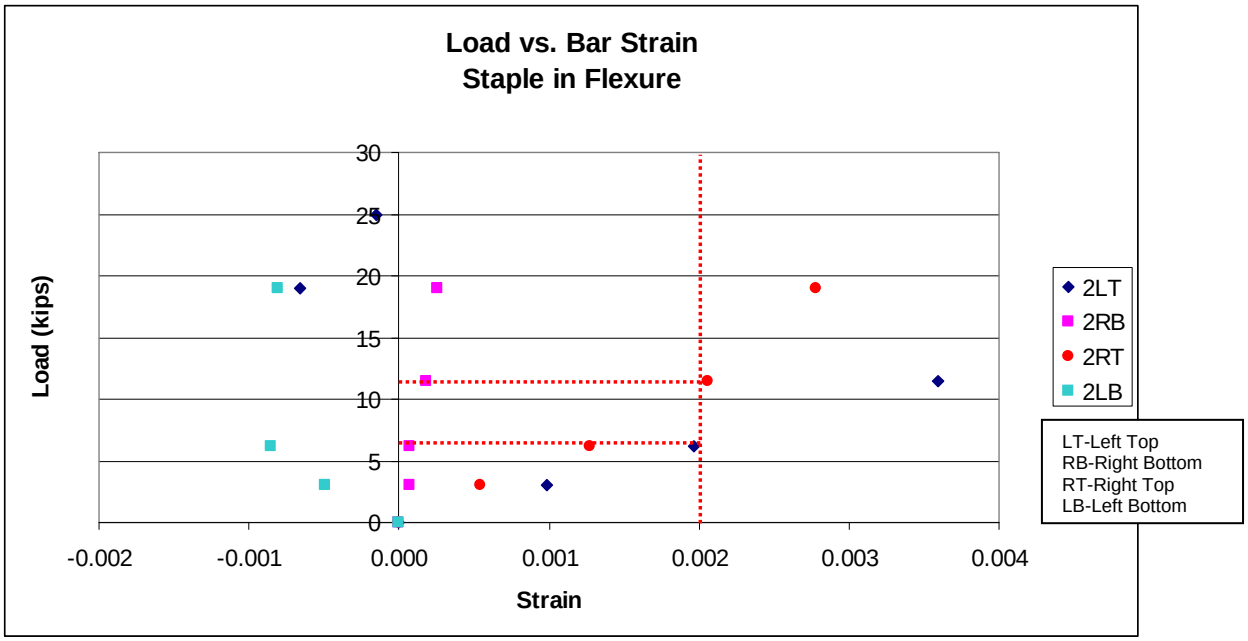

Figure 4.51: Staple Bar Strain Plot for Flexure Test

Slot Stitch

Figure 4.53 shows the specimen before loading commenced; Figures 4.54 through 4.56 shows the specimen at failure.

Figure 4.57 shows the load-deflection behavior for the specimen.

Figure 4.52: Slot Stitch Specimen Before Flexure Test

Figure 4.53: Slot Stitch Specimen at Failure

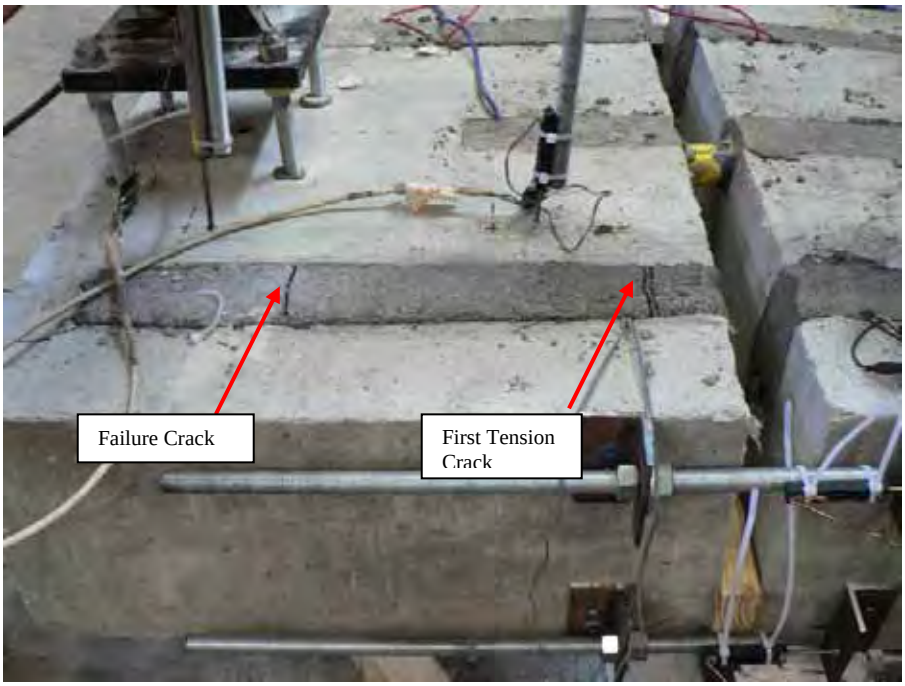

Figure 4.54: Cracks at Failure in Slot Stitch Specimen

Figure 4.55: Left Side of Slot Stitch Specimen at Failure

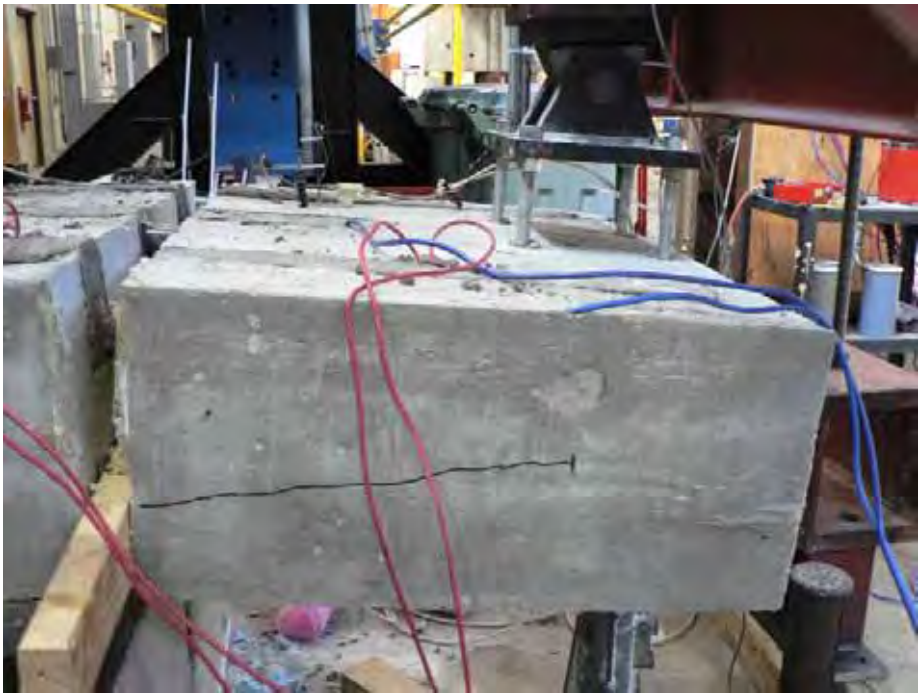

Figure 4.56: Right Side of Slot Stitch Specimen at Failure

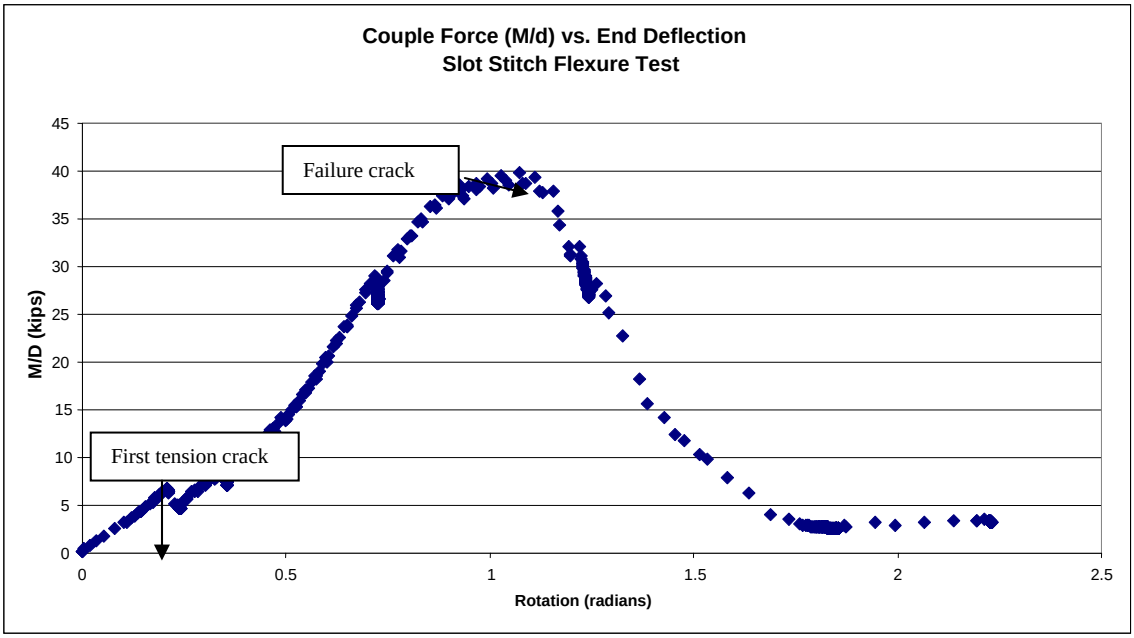

Figure 4.57: Couple Force vs. End Deflection for Slot Stitch Flexure Test

The "first tension crack," labeled in Figure 4.54, likely occurred around 7 k (the exact load was not recorded because the crack was not identified until it was fairly wide). The premature failure of this portion of the repair material was attributed to poor bonding to the walls of the slot. As the slots were being filled with repair material, a foam dam was installed in the simulated construction joint to prevent the repair material from leaking into the joint. This dam was somewhat flexible, and may have allowed the repair material to move away from the sides of the slot during curing, which would create poor bonding between the repair material and the concrete. As the specimen was loaded, the repair material lost bond, and the full value of stress present in the bar would have been transferred deeper into the slot (similar to the bond performance of steel bars in reinforced concrete beams as they crack). The bar would have been subjected to full tension strain at that point. Because the rigid repair material had very low tensile strength (like conventional portland cement concrete), it then cracked. A maximum load was reached at a coupled force of approximately 40 k, after which the load carrying capacity dropped sharply. Another tension crack formed in the repair material approximately two-thirds of the way into the slot at the maximum load. Additional cracking on the sides of the specimen were visible at failure, thought to be induced by radial bond stresses exerted by the repair bar on the repair material and propagating into the concrete.

For a point of reference, the bar force carried by each of the bars (20k each) is compared to the development length equations given in ACI 318-02 Section 12.2.2[3]. For the development

[3] Although the properties for portland cement concrete and the Sikaquick 2500 are not exactly the same, they are similar enough that the ACI development length equation can be used for an estimate of pullout strength. The assumed relationship between the modulus of rupture and compressive strength of concrete is given by Equation 9-10 (ACI 318-02):

$$f_r = 7.5\sqrt{f'c} \quad \text{or} \quad \frac{f_r}{\sqrt{f'c}} = 7.5$$

length that was provided for the stitch bar that failed, the ACI equation predicts bar pullout to occur at a bar force of about 32 k, which is higher than the actual load of 20 k. In the case of the test specimen, the bar did not pull out, but rather cracked the concrete in tension. This behavior, combined with the fact that the specimen failed at a load less predicted by the ACI equation, indicates that there was significant bending present in the bar (this is consistent with strain gage measurements) which induced additional tensile stresses in the concrete.

Tension Test

Shortly after commencing loading on the headed bar specimen (before yielding began), cracking occurred around the loading brackets on one end of the specimen. The test was stopped and a steel plate was installed in the simulated joint between the two ends of the specimen (Figure 4.60). The rams were re-set and loading restarted. Figure 4.58 shows the test data with the second test setup.

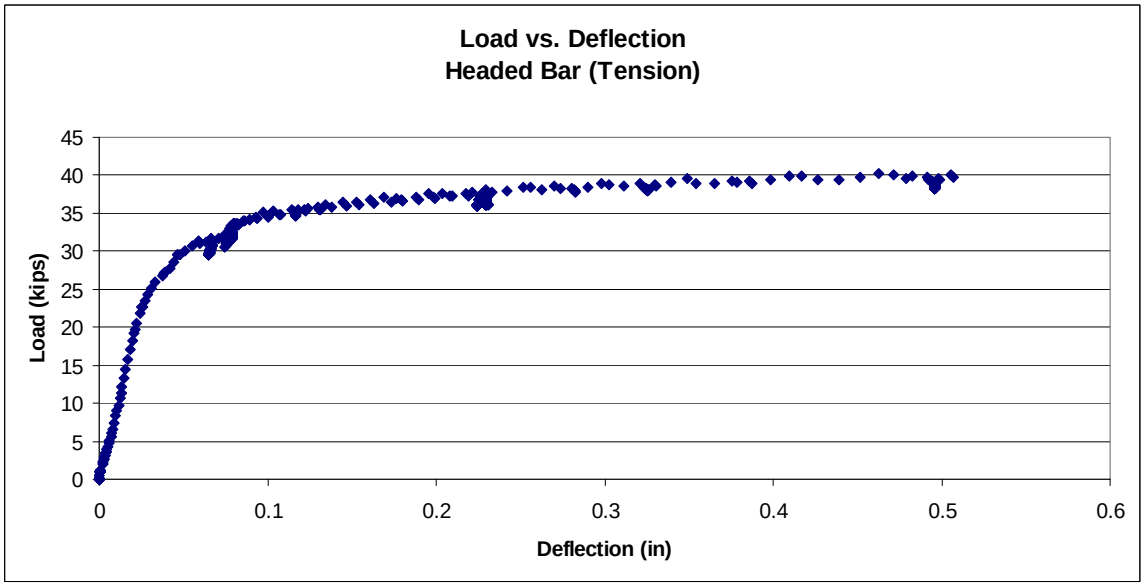

Figure 4.58: Load-Deflection Graph for Headed Bar Tension Test

The bar started to yield at a load of approximately 26 k, after which large deflections were observed. Noticeable cracking began to occur at around 32 k (Figure 4.60). Cracking patterns indicate a high concentration of bond stress near the edge of the specimen face around of

---

Using Sika's material specifications, $\frac{f_r}{\sqrt{f'c}}$ for Sikaquick 2500 is about 13.5, about twice the value for conventional concrete. Therefore the ACI development length equations should be conservative. Section 12.2.2 gives the following relationship:

$$l_d = \left(\frac{f_y \alpha \beta \lambda}{25\sqrt{f'c}} \right) d_b \text{ where } \begin{array}{ll} f_y = 60{,}000\,psi & f'c = 7125psi \\ \alpha = \beta = \lambda = 1.0 & l_d = 20.75in \end{array} \quad d_b = 0.75in$$

This equation is based on the assumption that 1.25 x f_y is to be developed. On this basis, for the embedment length provided to the bar that failed (taking into account the reduction due to the first early crack) the equation predicts that a bar force of 32k should be developed before the bar pulls out.

the bar. Cracks widened and eventually the concrete ruptured at a failure load of 40 k. See Figure 4.61 and 4.62 for the specimen at failure.

Figure 4.59: Cracking of Specimen at Loading Brackets

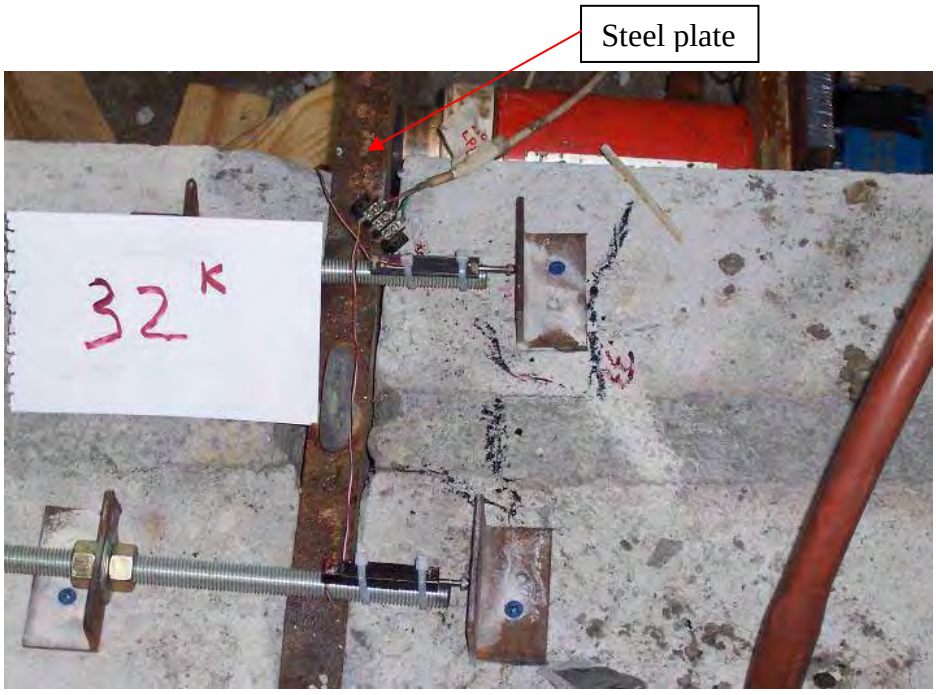

Figure 4.60: Headed Bar Specimen Cracking at 32 k

Figure 4.61: Headed bar Specimen at Failure

Figure 4.62: Headed Bar Specimen with Broken Concrete Removed

The specimen could likely have carried more load after test termination. After the completion of the test, the repair material was chipped out with a jackhammer in order to examine the condition of the bar heads. Figure 4.63 shows that they were in excellent condition. Had loading continued, the bar would likely have gone into strain hardening, and the heads would have increased capacity even further. However, the concrete around the remaining set of loading brackets ruptured at the same time as the concrete around the bar, so the test could not continue.

Figure 4.63: Exposed Head after Testing

4.2.4 Data Analysis

Comparison of Repair Methods

Shear Tests

Figure 4.64 shows the shear test load-deflection data for all specimens. All three specimens showed similar behavior to a load of approximately five kips. Past this point, significant differences in behavior between the specimens were observed. The cross stitch specimen showed significantly stiffer behavior to the point of failure load compared to the slot stitch and staple specimens. The staple specimen was the least stiff of the three, with the slot stitch specimen falling in between. The higher initial stiffness of the cross stitch specimen was attributed to the fact that the tension bar, (as noted above), which dominated the behavior of the specimen, had higher stiffness than the bars being bent primarily in flexure in the other two specimens. Note that the higher stiffness was not caused by different material properties, but rather the geometric orientation of the repair bars; a bar primarily loaded in tension is stiffer than a bar primarily loaded in flexure. The slot stitch bar showed stiffer behavior compared to the staple because of the stiffer repair material used to fill the slots. Appendix G gives repair material properties.

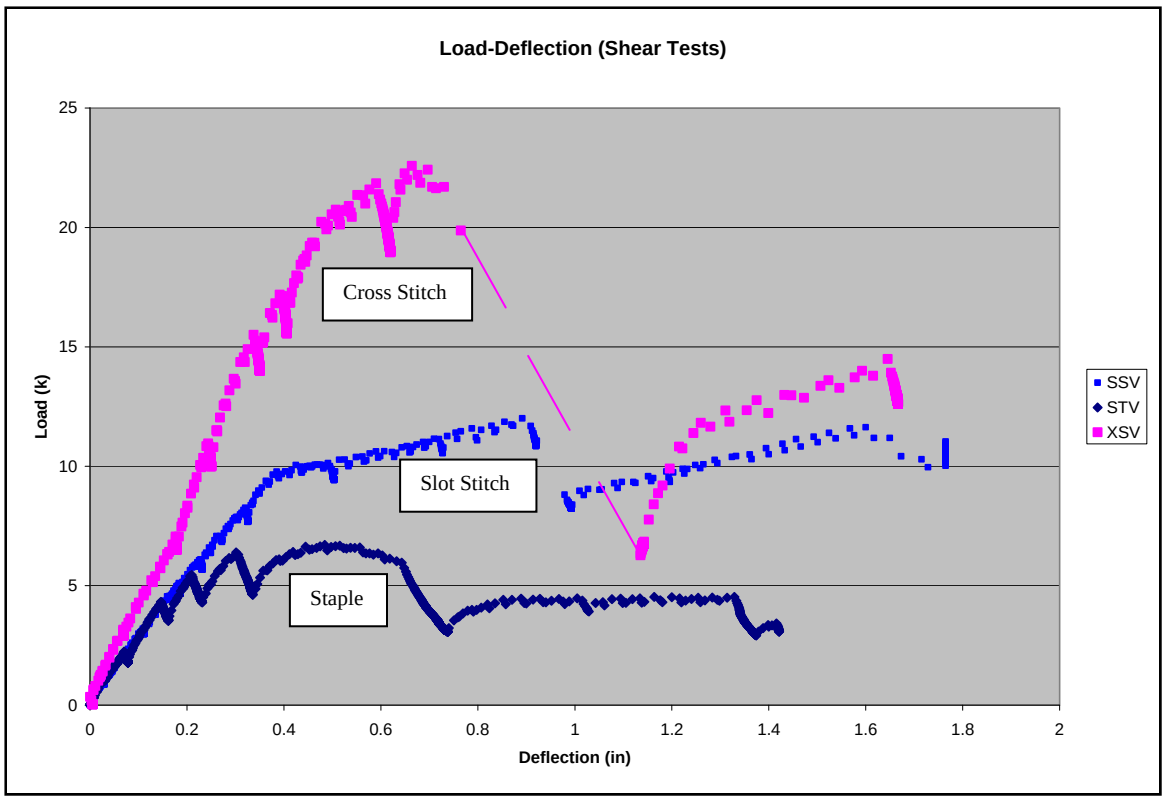

Figure 4.64: Load-Deflection Graph for Shear Tests

The cross stitch specimen resisted the largest load at 22.6 k, and the slot stitch and staple specimens resisted 12.0 k and 6.7 k, respectively. The ultimate load value for the cross stitch specimen may not be relied upon, however, because of the influence of the tension bar as noted above. In order to more accurately compare the results from each test, ultimate loads were adjusted to produce an ultimate-load-per-bar value. For the slot stitching and stapling specimens, this was accomplished by simply dividing the ultimate failure load by two to give the load per bar. The cross stitching specimen, however, did not share the load equally between the two bars as the other specimens did. The proportion of the load distributed to each cross stitch bar was estimated[4]. Ultimate load per bar values are summarized in Figure 4.65 below. Note that the values for the cross-stitch specimens are highly variable depending on the assumptions. A safe lower bound approach would be to assume the following: a truck driving along the edge of a pavement that is cross stitched would induce load into cross stitch tension bars and compression bars in an alternating pattern. When the tire is directly above a compression bar, assume the all the load is carried by that bar (no load sharing by adjacent bars). In that case, the maximum strength of the repair (per bar) would be limited to that of the compression bar.

Another approach is to assume that the wheel load would be distributed to a certain number of cross stitch bars. In that case, the behavior of the repair would be influenced by both the compression and tension bars. The failure load would fall in between the failure loads of the individual bars. To accurately determine the value of the failure load on this basis would require

[4] Significant bending of the compression bar was observed during testing. Plastic hinges appeared to form in the bar at the face of each side of the specimen. Assuming the plastic moment capacity of the bar is developed at each face, static analysis shows that the compression bar carried 4.2 k at failure. This means that the tension bar carried 18.4 k.

a level of structural analysis that is outside the scope of this study. Therefore the lower bound approach is used and the failure load of the cross stitching method is assumed to be at or near 4.2k.

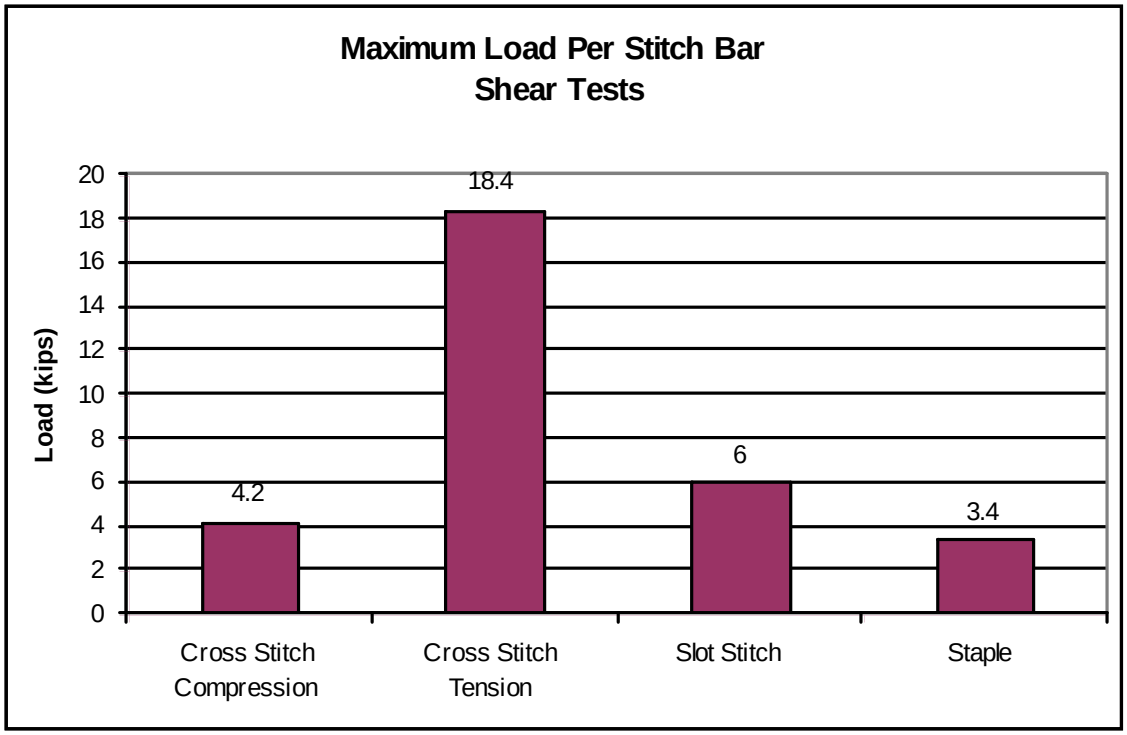

Figure 4.65: Maximum Load per Stitch Bar for Shear Tests

Ductility after first failure is worth noting, though it may not be especially influential in determining the most appropriate repair method for use in the field as noted in the conclusions. The cross stitch bar was the least ductile initially, exhibiting stiff behavior to the point of tension bar pullout, then exhibited a sharp drop-off in the load. Given the predicted failure mode of the compression bar under field conditions, the global performance in the field would most likely exhibit very brittle behavior. The slot stitch specimen was more ductile than the cross stitch specimen, showing bilinear load-deflection behavior before the first major drop in load. The staple specimen also showed significant ductility. A noticeable plateau occurred in the load-deflection graph before significant load drop-off.

Tests show that for loading conditions dominated by shear, the slot stitching performed the best of the three methods as it showed the highest load-carrying potential. Stapling and cross stitching showed less desirable behavior.

Flexure Tests

Figure 4.66 shows the M/d-Deflection curve for the flexure specimens. All three specimens showed similar initial stiffness. The staple specimen began to soften before the slot stitch specimen because one of the staple bars yielded before the other. It showed more ductile behavior than the slot stitch specimen due to the much lower elastic modulus of the Flexpatch in the staple specimen. The cross stitch specimen showed the least desirable behavior of the three

methods; a very low load level was achieved and very high deflections occurred. The staple specimen resisted the highest load at 26.7 k, followed by the slot stitch specimen at 11.3 k, with the cross stitch specimen resisting the smallest load at 3 k (Figure 4.67). The staple specimen clearly performed best for flexure type loading in terms of ultimate load.

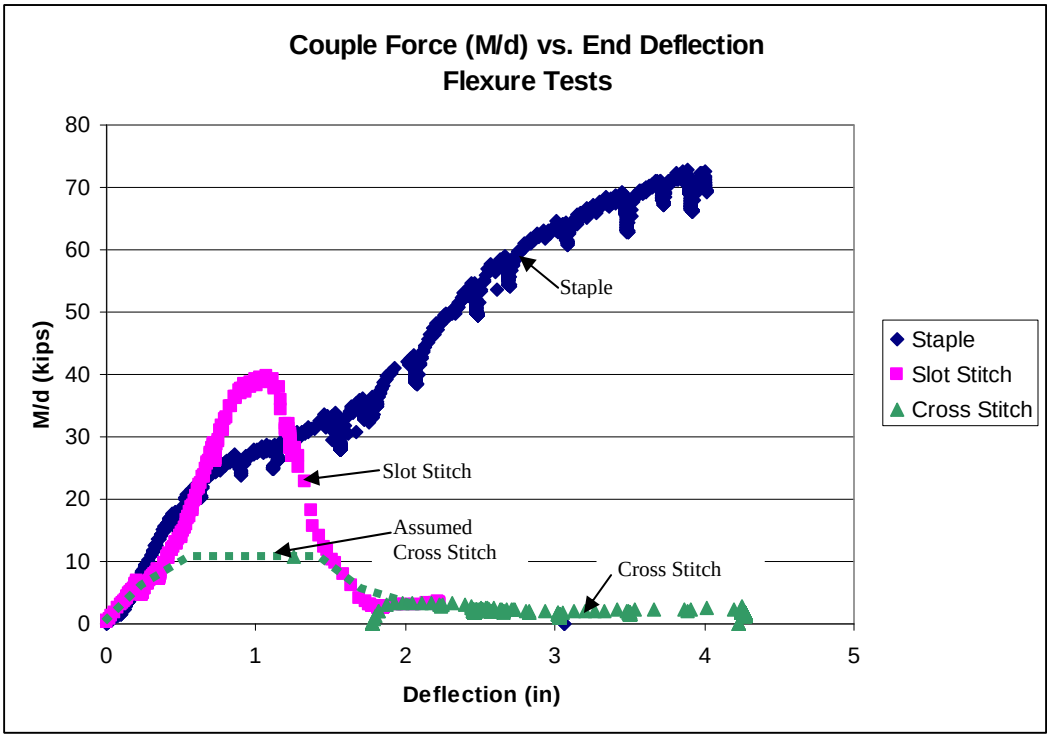

Figure 4.66: Couple Force-End Deflection Plot for Flexure Tests

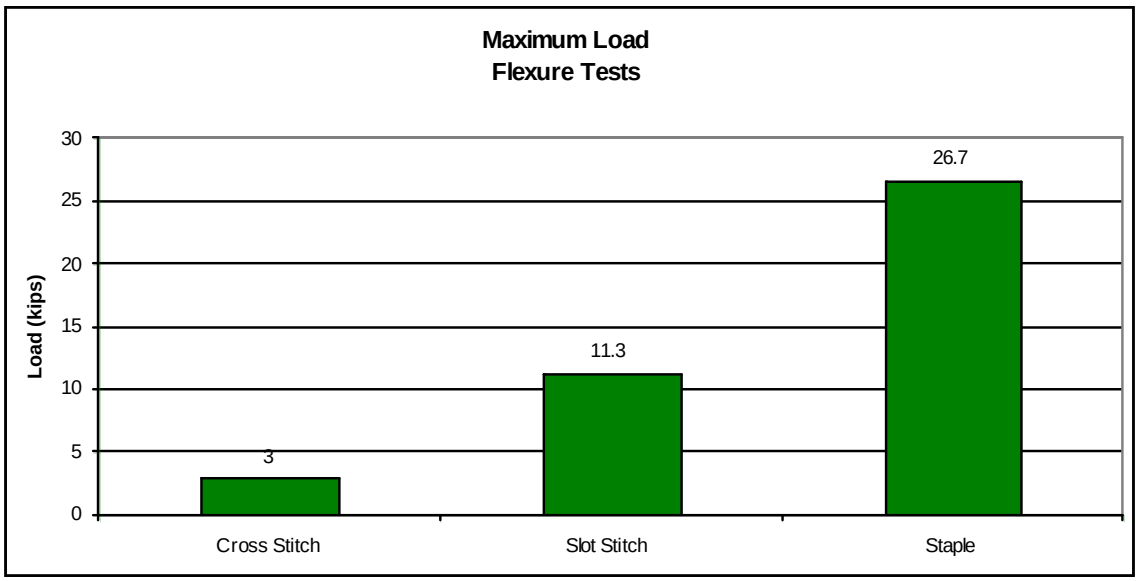

Figure 4.67: Maximum Load Summary for Flexural Tests

In choosing between staple and slot stitch methods for a particular application, one would need to decide upon a maximum allowable stress in the bar, and convert that to a bar force. The required bar force can be compared to Figure 4.66 to determine if slot stitching would perform acceptably or stapling would be required to resist the load. By the same token, an economic analysis can be performed to determine the most economical alternative between repairing with fewer staple bars or more slot stitch bars (Section 5.4.5 and Appendix H) At the present time, slot stitching appears to be the best alternative for flexural/tension loading. Field investigations show that the tension (shear) demand is likely more critical than flexure. If the bars for the flexural tests are assumed to have experienced pure tension (they in fact underwent tension and bending, but bending stresses were fairly small), then they can be compared to performance of tie bars observed in the field.

Tie bars that failed in the field had corroded bars. None showed signs of over-stressing (as cracking of concrete around the bar would show). The length of the tie bars (50 in. on new construction; 25 in. on each side of the joint) does not allow the full development of the bar in tension according to ACI 12.2.2, which requires 28 in. on each side in order to develop 125% of yield stress, or 67 ksi. Bars in the field, then, likely experience stress somewhat lower than yield stress. The slot stitching specimen failed when the bar stress reached approximately 45 ksi. If the maximum stress experienced by the bars is near this level, then slot stitching is clearly more desirable because of the lower cost (Appendix K gives material costs for each repair). In the future, as additional experimental testing is performed and repair methods are changed and refined, on economic analysis will be useful for comparison of alternatives.

Tension Test

The headed bar performed well, developing a higher load than the slot stitch bars in flexure. This was expected, as the slot stitch bars experienced combined tension and shear in the flexure tests, whereas the tension test induced pure tension. Headed bars would have a greater ultimate capacity in the field, but they do not offer any practical benefits over deformed, non-headed bars. In order to utilize the extra capacity of the heads, significant cracking must take place near the face of the concrete due to very high concentration of bond stress at that location. Cracking of such magnitude (at service levels) should not be tolerated for repairs of highway pavements, so the demand of the bar would be limited to a much lower level of stress. At this lower stress level, headed bars offer no advantages, and are actually less desirable due to higher cost.

Comparison of Test Data with Field Results

Cross Stitching

Data from the field suggest that the cross stitching experimental results are not representative of the global performance of the repair method in the field. Failures observed on US 59 in Queen City showed that breakout of the compression bars, which created spalling and cracking on the pavement surface, were the governing failure mechanism (Figure 4.68). This behavior highlights one of the primary differences between pavement in the field and laboratory specimens and illustrates the boundary conditions of in-place pavement. In the lab, specimens were not restrained because the width of the specimens and the loading and support conditions permitted relative translation and rotation of the segments across the joint. Much longer segments of the pavement containing at least 4 bar crossing the joint should have been tested.

The unsymmetrical loading condition on the bars (especially the cross-stitched bars) would not have occurred. The behavior of the compression bar would have been different.

Figure 4.68: Cross Stitching Distress on US 59

Quality control with regard to construction practices is likely a contributing factor in the failures seen on US 59. Many of the bars holes were drilled closer to the joint than that required. The closer the hole is to the joint, the higher the concrete stress and the likelihood of cracking and spalling. Cross stitching on SH 289 did not show this kind of distress. Construction practices there appeared to be more consistent, and although it cannot be conclusively stated that this is the sole cause of differing performance in the two areas, it is likely that it significantly contributed to the behavior.

Stapling

Field investigations did not uncover the kind of staple repair failures that were observed in the lab. Figure 4.69 below show bars on US 290 in Houston. The repair material appeared to have been worn off by traffic, but no evidence of further longitudinal joint separation was observed. No major faulting in the area was observed, and the pavement had 6 in. of asphalt-stabilized base when originally constructed, so the vertical loading condition simulated in the lab does not directly correlate with this particular section of pavement.

Figure 4.69: Deterioration of Stapling on US 290

Comparison of Test Data with FEM Results

Finite element modeling results were compared with testing data. Figure 4.70 summarizes the calculated maximum principle stress in the concrete for each of the loading cases.

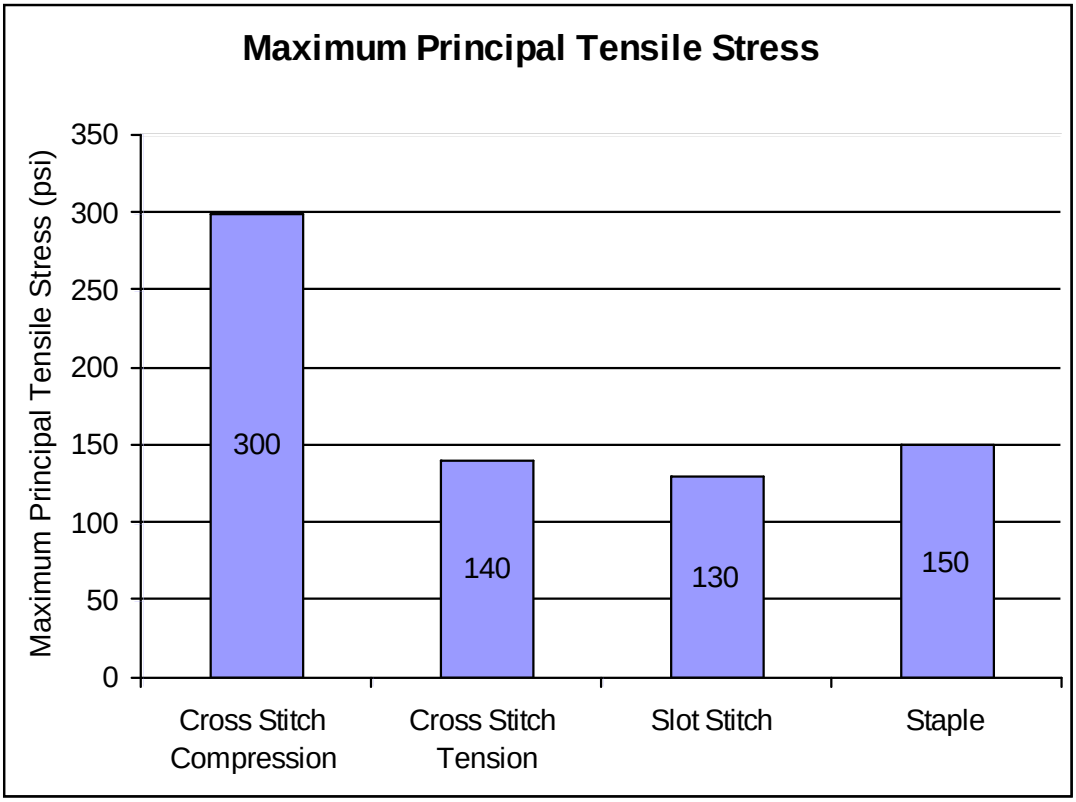

Figure 4.70: Maximum Principle Stress

Because different repair materials were used to fill the slots in the laboratory specimen, and those materials had different properties than plain concrete, the FEM results must be critically interpreted. The modeling results for slot stitching are likely the most comparable to lab testing conditions of the three repair types. Therefore the slot stitching lab specimen was used as a baseline for comparison of the methods.

Based on the FEM results, the staple specimen was expected to fail at a load 15 percent lower than the slot stitching specimen, had it been filled with the same type of repair material. The only difference between the two models was the placement of the bars within the slab (mid-depth vs. quarter-depth). This translated into a predicted maximum load in the lab of 5.2 k per bar for the staple specimen. The actual failure load, however, was 3.4 k. The additional reduction in load is most likely due to the weaker repair material used to fill the slots of the staple specimen.

The cross stitch bar in compression was expected to fail at 2.6 k, compared to the actual load of 4.2 k. The tension bar was expected to fail at 5.6 k, compared to the actual load of 18.4 k. One possible explanation for the higher-than-expected maximum load for the tension bar could be that the cross stitch bars used in the lab were approximately three inches longer than those assumed in the FEM. Because the governing failure mechanism for the tension bar was de-bonding of the bar with the concrete and/or epoxy, a longer bar would reduce the value of maximum bond stress, leading to a higher failure load. However, this factor alone does not explain the large discrepancy between modeling and testing data for the tension bar. Assumptions of the FE model should be re-examined and revised as needed in the future.

Qualitatively, the experimental testing results agreed with those of the FE modeling. Slot stitching induces lower stresses in the concrete than stapling, and testing showed that the slot stitch specimen carried a higher load than the staple. The cross stitch compression bar induced the highest amount of stress in the concrete, and resisted the smallest load during testing. The tension bar induced lower stresses in the concrete than the compression bar, and the tension bar resisted a higher load than the compression bar. Therefore the FEM results can be used to compare the expected field performance of each repair method in relation to the others.

Evaluation of Repair Materials

Shear Loading

Shear loading creates the tendency for a shear cone-type failure to occur in the specimens. In order for this failure mechanism to fully develop, the failure surface must propagate from the repair material into the concrete and engage the diagonal tension strength of the concrete. Bond strength, then, is the most important material property for this type of loading condition.

The Sikaquick 2500 performed very well in shear loading; the failure surface began at the bottom of the bars and propagated from the repair material into the concrete across the material interface. Bond strength was high enough to prevent the repair material from failing at the interface with the concrete. In effect, the repair material allowed the bars to behave as if they were embedded in monolithic concrete. The Flexpatch did not show great resistance to shear type loading. One slot failed in bond, and the other in shear (which is actually a diagonal tension failure). The full capacity of the repair material cannot be directly compared to that of the Sikaquick, though, because the staple bars were placed considerably closer to the surface of the specimen. If they had been embedded deeper, the specimen would likely have carried more load,

but the material would probably have still failed in bond, and therefore the strength of the concrete still would not be utilized.

The RedHead G-5 anchor bolt epoxy performed well. However, the material failed before the concrete, indicating that either the failure occurred in the epoxy itself or at the epoxy-concrete interface. The performance of this material is heavily dependent on construction methods. Good bond between the epoxy and the concrete requires cleaning of the holes and steps must be taken to ensure the epoxy does not flow out of the hole and into the joint or crack. The exact formulation of the epoxy is likely less important than quality control in the field.

Flexure Loading

Bond and tensile strength are the most critical material properties for flexural type loading. Some bending was present in the repair bars, but tension dominated, especially for small rotations such as would be common in the field. The repair material must have sufficient bond strength to prevent failure at the material/substrate interface. It must also have enough tension capacity to develop the stitch bar stress.

Sikaquick 2500 showed performance similar to that expected of portland cement concrete. Tension cracking of the repair material reflected its low tensile strength (similar to concrete) and failure was brittle. These characteristics make the repair material undesirable for applications dominated by flexure type loading.

Flexpatch material allowed a higher load to be developed in the repair bars in the staple specimen compared to the Sikaquick 2500 in the slot stitch specimen. The very high tensile strength (reflected in its flexural strength) enabled the bars to develop much higher stresses, likely into the strain hardening range. Although the bond strength of the material was lower, there was enough surface area along the walls of the slot to prevent a bond failure along the interface between the Flexpatch and the concrete substrate.

It was unclear exactly how effective anchoring the staple legs with Sikadur 35 was on the specimen's performance. Two specimens, one with straight bars and another with anchored legs, would need to be tested using the same loading conditions and repair materials in order to accurately determine this. Theoretically, though, they should increase the capacity of the specimen in flexure. Without anchorage of the legs, the repair bars would have visibly strained the Flexpatch and the load-deflection behavior of the specimen would have been less stiff. Therefore the technique of anchoring the staple legs with Sikadur 35 appears to be very effective.

Tension Loading

The Sikaquick 2500 performed very well in the tension test. Failure surfaces propagated through both the concrete and the repair material, indicating that the bond between the two materials was sufficient. The repair material effectively caused the specimen to behave as though it was encased in monolithic concrete, and perhaps even better (compressive strength of the Sikaquick was higher than the concrete at the time of testing—see Appendix I). Therefore the Sikaquick 2500 appears to be an excellent choice of material for tension loading.

Economic Analysis of Repair Methods

In this section, a general methodology for an economic analysis of repair methods is based on experimental testing results. The methodology is intentionally general so that it can be adapted for the variable condition encountered in a specific application. One example is given to show the procedure for a certain set of repair performance criteria.

The first step in the process is to choose performance criteria for the repair method. Assuming that each alternative has acceptable material properties, the performance criteria will take the form of maximum bar force and/or maximum deflection. Maximum bar force will be limited by the strength and serviceability of the repair methods--the repair must be able to resist the applied loads, including the effects of fatigue, with little or no deterioration of the bars or concrete surrounding the bars. Maximum deflection could be based on environmental loading such as the expected potential vertical rise of the soil beneath the pavement or on traffic loading. This would be converted into a maximum curvature or angle of rotation at the repaired joint or crack.

Performance criteria are then compared to established load-deflection (or moment-curvature, or force-curvature whichever is appropriate) curves for each repair type. For the bar force limit state, the expected load per foot of joint or crack is compared to the maximum resisting load per stitch bar to calculate the required number of bars. For the deflection limit state, the resisting bar force corresponding to the specified deflection value is compared to the expected load per foot of crack or joint width to determine the required number of bars. The governing limit state will be the one requiring the greater number of bars. Additional laboratory testing will need to be conducted to more accurately determine the capacity for each repair method.

Once a system is installed, routine evaluations of performance should be conducted so that a performance database is established within the Department.

4.2.5 Conclusions and Recommendations

1. Repair bars should be placed as close to mid-depth in the slab as possible.
2. Low-modulus material in slots is not beneficial for shear performance, but works well for tension or flexure, provided it has good tensile characteristics.
3. Cross stitching is still suspect because of field performance and lack of conclusive lab data.
4. Both cross stitching and slot stitching methods performed better in shear loading than stapling.
5. Stapling performed best in flexure type loading.
6. Headed bars offered no advantage over conventional rebar.
7. Separated joints and cracks should be repaired as soon as possible, and before wide separations occur. Wide joints translate into high concrete stresses, high bending stresses in the repair bars, and lower stiffness (load transfer efficiency).
8. Bond strength is the most important material property for shear loading.
9. Bond and tensile strength are the most important material properties for tension or flexure loading.

4.3 Dynamic Cone Penetrometer

Dynamic Cone Penetrometer (DCP) tests were performed on multiple field investigations to determine the modulus of the base and subgrade beneath the concrete pavement slabs. This is

one of the tests that researchers hoped might explain the peculiar behavior of the separated concrete pavements. These tests were conducted statewide to determine whether there was a direct correlation between DCP readings, or rather subgrade modulus, and the likelihood of longitudinal cracks, joint separations, and faulting.

4.3.1 Test Description

DCP tests were run in accordance with ASTM International Standard D6951-03 *Standard Test Method for Use of the Dynamic cone Penetrometer in Shallow Pavement Applications*. The DCP device is shown in Figure 4.71. The hammed is raised to the specified height (upper stop) and released, this is repeated several times, usually in increments of 10 depending on the penetration rate, and the corresponding penetration depth is recorded. This test was repeated in multiple locations during each field study, at locations near and far from longitudinal cracks and joint separations and at locations in between.

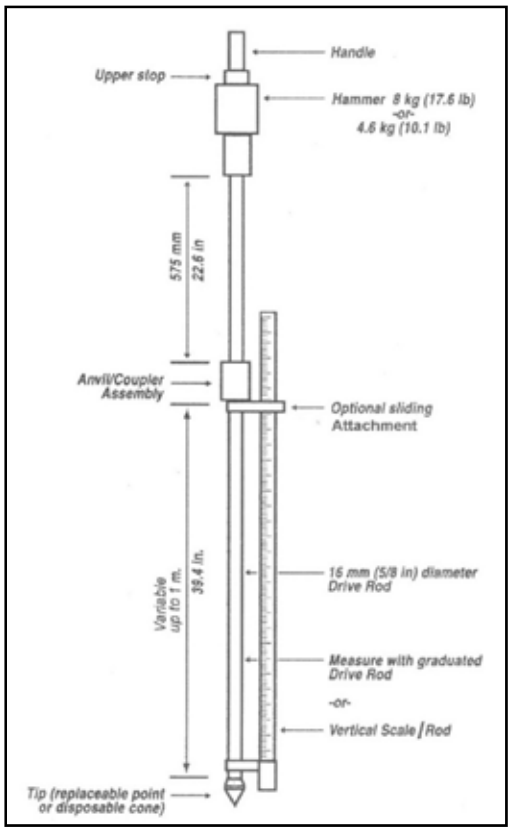

Figure 4.71: DCP Device

The DCP data collected is used to create a line graph of the cumulative number of blows vs. penetration dept. From the graph, many things can be determined, the most important of which is the slope(s) of the curve, the corresponding correlation coefficient(s), and the California Bearing Ratio (CBR) (Figure 4.72). Developed by the California Department of Transportation, CBR is an evaluation of the mechanical strength of road subgrades. The CBR calculated is then used to find the subgrade modulus values.

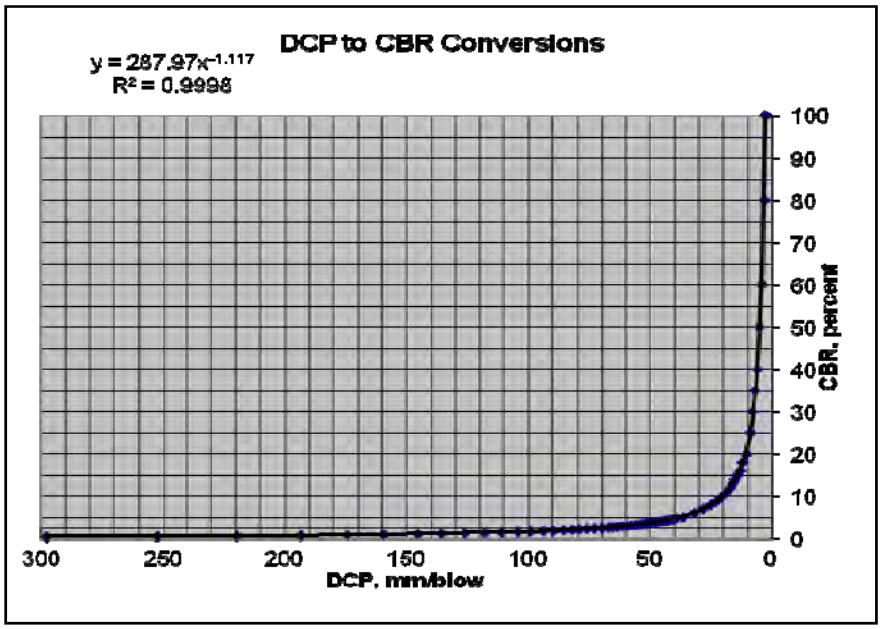

Figure 4.72: DCP to CBR Conversion Chart and Equation

The subgrade modulus value is calculated from the following equation derived in the paper *Field Performance Monitoring of Repair Treatments on Joint Concrete Pavements.*

E(psi)=2250*CBR^0.64

Modulus values of 15,000 psi and above are adequate and represent good subgrade conditions. Good subgrade conditions are important to the integrity of the pavement but are not the only influencing factor.

4.3.2 Data Collection

The research team performed DCP tests in various cities throughout the state. DCP data was gathered from Dallas, El Paso, Childress, Quanah, Sherman, Queen City, and Houston.

Dallas

Researchers performed a field investigation on September 13, 2007 along SH 66 at Centerville Road and on SH 289 at Preston Road. DCP tests were run in numerous locations along both highways in locations where the longitudinal cracking was bad and on the slabs adjacent to the longitudinal cracks (Figure 4.73). Along 289 longitudinal cracks were previously cross stitched, but the repaired cracks do not appear to be in good form. The epoxy sealing the longitudinal crack has eroded away (Figure 4.75).

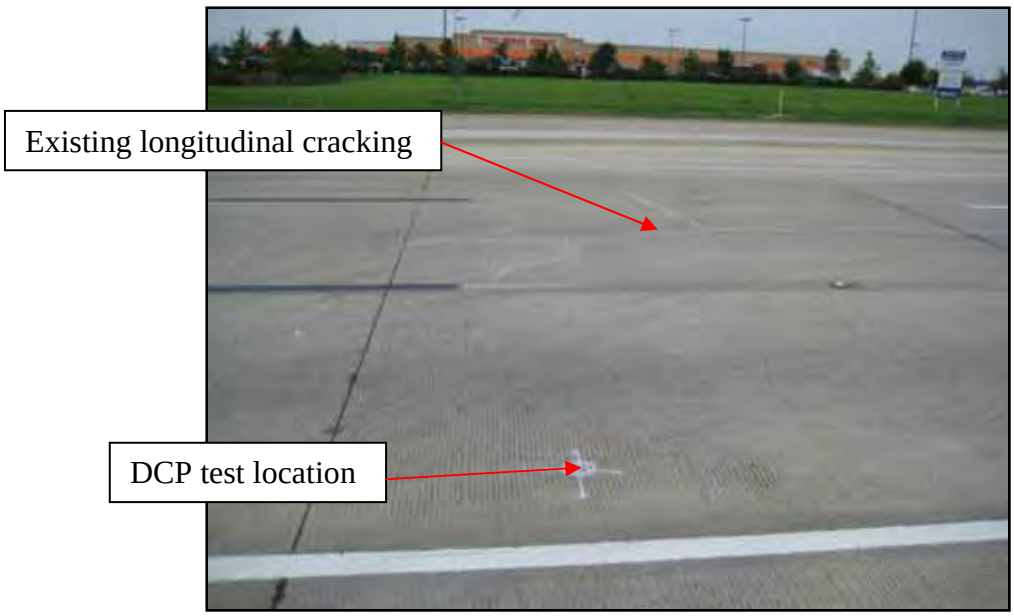

Figure 4.73: Dallas SH 66 DCP Test Location with Cracking Adjacent to Slab

Figure 4.74: Dallas SH 66 Longitudinal Joint Separation and Faulting

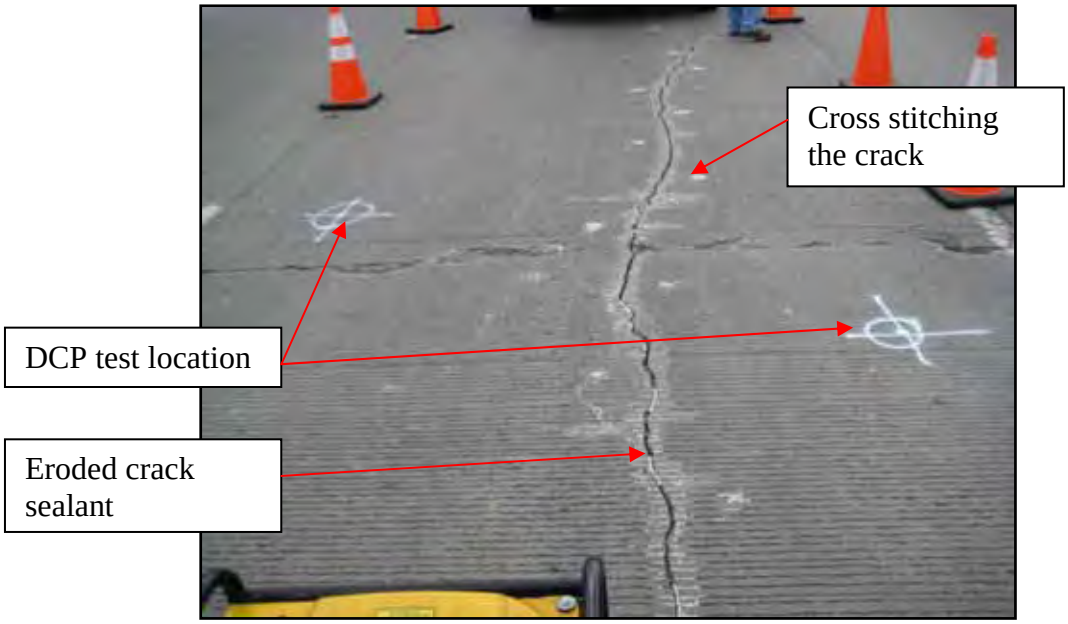

Figure 4.75: Dallas SH 289 DCP Test Location with Cracking

Tests indicated, for the most part, very poor subgrade material and wet subbase material was found at both locations. The graphs indicating number of blows vs. penetration depth and the subgrade modulus chart are shown in Figures 4.76 and 4.77.

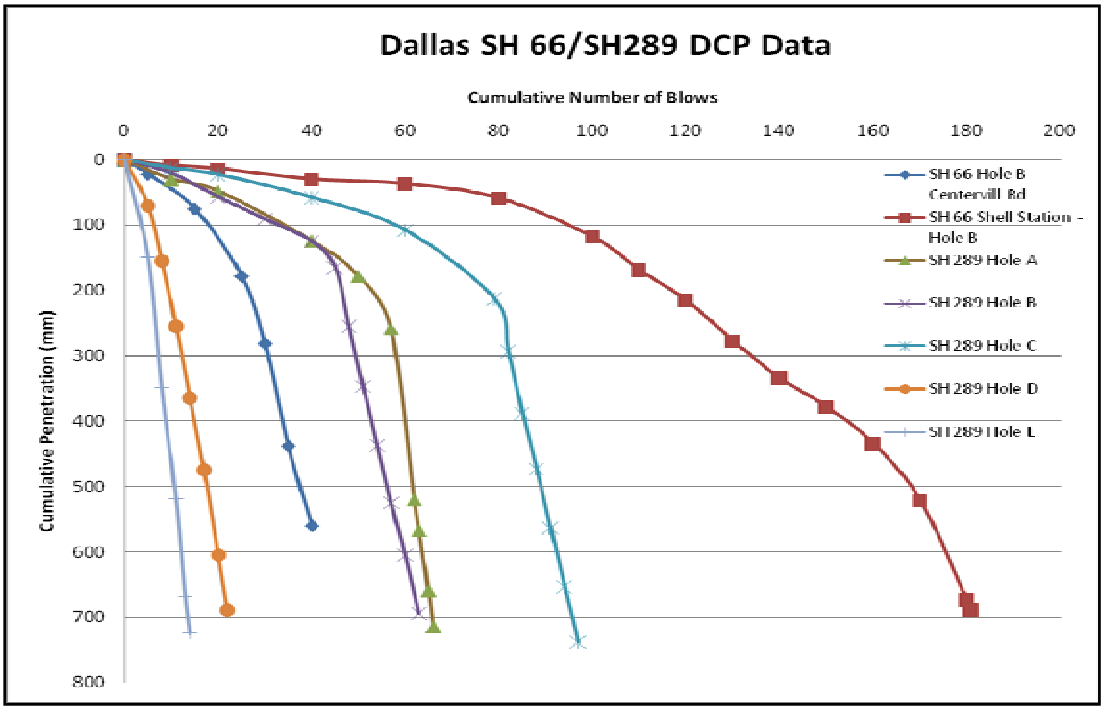

Figure 4.76: Dallas DCP Data

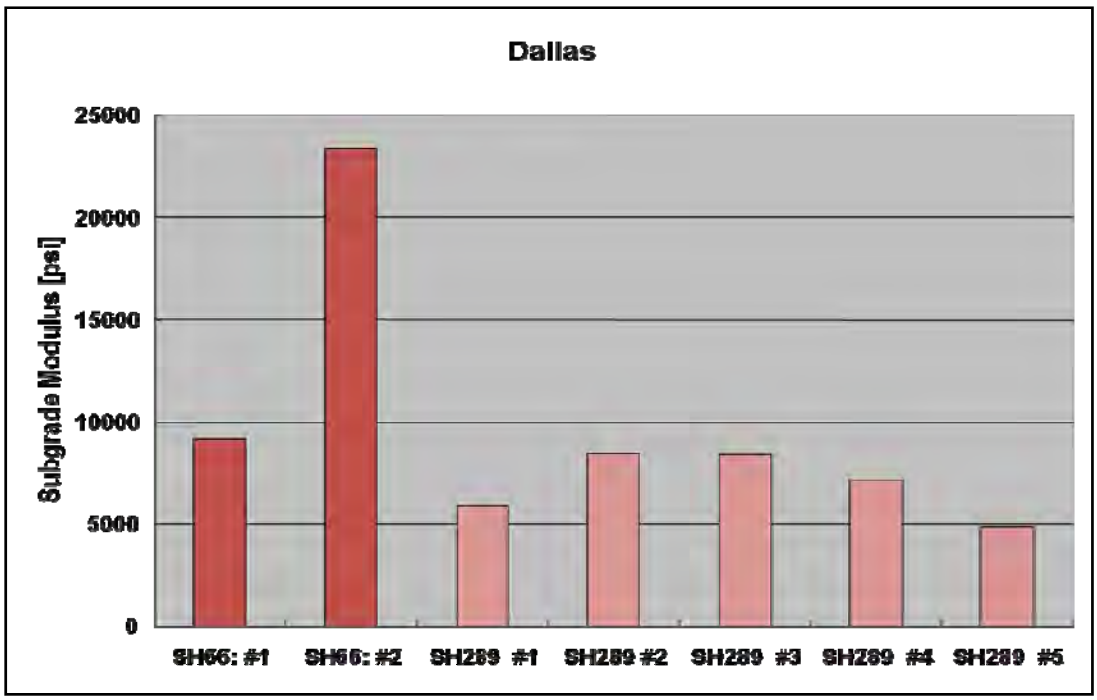

Figure 4.77: Dallas Subgrade Modulus Values

The DCP tests along SH 66 and 289, with the exception of one test along SH 66, showed very poor subgrade modulus values (below 10,000 psi). Along SH 66, crack widths from about 0.025 to 0.5 in. were observed as well as limited slab faulting (Figure 4.74). Researchers found one very good subgrade modulus value and one very poor value. These results are not necessarily conclusive due to the singular nature of DCP tests; DCP tests offer just a snapshot of the base material at a particular time (seasonal moisture condition) and location. Also, subgrade is only one of many factors affecting pavement conditions. After completing a visual study of SH 289, it was evident that the pavement was in poor condition. The pavement has numerous transverse and longitudinal cracks. The longitudinal cracks were previously repaired but the condition of the repair is poor. The modulus values calculated show very poor subgrade conditions. This and/or the wet subbase could be the cause of the concrete's extensive cracking problems. The modulus values were lower than those for SH 66, and this may be the reason that the crack widths and slab faulting observed were greater than the crack widths and slab faulting observed on SH 66.

El Paso

Field tests were performed November 14, 2007 on I10 near exit 22B along the eastbound outside lane. Multiple tests were run in locations with longitudinal cracks (Figures 4.78 and 4.79) or small joint separations and in locations without.

Figure 4.78: El Paso DCP Test Location

Figure 4.79: EL Paso Core Hole with Longitudinal Cracking

The data collected is presented in Figures 4.80 and 4.81.

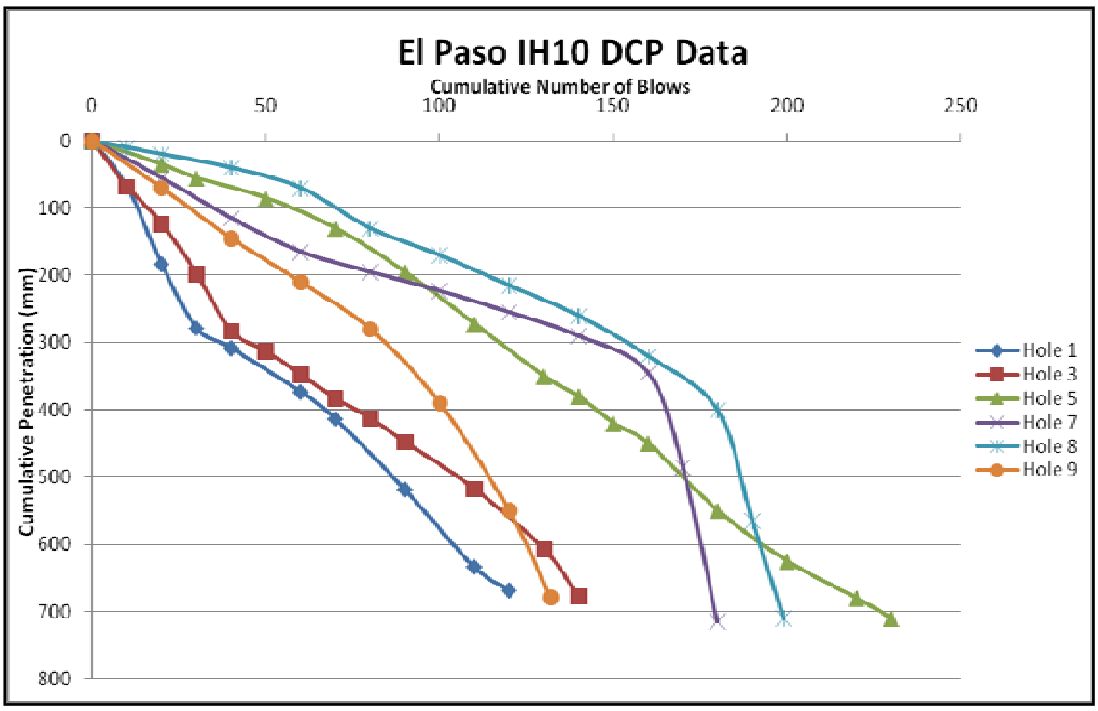

Figure 4.80: El Paso DCP Data

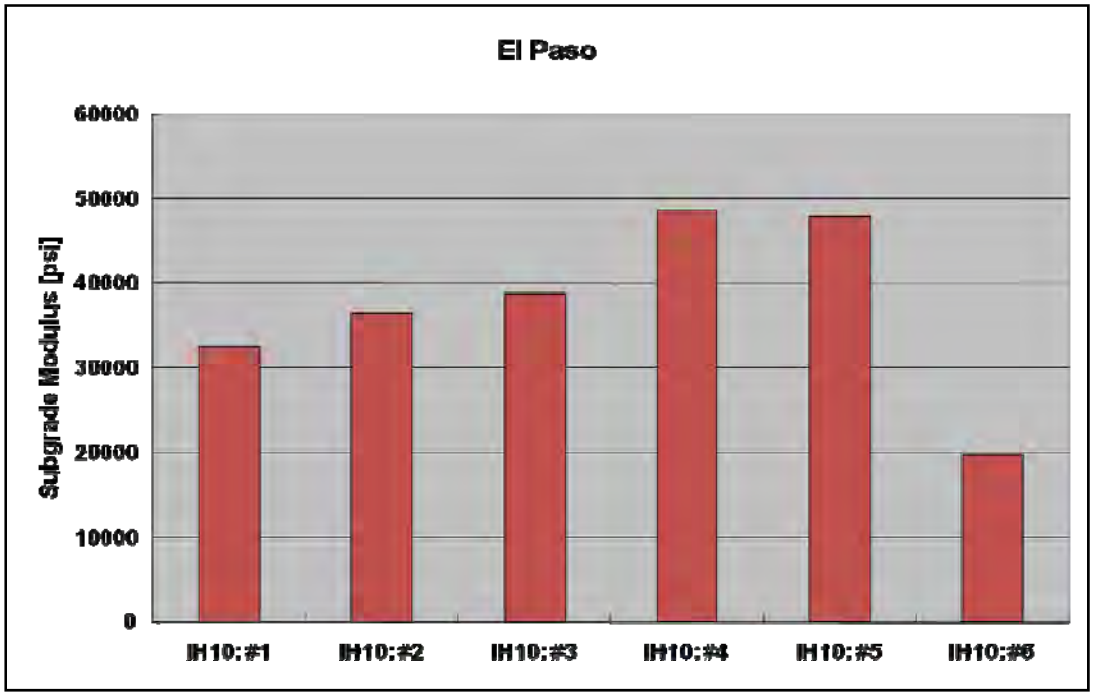

Figure 4.81: El Paso Subgrade Modulus Values

IH 10 showed very good subgrade modulus values (above 20,000 psi). Minimal faulting was observed, and the longitudinal cracks and separations observed in the test locations were relatively small. Although the concrete pavement on I10 in El Paso is mostly over 40 years old it

is still in pretty good condition. This probably is because good base conditions and good subgrade modulus values were found.

Childress and Quanah

Researchers performed field tests in Childress and Quanah on December 4, 2007 along IH287 at 3rd Street Avenue in Childress and at Main Street and Star Road in Quanah. In Childress, tests were run in locations where longitudinal cracks were present (Figure 4.82) and in locations without cracks. In Quanah, dowel bar retrofit was installed along the transverse joints (Figure 4.83) and the DCP tests were taken along the repaired portion of IH 287.

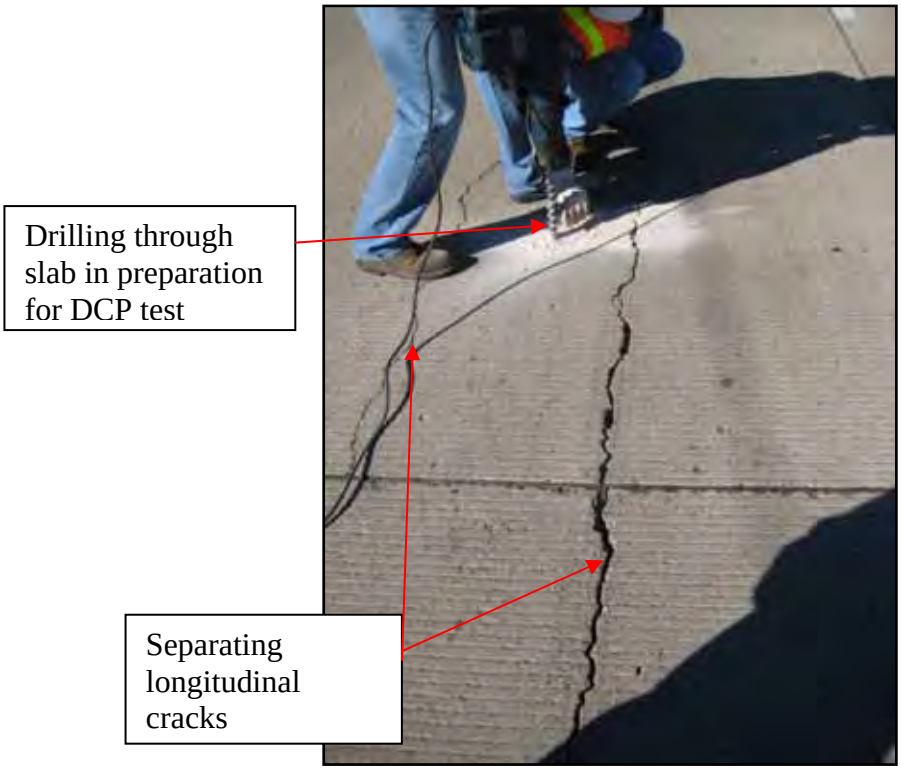

Figure 4.82: Childress DCP Test Location

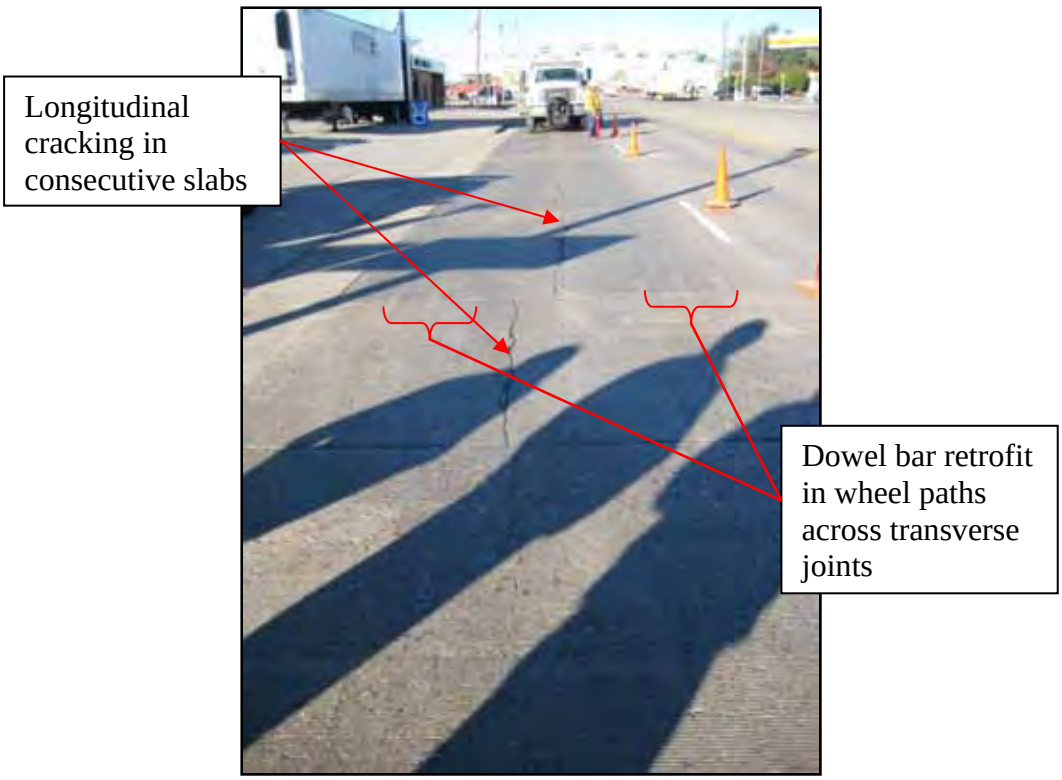

Figure 4.83: Quanah DCP Test Location

The number of blows vs. penetration depth graph and the subgrade modulus chart are shown in Figures 4.84 and 4.85.

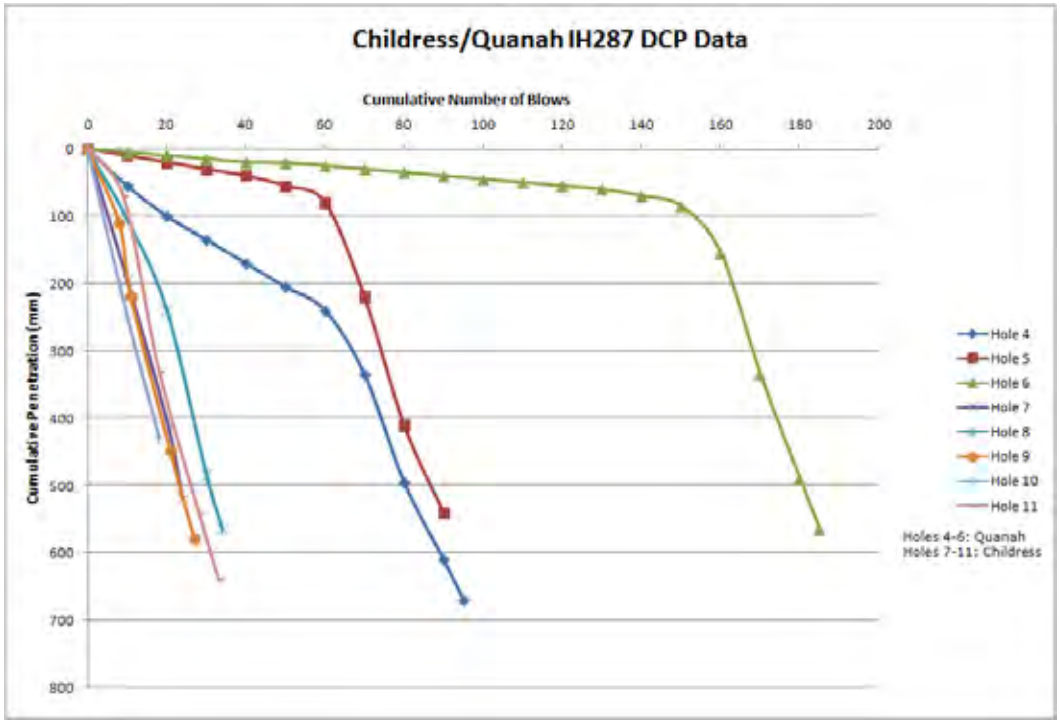

Figure 4.84: Childress and Quanah DCP Data

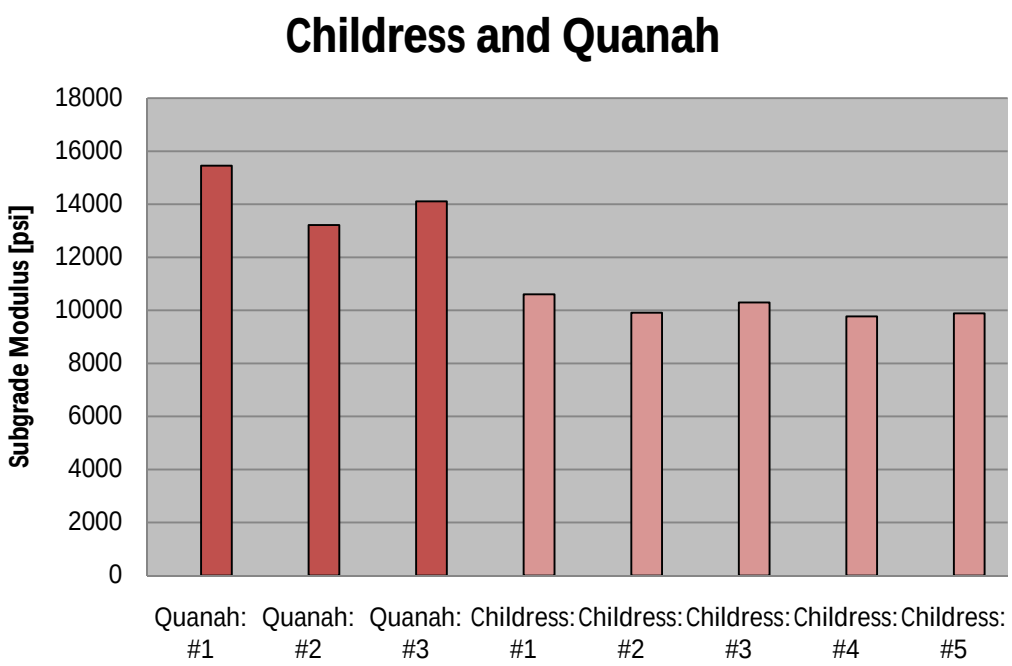

Figure 4.85: Childress and Quanah Subgrade Modulus Values

Childress and Quanah both have very bad longitudinal cracking along IH 287. DCP tests indicated for the most part poor subgrade material and both sections of IH 287 had poor subgrade modulus values. In Quanah researchers found slightly higher subgrade modulus values than in Childress (14,000 psi average in Quanah and 10,000 psi average in Childress).

Sherman

DCP tests were run during the field investigation (see Chapter 6) on March 31st –April 2, 2008. Longitudinal joint separations, faulting, and some cracking were evident. The field investigation began after an entrance ramp and just prior to exit ramp 68 along US 75 northbound on the two right-hand lanes. DCP tests were run in locations within the 14 contiguous slabs studied (Figure 4.86). DCP data and modulus graphs are shown in Figures 4.87 and 4.88.

Figure 4.86: Sherman Slab 3 DCP Test Location

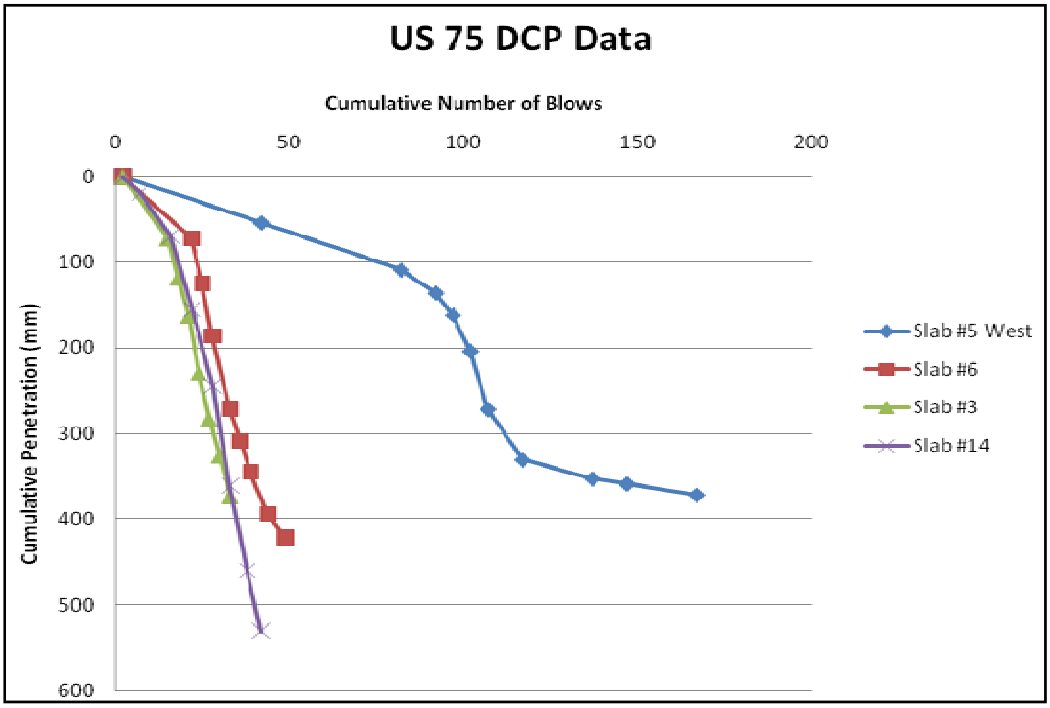

Figure 4.87: Sherman DCP Data

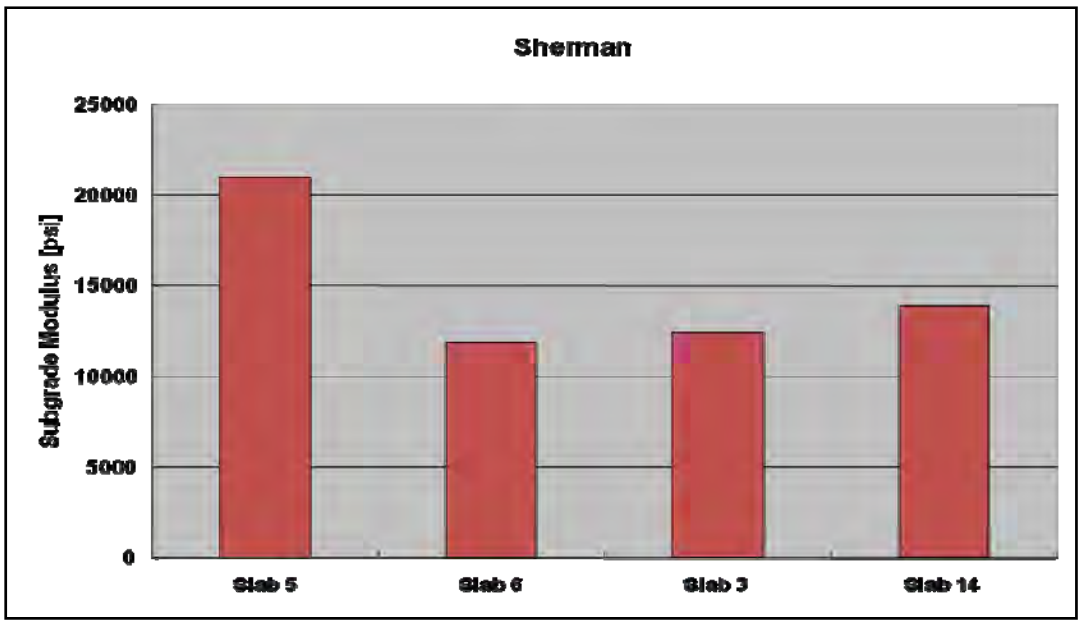

Figure 4.88: Sherman Subgrade Modulus Values

Subgrade modulus values for US 75 were poor with the exception of the modulus at slab 5 (about 21,000 psi). Despite the good and bad modulus values, Slabs 5 and 6 had the worst faulting of the slabs investigated. At those locations, the open construction joint allowed water to penetrate to the base. As a result pumping and faulting began to occur. This pumping of the slab is evident from the clean gravel (no fine materials) found at the base and resulted in an approximately 3 in. deep by 5 in. wide void under Lane 2's slab, see Chapter 6 for details and figures. DCP tests offer just a snapshot of the base material at a particular time and location. The DCP's singular nature can explain why poor pavement conditions can be observed despite good subgrade modulus values and illustrates that subgrade modulus is one of many factors affecting the condition of the pavement. This can explain the high subgrade modulus value calculated at Slab 5. There was a crack along Slab 3, which can explain the poor modulus value determined there. Slab 14 was in the best state of the slabs investigated (about 14,500 psi subgrade modulus value). It was also one of two slabs to have a keyed longitudinal construction joint. This keyed longitudinal joint offered more resistance to slab vertical movement and enhanced the slab's stability. Keyed joints do not allow the two ends of the slabs to deflect differently. They also allow less water penetration to the base compared to an un-keyed joint which in turn reduces the likelihood for slab pumping.

Queen City and Houston

DCP data were collected from Queen City and Houston by researchers and local TxDOT offices. In Queen City the data was taken on US 59 in front of Ken's Sporting Goods, near the intersection with Hickory Street on August 15, 2007 (Figure 4.89). In Houston data were taken along US290 near the Magnum exit. The data collected are shown in Figures 4.91 and 4.92.

Figure 4.89: Queen City US 59 DCP Test Location

Figure 4.90: Houston US 290 Joint Separation

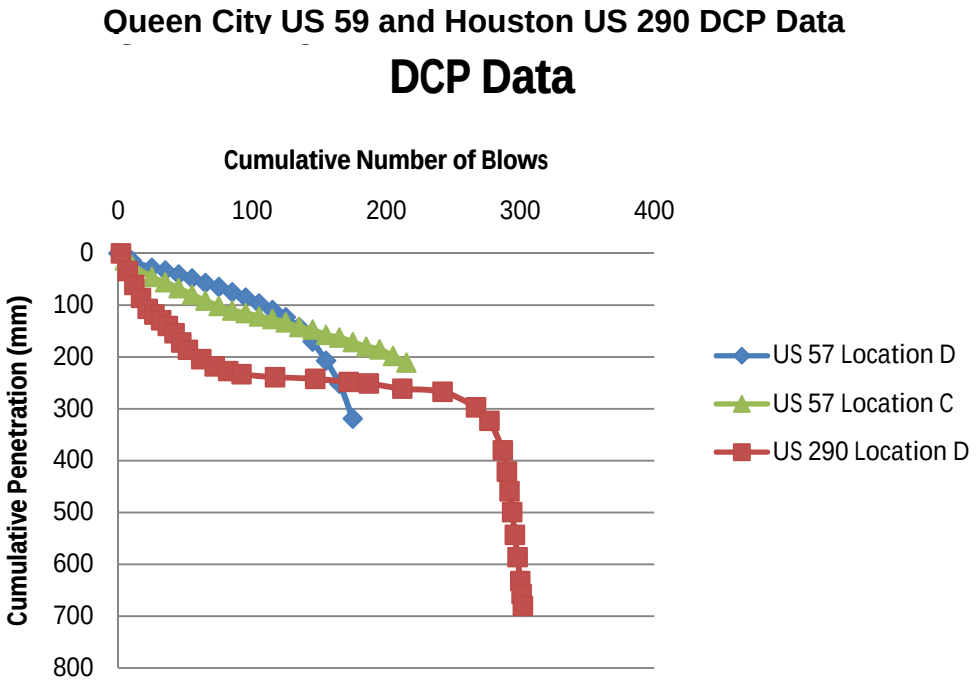

Figure 4.91: Queen City and Houston DCP Data

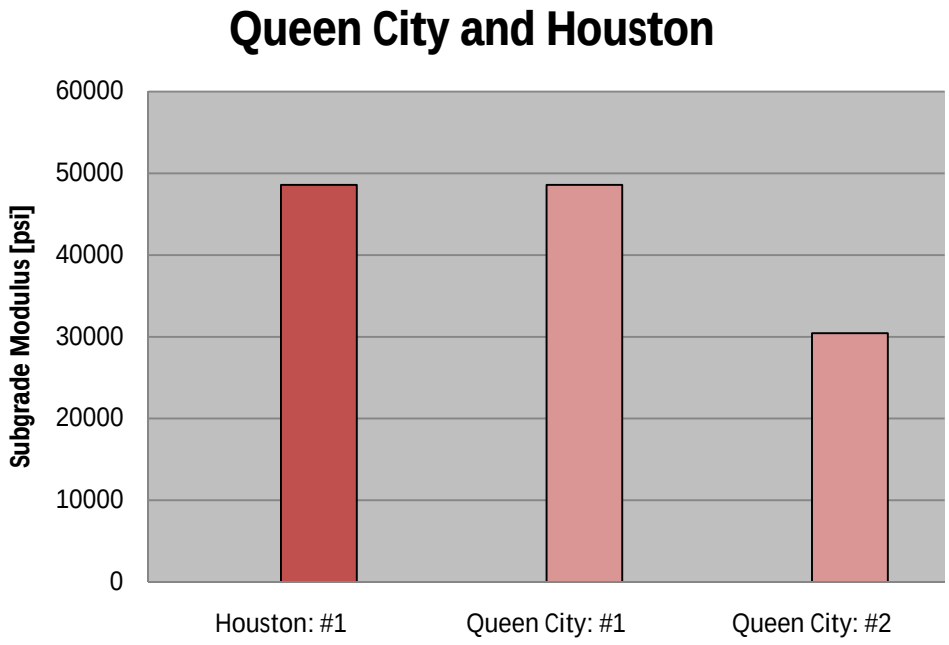

Figure 4.92: Queen City and Houston Subgrade Modulus Values

Queen City has had some major pavement issues along US59 and was repaired in 1997 and 2004. Repairs have included slab jacking, installation of pipe underdrain, joint sealing and cleaning, dowel bar retrofit, cross stitching and diamond grinding. A major cause of US 59's

problems is logging trucks that pass through the city that cause entire lanes to depress. Despite the pavement problems caused by the trucks, the base modulus values calculated in Queen City were very high (above 30,000 psi). These tests, however, were not run to the full depth; tests were stopped after penetrating approximately 8 in. into the base and do not give indications of subgrade conditions beneath the treated base. In Houston very wet climate conditions are encountered and good base preparation is always performed prior to any paving operations. The well-compacted base explains the high subgrade modulus values discovered. Also attributing to this is the fact that US 290 has keyed longitudinal joints and previous longitudinal crack repairs. The stapling method was used across the longitudinal joints to prevent further joint separation. Typical joint separation found along US 290 is shown in Figure 4.90.

4.3.3 Analysis of Results

The data collected from the DCP tests were used to calculate various soil properties, the most important of which was the soil's modulus value. Adequate modulus vales are at least 15,000 psi. The majority of the modulus values calculated for concrete paving sections with longitudinal separations were below this value. There were a few locations with good modulus values but the pavement condition was still poor. Therefore, a direct correlation between modulus value and likelihood of joint separations was not evident. More data would need to be collected to adequately access the likelihood of a correlation of DCP data and joint separations and faulting.

The data do, however, show that base conditions are an important aspect to the causes of longitudinal joint separations and cracking, but that they are not the only factor. In most of the locations studied, soils were very plastic. Good base conditions are vital to providing good LTE and having good LTE is very beneficial to a pavement's performance.

4.3.4 Conclusions

Researchers explored the possibility of a direct correlation between subgrade modulus values and pavement conditions implied by earlier TxDOT field notes. The data collected did not fully support this hypothesis. DCP tests offer just a snapshot of the base material at a particular time and location under seasonal subgrade moisture conditions. At different times of the year subsurface conditions can vary. Therefore more tests need to be run in additional locations and climate conditions before accurate conclusions can be constructed. Preliminary conclusions can be drawn regarding the DCP field studies, and they are listed below:

- Good subgrade conditions are important to have good pavement performance but they are not they only factor that determines the performance.
- No direct correlation was found between subgrade modulus value and pavement condition. In all conditions where poor subgrade modulus values were determined pavement performance was poor. When good subgrade modulus values were found, other factors present attributed to the poor performance of the pavements.
- High subgrade modulus values do not necessarily mean the pavement has good LTE.
- More DCP tests need to be run in more locations, multiple places at each location, and during different times of the year to accurately conclude if there is a correlation between subgrade modulus values and pavement conditions.

Chapter 5. Tie Bar and Transverse Steel Design

TxDOT's standards for tie-bar and transverse steel design utilize the subgrade drag theory (SGDT). Under SGDT the CRCP bar size and spacing for the two are the same. Longitudinal steel in CRCP is to keep transverse cracks that inevitably take place tight. Tight crack widths keep water and foreign materials from getting into cracks and provide good load transfer through aggregate interlock. If the transverse cracks are not kept tight, performance problems might result due to the ingress of water and poor load transfer. Transverse steel design, on the other hand, is based on the premise that once longitudinal cracks take place, the stress in the steel should not exceed ¾ of the yield strength of the steel. To compute adequate amount of transverse steel using the subgrade drag theory, it is assumed that there are no temperature variations through the slab depth. It is also assumed that the steel stress will be in equilibrium with concrete stresses caused by frictional resistance that develops between concrete slab and subbase, the magnitude of which is linearly proportional to the pavement width. Due to the assumption of temperature uniformity, the effects of warping and curling are completely ignored. SGDT requires that the amount of transverse steel needed be proportional to the pavement width. The number of lanes used in some urban areas is as many as 6 to 7 lanes. In these pavements, a substantial amount of transverse steel is used per SGDT. On the other hand, significant portion of early-age transverse cracks appears to take place at the locations of transverse steel. From a mechanistic standpoint, concrete stress concentrations will exist at the locations of transverse steel, which will result in transverse cracks. Over the years, the spacing of transverse steel has been reduced due to the increased number of lanes tied together. Spacing as small as 1 ft has been used in urban districts such as Houston. However, not much research has been done in this area to investigate whether transverse cracks that take place at the locations of closely spaced transverse steel might have adverse effects on long-term CRCP performance. Also, too much steel at one plane in concrete might increase the potential for delamination of concrete and resulting pavement distress. There is a research project currently underway to investigate horizontal cracking in CRCP, and this issue could be addressed in that study.

5.1 Tie Bar Design

In portland cement concrete (PCC) pavement, tie bars are installed at longitudinal construction joints primarily to keep the lanes together and secondarily to provide load transfer. In the design of tie bars using SGDT it is assumed that no temperature variations exist through the slab depth and, therefore, the slab displacements in the transverse direction are the same at all depths. Stresses in tie bars are computed from equilibrium between frictional resistance provided by the subbase as the slab displaces due to temperature variations and the forces in tie bars. The spacing for tie bars is determined by limiting the maximum steel stress in tie bars to a prescribed value, usually 75% of the yield strength. Due to the assumptions made in SGDT, tie bar spacing is inversely proportional to the widths of lanes tied together. SGDT is quite simple in concept and easy to implement. However, it has been demonstrated by a number of researchers that the basic assumption made in SGDT, uniform temperature distribution throughout concrete slabs, is not valid. Rather, as will be shown later, substantial temperature variations exist through slab depth, which will induce displacements in concrete slab in a vertical direction (curling). Figure 5.1 illustrates decomposition of non-linear temperature effects into three components that result

in the equivalent behavior of a concrete slab subjected to non-linear temperature variations through the slab depth. The first component is the axial strain, which SGDT addresses. SGDT does not consider the other two components. Ignoring the other two components could result in inaccurate estimation of tie bar stresses and unreasonable tie bar designs. To develop more rational tie bar designs, it is important that all three components be included in the analysis.

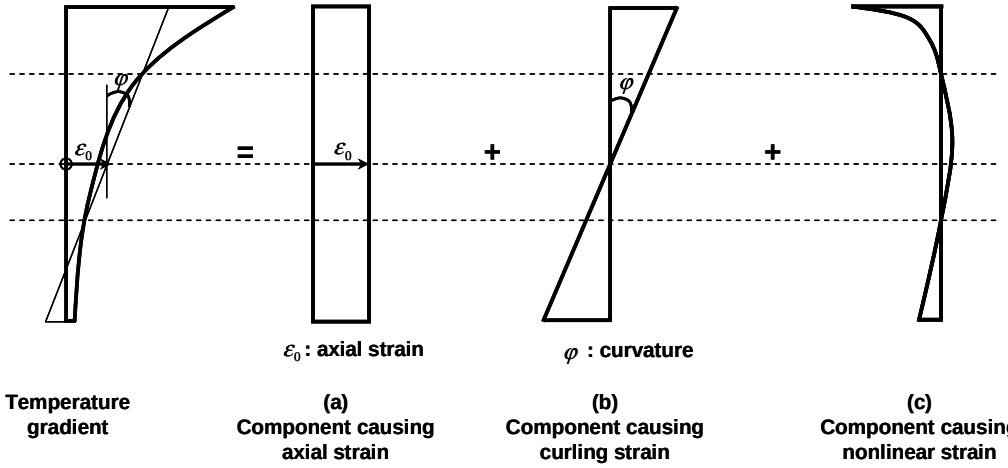

Figure 5.1: Decomposition of non-linear temperature effects

A field investigation was conducted to evaluate concrete displacements in vertical and transverse directions at the free edge. Figure 5.2 (a) shows the gage installed for the measurements of vertical slab displacements, and Figure 5.2 (b) illustrates the measured values for seven days. The slab was 15 in thick. Figure 5.2 (b) clearly illustrates the curling behavior of the concrete slab. In the x-axis, the whole number denotes midnight of the day after the concrete placement. For example, 15 means midnight of the 15^{th} day after concrete placement. The displacements at y-axis decrease if the slab is going down. It shows that the slab curls down in the late afternoon when top temperatures are higher than bottom temperatures. On the other hand, the slab curls up in the early morning when the top temperatures are lower than bottom temperatures. Figure 5.3 (a) shows gages installed to evaluate horizontal displacements of concrete slab at the free edge. This slab was 15 in thick. The displacements were measured at three depths of the slab: top (1 in), middle (7.5 in), and bottom (14 in). Figure 5.3 (b) illustrates the measurements. In the y-axis, as the slab is moving towards the free edge, the displacement number increases. For example, in the late afternoon, the top at the free edge moves towards the gages, while in the early morning, it moves away from the gages. It is shown that the displacements at the top and bottom are moving in opposite directions. The measured vertical and horizontal concrete displacements clearly indicate the existence of curling components in the slab movements. If the assumptions made in SGDT are correct, there should be no variations in the vertical displacements in Figure 5.2 (b), and the transverse displacements at three depths should be parallel to each other in Figure 5.3 (b). This finding indicates that SGDT alone may not be adequate to accurately estimate stresses that develop in tie bars due to temperature variations in concrete. More adequate evaluation methods need to be used to accurately estimate tie bar stresses and develop rational tie bar designs. In this investigation, both theoretical analysis and field evaluations were conducted to estimate tie bar stresses.

(a) Vertically installed crackmeter

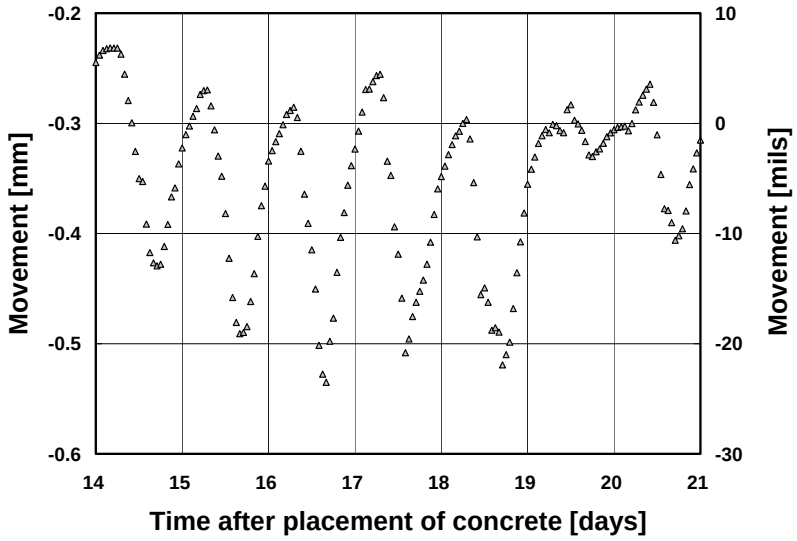

(b) Measured data

Figure 5.2: Measurement of vertical movement

(a) Crackmeters for transverse movement

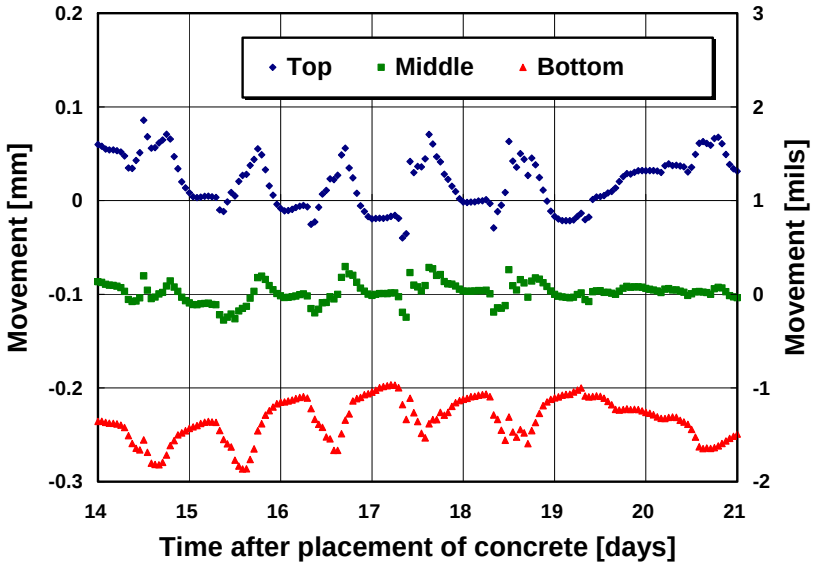

(b) Measured data

Figure 5.3: Measurement of transverse movement

5.1.2 US59 Field Investigation

To evaluate tie bar stresses in response to concrete temperature variations, field testing was conducted. The pavement section was located on US59 in Rosenberg, in the Houston District of the Texas Department of Transportation (TxDOT). The pavement type was continuously reinforced concrete pavement (CRCP) with a 15-in thick slab and the concrete was placed on July 11, 2007. The existing slab was 24 ft wide. A new 18-ft- wide slab was placed with a longitudinal construction joint in between. Steel strain gages were installed at various locations of a tie bar as well as temperature sensors at a number of slab depths. Figure 5.4 (a)

shows the testing setup, and Figure 5.4 (b) shows more detailed information on the locations of steel strain gages and temperature sensors. It shows that three steel strain gages were installed near the longitudinal construction joint, and one gage at the end of the tie bar. In Texas, two types of tie bars are used; one is a single-piece tie bar, and the other a multi-piece tie bar. In general, the multi-piece tie bar is more widely used. In this construction project, the contractor decided to use single-piece tie bars. Tie bars were inserted into fresh concrete manually after the paving machine passed. Before the paving of the next lane, the surface of a tie bar at planned gage installation locations was ground with a grinder, and then polished with sand paper to develop a flat and smooth surface for the steel strain gage installation. The accuracy of the steel strain measurements depends greatly on how smooth the surface is.

To investigate the effect of tie bar spacing on tie bar stresses, two additional tie bars were inserted at 1 ft spacing between two adjacent tie bars with normal 3 ft tie bar spacing. To evaluate the effect of tie bar depth on tie bar stress, one tie bar was installed at 5 in from the surface of the slab, instead of the normal 7.5 in depth.

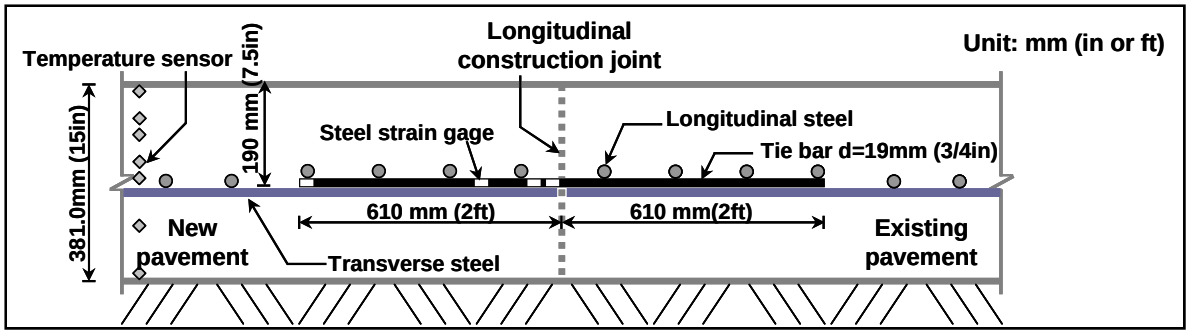

(a) Test setup

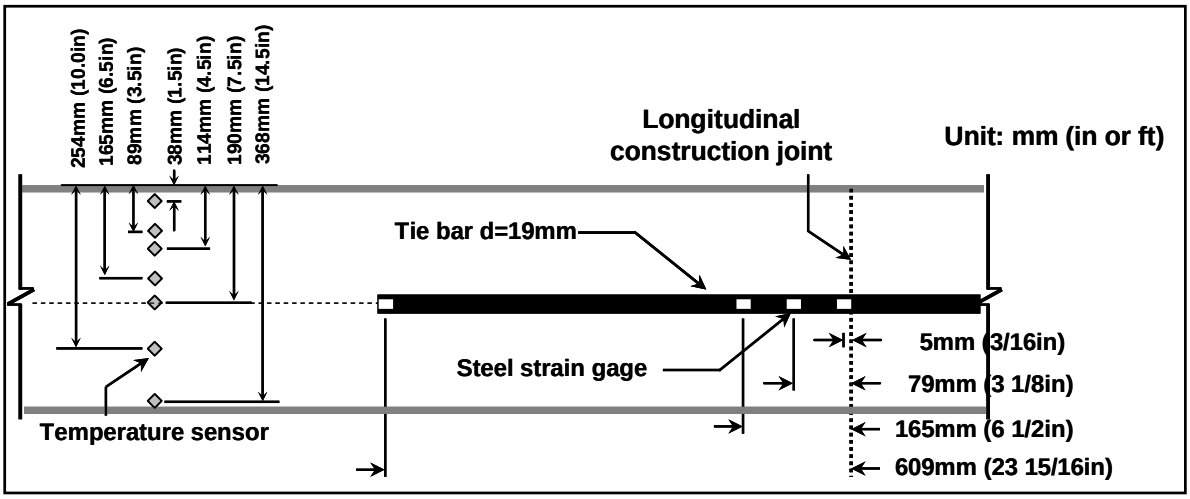

(b) Details on steel strain gages and temperature sensors

Figure 5.4: Test plan and details for gage installation

5.1.3 Analysis of Measured Data

Measured Temperature and Distribution of Tie Bar Strain

Figure 5.5 illustrates temperature variations at various depths from the placement of the concrete. It shows that the maximum concrete temperatures occurred at midnight on the day of concrete placement. It also shows a relatively large difference in concrete temperatures at various depths, even though they diminish with time as heat of hydration dissipates. It also illustrates that the maximum temperature changes occur near the top of the slab, while the temperature variations near the bottom of the slab are the smallest. This information again demonstrates the deficiency of SGDT in modeling real pavement behavior and the need for improved model to analyze tie bar stresses and design.

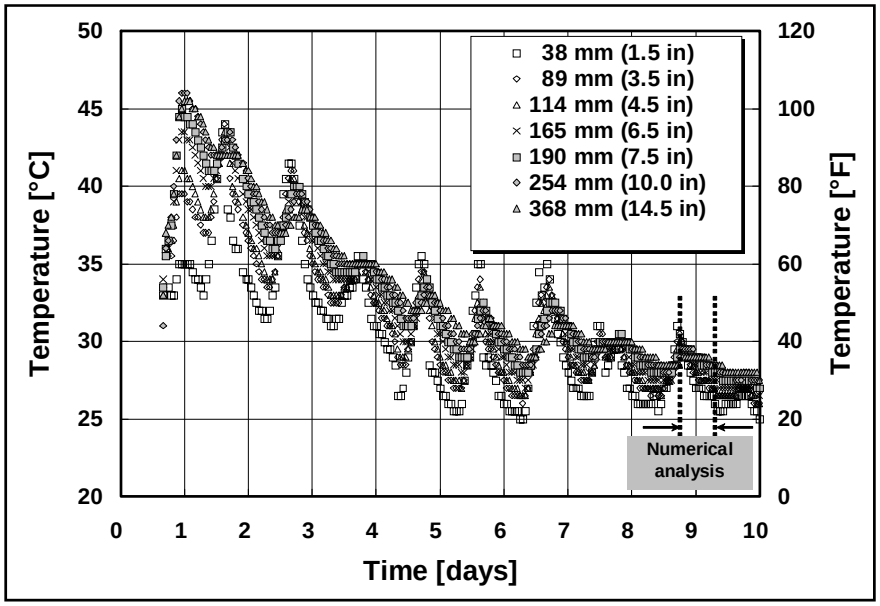

Figure 5.5: Measured temperature data

Figure 5.6 shows strains in a tie bar for 10 days after concrete placement at different locations from the longitudinal construction joint (LCJ). The numbers in the legend indicates the locations of the steel strain gages in terms of distance from the LCJ. As expected, the maximum strains occur in a gage installed near the LCJ, and very low strains are noted at the end of the tie bar. It also shows that maximum strains occur in the mornings and minimum strains in the late afternoon. It is also noted a rather rapid decrease in steel strain as it moves away from the LCJ. This implies potential bond-slip failures in the region between 3/16 in and 3 1/8 in from the LCJ. However, little difference is noted in steel strains in the region between 3 1/8 in and 6.5 in from the LCJ. For further theoretical analysis, the data from the evening of Day 8 to early morning of Day 9 was selected and detailed analysis results are presented later.

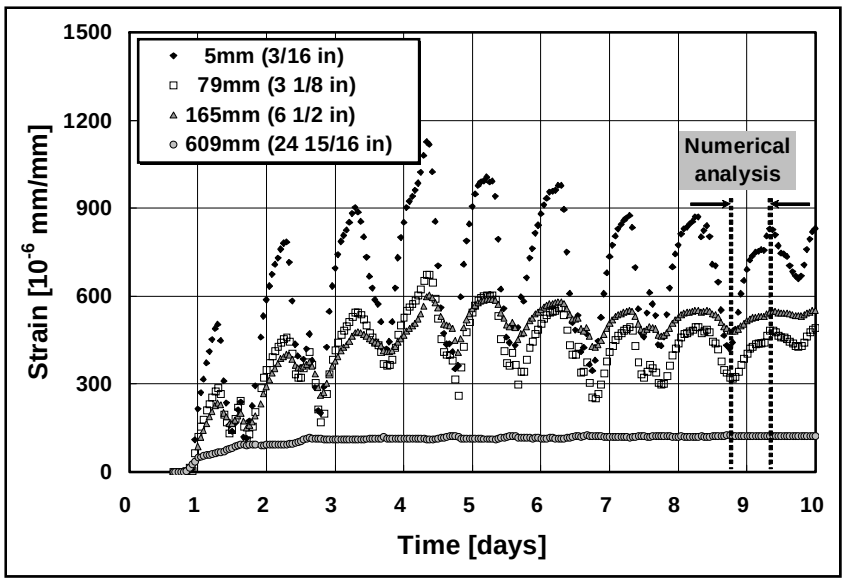

Figure 5.6: Measured steel strain

Figure 5.7 shows strains in tie bars placed at 1-ft spacing and 3-ft spacing. In the legend, the first number denotes the distance of the measured steel strain from LCJ, and the second number is tie bar spacing. It shows that much higher steel strain was obtained at LCJ in a tie bar with 3-ft spacing than that at LCJ in a tie bar with 1-ft spacing. It is as expected as tie bars placed at closer spacing have more steel cross-sectional area per unit length of concrete slab, which will result in lower steel stress.

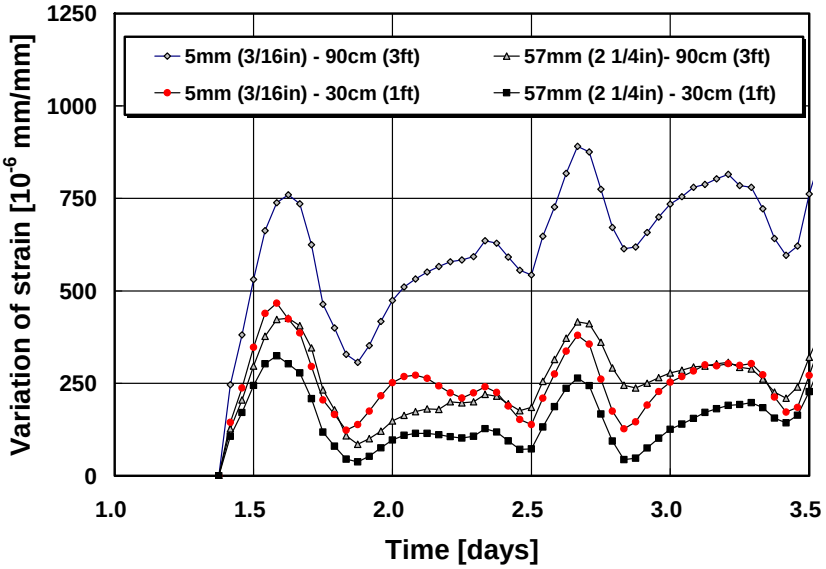

Figure 5.7: Effect of tie bar spacing on tie bar strain

Figure 5.8 shows strains in tie bars that were placed at two different depths. One was placed at 5 in from the top of the slab, and the other at 7.5 in from the concrete surface. It shows larger strain values in a tie bar placed at 5 in. from the concrete surface. These two bars were

within 12 ft, and it is considered that the only difference was the vertical location of the tie bars. The information in Figure 5.8 cannot be explained by SGDT. Rather, it can be explained only when the curling effect is taken into account. As will be discussed later in more detail, curling behavior at the LCJ could result much higher stresses in tie bars if they are placed closer to the slab surface.

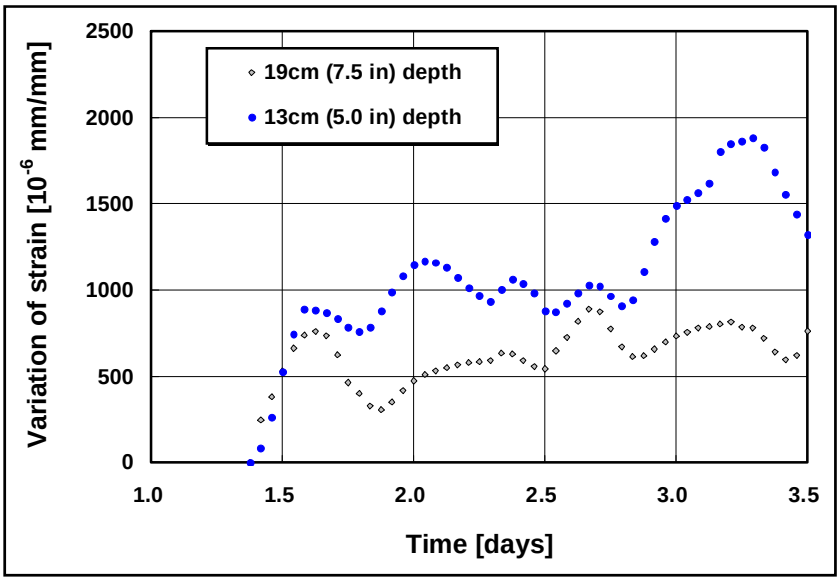

Figure 5.8: Effect of tie bar depth on tie bar strain

Numerical Modeling

In order to numerically investigate the effect of nonlinear thermal gradient on the stress in tie bars, the finite element program DIANA was used in the numerical analysis. Figure 5.9 (a) shows the finite element model of concrete pavement with tie bar at the LCJ. Plane strain and truss element were used to model the concrete and tie bar, respectively. Bond-slip behavior was considered in terms of relationship between the relative traction and slip in the structural interface. Spring elements in the horizontal and vertical directions were used to consider the subbase restraining effect. The tie bar was horizontally fixed at one end near the LCJ, considering the symmetry at the joint. Figure 5.9 (b) illustrates the deformation at the LCJ when the negative nonlinear temperature gradient was applied. As shown in Figure 5.1, the top and bottom portion concrete may contract and expand, respectively, depending on the degree of nonlinearity of temperature gradient. When the slab tries to expand at the bottom, this expansion would be restrained by another slab. To consider this restraining effect, a tensionless spring with sufficient stiffness in the compression was provided to the one node located at the bottom of concrete at the LCJ.

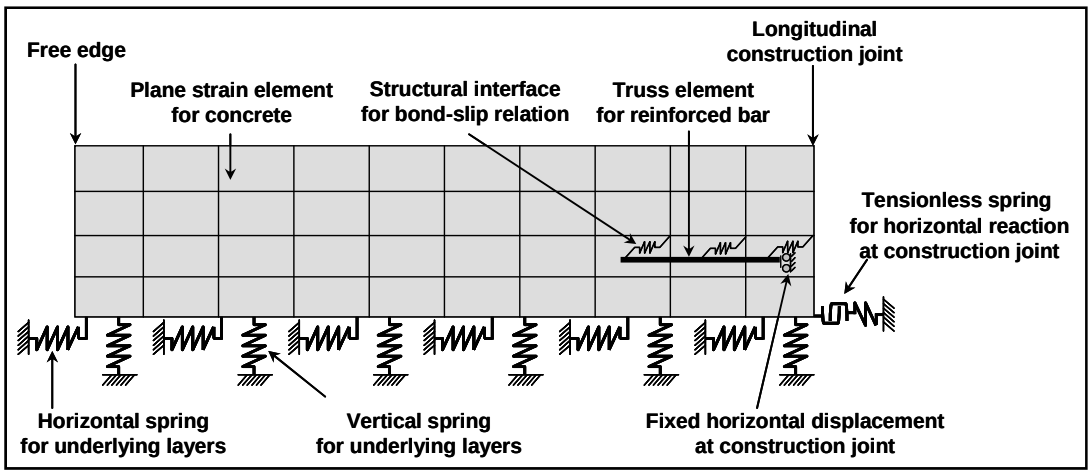

(a) Finite element modeling of concrete pavement

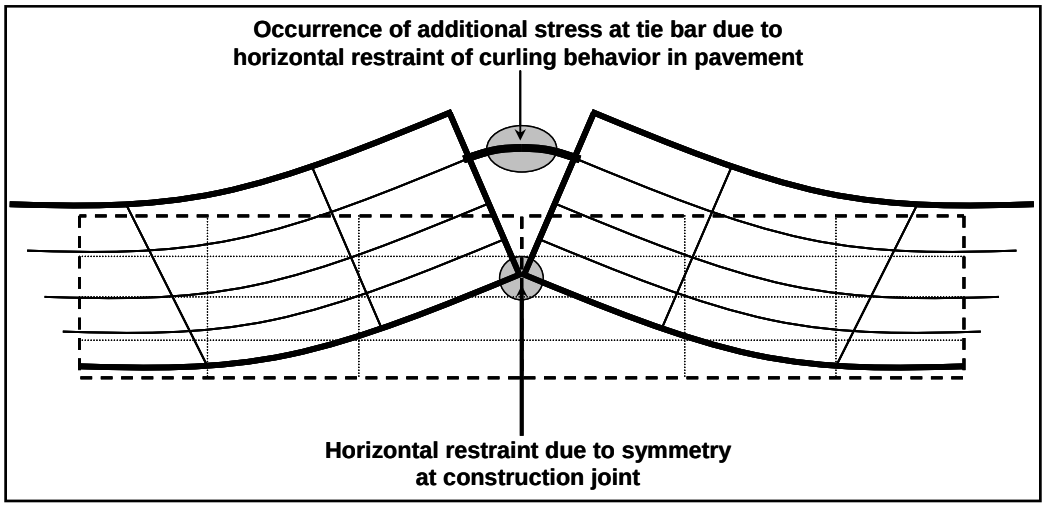

(b) Restraining effect at the bottom of concrete slab in the LCJ

Figure 5.9: Numerical modeling of concrete pavement with tie bar at the longitudinal construction joint.

Figure 5.10 (a) indicates the measured temperature profiles from 8th day evening (6:00 p.m.; 8.75 days) to 9th day morning (8:00 a.m.; 9.33 days), as was shown in Figure 5. As expected, the temperature at the top surface in the slab diminished significantly and the decrease was reduced as the depth was increased. Figure 5.10 (b) shows the temperature gradient applied to the numerical analysis. This period was selected in the analysis because the change of mechanical properties such as elastic modulus was relatively small compared to the values in the early ages. For the analysis, it was assumed that the changes in material properties during the analysis period could be negligible and the error associated with this assumption is quite small.

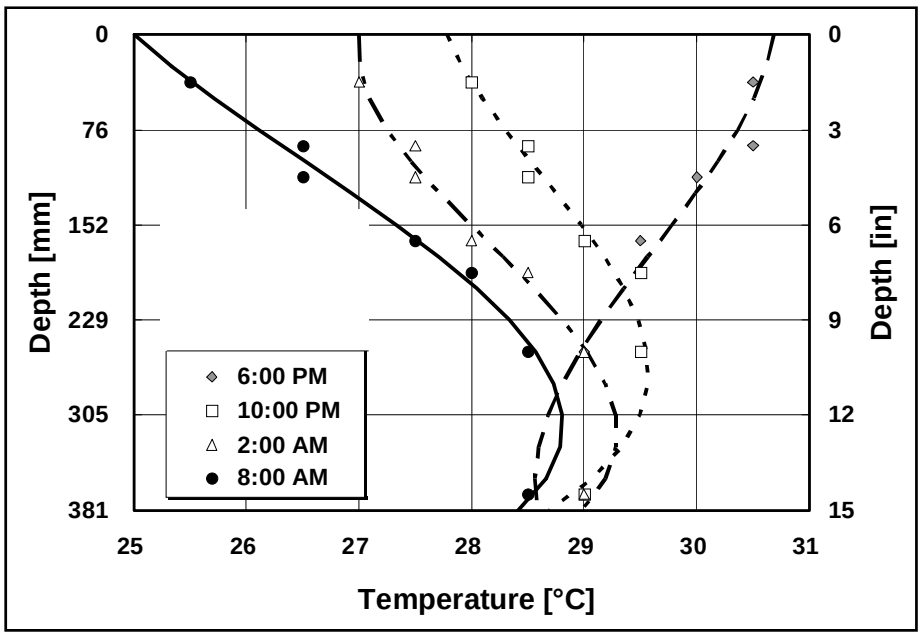

(a) Measured temperature profile at the concrete slab from 8.75 days to 9.33 days

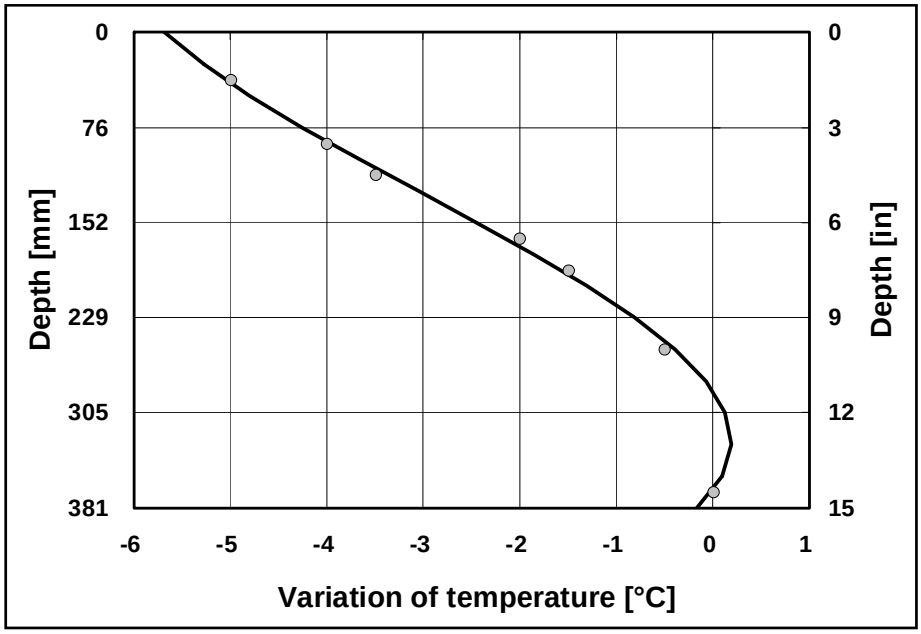

(b) Applied temperature gradient in the numerical analysis

Figure 5.10: Temperature profile and gradient in the numerical analysis.

Table 5.1 represents the geometric and material properties used in the numerical analysis. Based on CEB MC 90 model from the European International Code, development of elastic modulus with time was estimated from 28 days compressive strength and the maturity function which considers the effect of temperature on the development of hydration process. Average temperature was used to calculate the temperature-adjusted concrete age. The bond-slip model from the paper written by Kim, Won, and McCullough titled *Three-Dimensional Nonlinear*

Finite Element Analysis of Continuously Reinforced Concrete Pavements was adopted in this investigation.

Table 5.1: Geometric and Material Properties in the Numerical Analysis

Pavement width	5,486 mm (18 ft)	Pavement thickness	381mm (15 in)
Concrete modulus	$3.16X10^4$ MPa ($4.58X10^6$ psi)	Concrete Poisson ratio	0.15
28-day compressive strength	34.5MPa (5,000 psi)	Concrete CTE*	$7.2\ X10^{-6}$/°C ($4\ X10^{-6}$/°F)
Tie bar spacing	914 mm (3 ft)	Tie bar length**	609 mm (2 ft)
Tie bar diameter	19mm (3/4in)	Tie bar modulus	200 GPa ($29X10^3$ ksi)
Tie bar Poisson ratio	0.3	Tie bar CTE*	$11.5\ X10^{-6}$/°C ($6.4\ X10^{-6}$/°F)
Horizontal stiffness for underlying layer	0.04 MPa/mm (150 psi/in)	Vertical stiffness for underlying layer	0.1 MPa/mm (400 psi/in)
Yield slip between concrete and base	0.5 mm (0.02 in)		

* CTE: coefficient of thermal expansion

** Half length of tie bar was modeled due to symmetry

Numerical Analysis Results

Figure 5.11 (a) shows the distribution of tie bar stress variation from the numerical analysis along the tie bar from the LCJ. The dotted line represents predicted tie bar stress solely due to the axial component in concrete slab displacements shown in Figure 5.1. The solid line shows the predicted tie bar stress due to the combined effects of three components shown in Figure 5.1. Quite good agreement is shown between the predicated and measured tie bar stresses that include the effects of all three components of non-linear temperature distribution.

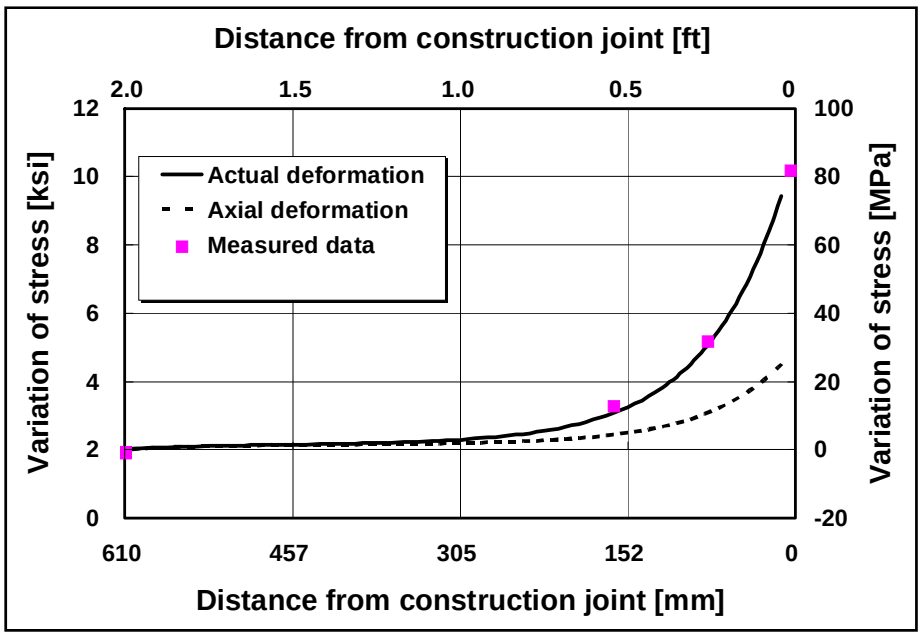

(a) Distribution of strain at the tie bar

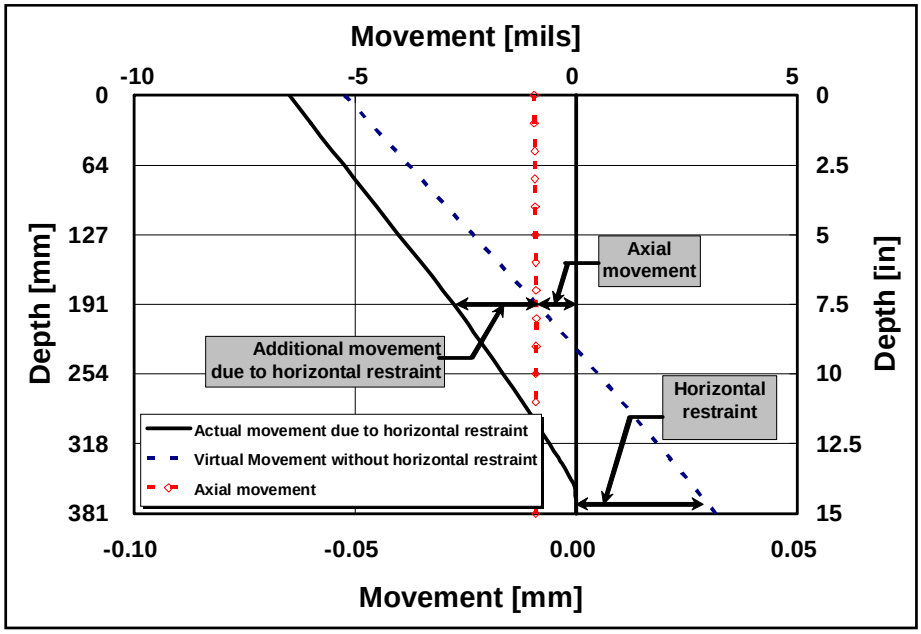

(b) Movement of construction joint in transverse direction

Figure 5.11: Tie bar strain and movement at construction joint

Figure 5.11 also shows rather rapid increase in tie bar stress as it gets closer to the LCJ. The information in this figure illustrates that tie bar stresses predicted by SGDT are much lower than actual stresses. This indicates that SGDT may not adequately assess stresses in tie bars, and consideration should be made to include the other two components shown in Figure 5.1 for proper design of tie bars. Figure 5.11 (b) shows the transverse movement of slab at the LCJ when the temperature gradient in Figure 5.10 (b) was applied. It explains the mechanism of tie bar stress development at the LCJ when all the three components are considered. The axial

contraction caused the frictional stress to develop at the interface between slab and subbase, which induced stresses in the tie bar. The concrete at the bottom of the slab would expand if there is no horizontal restraint. In the real pavement, restraint will exist at LCJ due to the symmetry condition shown in Figure 5.9 (b). The additional stress was produced when the expansion at the bottom was restrained. Figure 4.11 illustrates that the additional stress plays an important role in the development of stresses in tie bars.

5.1.4 Effect of Nonlinear Temperature Gradient on Tie Bar Stress

In order to investigate the effect of nonlinear temperature gradient on the stress of tie bars at the longitudinal construction joint, a 3rd degree of polynomial for the temperature profile along the depth was assumed as shown in Figure 5.12. The temperature differences between the top and the bottom of the concrete slab were assumed to be 5°C, 10°C, and 15°C in the numerical analysis. The values in Table 5.1 were used in this analysis.

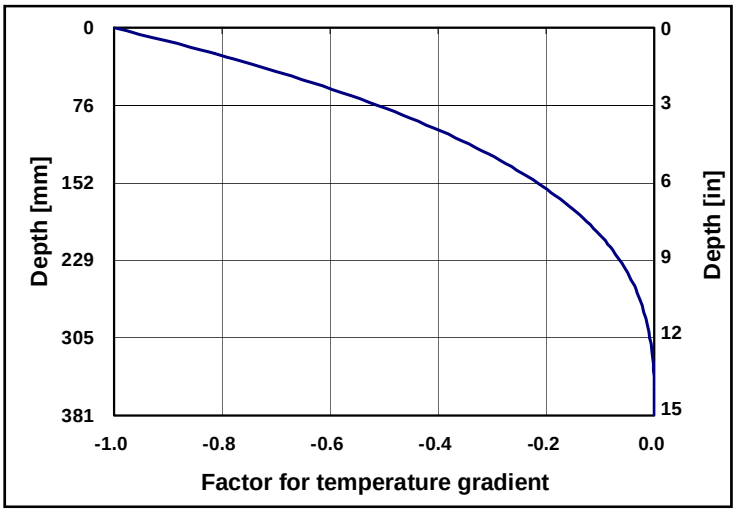

Figure 5.12: Assumed temperature gradient in the numerical analysis

Figure 5.13 (a) shows the effect of pavement width on the stresses in tie bars. The temperature difference of 15°C between top and bottom was assumed. As the pavement width increases, the tie bar stress due to the restraint of axial movement by frictional stress increased almost linearly as would be expected. This stress still underestimated the tie bar stress when axial and curling movement exists together in the actual pavement. Tie bar stress due to both frictional resistance and curling is much greater than the tie bar stress resulting solely from frictional resistance at the subbase interface. As pavement widths increase, tie bar stress will proportionately increase due to frictional resistance. On the other hand, tie bar stress due to both frictional resistance and curling will increase quite modestly. This difference is due to the fact that tie bar stress due to curling is not linearly proportional to the width of the pavement. The shape of the tie bar stress variation will follow Bradbury's curling coefficient curve quite closely; Bradbury's curling coefficient curve was illustrated in his book *Reinforced Concrete Pavements*. As the pavement widths increase greatly, it is possible that tie bar stress estimated from frictional resistance alone might surpass that due to both frictional resistance and curling. In other words, tie bar designs based on SGDT might not be adequate if the pavement widths are not large, and failures and distresses might result in the form of joint opening, intrusion of water to subbase,

and loss of load transfer efficiency at the LCJ. On the other hand, tie bar design based on SGDT might be adequate for pavements with large widths. This does not justify using SGDT for tie bar design. Accurate tie bar design should be based on the utilization of both frictional resistance and curling.

Figure 5.13 (b) shows the effect of temperature difference between the top and bottom of the slab and tie bar spacing on the tie bar stress. As expected, tie bar stress increased as the spacing increased. Furthermore, the temperature differential between the top and bottom of the slab had a substantial effect on the development of tie bar stress.

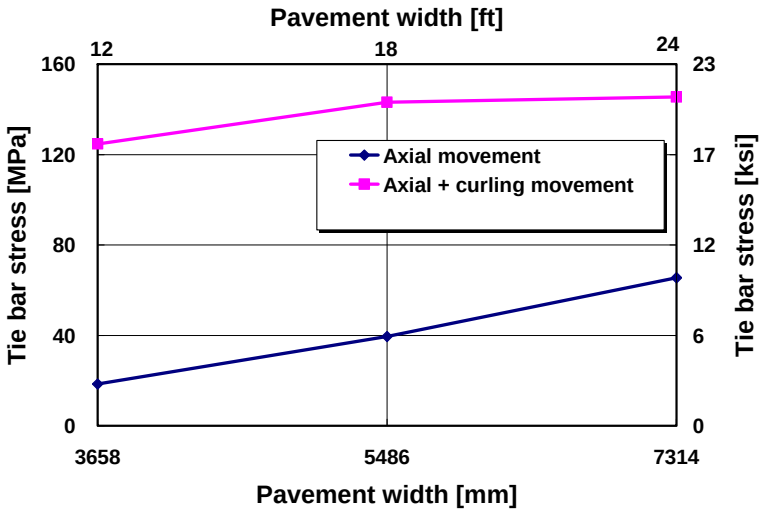

(a) Effect of pavement width

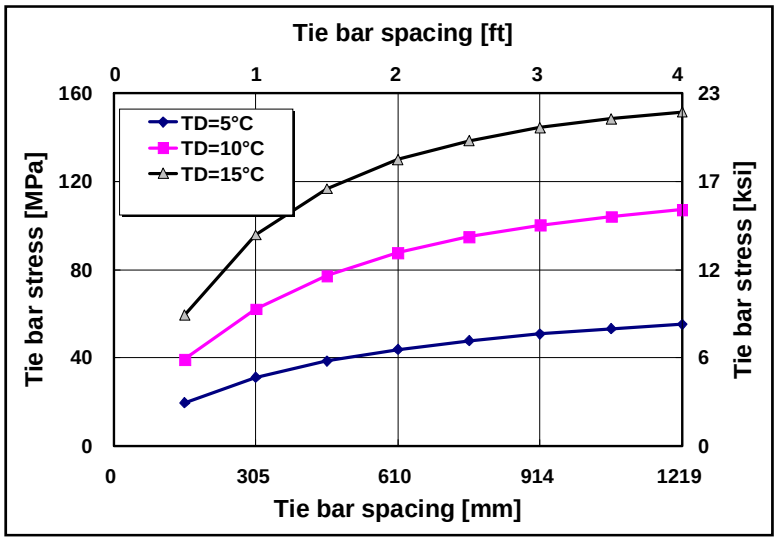

(b) Effect of tie bar spacing and temperature difference

Figure 5.13: Effect of various parameters on the stress of tie bar

5.1.5 Summary and Recommendations

Currently, tie bar design is based on subgrade drag theory (SGDT). In this study, the validity of SGDT for tie bar design was investigated. Concrete slab displacement behavior was evaluated at the free edge for vertical and transverse displacements. Tie bar stresses were evaluated in the field and by theoretical analysis considering frictional resistance at the interface only, and effects of both frictional resistance and slab curling. Based on the field experiment and theoretical analysis, the following conclusions are made:

- Concrete temperatures evaluated at various depths from the concrete placement showed substantial variations between the top and the bottom of the slab. This variation causes slab curling and does not support the assumption made in SGDT, which is there is no variation in temperature along the slab depth.
- Concrete slab displacement measurements at free edge exhibited daily curling behavior. This behavior violates one of the assumptions made in SGDT, which is that the slab moves uni-axially in a transverse direction due to temperature variations.
- Quite different stresses resulted in tie bars placed at different depths. Much higher stresses were obtained in a tie bar placed closer to the slab surface compared to the tie bar placed at the mid-depth of the slab. SGDT cannot explain this difference. This difference can only be explained if curling effect is taken into account.
- Comparison of the results from theoretical analysis and field measurements in terms of tie bar stresses indicates good correlation between them when both frictional restraint and curling effects are included in the analysis. On the other hand, when only frictional resistance is included in the analysis, which is the case when SGDT is applied, there was a large discrepancy between measured and predicted values.
- Due to the inherent limitations in the assumptions made in the development of SGDT, tie bar designs based on SGDT might not be adequate if the pavement widths are not large, and failures and distresses might result in the form of joint opening, intrusion of water to subbase, and loss of load transfer efficiency at LCJ.

Based on the findings in this study, it is recommended that tie bar designs should be developed considering not only frictional resistance at the interface between concrete slab and subbase, but also non-linear temperature effects. Tie bar designs thus developed are expected to provide better performance in terms of keeping the lanes together, minimizing the intrusion of water through joint, and providing good load transfer efficiency at the longitudinal construction joints. Guidelines for new tie bar construction have been developed and can be found in Appendix O.

5.2 Transverse Steel Design

5.2.1 Current Transverse Steel Design Philosophy in CRCP

Subgrade drag theory (SGDT) was used to develop transverse steel design in the current CRCP Standards and this section discusses SGDT in detail.

Current Transverse Steel Design

The current transverse steel design is based on the premise that steel stress should be limited to 40 ksi at longitudinal cracks. Steel stresses are computed from SGDT by the following equation.

$$A_s = \frac{\gamma_c h L f_a}{2 f_s}$$

where, A_s = the amount of steel required for the unit width of the slab,
L = pavement width,
h = slab thickness,
f_s = allowable steel stress,
γ_c = concrete unit weight (normally 150 lbs/cf or 0.0868 pci) and,
f_a = frictional coefficient between slab and subbase (normally 1.5).

According to the previous equation, the amount of steel that is needed is directly proportional to pavement width and slab thickness. Field testing was conducted to evaluate the adequacy of the use of SGDT in developing transverse steel design.

5.2.2 Forth Worth District

Measurements of Stresses in Transverse Steel and Tie Bars

CTR conducted field testing to evaluate steel stresses in tie bars and transverse steel. The testing was conducted on SH114B (Texan Trail) in the Fort Worth District on September 19, 2006. Figure 5.14 illustrates the geometry of the pavement section. CRCP was 8-in thick. One lane (12 ft) of concrete was placed next to the existing CRCP. A total of 8 steel strain gages were placed—three of them on a tie bar and the other 5 on transverse steel. The numeric portion in the gage designations indicates the distance in inches from the longitudinal construction joint. For example, TIE24 indicates a gage on tie bar at 24 in from the joint. Similarly, TR49 indicates a gage on transverse steel at 49 in from the joint. Figures 5.15 (a) and 5.15 (b) show close-up views of installed steel strain gages.

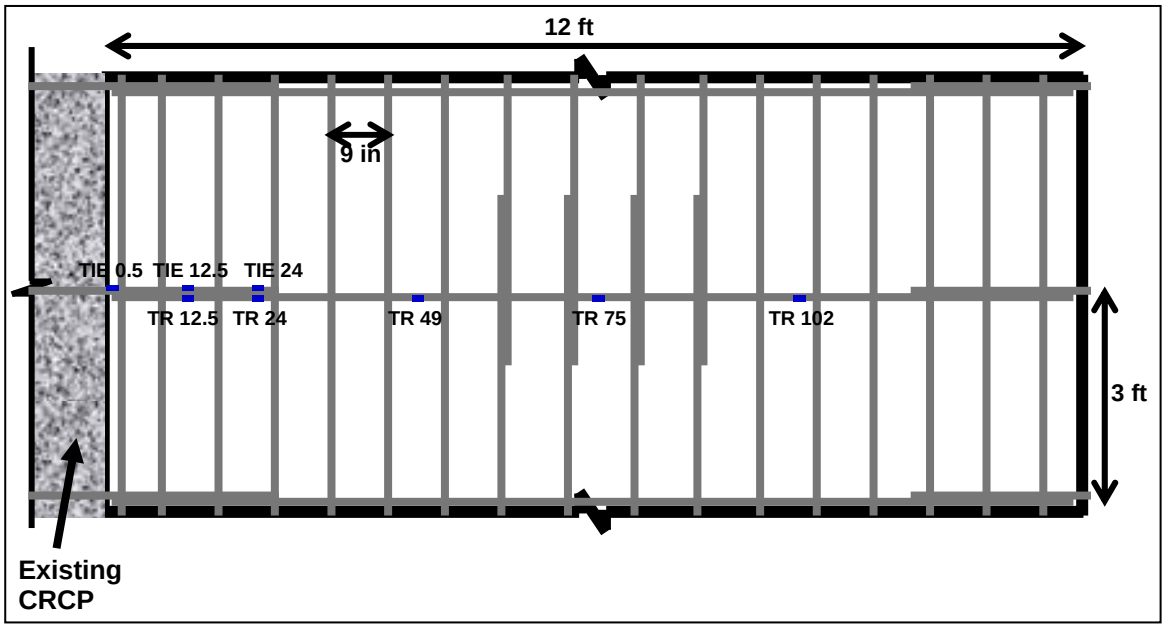

Figure 5.14: Testing layout for steel stress measurements

(a) Steel strain gages installed

(b) Steel gage at longitudinal joint

Figure 5.15: Strain Gage Installation

Concrete was place at 6 pm, and concrete setting temperature at the mid-depth was about 85 °F, that occurred at about 10 pm. Figure 5.16 shows concrete temperatures at three different depths and tie bar stress at longitudinal construction joint. A maximum steel stress of about 25 ksi is observed. The steel stress at the tie bar computed from the equation above results in about 12 ksi. It appears that warping and curling is responsible for rather high steel stress at the tie bar, and the current design for tie bars might not be adequate. Figure 5.17 illustrates the stresses in transverse steel at different locations. It is observed that the stress level is quite low at all locations. The comparisons of steel stresses at various locations are not meaningful because the values are so small and are within the measurements error range. These low stresses might be

due to the fact that the steel is located at the neutral axis and warping and curling has little effects on steel stresses.

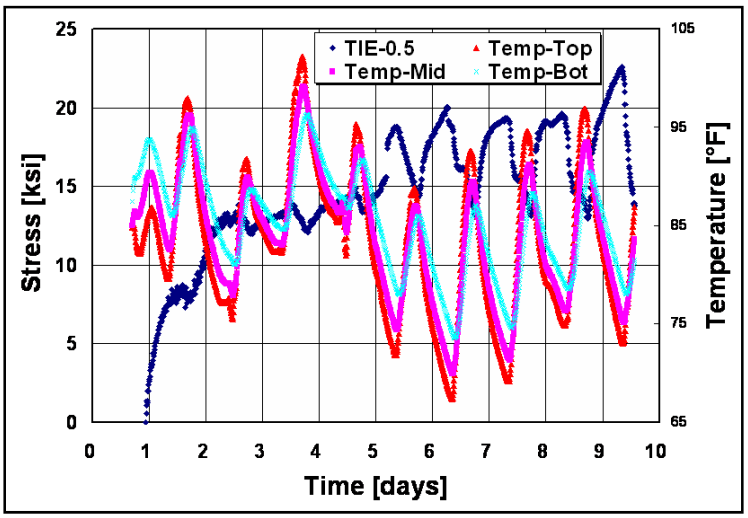

Figure 5.16: Tie bar stress at longitudinal construction joint

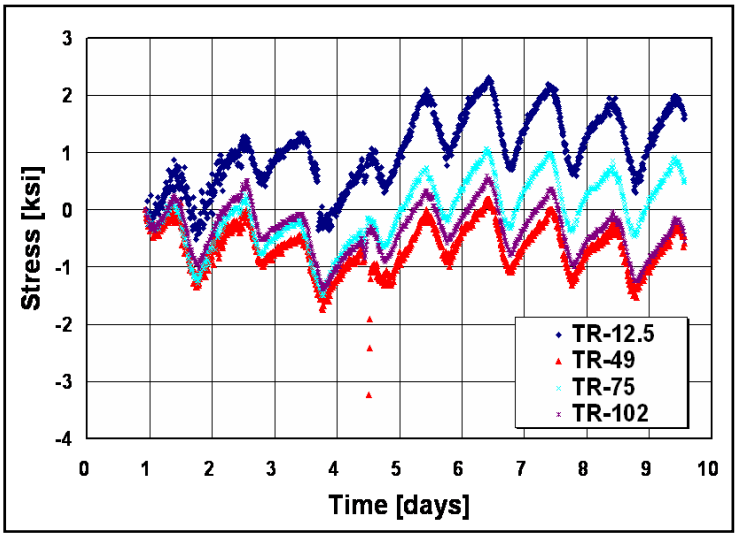

Figure 5.17: Stresses in transverse steel

To evaluate warping and curling in CRCP, CTR conducted field testing on US 183 in the Austin District. Figure 5.18 shows the testing setup. Figure 5.19 shows warping and curling of the CRCP at the edge of the slab shown in Figure 5.18. It is noted that, after day 5, curling of concrete is directly a function of air temperature, even though the trend is not that clear between days 3.5 and 5.

Figure 5.18: Field testing for curling measurement

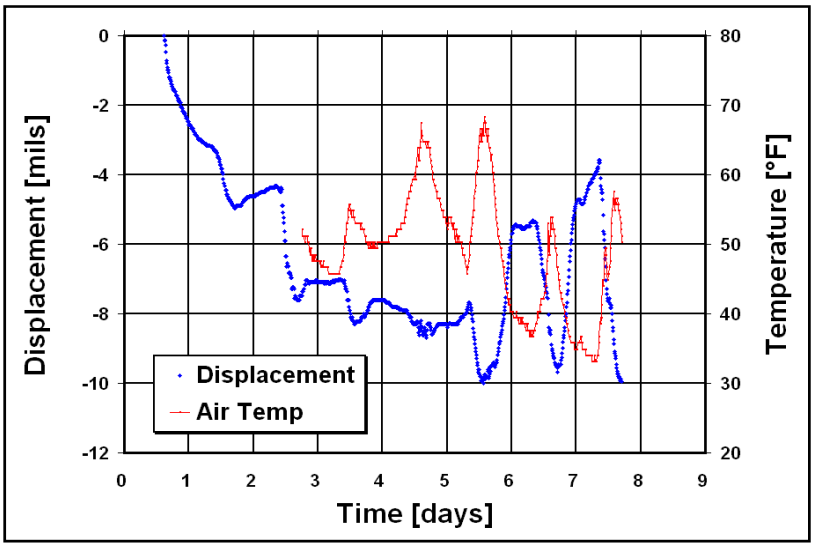

Figure 5.19: Air temperature variations and warping and curling of CRCP

It is noted that there were little variations in vertical slab movement between days 3.5 and 5. What happened was that there was a rain on day 3, and concrete volume changes due to moisture variations in concrete caused warping of the slab. Figure 5.19 shows the relative humidity (RH) measured in the air, which indicates quite high RH between days 3.5 and 5. The combined effects of temperature and moisture variations in this time period resulted in little variations in vertical slab movement.

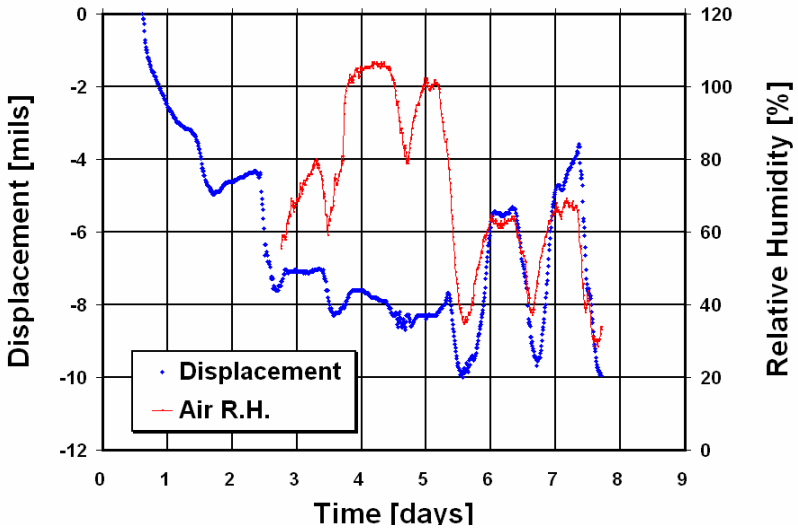

Figure 5.20: Variations in air relative humidity and warping & curling of concrete

Figures 5.19 and 5.20 indicate a maximum warping and curling of more than 6 mils was observed. This implies that the slab and subbase might not be in full contact in this area, nullifying one of the assumptions in SGDT.

5.2.3 Summary & Recommendations

Subgrade drag theory does not appear to describe concrete slab behavior in CRCP properly. Rather, warping & curling might be a dominant factor in determining concrete slab behavior. The reason why SGDT is not applicable to the proper analysis of CRCP slab behavior is described below:

- An assumption made in SGDT that temperature is uniformly distributed through slab depth is not valid
- Concrete slab displacements are not one-dimensional, as assumed in SGDT. (Figure 5.19)
- An assumption that concrete slab and subbase are always fully contacted is not valid, especially near the edge of the pavement slab (Figure 5.19)
- Concrete stresses computed by SGDT indicate that longitudinal cracks will not take place even when the pavement width is more than 150 ft. Field evidence shows that when the slab width is more than 17 ft, potential for longitudinal cracks increases substantially.

Because relief joints (longitudinal construction and warping joints) are provided every 12 ft, the potential for longitudinal cracking in CRCP will be minimal, as long as proper joint construction practices are exercised. That's one of the reasons why no transverse steel is used in jointed concrete pavements. Transverse steel in CRCP is needed to provide support for longitudinal steel. However, the amount of transverse steel needs to be determined using a proper theory. At this point, warping and curling theory describes the CRCP behavior better and appears

to be more appropriate for that purpose, not SGDT. Based on the past practice in Texas and the practices of other states, it is recommended that, until more definite research findings are available, 3 ft spacing with #6 bars be used for transverse steel in CRCP regardless of pavement widths. This will alleviate the potential for adverse effects such as too close transverse cracks.

As for the design of tie bars, stresses in tie bars should be theoretically analyzed and field monitored. With sufficient field data, if warranted, new designs for tie bars should be developed.

- Slabs show flexural behavior and, therefore, do not follow the behavior assumed in SGDT.
- Current practice of tie bar spacing determination using SGDT could result in excessive stresses in tie bars for PCC pavements of small widths.
- There appears no stress transfer from tie bars to transverse steel, and stress level in transverse steel is quite low.
- Depth and spacing of tie bars have substantial effects on steel stress. Tie bars placed above the mid-depth or missing tie bars could result in excessive stresses in tie bars.

Recommendations

- Transverse steel spacing could be increased to 3 ft or more, regardless of slab widths.
- New methodology for tie bar size and spacing determination, which accounts for curling behavior and thickness of slabs and load transfer aspect, is needed.
- Warping joint saw-cut depth could be 1/3 of slab thickness regardless of coarse aggregate type.
- Saw cut depth could be checked as a job acceptance testing.
- Including tolerances for tie bar depth in the Standards could be beneficial.

Financial Impact

- At the current price of steel, increasing transverse steel spacing from 1 ft to 3 ft will reduce the construction cost by $300k per mile for 100 ft wide section.

Guidelines for transverse steel design have been developed and are in Appendix P.

Chapter 6. Implementation of US 75 in Sherman, Texas

6.1 Background and Scope of Activities

US 75 in Sherman was constructed in the mid 1980s. The section of US 75 that was investigated consisted of 10 in. thick, 3-lane JCP with tied, keyed, and unkeyed longitudinal joints. The section investigated was 14 contiguous slabs between lanes 2 and 3 on the northbound side of US 75 after the entrance ramp and just prior to the exit ramp 68 (Crawford Street). Figure 6.1 shows a satellite image of the section.

Figure 6.1: Satellite Image of Section

Researchers conducted field investigations on the 14 slabs on March 31 through April 2, 2008. The slabs were numbered sequentially from the southern-most northward in a section located just prior to the exit ramp 68 on US 75. The worst faulting occurred at slabs numbered "5" and "6" and gradually tapered off to essentially no faulting at slabs "12" and "13." The objective of this investigation was to determine a location suitable for a field trial section to evaluate and monitor guidelines and methods for rehabilitation that was proposed by the researchers. Once the field trial is completed, guidelines can be adjusted to accommodate findings. Activities performed included:

1. Visual Inspection: Location displaying both bad faulting and almost no faulting at the longitudinal construction joint was selected. Longitudinal cracks and joint separations were inspected; crack widths and degree of slab faulting were recorded.
2. Falling Weight Deflectometer: FWD tests were conducted at multiple locations along the longitudinal construction joints. Load transfer efficiency (LTE) was calculated for joint separations of various widths.

3. Ground Penetrating Radar: GPR tests were conducted and tie bar locations were detected.
4. Dynamic Cone Penetrometer: DCP tests were performed in both faulted and stable slabs to determine the subgrade modulus.
5. Coring: Cores were taken at 4 locations along the longitudinal joints over tie bars in both the faulted and stable areas.

6.2 Pavement Condition Report

There were many problems observed along US 75: shattered and depressed slabs, tie bar exposure, faulting along longitudinal joints, transverse cracks in CPCD sections, and poor base conditions including standing water in the base material.

Using the GPR to locate the reinforcement, at least six tie bars were found in every 15-ft long slab at the longitudinal joint and ten dowel bars were found at the transverse joints. Figure 6.2 shows the ties bars located by the GPR.

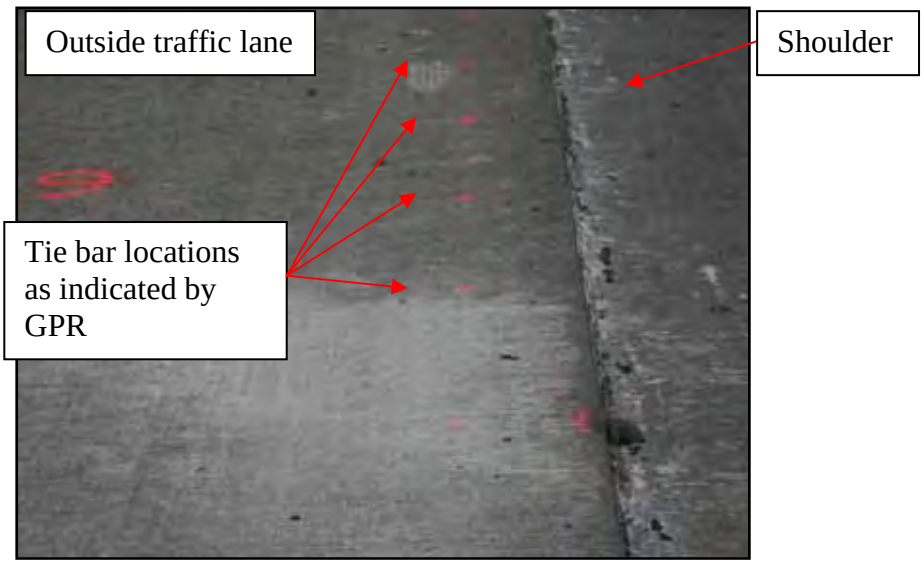

Figure 6.2: Slab 6 Tie Bar Locations Between Shoulder and Outside Traffic Lane

Load deflections and load transfer efficiency along the longitudinal joint of each slab was measured using the FWD in several locations along each slab: at the left transverse joint, at the tie bar, and at the right transverse joint, see Figure 6.3. The deflections plot in Figure 6.4 shows that the dowel bars at the transverse joint are mostly providing good load transfer (red circle and green square for two adjacent slabs are close together) and it illustrates the curling effect occurring along each slab. The curling effect causes the slab ends to deflect (curl) vertically upward or downward depending on the temperature (time of day) and moisture content at the particular slab's location. When the top and bottom of the slab are at different temperatures one side wants to contract while the other wants to expand. If the top of the slab is warmer than the bottom of the slab it will want to expand and will curl downwards (creating and upside down

"U" shape). In Sherman, the slabs were cooler on the top then on the bottom and were curling upwards. Moisture often serves as a mitigating factor to the curling effect.

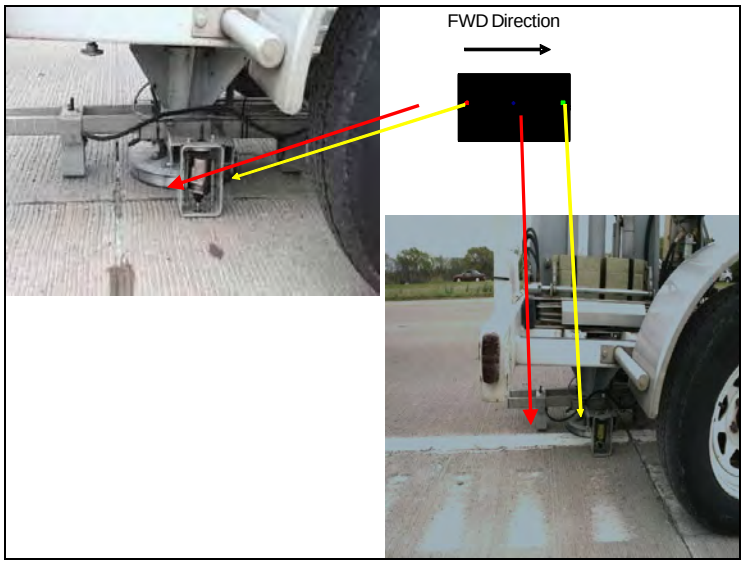

Figure 6.3: FWD Setup Diagram

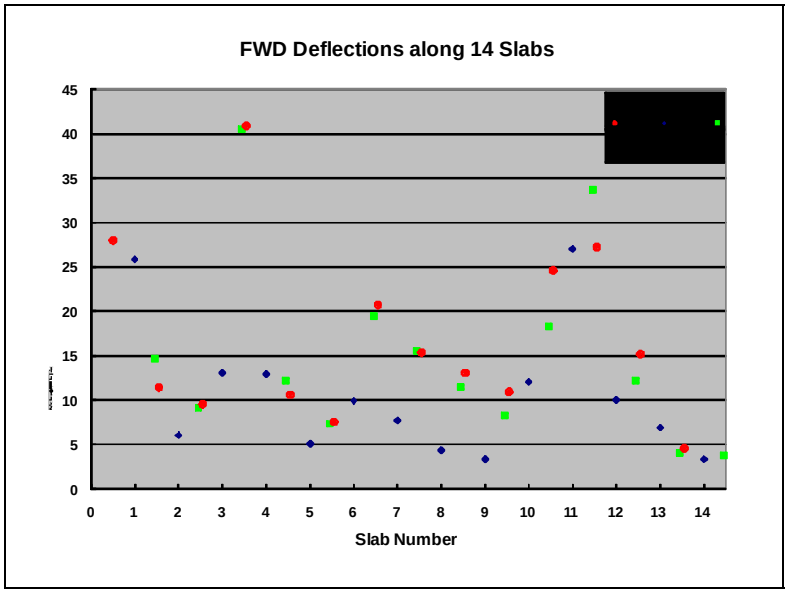

Figure 6.4: FWD Deflections Along Slabs

DCP tests were run in both the faulted and non-faulted areas. The subgrade modulus values were poor with the exception of the modulus at Slab 5. Slab 5 and 6 had the worst faulting of the 14 slabs investigated; see Section 4.3 for more information.

The cores were taken along the longitudinal joint in both the faulted and non-faulted regions. The cores retrieved from the faulted areas showed shear failure of the tie bar as well as corrosion of the tie bar. These tie bars were #4 bars. Evaluation of these core holes indicated

voids under the longitudinal joint. Where the faulting was greatest (Slabs 5 and 6) (Figure 6.7), the subbase material obtained from the hole was clean gravel, with almost no fine materials indicating pumping of the slab (Figure 6.5). In contrast, the subbase material obtained from core holes in non-faulted areas contained both gravel and fine materials (Figure 6.6).

Figure 6.5: Subbase Material Resulting from Slab Pumping at Slab 5

Figure 6.6: Good Subbase Material at Slab 14

Figure 6.7 shows a section through the pavement along the longitudinal construction joint. This condition was observed where faulting was the greatest. A core was taken at the joint and the base material was observed. The construction joint had allowed water to penetrate to the base and pumping began to occur from the faulted slab in Lane 2. This pumping of the slab is evident from the clean gravel (no fine materials) found at the base and the approximately 3 in. deep by 5 in. wide void detected under the Lane 2 slab (Figure 6.86).

The mechanics of the slab faulting is an iterative process. The faulting is a result of joint separation, which leads to water infiltrating into the joint. The water infiltration leads to deteriorated base and softening of the subgrade which leads to deflection of the slab. This deflection leads to pumping out of fine materials from the base and that leads to the creation of voids under the slabs. The voids allow larger slab deflections which leads to cracking, spalling and larger separations.

Figure 6.7: Faulted Slab 5

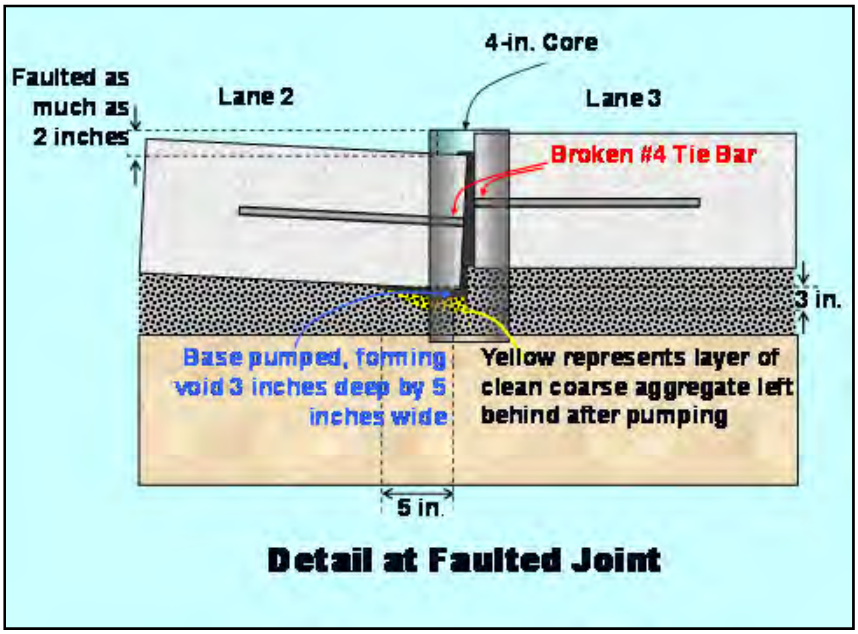

Figure 6.8: Faulted Joint Detail

Researchers additionally found keyed joints where faulting was minimal or non-existent, but none where faulting was greatest. These keyed joints occurred at Slabs 13 and 14 and cores were taken at a tie bar. At the Slab 13 joint, a small separation had occurred and the tie bar at that location has corroded as shown in Figures 6.9 and 6.10. In contrast, the Slab 14 joint is much tighter and its tie bar is in much better condition. The cracking around the Slab 14 keyed joint shows signs of imminent failure. The cracking around the key way can be seen in Figure 6.11.

Figure 6.9: Slab 13 Keyed joint

Figure 6.10: Slab 13 Corroded tie bar in keyed joint

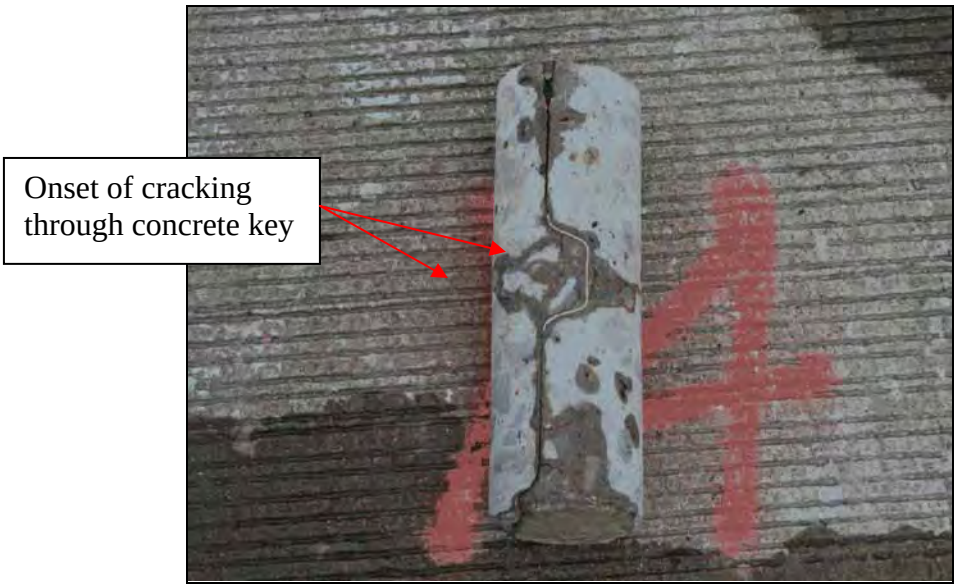

Figure 6.11: Slab 14 tight keyed joint

6.3 Analysis of Findings

The condition of the section analyzed along US 75 is summarized in the following deflection and LTE graph (Figure 6.12). There is a direct relationship between FWD deflections and LTE; the higher the LTE observed the lower the deflection and vice versa. This relationship was confirmed upon testing; when there was good LTE across the longitudinal joint there was minimal slab deflection observed.

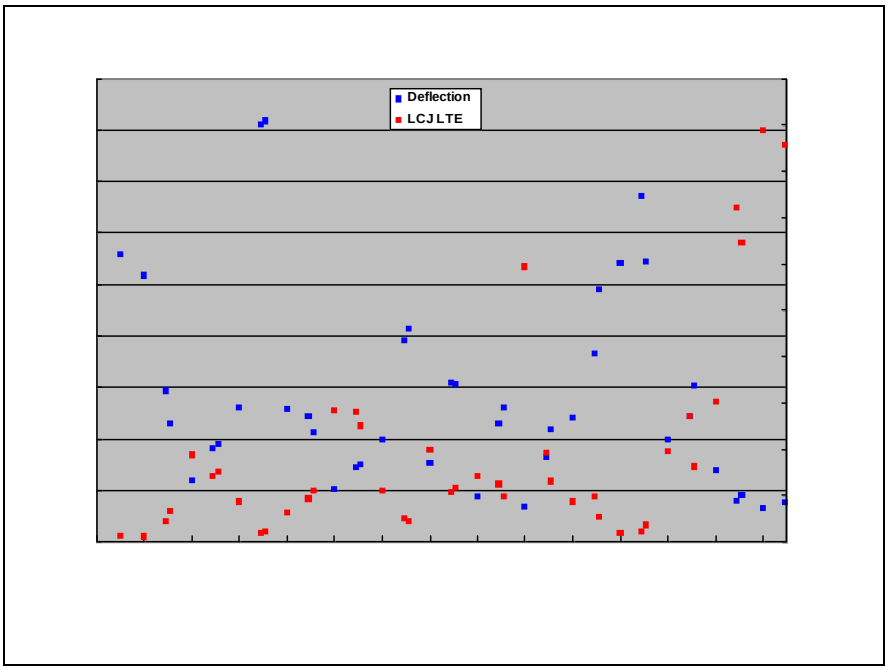

Figure 6.12: FWD Deflections and LTE at LCJ

Average LTE was very low (less than 30%) along the longitudinal joint but was quite high along all transverse joints. Slabs 5 and 6 had the worst faulting. Slab 5 had a good subgrade modulus (approximately 21,000 psi) while Slab 6 did not (approximately 11,500 psi). Despite the good subgrade modulus at slab 5, LTE was not good (approximately 30%). Slab 13 and 14 both have keyed joints and exhibit the best LTE of the slabs tested. Slab 14 shows higher LTE than Slab 13 (80 to 90% vs. 65 to 75%) because of a small separation of the construction joint occurring at Slab 13, see Figure 6.9. The high LTE at Slabs 13 and 14 is a direct result of the keyed joints. The high deflection found at Slab 3 was due to the large crack running across the slab. The LTE at Slab 9 is much higher than the previous slabs because the tie bars were not broken (LTE is about 60%). While LTE was not very high at Slab 9, it was at least twice as much as the LTE at Slabs 1 to 8 and 10 to 12. This shows the effect tie bars have in pavement performance and illustrates the importance of well placed and working bars.

During the field study researchers also explored the effect the distance from the corner of the pavement has on pavement deflections. The data presented in Figure 6.13 illustrates the warping effect that takes place across the width of the pavement. There are much higher deflections at the corners of the slab than at the center of the slab.

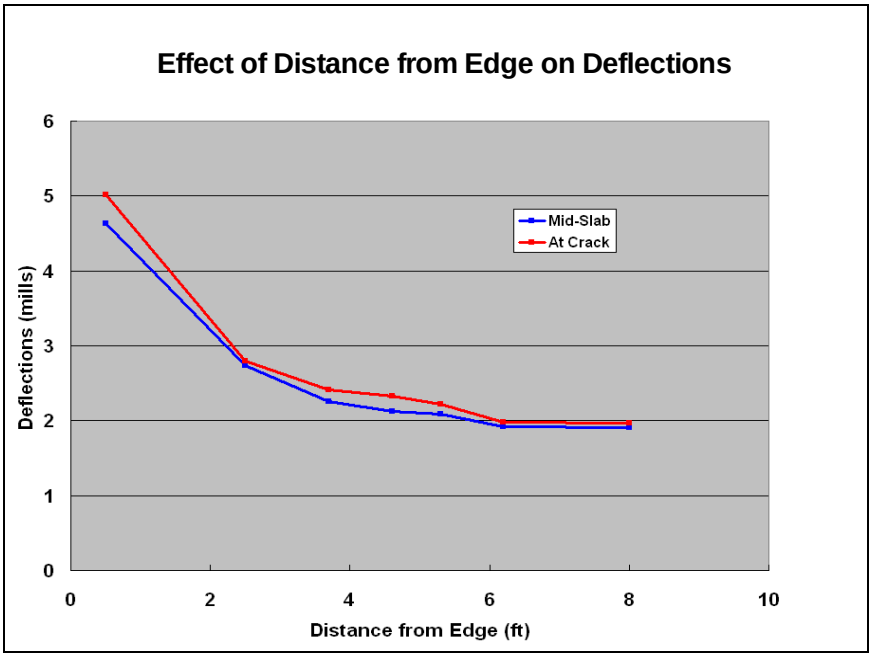

Figure 6.13: Edge Distance vs. Deflection

The effect of subgrade modulus (stiffness) and deflections was also investigated during the field study. Higher subgrade modulus resulted in lower observed deflections. The data presented in Figure 6.14 displays the effect of subgrade modulus and deflection for both the interior and edge condition. The graph shows that subbase stiffness does not have substantial effects on deflections. The three most important factors affecting deflections are slab thickness, loading condition, and whether there is void present.

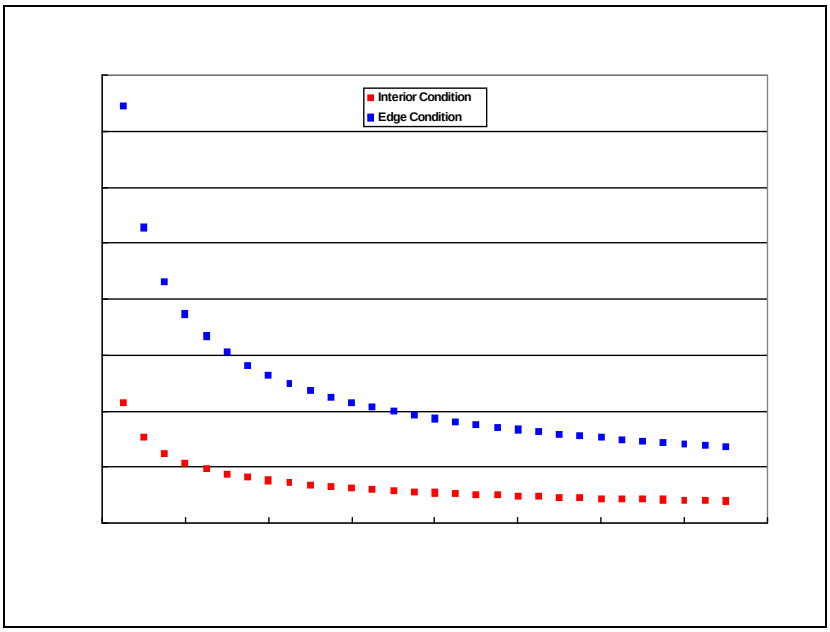

Figure 6.14: Subgrade Reaction Modulus vs. Deflections

Slab 14 had the highest LTE of all the slabs observed. Currently it is in good form but it is starting to deteriorate, as evident by the cracking to the left of the key. The keyed joint provides the tie bars extra vertical resistance and strength. Support conditions are very important to integrity of the keyed joint, if there is a loss in support, aggregate interlock will be the only factor preventing the key from shearing off. Once that happens the performance of Slab 14 will begin to deteriorate and resemble the middle slabs (Slabs 5 to 9). It is important to restore slab 14 before its LTE drops significantly before it causes more problems along US 75 and becomes very costly to repair. Figure 6.15 shows the current LTE values and corner deflections for each slab and where the LTE and corner deflections of slab 14 will end up if the pavement issues along US 75 are not addressed properly and in a timely manner. The failing longitudinal joints were between the outside travel lane and the paved shoulder. The section examined was just north of the entrance ramp from Loy Lake Road onto northbound US 75 north of Sherman, TX (south of northbound US 75 Exit 68, Crawford Street).

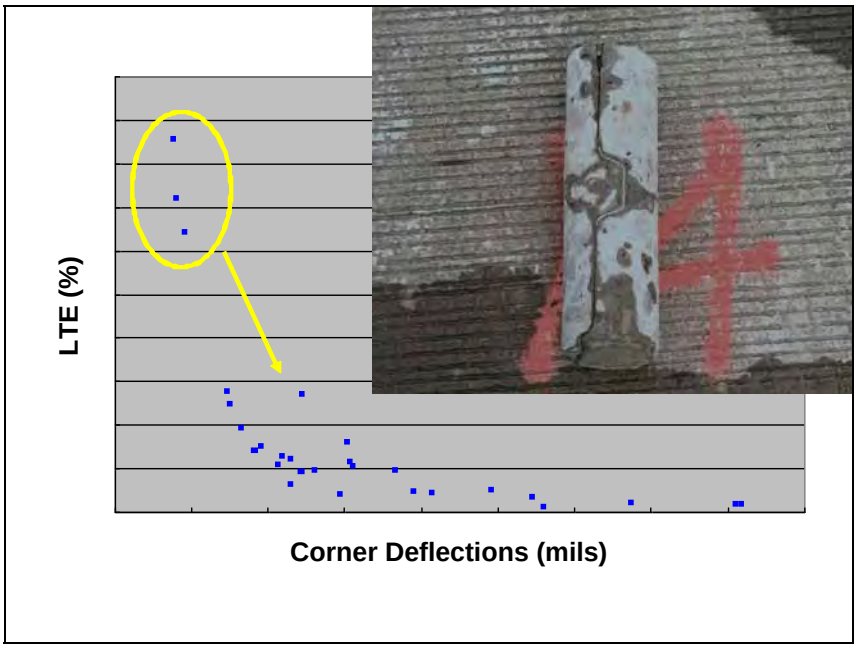

Figure 6.15: Corner Deflections vs. LTE for Slab 14 (at longitudinal joint between outside travel lane and shoulder, 14th slab immediately north of entrance ramp from Loy Lake Road on northbound US 75 north of Sherman, TX)

6.4 Conclusions/ Findings

Based upon the observations made during the field investigation the research team reached the following conclusions:

- Lane 2 faulting at Longitudinal Joint with Lane 3
- Pavement stained from pumping
- Distresses due to edge loading and resulting pumping
- Distresses similar to those at AASHO Road Test
- FWD indicates high deflections and minimal load transfer across longitudinal joint
- Good subgrade conditions are necessary for good LTE
- Very few shattered slabs (none in the northbound inspected section)
- Poor base support on faulted edge
- Virtually no load transfer

The research team recommends the following rehabilitation:

- Rehab with minimal slab replacement
- Restore LTE at longitudinal joints to improve the performance.
- Utilize new tie bar design concept
- Restore base support

- Restore tie bars
- Restore grade on faulted slab to height of Lane 3

6.5 US 75 Repair Procedures

Upon performing the field investigation along US 75 a suitable field trial section was determined. This section contains many problems that have been seen throughout the state. The US 75 field trial is an excellent culmination of the entire research project and will allow for the evaluation and monitoring of guidelines and specifications that have been proposed. Once the rehabilitation job is completed, guidelines will be adjusted to accommodate findings. This section describes the proposed repair procedures for the US 75 field trial section. Guidelines and specifications for repair of longitudinal cracking and joint separations are shown in Appendix M. Specifications for construction of longitudinal joints are shown in Appendix N.

6.5.1 Description of Repair Procedures for Depressed Slabs

1. Restore base support where possible (as shown in Figure 6.16)
2. Restore load transfer using retrofit tie bars (Figure 6.17)
3. Restore smooth transition across joint (Figures 6.18 and 6.19)

Restore support

Pump Grout Under Slab

1. Drill injection holes at longitudinal joint
2. Cementitious grout
3. Low pressure
4. Fill void only (no slab-jacking pressures)
5. Slowly fill until grout begins to flow out of joint or adjacent injection port

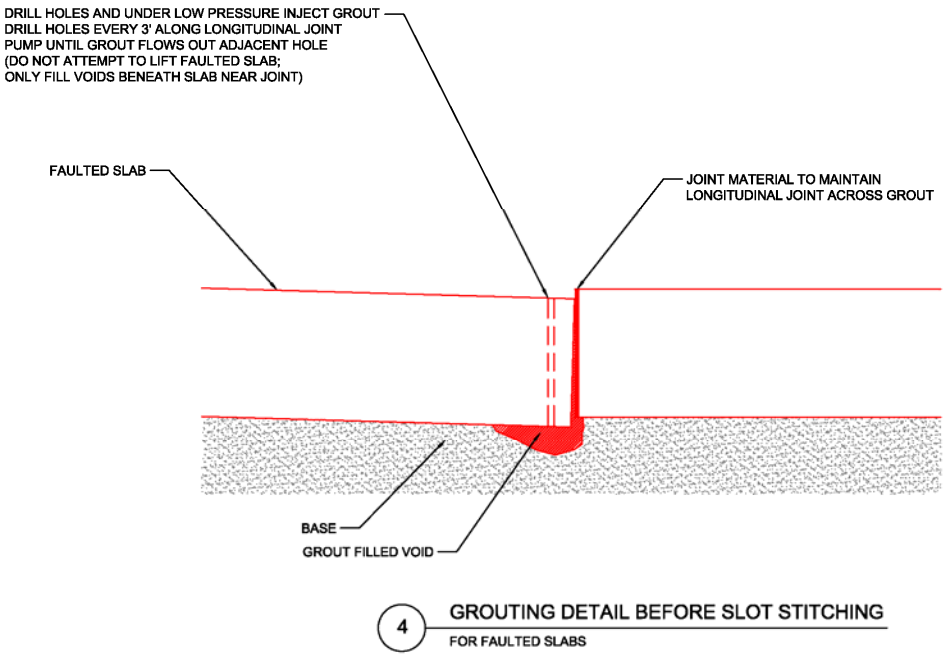

Figure 6.16: Restore Base Support—Grouting Detail

Restore Load Transfer

Preparing the slot specification drafted

1. Saw at least 3 parallel transverse cuts and break out resulting ridges to make 1 ¾ inch wide slots
2. 6 inches deep x 60 inches long
3. Slots 3 feet apart
4. Perpendicular to and Centered over Longitudinal Joint

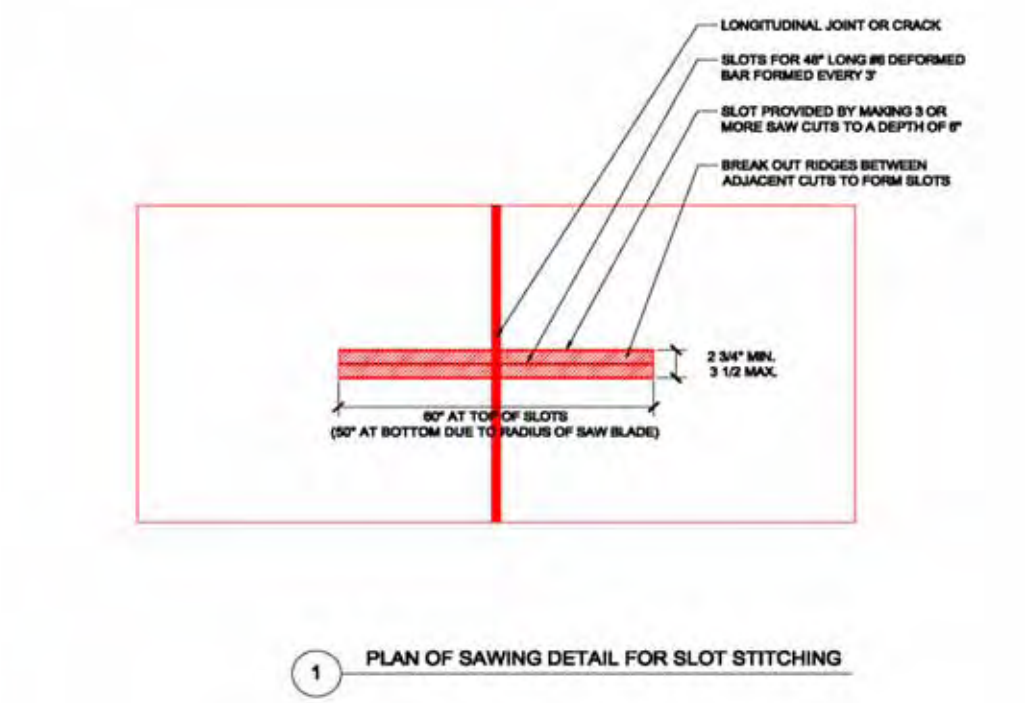

Figure 6.17: Restore Load Transfer- Sawing Detail

- Slots must be sand blasted & blown out with clean dry air to remove all dust and debris
- Filling the slots
- 48-inch No. 6 bars on chairs in the slot
- Allow at least 1 inch grout beneath the bar and ½ inch grout on each side of the bar
- Fill with grout surface of the slabs

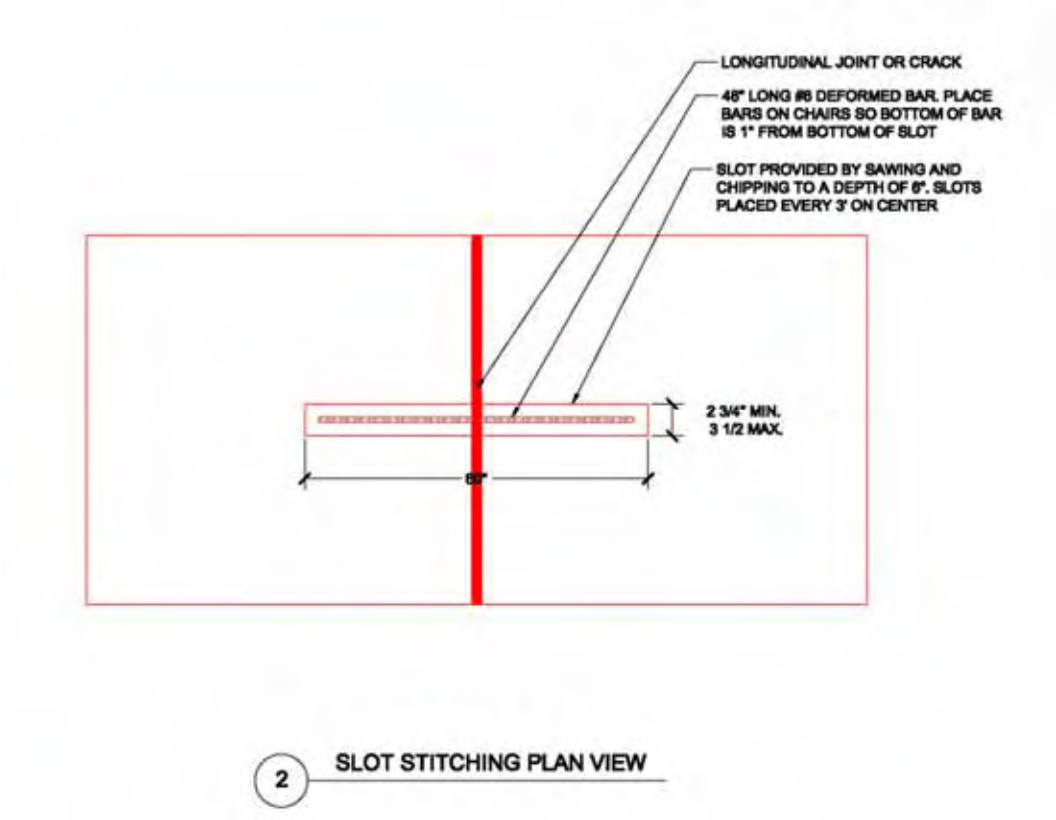

Figure 6.18: Restore Load Transfer—Slot Stitching Plan

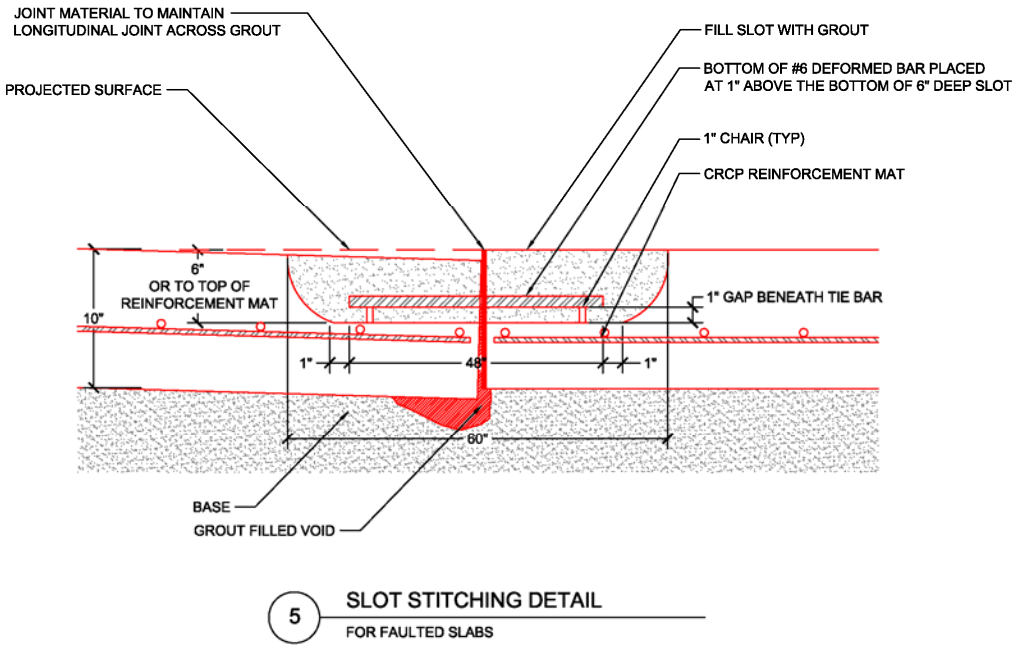

Figure 6.19: Restore Load Transfer—Slot Stitching Detail

Restore smooth transition across joint

- Mill depressed slab (milling detail shown in Figure 6.20)
    - Reduce high end of faulted slab
        - Reduce to allow for a minimum of 1” depth of overlay
        - Shot blast to provide clean and dry substrate for overlay

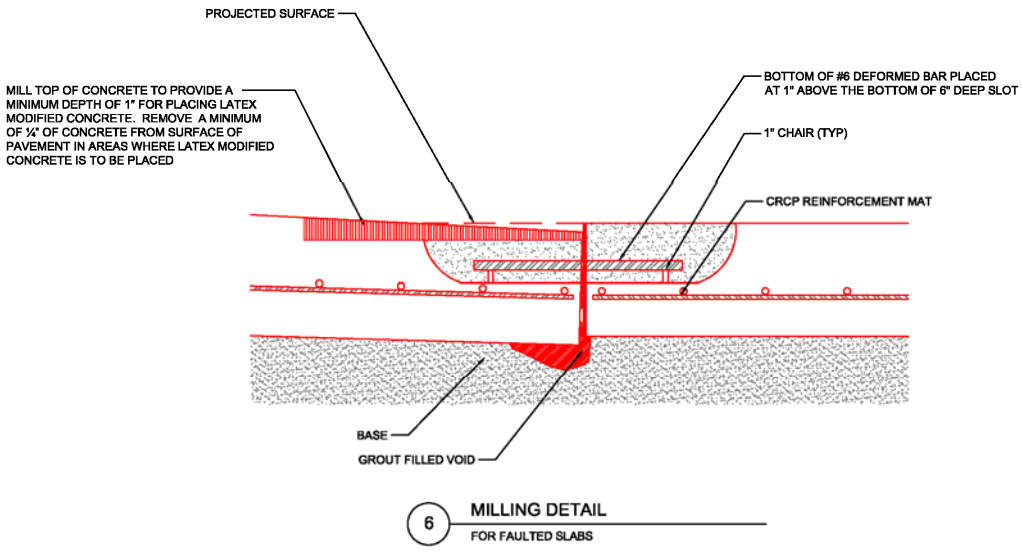

Figure 6.20: Restore Smooth Transition—Milling Detail

- Level Up at Longitudinal Joint with High Slab (Figure 6.21)
    - Use rapid setting latex-modified concrete overlay

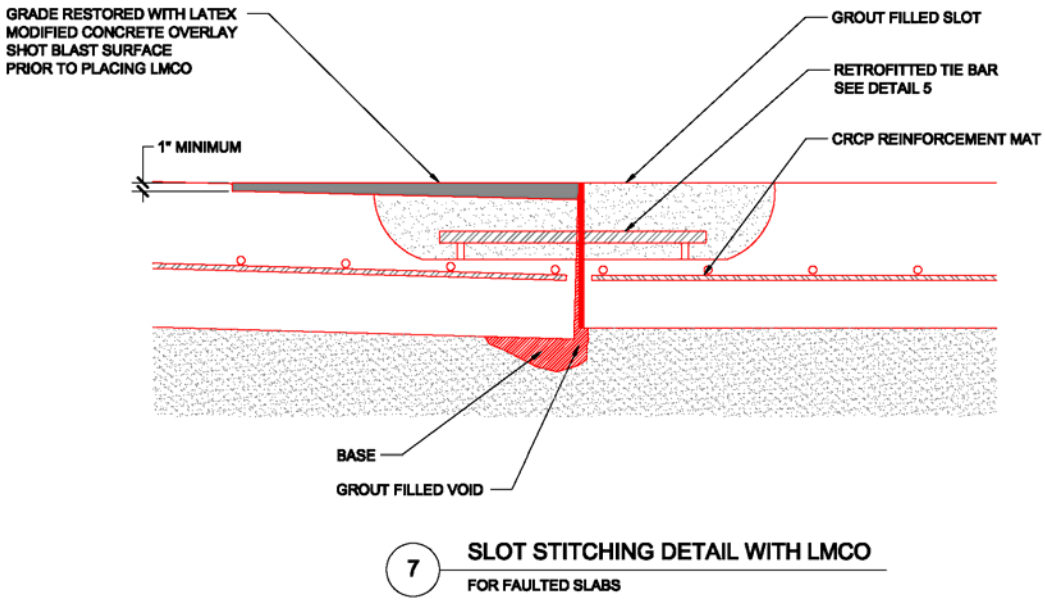

Figure 6.21: Restore Smooth Transition—Slot Stitching with LMCO

6.5.2 Description of Repair Procedures for Longitudinal Cracks

- For longitudinal or other cracks that require repairing, slot stitching should be used.

Chapter 7. Summary and Conclusions

7.1 Summary

Longitudinal cracking and longitudinal joint separations in concrete pavements have plagued the state of Texas and have become an expensive maintenance endeavor. This uncontrolled cracking and joint separation at the longitudinal construction joint has often led to corrosion of the steel reinforcement and the erosion and pumping of the base layer due to moisture penetration through the cracks and joints. This then results in open cracks, spalling, and slab faulting, researchers examined the causes of the distress and developed and tested methods for repair and prevention. Email and phone surveys were distributed to TxDOT engineers, other state Departments of Transportation and industry organizations, and a literature review was conducted to determine the current state of practice. Field investigations were conducted on numerous concrete pavements throughout the state to determine the cause(s) of distress and to determine if anything has been successful in mitigating the distress. Finite element modeling was conducted to examine the relative magnitude of stress that proposed repair methods introduced onto the concrete pavement. Experimental tests were conducted to determine strengths and weaknesses of each repair method under various loading conditions encountered in the field. Various sizes, spacings, shapes, and placement methods for transverse steel and tie bars were investigated and evaluated. Lastly, a field trial section was selected, so the findings from this research project can be evaluated. The field trial section will not only implement and assess slot stitching, but will also include leveling up depressed slabs with a latex modified concrete overlay.

7.2 Conclusions

Upon completion of the research project, the researchers have developed repair and new construction procedures for longitudinal cracking and joint separations in concrete pavements have been determined (Appendix M and N). Also tie bar and transverse steel designs have been developed (Appendix O and P). The Districts should monitor their pavements carefully, noting any longitudinal cracks or joint separations. Once cracks or separations have been identified, FWD tests should be performed on a representative sampling of locations, including the best and worst instances of the distress.

The following conclusions regarding longitudinal cracking and joint separations in concrete pavements have been made upon completion of the research project:

1. Longitudinal cracking in JCP is most often caused by shallow and possible late saw cutting of longitudinal warping joints.
2. Longitudinal joint separations are caused by corrosion of tie bars in conjunction with dynamic traffic loading.
3. Longitudinal cracks should be repaired as soon as possible after identification to prevent further deterioration and separation. Repairing the cracks early saves money in the long term.
4. Cross stitching should be used to repair cracks/separations that are fairly tight. For wider cracks/separations slot stitching should be used.

5. Slot stitching is the most economical repair method for restoring load transfer, preventing separations, and improving performance of longitudinal joints and wide cracks.
6. Corrosion and shear were found in association with tie bar failures, therefore #6 bars should be used instead of the specified #4 bars.
7. In this study, there was no direct correlation found between DCP readings and the likelihood of longitudinal cracking or joint separations. But when lower modulus values were found, the possibility of problems with longitudinal cracking and joint separations was greater.
8. Voids were found under faulted slabs. An underseal should be inserted into the voids to re-establish uniform support for the slabs.
9. When taking LTE readings, the deflections associated with the LTE test locations need to be known to determine the condition of the pavement. A high or low LTE reading can be misleading; a high LTE reading does not necessarily mean the pavement is in good condition. However high measured deflections always means the slabs have low LTE.

References

American Concrete Institute (2002). Building Code Requirements for Structural Concrete (ACI 318-02) and Commentary (ACI 318R-02). American Concrete Institute: Farmington Hills, NM.

American Concrete Pavement Association (ACPA) (1995). “How to Reseal Pavement Joints”. Concrete Repair Digest (April/May).

American Concrete Pavement Association (ACPA) (2001) Stitching Concrete Pavement Cracks and Joints. Special Report SR903P. American Concrete Pavement Association: Skokie, IL.

American Concrete Pavement Association (ACPA) (2006). Repair Techniques that are both Corrective and Preventative. Available from http://www.acpa.org/. American Concrete Pavement Association: Skokie, IL.

Ardani, A, Hussain, S, and LaForce, R. (2003) Evaluation of Premature PCCP Longitudinal Cracking in Colorado. Report No. CDOT-DTD-R-2003-1. Colorado Department of Transportation: Denver, CO.

ASTM International (2007). Standard Test Method for Use of Dynamic Cone Penetrometer in Shallow Pavement Applications. Designation: D 6951-03. ASTM International: West Conshohocken, PA.

Bradbury, R.D., Reinforced Concrete Pavements, Wire Reinforcement Institute, Washington D.C., 1938

Buch, N, Frabizzio, M, and Hiller, J. (2000) “Impact of Coarse Aggregates on Transverse Crack Performance in Jointed Concrete Pavements”. ACI Structural Journal (May-June).

California Department of Transportation (Caltrans) (2004a). Concrete Pavement Design Overview. Available from http://dot.ca.gov. California Department of Transportation: Sacramento, CA.

California Department of Transportation (Caltrans) (2004b). Interim PCC Pavement Rehabilitation Guidelines. Available from http://dot.ca.gov. California Department of Transportation: Sacramento, CA.

California Department of Transportation (Caltrans) (2004c). Slab Replacement Guidelines. Available from http://dot.ca.gov. California Department of Transportation: Sacramento, CA.

Chen, Dar Hao and Won, Moon (2007). Field Performance Monitoring of Repair Treatments on Joint Concrete Pavements.

Comité Euro-Internaltional du Béton-Fédération International de la Précontrainte (CEB-FIP), CEB-FIP model code 1990, Design code, Thomas Telford, 1993

Construction Technology Laboratories (2002). Summary of CRCP Long-Term Performance. Concrete Reinforcing Steel Institute: Shaumburg, IL.

DIANA, release 9.1., Division of Engineering Mechanics and Information Technology, TNO Building and Construction Research, Delft, The Netherlands, 2007

Eddie, D, Shalaby, A, and Rizkalla, S. (2001). "Glass Fiber-Reinforced Polymer Dowels for Concrete Pavements". ACI Structural Journal (March-April).

Federal Highway Administration (FHWA) (1997). LTPP Data Analysis: Frequently Asked Questions About Joint Faulting With Answers From LTPP. Publication No. FHWA-RD-97-101. Federal Highway Administration: McLean, VA.

Federal Highway Administration (FHWA) (2003). Evaluation of Joint and Crack Load Transfer. Publication No. FHWA-RD-02-088. Federal Highway Administration: McLean, VA.

Federal Highway Administration (FHWA) (2005). Structural Factors of Jointed Plain Concrete Pavements: SPS-2- Initial Evaluation and Analysis. Publication No. FHWA-RD-01-167. Federal Highway Administration: McLean, VA.

Federal Highway Administration (FHWA) (2006a). Materials and Procedures for Repair of Joint Seals in Portland Cement Concrete Pavements. Publication No. FHWA-RD-99-146. Federal Highway Administration: McLean, VA.

Federal Highway Administration (FHWA) (2006b). Resealing Concrete Pavement Joints. Publication No. FHWA-RD-99-137. Federal Highway Administration: McLean, VA.

Fowler, D, and Zollinger, D. (2005a). Investigation of Repair Materials for Spalling Concrete Pavement. Center for Transportation Research: Austin, TX.

Fowler, D, Whitney, D, and Jirsa, J. (2005b). Project No. 0-5444: Rehabilitation Procedures for Longitudinal Cracks and Joint Separations in Concrete Pavement. Unpublished project agreement available from the Center for Transportation, Austin, TX.

Ghali A. and Favre R., Concrete Structures: Stresses and Deformations, 2nd edition, E&FN SPON, London, 1994

Huang, Y. H., Pavement Analysis and Design, 2nd edition, Pearson Education, Inc., New Jersey, 2004

Kansas Department of Transportation (KDOT) (1990a). Cross Stitching Longitudinal Cracks in Concrete Pavement. Special Provision to the Standard Specifications, Edition of 1990. Kansas Department of Transportation: Topeka, KS.

Kansas Department of Transportation (KDOT) (1990b). Tie Bar Insertion. Special Provision to the Standard Specifications, Edition of 1990. Kansas Department of Transportation: Topeka, KS.

Kansas Department of Transportation (KDOT) (2005). Personal Communication via Email.

Kasmierowski, T. (2004). Personal Communication via Email.

Kazmierowski, T. (2005) Personal communication via Email.

Kim S., Won M., and McCullough B. F., Three-Dimensional Nonlinear Finite Element Analysis of Continuously Reinforced Concrete Pavements, Research Report 1831-1, Center for Transportation Research, The University of Texas at Austin, 2000

Mangum, W, Bermudez-Goldman, A, Whitney, D, Fowler, D, and Meyer, A. (1986) Repairing Cracks in Portland Cement Concrete Using Polymers. Center for Transportation Research: Austin, TX.

Masten, M. (2005). State of Minnesota Office Memorandum Transmitted via Personal Email.

Medina-Chavez, Dossey, and McCullough. "Prediction of Long-Term Minimum Concrete Temperature Using Climatic Variables". Presented at the 2005 Annual Meeting of the Transportation Research Board.

Merryman (2005). Electronic Survey Response.

Minnesota Department of Transportation (MnDOT) (2003). Concrete Pavement Rehabilitation, Section 5-694.900, Concrete Manual. Minnesota Department of Transportation: Saint Paul, MN.

Mohamed A. R. and Hansen W., Effect of Nonlinear Temperature Gradient on Curling Stress in Concrete Pavements, Transportation Research Record 1568, TRB, National Research Council, Washington D.C., 1997, pp. 65-71

New York Department of Transportation (NYSDOT) (2002a). Pavement Joints, Chapter 8, Comprehensive Pavement Design Manual. New York Department of Transportation: Albany, NY.

New York Department of Transportation (NYSDOT) (2002b). Rehabilitation, Chapter 5, Comprehensive Pavement Design Manual. New York Department of Transportation: Albany, NY.

New York Department of Transportation (NYSDOT) (2003). Portland Cement Concrete Pavement Restoration Interim Design Guidelines

New York Department of Transportation (NYSDOT) (2005). Comprehensive Pavement Design Manual. New York Department of Transportation: Albany, NY.

Pierce, L. (2006). Presentation Transmitted via Email.

Pierce, L, Uhlmeyer, J, and Weston, J. (2003). Dowel Bar Retrofit—Do's and Don'ts. Report WA-RD 576.1. Washington State Department of Transportation: Olympia, WA.

Texas Department of Transportation (TxDOT) (1993). Crack and Spall Repair (Elastomeric Patching Material). Special Specification 3408. Texas Department of Transportation: Austin, TX.

Texas Department of Transportation (TxDOT) (1994a). Concrete Pavement Details—Contraction Design. Detail CPCD-94. Texas Department of Transportation: Austin, TX.

Texas Department of Transportation (TxDOT) (1994b). Full Depth Repair for Concrete Pavement. Detail FDR (CP)-05. Texas Department of Transportation: Austin, TX.

Texas Department of Transportation (TxDOT) (1994c). Concrete Paving Details—Joint Seals. Detail JS-94. Texas Department of Transportation: Austin, TX.

Texas Department of Transportation (TxDOT) (2003). Continuously Reinforced Concrete Pavement. Detail CRCP (1)-03. Texas Department of Transportation: Austin, TX.

Texas Department of Transportation (TxDOT) (2004a). Cross-Stitching Cracks and Longitudinal Joints in Concrete Pavement. Special Specification 3054. Texas Department of Transportation: Austin, TX.

Texas Department of Transportation (TxDOT) (2004b). Slot Stitching (Epoxy Coated). Special Provision SP-215, Section 02755S. Texas Department of Transportation: Austin, TX.

Texas Department of Transportation (TxDOT) (2004c). Longitudinal Crack Repair. Texas Department of Transportation: Houston, TX.

Texas Department of Transportation (TxDOT) (2004d). Standard Specifications for Construction and Maintenance of Highways, Streets, and Bridges. Texas Department of Transportation: Austin, TX

Texas Department of Transportation (TxDOT) (2005a). Miscellaneous Roadway Details Texas Department of Transportation: Kaufman County, TX.

Texas Department of Transportation (TxDOT) (2005b). DMS-6140, Elastomeric Concrete for Bridge Joint System, In Departmental Material Specifications. Texas Department of Transportation: Austin, TX.

Texas Department of Transportation (TxDOT) (2006). DMS-6100, Epoxies and Adhesives, In Departmental Material Specifications. Texas Department of Transportation: Austin, TX.

Voigt, Gerald F. (2000). Specification Synthesis and Recommendations for Repairing Uncontrolled Cracks that Occur During Concrete Pavement Construction. American Concrete Pavement Association: Skokie, IL.

Washington State Department of Transportation (WSDOT) (1995). Departmental Change Order via Email.

Washington State Department of Transportation (WSDOT) (2001). Dowel Bar Retrofit In Tech Notes. Washington State Department of Transportation: Olympia, WA.

Washington State Department of Transportation (WSDOT) (2003). Dowel Bar Retrofit In Tech Notes. Washington State Department of Transportation: Olympia, WA.

Won, M. (2006a). Unpublished Research Information via Email.

Won, M. (2006b). Unpublished Research Information via Email.

Appendix A: Rationale for New FWD Sensor Arrangement

Figures A.1 and A.2 show the conventional sensor arrangement for conducting FWD tests.

Figure A.1: Conventional FWD setup in the Field

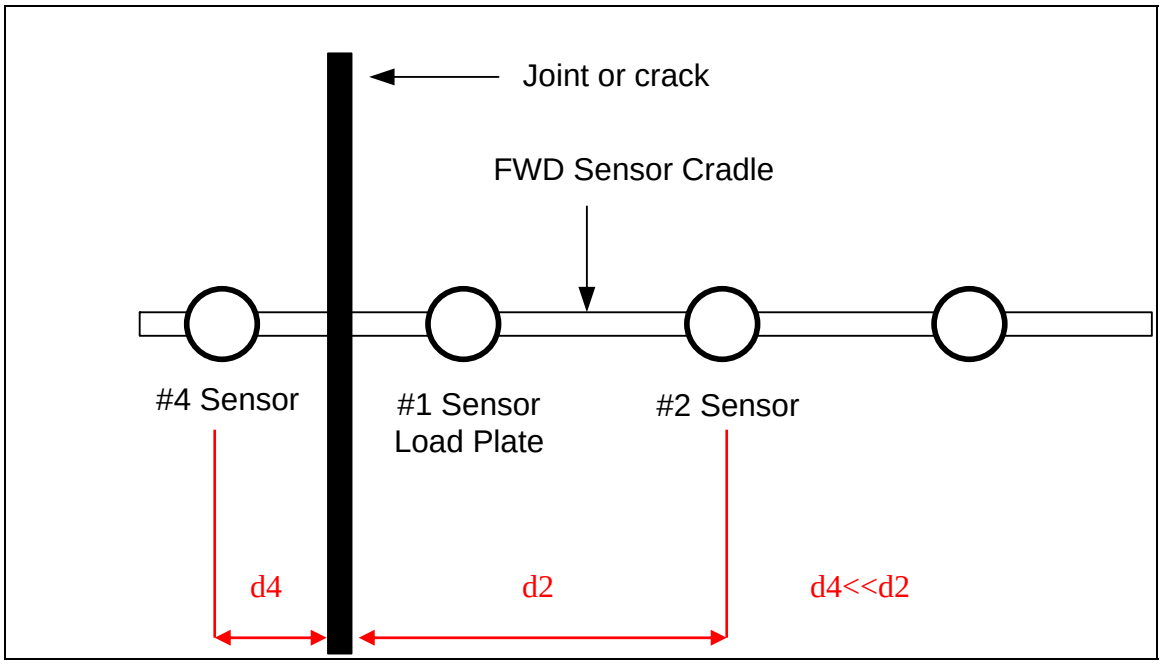

Figure A.2: Diagram of FWD Sensors

Figure A.3 shows values of #1 sensor deflection for various distances away from the pavement longitudinal free edge. It can be seen that for distances less than two feet away from the edge, deflection varied significantly with distance. The conventional FWD sensor arrangement causes the distance between the longitudinal joint and the #2 sensor to be at least double the distance from the joint to the #4 sensor. Joints, especially separated ones, act like free edges because no restraint exists.

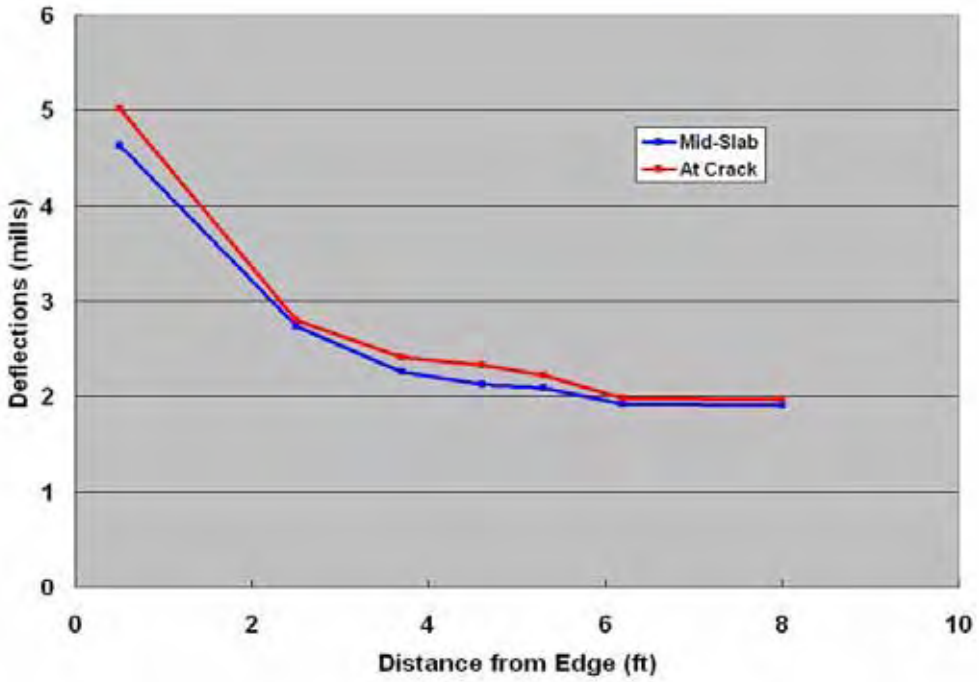

Figure A.3: Deflection at Different Edge Distances (Won, 2006b)

Recall the relationship between LTE and sensor deflections:

$$LTE = \frac{\Delta_{\#4}}{\Delta_{\#2}} \times 100$$

Theoretically, a monolithic pavement will have 100% LTE. With the conventional sensor arrangement, though, values greater than 100% were commonly calculated. One reason is that the #2 deflections are lower because of the larger distance from the joint to the sensor. Lower #2 deflection translates into higher LTE. Ideally, the #2 and #4 sensors should be the same distance away from the joint for more accurate tests. This was the impetus for the development of a modified sensor arrangement. Dr. Moon Won of the Center for Transportation Research and Mr. Randy Beck of TxDOT developed a piece of equipment to attach to existing FWD machines to address this problem. The modified sensor arrangement is shown in Figures A.4 and A.5.

Figure A.4: New FWD Setup in the Field

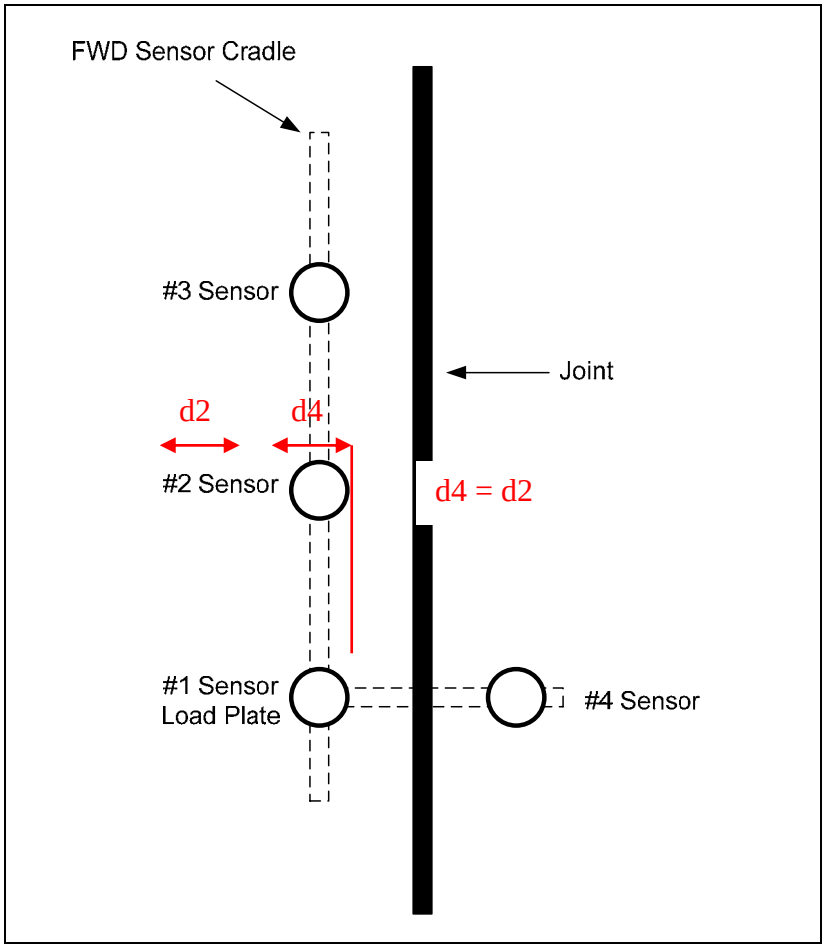

Figure A.5: New FWD Sensor Arrangement

Appendix B: TxDOT Pavement Details

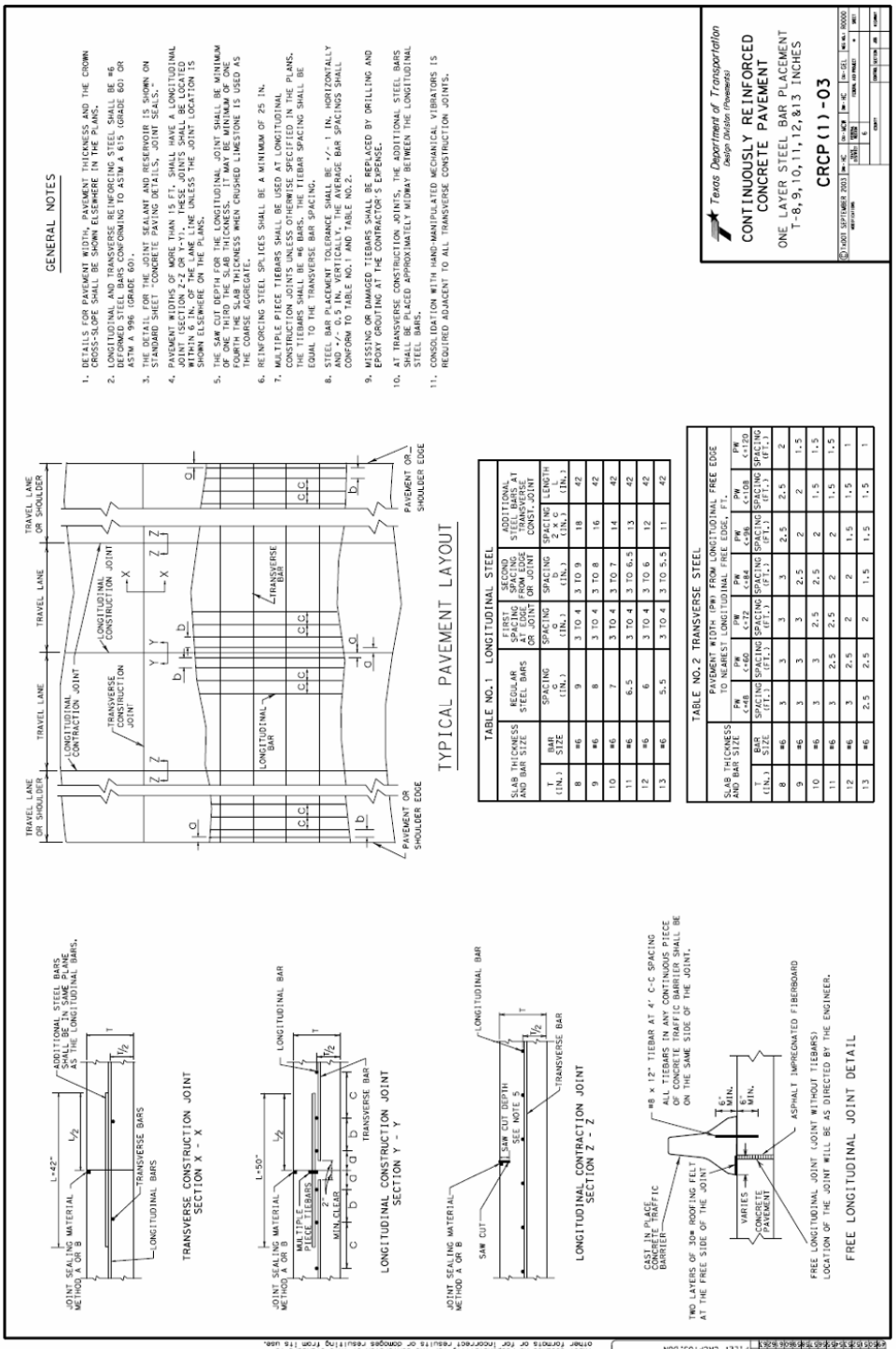

Figure B.1: TxDOT CRCP Detail (TxDOT 2003)

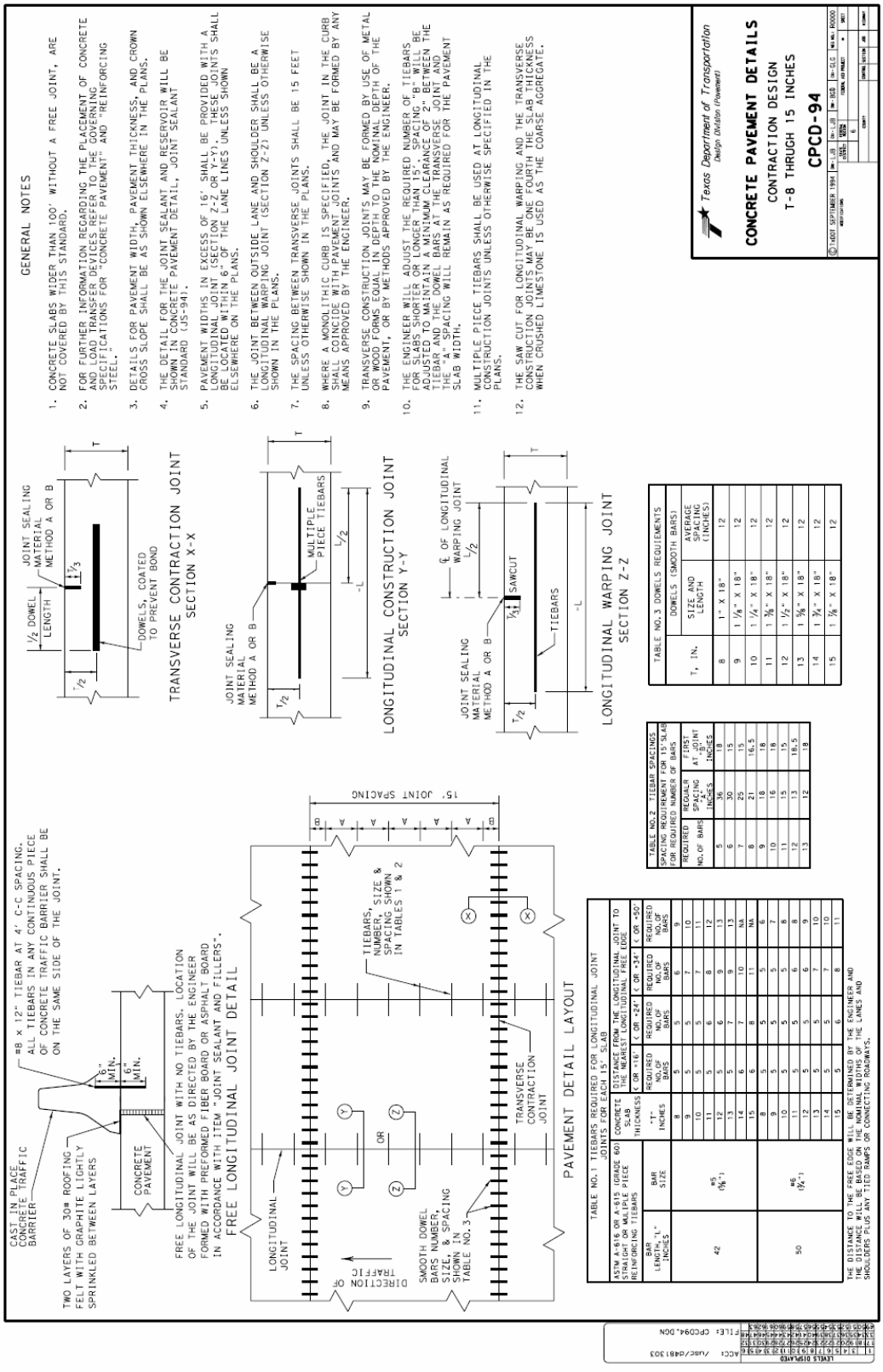

Figure B.2: TxDOT CPCD Detail (TxDOT 1994a)

Appendix C: Stapling Specifications and Details

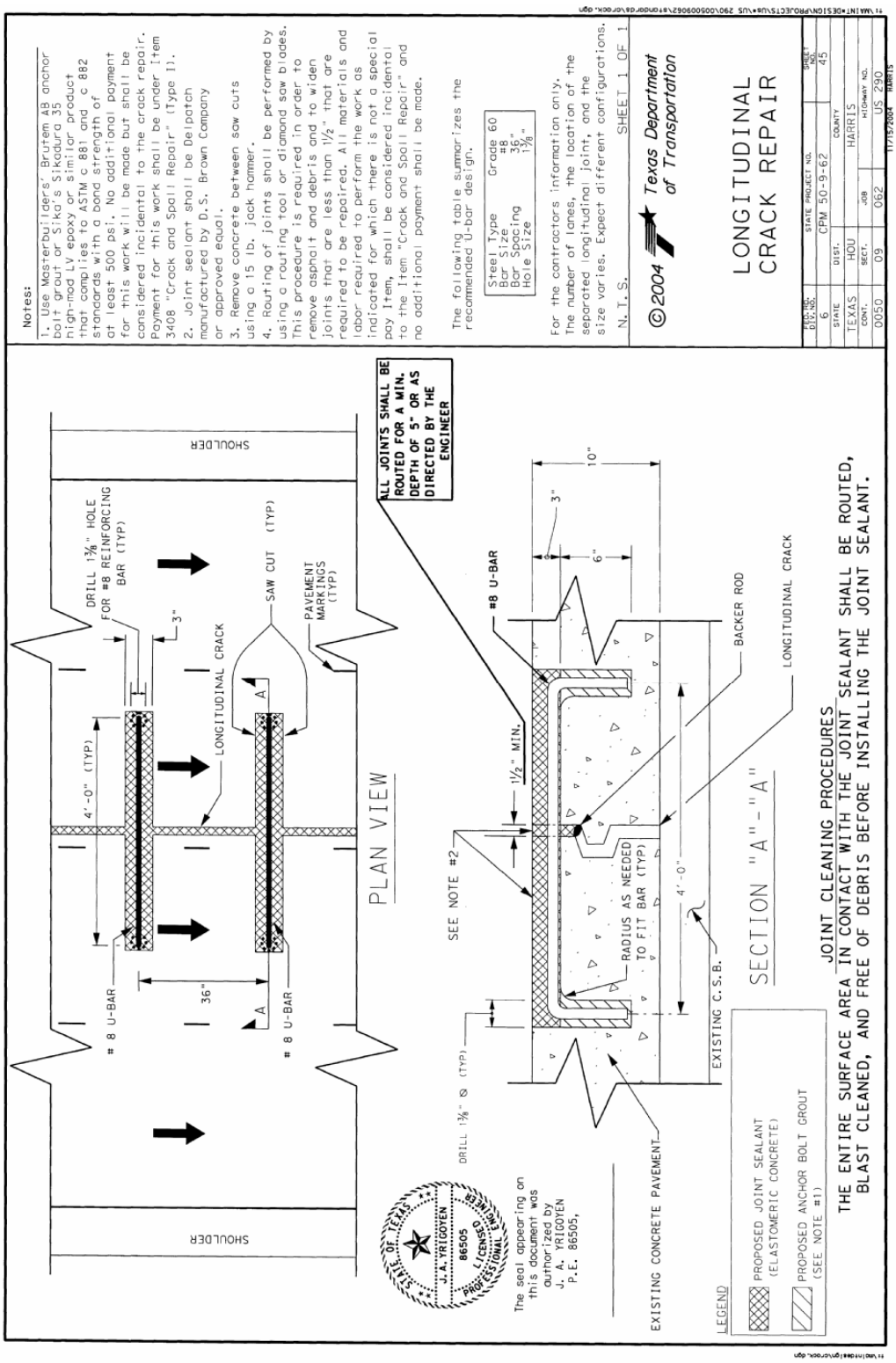

Figure C.1: TxDOT Stapling Details (TxDOT 2004c)

SPECIAL SPECIFICATION

3408

Crack and Spall Repair (Elastomeric Patching Material)

1. **Description**. This Item shall govern for the furnishing and installation of elastomeric patching material for the repair of random cracks and spalls in existing Portland cement concrete pavement in accordance with the requirements herein and the details shown on the plans.

2. **Materials.** The repair material shall be an elastomeric patching material consisting of a fluid polyurethane base or binder with a sand and with or without fiberglass aggregate system to provide a product that mixes in 5 minutes or less, flows readily, adheres to concrete, and requires no external application of heat for curing. This material shall be Delpatch (TM) and Delcrete (TM) Elastomeric Concrete as manufactured by D. S. Brown Company, or equal, as approved by the Engineer.

   The materials shall meet the following physical properties:

Binder Only

Test		Test Method	Specification
Original Properties (after conditioning at 100 F for 7 days)	Tensile Strength, psi	TEX-618-J	1,100 Min.
	Tensile Stress, psi	TEX-618-J	500 Min.
	Elongation, %	TEX-618-J	200 Min.
	Hardness, Durometer D	ASTM D2240	90 + 3 A
Tensile Properties (after oven aging 7 days @ 158 F ASTM D573	Tensile Strength, psi	TEX-618-J	1,100 Min.
	Tensile Stress, psi	TEX-618-J	500 Min.
	Elongation, %	TEX-618-J	200 Min.
	Hardness, Durometer D	ASTM D2240	90 + 3 A

   Properties for the binder and aggregate shall be submitted by the Manufacturer to the Engineer for approval.

   The size of the aggregate and binder to aggregate ratio shall meet one of the following mix types:

Figure C.2: TxDOT Stapling Specifications (1 of 3) (TxDOT 1993)

Type 1. The aggregate shall consist of fine silica sand passing the No. 30 sieve size. The composition of the mix shall be approximately 15 lb. of aggregate per 1 gal. of binder.

Type 2. The aggregate shall consist of fine silica sand passing the No. 6 sieve size. The composition of the mix shall be approximately 30 to 40 lb. of aggregate per 1 gal. of binder.

Type 3. The aggregate shall consist of sand of the size selected by the Manufacturer. The composition of the mix shall be approximately 60 lb. of aggregate per 1 gal. of binder.

The type of mix required for the project shall be as indicated on the drawings.

The elastomeric patching material shall be gray in color. The material shall be kept dry and above freezing temperatures. During hot weather the material shall be kept in the shade and/or as directed by the Manufacturer.

3. **Construction Methods.** Prior to beginning operations, the Contractor shall submit a statement from the elastomeric concrete manufacturer showing the recommended equipment and installation procedures to be used. All equipment and procedures will be subject to approval by the Engineer.

The use of any equipment which damages dowels, reinforcing steel, concrete, base, subbase or subgrade shall be discontinued, and the joint and/or crack shall be cleaned by other methods which do not cause such damage.

(A) Crack And Spall Preparation. At the time of sealing, the crack or spall shall be free of all debris, dirt, dust, saw cuttings or other foreign material.

The cracks shall be cleaned by a method approved by the Engineer. Unless otherwise shown on the plans, hand tools, air guns, power routers, abrasive blasting equipment or other equipment may be used to clean the cracks.

Unsound concrete shall be removed to the dimensions indicated on the plans or as directed by the Engineer. Prior to application of the elastomeric patching material, the surface shall be dry and shall be sandblasted to ensure it is free from dirt, grease, oil, laitance or other foreign material which may reduce the bond between the elastomeric patching material and the existing concrete pavement. There shall be no dust from the sand blasting operation in the area to be repaired.

(B) Primer. After sandblasting, a primer supplied by the manufacturer shall be applied to the area to be repaired and allowed to cure for a minimum of 30 minutes before placing the elastomeric patching material. The primer shall be re-applied if 6 hours pass prior to introduction of the elastomeric patching material, or if a rain occurs.

(C) Application. Elastomeric concrete components shall be weighed and mixed in accordance with the manufacturer's recommendations. The material shall be placed into the area to be repaired within 4 minutes of the initial mixing. If there is a sloped condition in the roadway, placement shall begin at the lower end. Upon initial cure, a notched trowel shall be used to provide a non-skid finish to the surface.

Figure C.3: TxDOT Stapling Specifications (2 of 3) (TxDOT 1993)

An experienced manufacturer's representative or agent of the manufacturer shall be present during the installation of the elastomeric patching material.

4. **Measurement.** This Item will be measured by the mixed gallon of elastomeric patching material, complete in place, of the type specified.

5. **Payment.** The work performed and materials furnished in accordance with this Item and measured as provided under "Measurement" will be paid for at the unit price bid for "Crack and Spall Repair Type 1", "Crack and Spall Repair Type 2" or "Crack and Spall Repair Type 3". This price shall be full compensation for furnishing all materials; for all routing and chipping, removal of loose concrete and cleaning; furnishing and installing "Elastomeric Patching Material and Primer"; and for all manipulations, labor, equipment, tools and incidentals necessary to complete the work.

Figure C.4: TxDOT Stapling Specifications (3 of 3) (TxDOT 1993)

Appendix D: Full Depth Repair Details

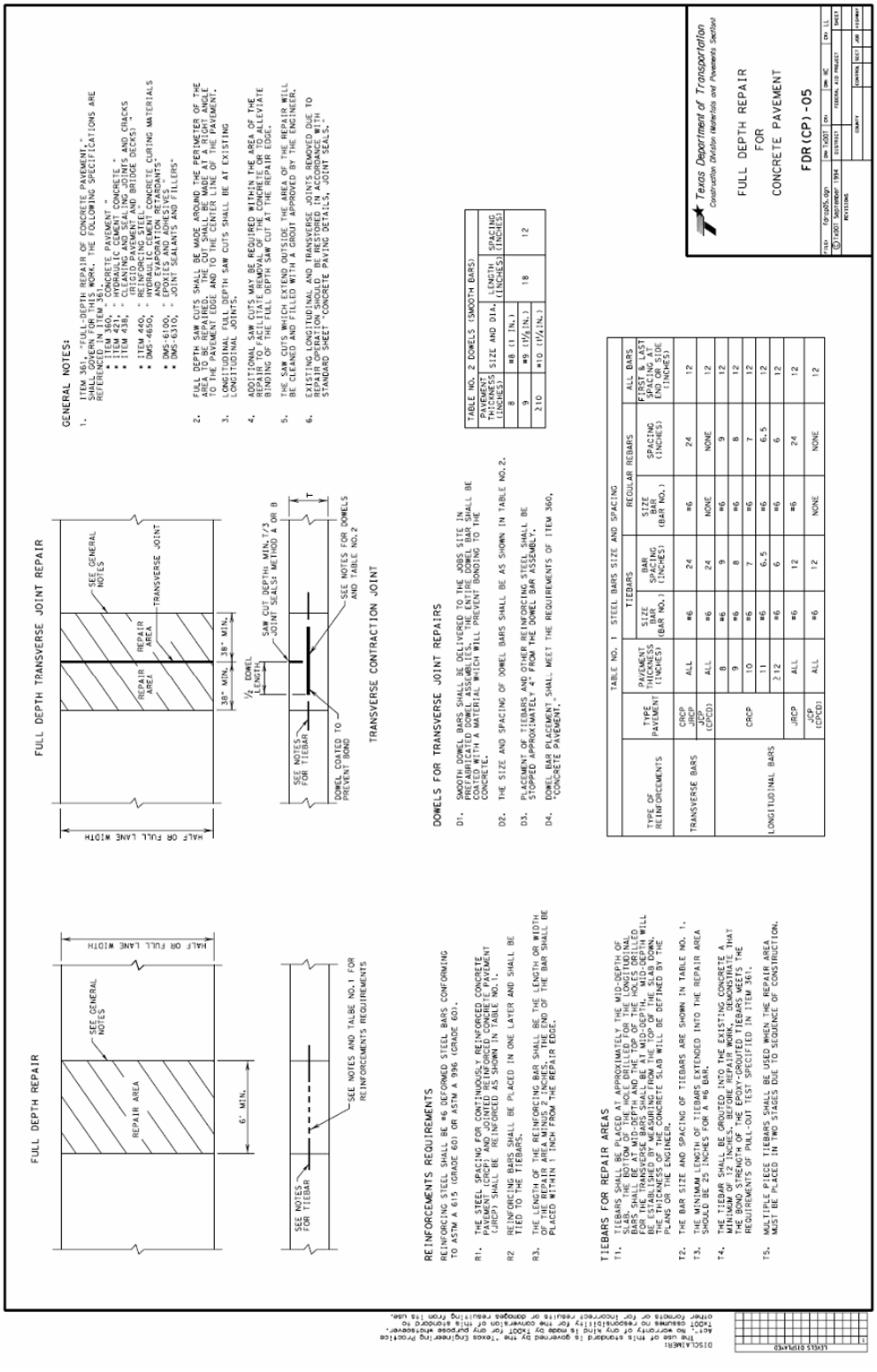

Appendix D.1: TxDOT Full Depth Repair Details (TxDOT 1994b)

Appendix E: Statistical Data for FWD tests

Table E.1: Statistical Data for FWD Tests on US 59 and IH 10

US 59

Cross Stitched areas

	Joint width (in)	LTE (%)	#1 defl (mils)
AVG	0.76	38.5	4.94
STDEV	0.18	17.8	2.09
COV	0.24	0.5	0.42

Unrepaired Areas

	Joint width (in)	LTE (%)	#1 defl
AVG	0.90	33.5	4.86
STDEV	0.51	20.7	1.19
COV	0.56	0.6	0.24

IH 10

Eastbound

	Joint width (in)	LTE (%)	#1 defl
AVG	1.048	40.0	11.417
STDEV	0.396	22.8	3.407
COV	0.378	0.571	0.298

Westbound

	Joint width (in)	LTE (%)	#1 defl
AVG	1.713	38.0	12.842
STDEV	0.734	23.4	3.836
COV	0.429	0.617	0.299

Table E.2: Statistical Data for FWD Tests on IH 27

IH 27

Center Joint Unrepaired

	Joint width (in)	LTE (%)	#1 defl
AVG	1.083	71.1	5.537
STDEV	0.154	7.6	0.884
COV	0.142	0.107	0.160

Center Joint FDR

	Joint width (in)	LTE (%)	#1 defl
AVG		91.6	3.710
STDEV		7.3	0.583
COV		0.080	0.157

Shoulder Joint

	Joint width (in)	LTE (%)	#1 defl
AVG	1.01	57.9	6.72
STDEV	1.05	11.9	1.57
COV	1.10	0.21	0.23

Table E.3: Statistical Data for FWD Tests on SH 289 and SH 66

SH 289

Unrepaired Cracks

	Crack width (in)	LTE (%)	#1 defl
AVG	0.235	88.1	6.166
STDEV	0.148	12.7	1.617
COV	0.630	0.144	0.262

Repaired Cracks

	Crack width (in)	LTE (%)	#1 defl
AVG	0.105	94.1	5.332
STDEV	0.032	3.0	1.498
COV	0.302	0.032	0.281

SH 66

100 deg F

	Crack width (in)	LTE (%)	#1 defl
AVG	0.165	95.9	2.088
STDEV	0.180	1.4	0.290
COV	1.090	0.015	0.139

70 deg F

	Crack width (in)	LTE (%)	#1 defl
AVG	0.204	84.8	3.175
STDEV	0.164	11.8	1.325
COV	0.803	0.139	0.417

Appendix F: Cross Stitching Specifications

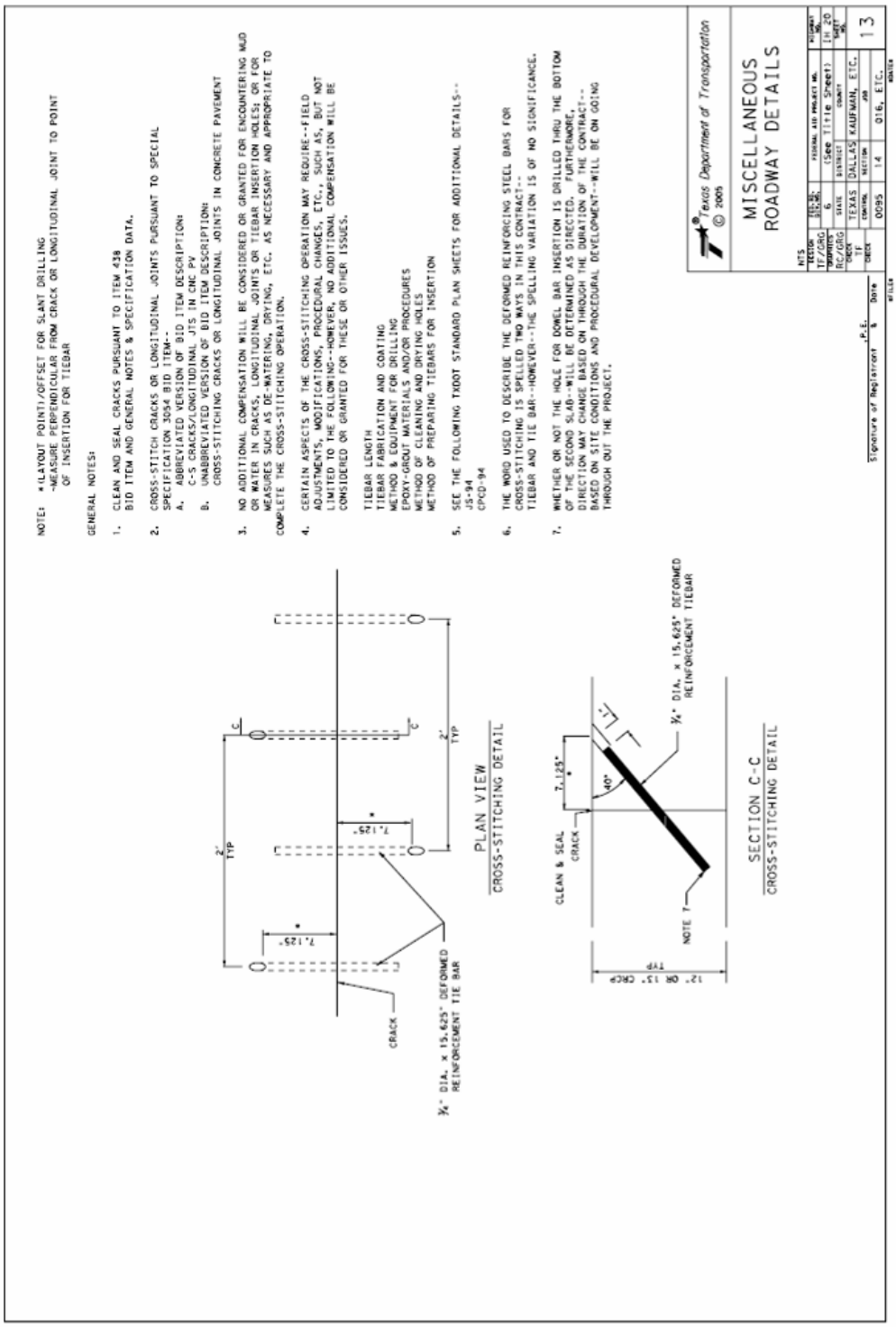

Figure F.1: TxDOT Cross Stitching Details (TxDOT (2005a)

SPECIAL SPECIFICATION

3054

Cross-Stitching Cracks and Longitudinal Joints in Concrete Pavement

1. **Description.** Drill holes and anchor deformed tie bar reinforcement diagonally across cracks or longitudinal joints in concrete pavement in accordance with the details shown on the plans and the requirements of this Item.

2. **Materials.** Unless otherwise shown on the plans or directed by the Engineer, use materials that meet the requirements of the pertinent items as follows:

   A. Item 440, "Reinforcing Steel"

   B. DMS-6100, "Epoxies and Adhesives," Type VIII (Grout) Class B

3. **Equipment.** Provide tools and equipment necessary for proper execution of the work.

   A. Drill. Use a maximum 40 lb. hydraulic drill with tungsten carbide bits.

   B. Air Compressor. Provide compressor capable of delivering air at 120 cu. ft. per minute and with a minimum 90 psi nozzle pressure.

4. **Construction.** Provide the anchoring material Manufacturer's written recommendations to the Engineer. Demonstrate the cross-stitching work to receive approval of the operation procedure and the use of equipments.

   A. **Drill Holes.** Use drilling operations that do not damage the surrounding concrete. Drill the end holes in a slab at the offset, depth, and angle as shown on the plans. Ensure that the holes are drilled perpendicular to the longitudinal joint or crack (in plan view) at each location being drilled. Drill adjacent holes in opposite directions across the joint or crack. Ensure that the holes diameters are no more than 3/8 in. larger than tie bar diameter.

   B. **Clean Holes.** Clean holes with oil-free and moisture-free compressed air and a wire brush to remove all cuttings, dust, and other deleterious material. Check the compressed air stream purity with a clean white cloth. Insert the nozzle to the back of the hole to force out all dust and debris. Alternate use of the wire brush and compressed air as necessary until all loose material has been removed.

   C. **Insertion of Tie Bar.** Place the anchoring material into the back of the hole using a nozzle or wand of sufficient length. Insert the tie bar such that the anchoring material is evenly distributed around the tie bar and slightly extrudes out the hole. Trowel the anchoring material smooth to the pavement surface.

Figure F.2: TxDOT Cross Stitching Specifications (TxDOT 2004a)

Appendix G: Repair Material Properties and Costs

SSI Flexpatch

Data from (Fowler et al, 2005a)		Test Method	Time	Temp
Compressive Strength	too flexible to test			
Flexural Strength	2281 psi	ASTM C78	1 day	70 deg F
Bond Strength	92 psi	ACI 503R	1 day	70 deg F
Elastic Modulus	1.20E+05	ASTM C469	1 day	70 deg F
Coeffiecient of Thermal Expansion	1.65E-05	Tex-428-A	1 day	70 deg F
Cost	$115/cu. ft.			
Data from manufaturer:				
ASTM C 579	1500	ASTM C 579	4 hrs	not given
	2400	ASTM C 580	1 day	not given
Bond	650 psi	ASTM C882	not given	not given

Sika Sikaquick 2500

Data from manufaturer:	Values for conrete (mixed with 25-30 lbs. of 3/8 in. aggregate)			
		Test Method	Time	Temp
Compressive Strength	5000 psi	ASTM C-39	1 day	73 deg F
	5500 psi	ASTM C-39	28 days	73 deg F
Flexural Strength	600 psi	ASTM C78	1 day	73 deg F
	1000 psi	ASTM C78	28 days	73 deg F
Bond Strength	300 psi	ACI 503	28 days	73 deg F
	1500 psi	ASTM C882	1 day	73 deg F
	2700 psi	ASTM C882	28 days	73 deg F
Elastic Modulus	4.60E+06	ASTM C469	28 days	73 deg F
Cost	$47/cu.ft.	grout only		
	$34/cu ft	w/agg		

Sikadur 35

Data from manufaturer		Test Method	Time	Temp	Curing
Compressive Strength	6000 psi	ASTM D695	1 day	73 deg F	
	12000 psi		14 days	73 deg F	
Bond Strength	2800 psi	ASTM C882	14 day		Dry
Flexural Strength	14,000 psi	ASTM D790	14 day		
Tensile Strength	8900 psi	ASTM D638	7 day		
Cost	$817/cu.ft.				

Redhead G-5

Data from manufaturer		
Max tensile load for #6 rebar	27.7 kips	6-3/4 in. embedment
embedded in 4 ksi concrete	47.9 kips	9 in. embedment
Compressive Strength	10,344 psi	ASTM D695
Cost	$31.27 per 22 oz. cartridge	
	1 cartridge fills 12 holes with 15" long #6 bar	

*Material costs were determined in 2007

Appendix H: Economic Analysis Method for Selecting a Repair

The following economic analysis technique can be employed to select the most effective and economical repair method for any application. The general approach involves selecting force and/or displacement criteria for the job, determining the capacity of each repair method, and finding the lowest cost solution. For example, suppose District X wants to repair a separated longitudinal joint, and is considering using slot stitching and stapling. Laboratory testing has provided data shown in Figure H.1 for flexural loading, which is most similar to what the District Engineer expects to occur in the field (tests were performed using two bars, so the force per bar is attained by dividing the value from the graph by two)

Force analysis

Analysis has shown that each 10 ft. of repair would need to resist 100 kips of bar force total. Engineers have determined that the maximum serviceable load for each staple bar to be 35 kips and 20 kips for each slot stitch bar. Therefore 5 slot stitch bars or 3 staple bars would be required every 10 ft.

Displacement Analysis

Engineers have determined that the maximum acceptable rotation for the repair is 0.03 radians. For each repair method, the resisting bar force corresponding to a rotation of 0.03 radians is determined from the force-rotation graph. Figure H.1 shows that the stapling method resists 14 kips per bar while the slot stitching method resists 20 kips per bar. This translates into 5 bars per 10-ft. section for slot stitching and 8 bars for stapling.

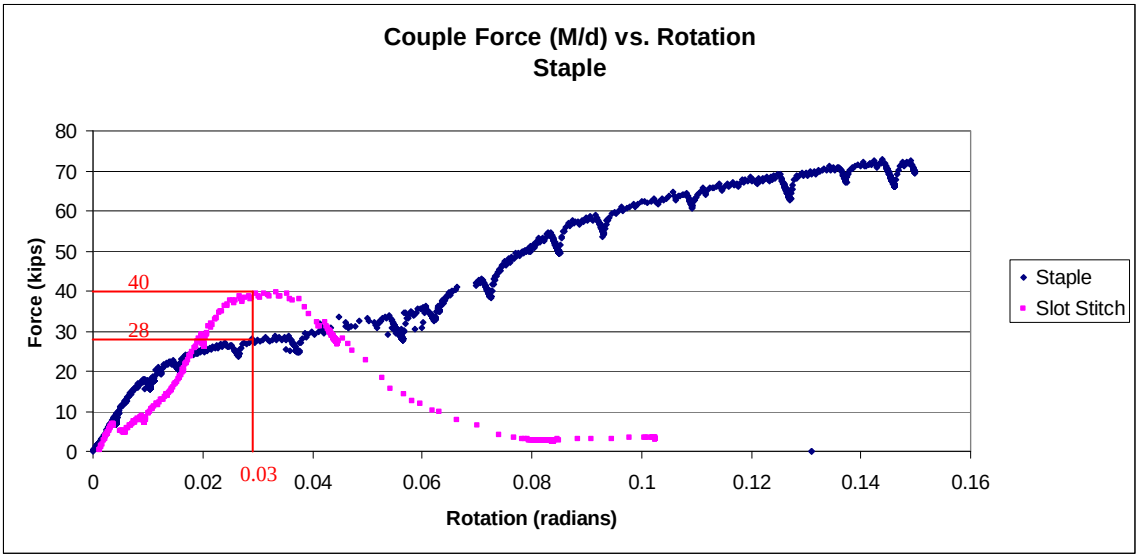

Figure H.1: Bar Force vs. Rotation

The results of the two analyses must be combined to determine the worst case for each repair method. The stapling method is governed by the displacement demand; eight bars per 10-ft. section are required. Slot stitching has the same demand for both force and displacement demand at five bars per 10-ft. section. Therefore slot stitching should be chosen if it is less than 8/5 of the cost of stapling.

Implementation

Two primary approaches can be employed in the implementation of this analysis method: (1) Set the performance criteria at the State level and perform the economic analysis to select a repair method for State-wide use, (2) Allow the District Engineers to set the performance criteria and select the repair method for each individual job. See Figure H2 for a flow chart of the different approaches.

There is a case to be made for option #2: each pavement will have much different conditions, including soil type, weather conditions, drainage, base and subgrade type, width of pavement, type of pavement construction (CRCP vs. JCP), etc. Any state-wide repair method would necessarily be a lower bound solution, taking into account the worst conditions possible in the field. By allowing the individual districts control over the repair selection process, better economy is achieved.

However, for the example given here, taking into account the current material costs for the repairs shown in Appendix J, slot stitching should clearly be chosen in all cases. Perhaps the process could be kept at the State level for simplicity. The decision would rest with TxDOT. Note that the example given here is not reflective of actual field conditions and should not be used for implementation purposes.

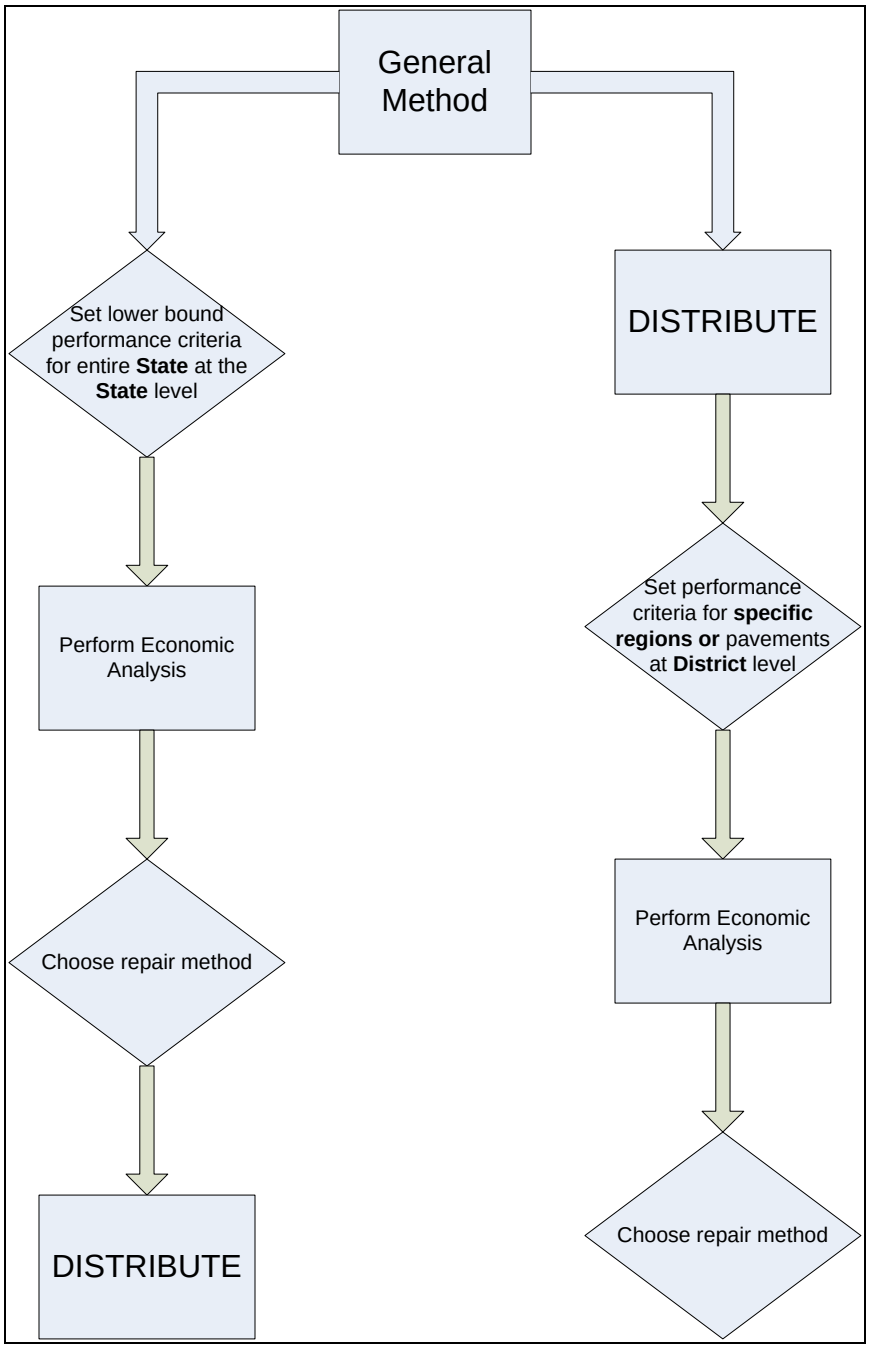

Figure H.2: Economic analysis flow chart

Appendix I: Laboratory Specimen Material Strengths

Shear Tests
Concrete fc= 5920 psi
Slot Stitch
Sikaquick fc= 7081 psi

Flexure Tests
Concrete fc= 5920 psi
Slot Stitch
Sikaquick fc= 7125 psi

Tension Test
Concrete fc= 5176 psi
Sikaquick fc= 6691 psi

Appendix J: Description of Sensors

Vibrating wire strain gages from Geokon were used in conjunction with electrical resistance gages to determine their suitability for field use. Long-term monitoring of joint and crack repair bars would provide very valuable information regarding the demand on such repairs, and would help engineers develop more durable repairs. Figure J.1 shows the strain gages.

Jointmeters (also vibrating wire type from Geokon) were included in the test specimens to determine their durability under severe loading. Jointmeters would be installed across joints or cracks to monitor the separation or contraction over time. The advantage of such an approach is that readings can be collected by a data logger, and can be downloaded periodically without interrupting traffic. Figure J.2 shows the jointmeters.

One vibrating wire tiltmeter was also tested. Pavement "flapping" due to shrinking and swelling of soil under changing moisture conditions could be calculated by monitoring slab tilt. Figure J.3 shows the tiltmeter.

Sensors performed very well in all tests. Strain gages gave consistent results, and jointmeters withstood significant amounts of shear without breaking. The drawback to the jointmeters is their size. The tiltmeter also performed very well, giving readings through the end of the test. All Figures were taken from Geokon's website: www.geokon.com

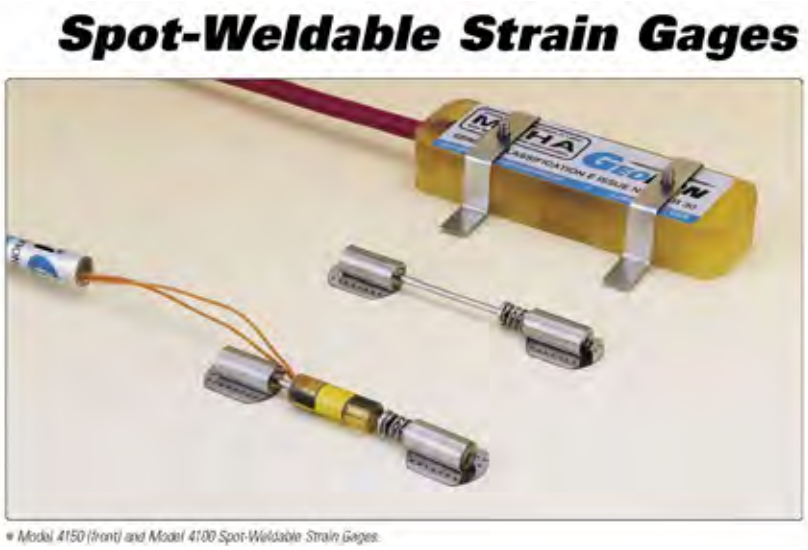

Figure J.1: Strain Gages

Figure J.2: Jointmeter

Figure J.3: Tiltmeter

Appendix K: Repair Material Costs

The costs presented in Table K.1 reflect only those of the repair materials; labor and traffic control are not included as they vary significantly between the Districts.

Table K.1: Repair Material Costs

Slot Stitching

Material	Volume	Unit Cost	Total Cost
Sikaquick 2500	0.5 cu ft	$34	$ 17.00
		Total Cost Per Bar=	***$ 17.00***

Stapling

Material	Volume	Unit Cost	Total Cost
Flexpatch	0.25 cu ft	$115	$ 28.75
Sikadur35	0.0625 cu ft	$817	$ 51.06
		Total Cost Per Bar=	***$ 79.81***

Cross Sitching

Material	Volume	Unit Cost	Total Cost
Redhead G-5	1.83 oz	$1.43	$ 2.62
		Total Cost Per Bar=	***$ 2.62***

*Material costs were determined in 2007

Appendix L: Required Repair Material Properties

Slot Stitching

Slot patch material:

Compressive Strength at 3 hours = 3,000 psi minimum (ASTM C-109)
Compressive Strength at 24 hours = 5,000 psi minimum (ASTM C-109)
Length Change at 28 days = 0.15 percent maximum (ASTM C-157)
Bond strength at 24 hours = 1,000 psi minimum (ASTM C-882)

Joint or crack sealant:

Conform to TxDOT DMS-6140 (Figures L.1 and L.2)

Cross Stitching

Bar Epoxy:

Conform to TxDOT DMS-6100 (Figures L.3 and L.4)

Crack sealant:

Conform to TxDOT DMS-6140 (Figures L.1 and L.2)

DMS-6140, Elastomeric Concrete for Bridge Joint Systems

Overview

Effective Date: March 2005 (refer to 'Archived Versions' for previous versions).

This Specification governs for the Quality Monitoring Program (QMP) for elastomeric concrete bridge joint systems. This Specification also describes the requirements and procedures for the QMP and describes the material requirements for the elastomeric concrete.

Materials

Elastomeric Concrete

Two types of elastomeric concrete are described. Both types consist of a two-component binder and an aggregate system that when blended will form a mortar for nosing or joint repair.

- Type I consists of a fluid thermosetting binder that is a two-component, rapid curing elastomer. When combined with the aggregate, the system will form a semi-flexible and resilient material.
- Type II consists of a two-component, rapid-curing liquid polymer. When combined with the aggregate, the system will form a semi-rigid and higher compressive strength material.

Quality Monitoring Program

The QMP is a Department program where materials are submitted on a periodic basis for testing and verification of specification compliance.

Material Producer List (MPL)

The Materials and Pavements Section of the Construction Division (CST/M&P) maintains a list of all materials conforming to the procedures and requirements of this program. Products on the MPL require no further testing unless deemed necessary by the Project Engineer. To obtain a place on this list, the producer must be accepted into the QMP.

The MPL contains the prequalified elastomeric concrete suppliers for bridge joint systems. This will include the specific binder and aggregate used by the manufacturer. The contractor, supplier, or producer cannot substitute any of the components without prior notice to CST/M&P.

Figure L.1: Page 1 of TxDOT DMS 6140 (TxDOT, 2005b)

- The elastomeric concrete must be able to carry traffic within 3 hr. of placement.
- The elastomeric concrete is resistant to chemicals, weather, and abrasion.
- The aggregate types used are those specified by the manufacturer.
- Elastomeric concrete must not be installed at temperatures below 10°C (50°F).

Type I Requirements

Binder components are tested with and without the aggregate system. The binder and binder-aggregate system must meet the following requirements.

- Type I Binder

Type I Binder Requirements

Test	Method	Requirements
Gel Time, min.	"Tex-614-J, Testing Epoxy Materials"	5 Min
Tensile Strength, MPa (psi)	"Tex-618-J, Testing Elastomeric Concrete"	3.4 (500) Min
Ultimate Elongation, %	"Tex-618-J, Testing Elastomeric Concrete"	100 Min

- Type I Complete Binder-Aggregate Mixture

Type I Complete Binder-Aggregate Mixture Requirements

Test	Method	Requirements
Wet Bond Strength to Concrete, MPa (psi)	"Tex-618-J, Testing Elastomeric Concrete"	1.55 (225) Min
Compressive Strength, 24 hr. MPa (psi)	ASTM C 579, Method B	5.2 (750) Min
Compressive Stress, MPa (psi)	"Tex-618-J, Testing Elastomeric Concrete"	5.2 (750) Min
Resilience, %	"Tex-618-J, Testing Elastomeric Concrete"	85 Min

Type II Requirements

Binder components are tested with and without the aggregate system. The binder and binder-aggregate system must meet the following requirements.

- Type II Binder

Type II Binder Requirements

Test	Method	Requirements
Gel Time, min.	"Tex-614-J, Testing Epoxy Materials"	5 Min
Tensile Strength, MPa (psi)	"Tex-618-J, Testing Elastomeric Concrete"	6.2 (900) Min
Ultimate Elongation, %	"Tex-618-J, Testing Elastomeric Concrete"	40 Min

Figure L.2: Page 5 of TxDOT DMS 6140 (TxDOT, 2005b)

- Type II Complete Binder Aggregate Mixture

Type II Complete Binder-Aggregate Mixture Requirements		
Test	**Method**	**Requirements**
Wet Bond Strength to Concrete MPa (psi)	"Tex-618-J Testing Elastomeric Concrete"	1.55 (225) Min
Compressive Strength, 24 hr. MPa (psi)	ASTM C 579, Method B	13.8 (2,000) Min
Compressive Stress MPa (psi)	"Tex-618-J Testing Elastomeric Concrete"	13.8 (2,000) Min
Resilience %	"Tex-618-J Testing Elastomeric Concrete"	70% Min

Packaging and Labeling Requirements

Package components in airtight containers and protect from light and moisture. Include detailed instructions for the application of the material and include all safety information and warnings regarding contact with the components.

Labels must include the following information:

- name of manufacturer
- brand name
- resin or hardener components
- ratio of components to be mixed by volume
- unique batch number
- temperature range for storage
- date of manufacture
- expiration date of elastomeric concrete

Archived Versions

The following archived versions of "DMS 6140, Elastomeric Concrete for Bridge Joint Systems" are available:

- 6140-0898 for the Specification effective August 1998 through October 2001.
- 6140-1101 for the Specification effective November 2001 through February 2005

Figure L.3: Page 6 of TxDOT DMS 6140 (TxDOT, 2005b)

DMS-6100

Epoxies and Adhesives

Overview

Effective Date: May 2006 (refer to "Archived Versions" for previous versions).

This Specification details requirements for various types of epoxy and adhesive materials suitable for highway use. These materials consist of a resin component and a hardener component or a catalyzing agent mixed to produce the finished product.

All epoxies and adhesives must be resistant to the action of weathering, moisture, acids, alkalis, and other environmental factors.

This Specification describes the following types of epoxies and adhesives:

- Type I (Classes A, B, and C): precast concrete segment adhesive
- Type II: traffic marker adhesives
- Type III (Classes A, B, and C): dowel and tie bars adhesives
- Type IV: bridge deck sealant and adhesive
- Types V and VII: concrete adhesives
- Type VIII (Classes A and B): binder for producing grout or concrete
- Type IX: epoxy for crack injection
- Type X: epoxy coating for concrete.

Units of Measurement

The values given in parentheses (if provided) are not standard and may not be exact mathematical conversions. Use each system of units separately. Combining values from the two systems may result in nonconformance with the standard.

Material Producer List (MPL)

The Materials and Pavements Section of the Construction Division (CST/M&P) maintains a quality monitoring program (QMP) for epoxies and adhesives outlined in "DMS-6110, Quality Monitoring Program for Epoxies and Adhesives." Prequalified materials are on the MPL entitled "Epoxies and Adhesives." Products on this list do not need further testing unless deemed necessary by the Engineer.

Figure L.4: Page 1 of TxDOT DMS-6100 (TxDOT, 2006)

Type III - Dowel and Tie Bars Adhesives

- Description

  Type III adhesives are:

  - used to anchor dowels and tie bars in concrete and
  - suitable to bond steel to hardened concrete.

  There are three classes, which are:

  1. Class A is a bulk material used in horizontal applications.
  2. Class B is a bulk material used only in vertical applications.
  3. Class C is either a cartridge dispensed material or a bulk material for machine application only. Class C is used for either horizontal or vertical application.

- Physical Requirements

  The following table describes the requirements for dowel and tie bar adhesives.

Type III				
		Requirements		
Physical Property	**Test Method**	**Class A**	**Class B**	**Class C**
Gel Time, min.	Tex-614-J	25 Min	25 Min	6 Min
Viscosity of mixed components, poise (Pa-s)		1,200 (120) Max	20 (2) Min 150 (15) Max	-
Tensile Bond @ 6 hr., psi (MPa)		200 (1.40) Min	200 (1.40) Min	200 (1.40) Min
Tensile Bond @ 120°F (49°C), psi (MPa)		400 (2.8) Min	400 (2.8) Min	400 (2.8) Min
Thixotropy @ 120°F (49°C), mils (mm)		30 (0.75) Min	-	30 (0.75) Min
Wet Pullout[1] Strength, lbf. (kN)		4,500 (20) Min	4,500 (20) Min	4,500 (20) Min
[1]The wet pullout test determines the strength of the adhesive bond between a steel anchor and the surface of a hole in concrete or masonry units.				

- General Requirements
  - The producer must distinctly pigment each component of adhesive to produce a third color when properly mixed.
  - The fillers present in Class A and B must not abrade or damage the dispensing equipment.
  - Use a 1:1 extruder with fully contained proportioning and dispensing system for two-component adhesives to handle the viscosity range defined in this Specification for Class A (horizontal) and Class B (vertical) applications.

Figure L.5: Page 5 of TxDOT DMS-6100 (TxDOT 2006)

ITEM 720

REPAIR OF SPALLING IN CONCRETE PAVEMENT

720.1. Description. Repair spalling and partial-depth failures in concrete pavement.

720.2. Materials. Furnish either rapid-set concrete or polymeric patching material unless otherwise shown on the plans.

A. Rapid-Set Concrete. Provide concrete that meets DMS-4655, "Rapid-Hardening Cementing Materials for Concrete Repair."

Use a packaged blend of hydraulic cement, sand, and gravel (maximum size 3/8 in.) which requires the addition of water and has a maximum shrinkage of 0.15% in accordance with ASTM C 928. Do not use chlorides, magnesium or gypsum to accelerate setting time. Before spall repair operations, demonstrate that the mixture achieves flexural strength of at least 425 psi in 5 hr., a minimum compressive strength of 5,100 psi in 7 days, and 6,300 psi in 28 days. Test in accordance with Tex-418-A and Tex-448-A.

B. Polymeric Patching Material. Provide polymeric patching material that meets DMS-6170, "Polymeric Materials for Patching Spalls in Concrete Pavement," and matches the color of the pavement.

720.3. Equipment. Furnish equipment in accordance with Item 429, "Concrete Structure Repair," or as approved.

720.4. Work Methods. Repair areas as shown on the plans or as directed. Dispose of debris off the right of way in accordance with federal, state, and local regulations.

A. Hydraulic Cement Concrete Material. Saw at least 1 1/2 in. deep around repair area before concrete removal, unless otherwise directed, providing a vertical face around the perimeter of the repair area. Provide a uniform rough surface free of loose particles and suitable for bonding. Remove concrete to a depth of 1 1/2 in. or the depth of deteriorated concrete, whichever is greater. Use chipping hammers not heavier than the nominal 15-lb. class or hydro-demolition equipment for the removal of concrete below 1 1/2 -in. depth. Mix, place, and cure in accordance with manufacturer's recommendations. Do not place concrete if the air temperature is below 40°F. Screed concrete to conform to roadway surface. Provide a rough broom finish.

Polymeric Patching Material. Submit for approval a statement from the manufacturer identifying the recommended equipment and installation procedures. Remove the deteriorated concrete to the dimensions shown on the plans or as directed. Dry and abrasive-blast the repair area to ensure it is free from moisture, dirt, grease, oil, or other foreign material that may reduce the bond. Remove dust from the abrasive blasting operation. Apply primer to the repair area. Reapply primer if conditions change before placing patching material. Mix, place, and cure in accordance with manufacturer's recommendations. Begin

Figure L.6: Page 6 of TxDOT Item 720 (TxDOT 2004d)

A. placement of material at the lower end of sloped areas. Screed polymeric patching material to conform to the roadway surface. Provide a non-skid finish with a notched trowel.

720.5. Measurement. This Item will be measured as follows:

A. Hydraulic Cement Concrete Material. By the cubic foot of concrete repair material placed.

B. Polymeric Patching Material. By the gallon of polymeric patching material placed.

720.6. Payment. The work performed and materials furnished in accordance with this Item and measured as provided under "Measurement" will be paid for at the unit price bid for "Spalling Repair" of the type (Hydraulic Cement; Polymeric, Flexible; or Polymeric, Semi-rigid) specified. This price is full compensation for sawing, chipping, milling, cleaning, abrasive-blasting, repairing spalled concrete pavement, disposal of materials, materials, equipment, labor, tools, and incidentals.

Figure L.7: Page 7 of TxDOT Item 720 (TxDOT 2004d)

Figure L.8: TxDOT Joint Sealant Details (TxDOT 1994c)

Appendix M: Guidelines and Specifications for Repair of Longitudinal Cracks and Joint Separations

Research Study 0-5444
Submission of Recommended Repair Details and Specifications
For U.S. 75 near Sherman
August 29, 2008

Recommendations for repair of U.S. 75 are included for the faulted slabs located near Sherman. The exact location of the repairs will be determined in early September as part of the implementation project 5-5444 that will begin September 1, 2008.

The following items are included:

1. Construction Sequence and Materials Estimates for US 75 Repairs
2. Details, construction specifications and material specifications for filling the sub-slab voids with grout
3. Details, construction specifications, tie bar specifications and grout specifications for filling retrofit tie-bar slots
4. Details for milling and preparing surface for LMC overlay, details for placement of LMC overlay with construction and materials specifications for installation of the LMC overlay for leveling faulted slabs. (Also a copy of the ASTM C 1583 Pull-off test method for bond strength)

1. Construction Sequence

1. Fill the voids along edges of faulted slabs caused by pumping of base material, providing more uniform support along the joint and preventing further pumping. Low pressure grouting using hydraulic cements will be used such that slabs will not be lifted during grouting.
2. Lock the slabs with retro-fitted tie bars using slot stitching to prevent further separation and to provide load transfer across the joint. The integrity of the joint will be maintained during the installation of the tie bars.
3. Restore the original grade of the faulted slab by overlaying the depressed pavement sections with latex modified concrete (LMC) that will result in restoration of ride quality. Milling will be required to (1) provide a clean, rough surface to bond the LMC and (2) to provide a minimum thickness of 1 inch for the LMC overlay.

Materials Estimates for US 75 Longitudinal Joint Repairs near Sherman, Texas

Tie bars- (No. 6, deformed, 48 inches long) = 110 each

Estimate 5/ slab x 20 slabs = 100 + 10% contingency = 110

Epoxy grout- 30 cu. ft.

Estimate slot for tie bar = 1-3/4 in. wide x 5* in. deep x 54** in. = 473 cu. in.

Vol. of tie bar = 48 in. long x $(3/8 \text{ in.})^2$ x 3.14 = 21.2 cu. in.

Volume to be filled with epoxy grout = 473 – 21 = 452 cu. in.

100 slots x 452 cu. in. / slot = 45,200 cu. in. or 26 cu ft. Order 30 cu. ft.

* Do not fill top 1 in. of 6-in. deep slot to leave room for milling.

**54 is average width of trapezoid 48-in. bottom, 60-in. top.

Rapid-Setting Latex-Modified Portland Cement Mortar = 16 cu. yd.

Estimate for 20 slabs (12 feet wide x 15 feet long x 1 inch thick)

= 300 cubic feet (12 cubic yards). Order materials for 16 cu. yd.

(includes 30% overage for priming, QC testing, and waste)

Dow-Reichhold Modifier-A SBR Latex Emulsion = 735 lb.

Assume 7-sack mix: 94 lb. x 16 cu. yd. concrete

= approximately 1504 lb. cement

Assume emulsion is 40% latex solids and is used in the mortar at 37.5% of the weight of the cement. 1504 lb cement x .35 emulsion = 530 lb emulsion

2. Filling and Undersealing Sub-Slab Voids with Low-Pressure Grouting

1. Special Specification for Filling and Undersealing Base Voids with Low-Pressure Grout
2. Grouting Detail Before Slot Stitching

SPECIAL SPECIFICATION
ZZZZ

Filling and Undersealing Base Voids with Low-Pressure Grout

1) **Description.** This Item shall govern for the filling and sealing of existing voids under the concrete pavement at locations shown on the plans or designated by the Engineer. This work shall include drilling injection holes, placement of undersealing material, monitoring to avoid lifting slabs, clean up and other related work.

2) **Special Requirements**. The Contractor shall use a crew experienced and competent in the work of pressure grouting and pavement undersealing. The crew and equipment furnished by the Contractor shall have satisfactory production capabilities in the judgment of the Engineer.

3) **Materials.** The materials shall consist of a mixture of Type I, II or III Portland cement, a fluidifier, fly ash and water. All materials shall be furnished by the Contractor.

   Type I, II or III Portland cement shall conform to the requirements of DMS-4600, "Hydraulic Cement."

   The fluidifier shall be a cement dispersing agent possessing such characteristics that will inhibit early stiffening of the pumpable mortar, tend to hold the solid constituents of the fluid mortar in suspension and prevent completely all setting shrinkage of the grout.

   Water shall conform to Item 421, "Hydraulic Cement Concrete".

   Use fly ash that meets the requirements of DMS-4610. Select the fly ash from an approved source. The Materials and Pavements Section of the Construction Division maintain a list of approved sources.

4) **Equipment**. The equipment used shall be that customarily used in the pressure grouting of earthen embankments or pressure grouting of concrete pavement. It shall consist of at least the following:

   (1) Air compressors of sufficient capacity for operating pneumatic hammers.

   (2) Pneumatic hammers equipped with drills that will cut 1-1/2 in. diameter or other approved diameter holes through the rigid pavement. The equipment shall be in satisfactory operating condition and operated in such a manner so as to prevent unnecessary damage to the slab. The pneumatic hammer shall not be heavier than 60 lb. and the down feed pressure whether by hand or mechanical means shall not exceed 200 lb. The Contractor shall furnish a blow pipe with sufficient air pressure to dislodge loose debris from the drill holes.

(3) Cylindrical wooden plugs or other approved plugs that satisfactorily plug holes until the grout has set.

(4) Equipment for accurately measuring and proportioning by volume or weight the various materials composing the grout.

(5) A colloidal mixer that is capable of operating in a range from 800 rpm to 2,000 rpm and thoroughly mixing the various components of the grout in an approved manner.

(6) A positive action pump that is capable of forcing grout through a drilled hole into voids and cavities beneath the pavement slab. The pump shall be capable of supplying a varying pressure up to a maximum of one hundred pounds per square inch at the end of the discharge pipe, when pumping grout of the specified consistency. The injection pump shall be capable of continuous pumping at rates as low as 1-1/2 gallons per minute.

The discharge line shall be equipped with a positive cut-off valve at the nozzle end, and a bypass return line for recirculating the grout back into a holding tank or mixer unless otherwise approved by the Engineer.

(7) A stop watch and flow cone conforming to the dimensions and other requirements of Test Method Tex-437-A, "Method of Test for Flow of Grout Mixtures (Flow-Cone Method)".

(8) The Contractor shall supply equipment to measure slab lift. This equipment shall be capable of detecting the lift of slab in the area of pumping. The equipment shall have the capability of making this measurement as the slab is being pumped and be fast enough in response to insure that the slab will not be raised above the limit set in this specification.

(9) The Contractor shall furnish a vehicle having a single rear axle with dual tires that can be loaded to 18 kips evenly distributed between the inside and outside wheel path, a vehicle driver and sufficient manpower to assist in the operation of the static load measuring gauges. Maintain the tire pressure at 70 psi.

5) **Proportioning Grout Mixture**. The mixture used in pressure grouting, herein referred to as "Grout Slurry," shall consist of proportions of Portland cement, fly ash, fluidifier and water.

The Contractor shall furnish the Engineer the proposed mix design meeting the following requirements:

- The grout slurry shall remain fluid and not exhibit a resistance to flow for a minimum of one hour.

- The time of efflux from the flow cone shall be between 10 and 20 seconds. Perform the flow test in accordance with Test Method Tex-437-A, "Method of

Test for Flow of Grout Mixtures (Flow-Cone Method)."

- The grout slurry shall achieve initial set in less than 4 hours. Do not allow the grout slurry to carry traffic until which time it has set to the satisfaction of the Engineer; or until which set time, as determined with Test Method Tex-302-D, "Time of Setting of Hydraulic Cement by Gillmore Needles," has been reached.

- The 7 day compressive strength of the grout slurry shall not be less than 200 psi. The compressive strength shall be determined in accordance with Test Method Tex-307-D, "Compressive Strength of Hydraulic Cement Mortars."

6) **Deflection Testing**. Each joint and slab on the project or within designated areas of the project is subject to be tested by the Engineer in cooperation with the Contractor using the Falling Weight Deflectometer (FWD). Test joints in question before and after pressure grouting. If the deflection testing is done after grouting, then it will be done the next day before 11:00 a.m. All testing shall be limited to the hours between daylight and 11:00 a.m. The Engineer will use the deflection data to determine where re-grouting is necessary. A maximum of 2 properly performed groutings will be required. The Engineer will determine the specific joints that are to be tested.

7) **Construction Methods**. Drill 1-1/2 in. diameter (or other approved diameter) holes through the concrete pavement at the locations indicated on the plans or designated by the Engineer. Drill these holes to a depth sufficient to penetrate any stabilized base and into the subgrade. Subgrade penetration shall not exceed 3 in. For holes nearest the edges of the slab, the joints or a major crack, a maximum of 3 in. from the precise marked location is considered to be reasonable. For other holes a maximum 6 in. tolerance is considered to be reasonable. Rotate the drills to avoid cracking the pavement and to provide satisfactory holes of the proper diameter for effective operations in pressure grouting. When drilling holes, the drills shall be held as nearly perpendicular as possible to the pavement surface. Irregular or unsatisfactory holes which cannot be satisfactorily used in pressure grouting shall be filled with grout and new holes shall be drilled. The Contractor shall exercise sufficient precautions during all operations to insure that slabs are not broken or cracked. Any slab that develops a crack that extends through the drill hole will be considered to have been damaged during the process of the work and it shall be repaired or replaced at no cost to the Department. Repair or replacement will be in accordance with techniques approved by the Engineer. No more holes shall be drilled during a day's operations than can be grouted during the same day, unless specific approval is given by the Engineer.

After drilling the holes, lower a pipe connected to the discharge hose on the pressure grout pump into the holes. The discharge end of the pipe shall extend below any overlays which might exist, but not below the lower surface of the concrete pavement.

To fill all voids, pumping of grout will be required in holes designated by the Engineer. During the subsealing operation, use a positive means of monitoring lifts. The upward movement of the pavement should not be greater than 0.25 in. or as

directed by the Engineer. Pump each hole until maximum pressure is built-up, grout is observed flowing from hole-to-hole, or as directed by the Engineer. Maximum allowable pressure shall not exceed 20 psi., except for the allowance of a short surge to 150 psi when starting to pump.

Monitor the pressure by an accurate pressure gauge in the grout line that is protected from the grout slurry. Water displaced from the void structure by the grout shall be allowed to flow out freely, but shall not interfere with adjacent traffic. Excessive loss of grout through cracks, joints, or from backpressure in the hose or in the shoulder area shall not be tolerated.

Do not perform pressure grouting when pavement surface temperatures are below 35ºF or if the subgrade and/or base course material is frozen.

After the completion of grouting in any 1 hole, withdraw the discharge pipe from that hole and plug the hole immediately. Temporary plugs may be used since additional grout may be placed in particular holes to complete the required work in that area.

Remove temporary plugs when sufficient time has elapsed to permit the grout to set sufficiently so that back pressure will not force it through the hole, fill the space occupied by the plug with a reasonably stiff grout or an approved concrete mixture, and then compact.

In the event the Engineer determines that continued grout injection at any specific location is no longer economically feasible, he may direct the Contractor to cease grout injection at that location.

The Engineer may modify the construction methods outlined above, for sufficient justification, as field conditions dictate.

The Contractor shall use such approved measures as are necessary to keep all pavement surfaces adjacent to the actual grouting operation in progress reasonably clean of excess grout and other materials at all times.

Prior to the placement of traffic on the work area, clean the pavement (including adjacent shoulders) to the satisfaction of the Engineer.

Keep all traffic off the grouted slab for at least 4 hours unless otherwise directed by the Engineer.

8) **Measurement.** Drilled holes will be measured by each drilled hole actually drilled and filled as necessary to accomplish the work provided herein.

The undersealing grout slurry, mixed and placed as specified herein, will be measured by the cubic foot (dry measure) of each material (cement and fly ash) incorporated into the underseal, prior to mixing.

9) **Payment**. The work performed and materials furnished in accordance with this Item and measured as provided under "Measurement" will be paid for at the unit price bid

for “Drilled Holes” and “Grout Slurry.”

These prices shall be full compensation for all work covered by this Item, including but not limited to, drilling, temporary plugging and final sealing of holes in the concrete slabs; for securing and furnishing all materials including fluidifier and water; including all royalty, freight and storage involved; for mixing, proportioning and pumping the undersealing slurry grout into the voids under the concrete slabs; for cleaning up and for all manipulation, labor, tools, equipment and incidentals necessary to complete the work.

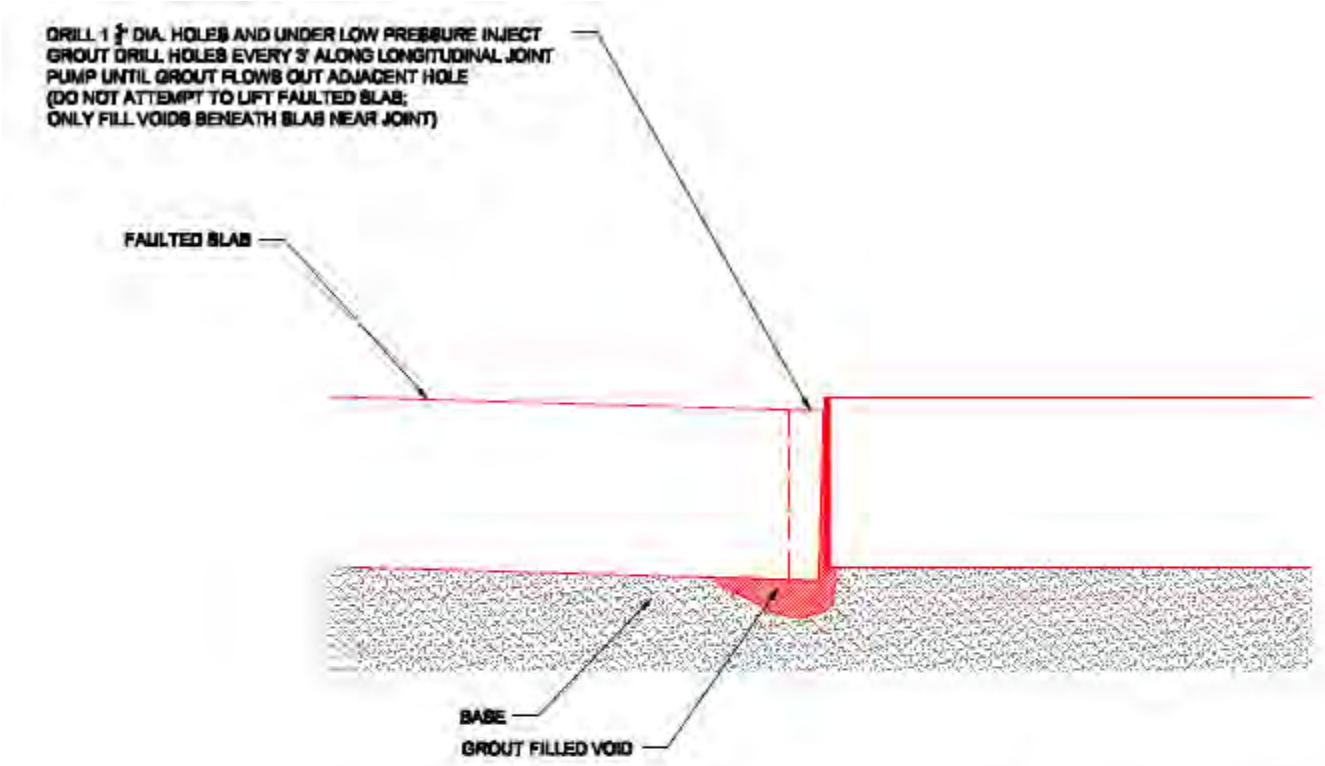

GROUTING DETAIL BEFORE SLOT STITCHING

FOR FAULTED SLABS

3. Slot Stitching

1. Special Specification for Slot Stitching Longitudinal Joints in Concrete Pavement
2. Plan View of Sawing Detail for Slot Stitching
3. Slot Stitching Plan View
4. Slot Stitching Section for Unfaulted Slabs
5. Slot Stitching Section for Faulted Slabs

SPECIAL SPECIFICATION

8888

Slot-Stitching Longitudinal Joints in Concrete Pavement

1. **Description**. Install tie bars across longitudinal cracks or joints in concrete pavement in accordance with the details shown on the plans and the requirements of this item.

2. **Materials**. Furnish the following materials, unless otherwise shown on the plans or directed by the Engineer:

    a. **Concrete**. Provide Class HES concrete conforming to Item 421, "Hydraulic Cement Concrete," with the following exceptions or additions:

        i. Design concrete mix with a maximum water to cement ratio of 0.38, and a minimum average flexural strength of 700 psi at the age of 48 hours. Test in accordance with Tex-448-A.

        ii. Use aggregate from siliceous sources only. Provide washed aggregate with 100% passing the 1/2 in. sieve. No more than 15% of the mix must be of any one size of aggregate.

        iii. Use shrinkage reducing or compensating admixtures, or water reducing admixtures as approved to achieve a fluid non-segregating mixture. Do not use retarding admixtures. When using any admixtures, document the type, quantity, and location of mix placement on a copy of the final plans.

        iv. The use of proprietary, high strength, rapid setting mixes may be approved when the materials demonstrate the satisfied performance. Obtain approval for the materials and proportions before using. Document the placement locations and material properties of proprietary materials on a copy of the final plans.

    b. **Steel Tie Bars**. Provide 48-in. long No. 6 deformed steel tie bars in accordance with Section 360.2.B, "Reinforcing Steel."

    c. **Epoxy**. Provide epoxy materials for bonding new concrete to old concrete or for concrete repair materials that conforms to DMS-6100, "Epoxy and Adhesives."

    d. **Membrane Curing Compound**. Provide membrane curing compounds that conform to the requirements of DMS-4650, "Hydraulic Cement Concrete Curing Materials and Evaporation Retardants", Type 2, Class A.

3. **Construction Methods**. Demonstrate slot-stitching work for approval of all the equipment and procedures. Provide tie bars at locations and spacing as detailed in the plans.

    a. **Slot Formation**.

        i. Provide slots using multiple saw cuts made with a diamond impregnated saw blade to a depth of 6 in. This depth will provide the needed clearance under the tie bars for the support devices and for encasing the tie bars in the repair material.

        ii. The slot is 2 3/4 in. minimum and at most 3 1/2 in. wide.

        iii. Provide enough length of the cut to allow the tie bar to be placed at the mid-depth of the slab with a 1-in. space between the ends of the tie bar and the ends of the slot.

        iv. Use lightweight jackhammers less than 30 lb. or hand tools to remove the "fins" formed by sawing.

        v. Do not spall or fracture concrete adjacent to the slots. Repair damages to concrete pavement caused by Contractor's operation without any additional compensation. Repair in accordance with Item 361, "Full-Depth Repair of Concrete Pavement" or Item 720, "Repair of Spalling in Concrete Pavement" if spalls are 0.25 to 3 in. in depth, or as approved.

    b. **Tie Bar Placement**.

        i. Rinse the slot with potable water, sand blasted, and blown clean and dry with high pressure oil-free air to remove sand, water and dust.

        ii. Place tie bars at locations and spacing as detailed in the plans. Place the tie bars on support chairs so that the tie bars rest horizontal at the mid-depth of the slab.

    c. **Repair Material Placement**.

        i. Do not place concrete when the air temperature is below 65ºF. Use a vibrator head at most 1 in. in diameter to consolidate the concrete repair material. Do not dislodge or move the tie bar out of position, but the repair material must fill the space under the bar.

        ii. Finish the repair material level with the existing slab surfaces.

        iii. Cure the repair surface in accordance with Section 360.4.I. If a proprietary mix is used, use manufacturer's curing procedure.

        iv. Use insulation blankets to facilitate curing and the strength gain of

repair areas if desired. Provide insulating blankets with a minimum thermal resistance (R) rating of 0.5 hour-square foot °F/BTU and in good condition.

v. Make and cure concrete compressive strength test specimens as directed.

d. **Opening to Traffic**. The pavement may be opened to traffic after all tie bars have been installed at a joint and the concrete has obtained a minimum average flexural strength of 700 psi or as directed by the Engineer. Determine the flexural strength in accordance with Tex-448-A by using concrete specimens cured at the job site under the same conditions as the pavement. Opening the pavement does not relieve the Contractor from his responsibility for the work in accordance with Item 7, "Legal Relations and Responsibilities." Seal all joints and clean the pavement before opening the pavement to traffic.

4. **Measurement**. This Item will be measured as each completed and accepted tie bar complete in place.

5. **Payment**. The work performed and materials furnished in accordance with this Item and measured as provided under "Measurement" will be paid for at the unit price bid for "Slot-Stitching Longitudinal Joints in Concrete Pavement". This price is full compensation for furnishing all materials, tools, labor, equipment and incidentals necessary to complete the work. No payment will be made for extra work required to repair damage to the adjacent pavement that occurred during sawing.

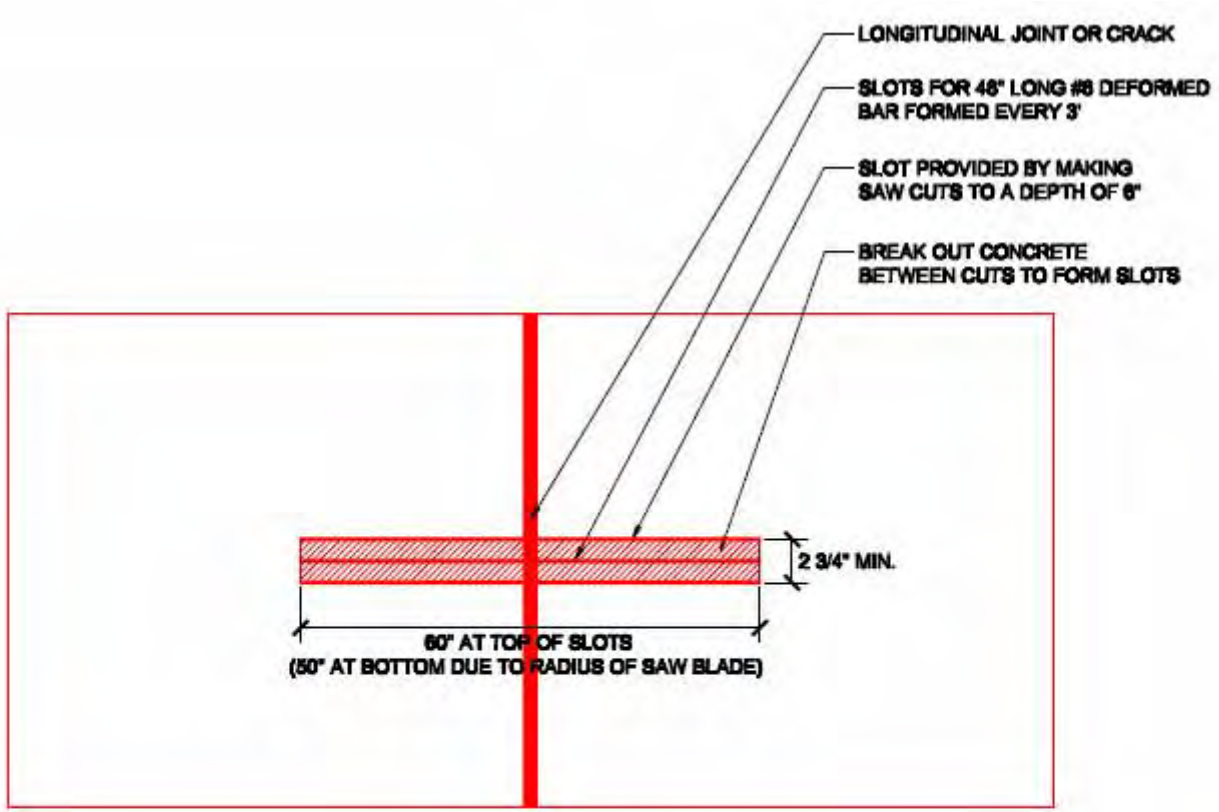

PLAN OF SAWING DETAIL FOR SLOT STITCHING

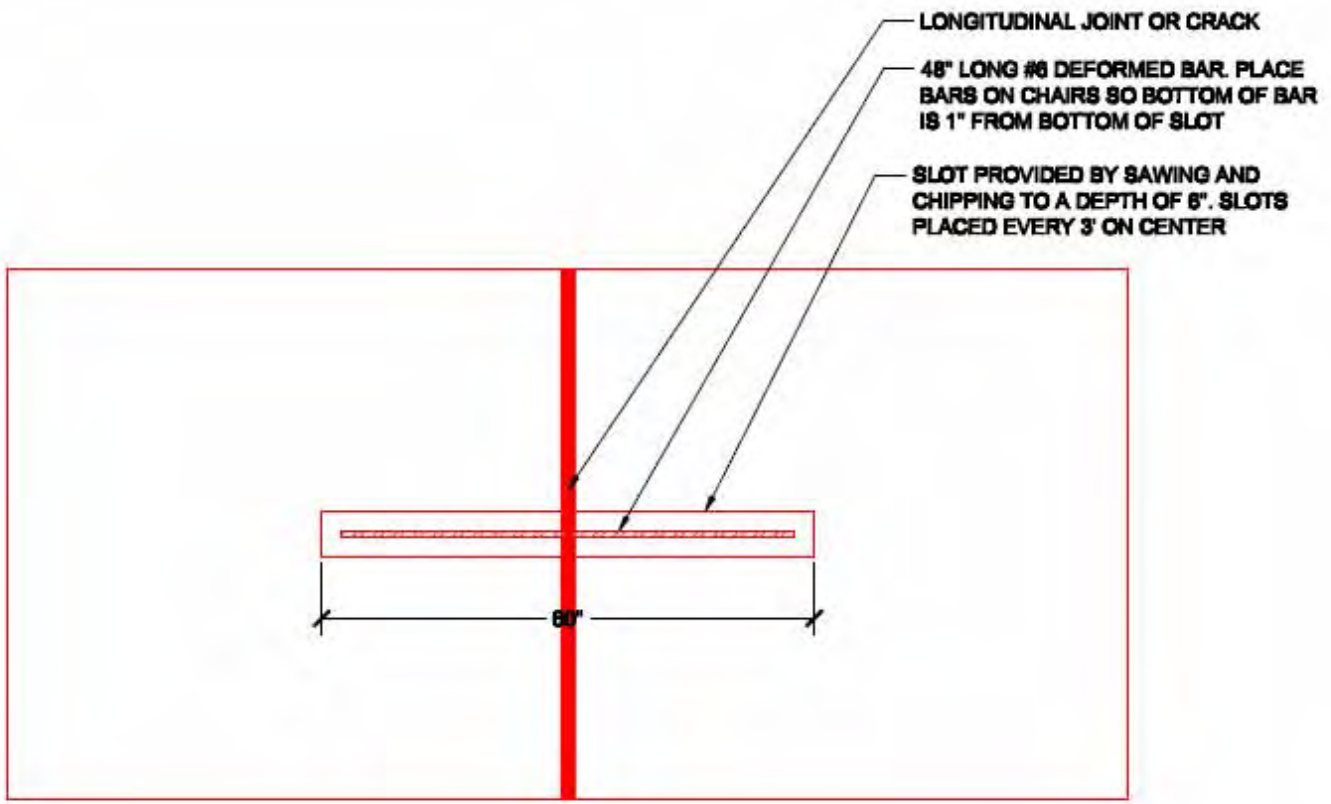

SLOT STITCHING PLAN VIEW

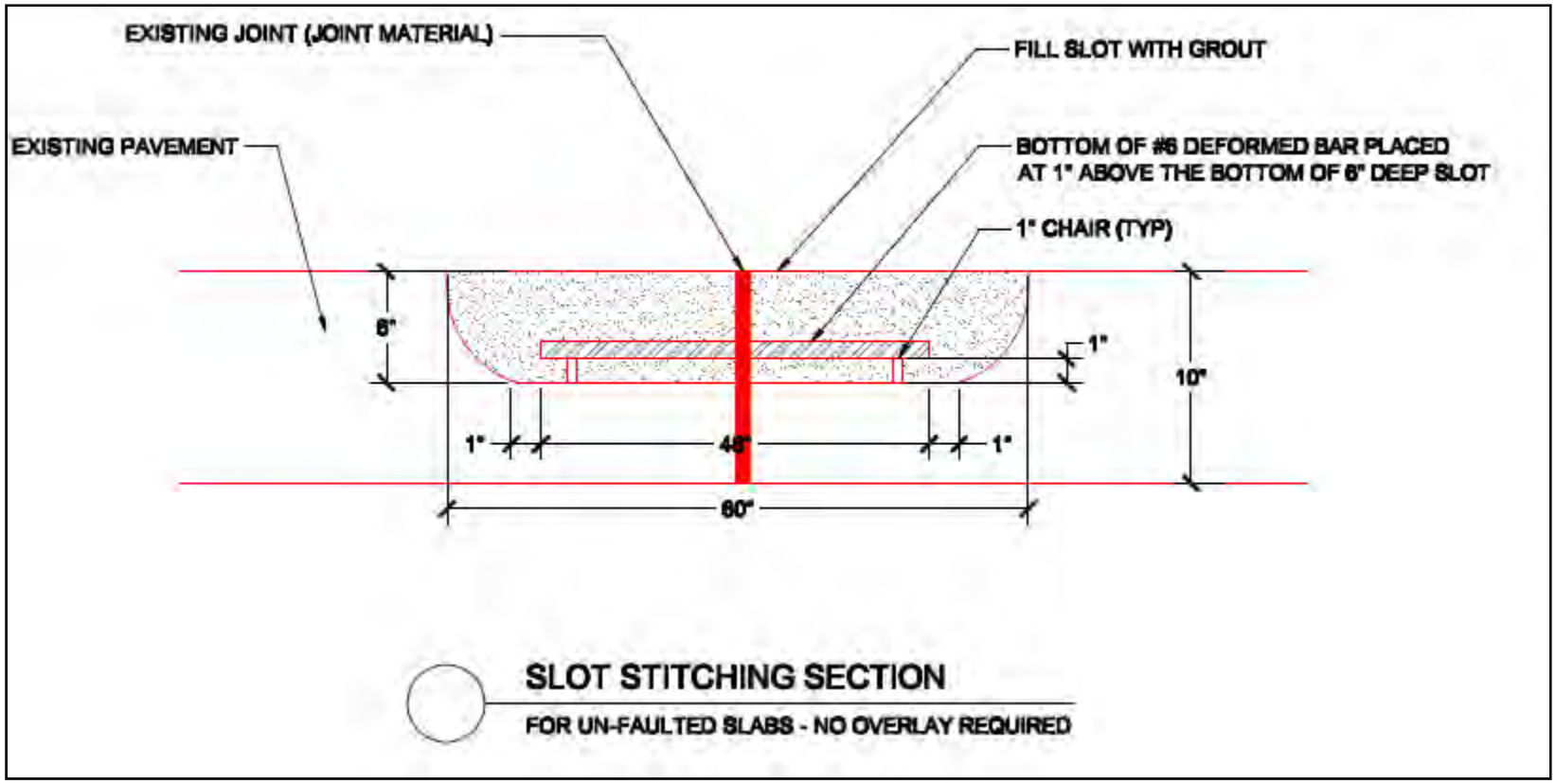

SLOT STITCHING SECTION

FOR UN-FAULTED SLABS - NO OVERLAY REQUIRED

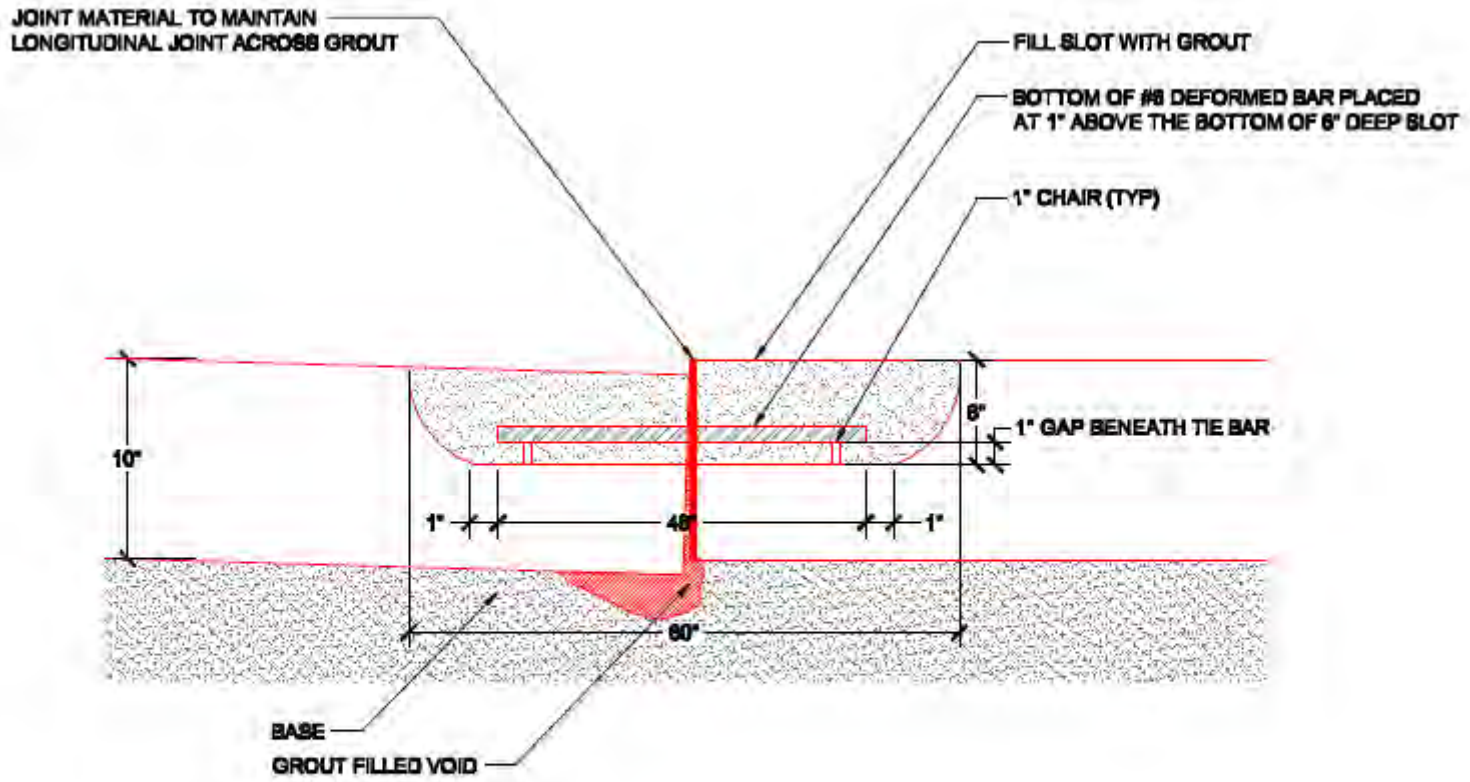

SLOT STITCHING DETAIL

FOR FAULTED SLABS

4. Restoring Grade for Faulted Slabs

1. Special Specification for Cold Milling Concrete Pavement Prior to Overlay
2. Milling Detail
3. Special Specification for Cleaning Milled Concrete Pavement
4. Special Specification for Latex Modified Concrete Overlay
5. ACI 548.4 Standard Specification for Latex Modified Concrete Overlays
6. Guide for Rapid Set Latex Modified Concrete
7. AASHTO Guidelines for Rapid Set LMCO
8. SHRP Guidelines for the Use of Rapid Set® Cement in Latex-Modified Concrete Overlays
9. Slot Stitching Detail with LMCO for Faulted Slabs

SPECIAL SPECIFICATION

MMMM

Cold Milling Concrete Pavement for Bonded Concrete Overlay

1. **Description**. Cold milling shall consist of removing existing surfacing material including some of the concrete substrate as shown in the plans. Non-portland cement concrete overlay materials shall be milled off completely and the concrete surface shall be milled to create an area to place a rapid-setting latex-modified concrete inlay or overlay. The concrete surface shall be milled down to a uniform depth in specified areas a shown in the plans or described in the special provisions.

2. **Materials.** Essentially all of the milled material shall be pulverized to pass a 1-inch sieve.

3. **Equipment.** The milling shall be done with a commercially manufactured machine able to perform this work to the Engineer's satisfaction. The milling machine shall be self-propelled and shall have sufficient power, traction, and stability to maintain an accurate depth of cut.

   a) The cold milling machine shall be equipped with automatic controls for establishing profile grades at each edge of the machine. The reference shall be the existing pavement or taut reference lines erected and maintained by the Contractor true to line and grade. A single reference may be used if the machine can maintain the designated transverse slope.

      When referenced from existing pavement, the cold milling machine shall be controlled by a self-contained grade reference system provided by the machine's manufacturer for that purpose. The sensing point shall react to compensate for 25 percent of the actual change in elevation due to a hump or dip that is 3 feet or less in length. The self-contained grade reference system shall be used at or near the centerline of the roadway. On the adjacent pass with the milling machine, a joint matching shoe may be used.

   b) Broken, missing, or worn teeth shall be replaced if the machine is unable to maintain the surface texture requirements.

   c) The machine shall be equipped with a loading elevator to remove the milled material from the roadway surface.

   d) The machine shall be equipped with means to effectively control dust generated by the cutting operation.

4. **Construction Methods**. Before beginning work on roadway demonstrate the milling machine to assure proper condition and operation of equipment to the satisfaction of the engineer.

   a) The milled surface shall not be open to traffic.

   b) When milling removes pavement markings, the Contractor must place temporary pavement marking before opening the road for public use.

   c) The texture produced by the cold milling operation shall be uniform, and continuous longitudinal striations will not be allowed.

   d) When milling is done under traffic maintained conditions, the Contractor shall uniformly mill the partial-lane width with one machine.

   e) The milling must result in a vertical longitudinal face between 1-1/2 inch and 2-1/2 inch in depth between the lanes. At the end of each day, no milled surface will be present to vehicular traffic. Work shall be scheduled so that the milled surface will not be present between traffic lanes over weekends, holidays, or other extended periods when work is not being performed.

   f) Transitions between milled and unmilled surfaces <u>will not</u> be feathered either by milling or with wedges of bituminous material (maximum slope 1 horizontal to 4 vertical).

   g) Surfacing material that cannot be removed by cold milling equipment because of physical or geometric constraints may be removed by other methods approved by the Engineer.

   h) If traffic has been detoured from the milled area, the surface shall be swept once per day. When milling is performed under traffic maintained conditions, the milled surface shall be inlaid with rapid-setting latex-modified Portland cement concrete that has achieved at least 2500 psi compression strength before traffic is placed on it.

   i) The Contractor shall mill curbs in accordance with the plans.

   j) The Contractor shall prepare stockpile sites by removing all vegetation on the portion of the site on which the material will actually be placed. The stockpile area shall be graded so that water will drain away from the stockpiled material. Unsurfaced areas upon which material is stockpiled shall be smoothed and rolled so that the salvaged material may later be removed with a minimum of loss.

   k) The Contractor shall stockpile salvaged material for the Department at the locations shown in the plans or special provisions.

   l) The Engineer shall locate each stockpile. The maximum height of stockpiles is 10 feet. Equipment shall not be driven over the stockpiled material.

   m) Concrete millings from inlays will not be salvaged but shall be disposed of in

accordance with the specified removal requirements.

5. **Method of Measurement**. The bid proposal "Schedule of Items" shall indicate whether the milling will be measured for payment by the ton, station, or square yards of completed and accepted work.

    a) Roadways that are measured by the station (100 feet) shall be measured horizontally along the project centerline between the beginning and ending points of the work.

    b) Areas outside the typical cross section shown in the plans will be measured in equivalent stations based on one station's area for the immediately adjacent roadway.

    c) Since the entire roadway width is not milled, the length of the milled roadway shall be added for the payment.

    d) Each milled slab will be measured separately in stations of 20 feet without regard to width. Stations will be measured horizontally along the project centerline between the beginning and ending points.

    e) Roadways that are measured by the square yard shall be measured to ± 1 SY.

    f) Areas outside the typical cross section shown in the plans will also be measured to ± 1 SY.

    g) Deductions will be made for all areas greater than 1 SY that are not milled.

    h) Measurement of temporary traffic control devices will be made in accordance with Section 422.

    i) Milling concrete for inlays will be measured for payment by the each.

    j) Milling concrete curb is measured in linear feet along the back face of the curb.

6. Basis of Payment

    a) <u>Pay Item Pay Unit</u>
    Concrete Surface Milling Station (Sta)
    Concrete Surface Milling Square Yard (SY)
    Milling Concrete for Inlays Each (ea)
    Payment for temporary traffic control devices will be made in accordance with Section 422.

    b) Payment is full compensation for all work prescribed in this Section.

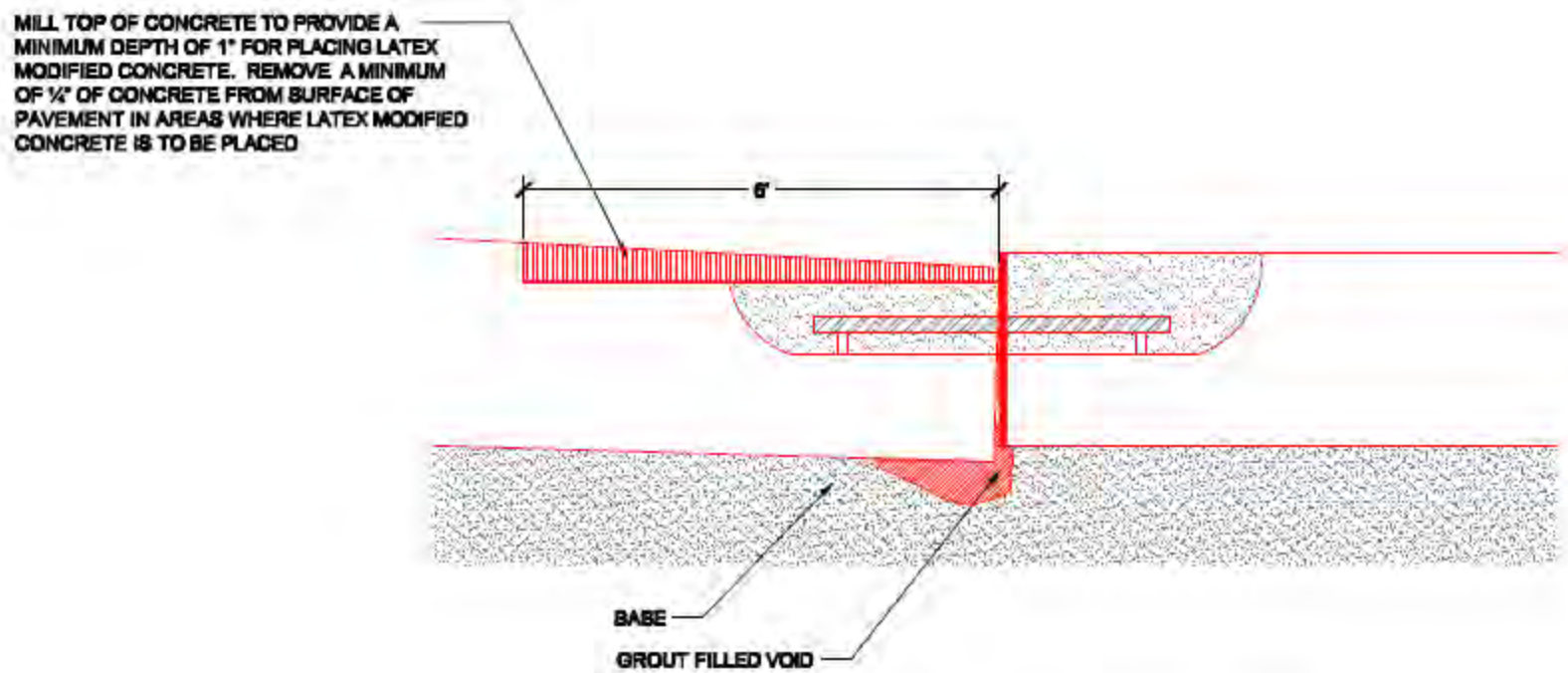

NOTE:
THE END OF MILLING RUNS MUST BE CHIPPED OUT TO THE EDGE OF THE SLAB TO PROVIDE SQUARE ENDS

MILLING DETAIL

FOR FAULTED SLABS

SPECIAL SPECIFICATION

3049

Cleaning Milled Concrete Pavement

1. **Description**. This Item shall govern for the cleaning by steel shot abrasion media of existing hydraulic cement concrete pavement surfaces at the locations shown on the plans or as directed by the Engineer and in accordance with the requirements herein.

2. **Equipment**. The abrasion cleaning shall be done by a machine designed and built for high production pavement texturing. Each machine shall have a minimum average production rate of 1200 sq. yd. per hour for concrete surfaces. The machine shall employ the HVIM (High Velocity Impact Method) by hurling steel abrasive media at high velocity to abrasively clean and texture the surface. The machine shall be capable of varying the velocity of the steel abrasive as well as the speed of the machine to provide the desired surface texture. Utilization of radial blades in multiple centrifugal wheels shall produce a continuous, minimum six-foot wide swath. This is synchronous to the recycling of the abrasive and vacuuming of surface materials into a self-contained vacuum unit of 6 cu. yd. or more, meeting or exceeding all environmental quality standards. No objectionable dust shall be emitted during the work. The machinery shall direct the velocity of abrasion in a bi-directional fashion, giving uniform abrasion to the surface. When transverse curves are present, the abrasion will be at an angle transverse to the grooves to give equal texture to the grove edges.

   On-board controls capable of providing and monitoring uniform velocity and direction will be required. Self contained lighting for night operations will be required.

   A generator driven electromagnet equal in width and production to the texturing machine will be available on the project. It will be used to pick up any steel abrasive left behind the machine if deemed necessary by the Engineer.

   Verifiable proof of prior major pavement texturing, in accordance with the specification, or satisfactory test sections performed at the Contractor’s expense will be necessary before the equipment will be approved.

3. **Construction**. Steel blast abrasion cleaning shall be done on the areas indicated on the plans. It shall be performed in a continuous operation of consecutive passes up to 6 ft. in width (if necessary), parallel to the centerline, so that one 12 ft. lane can be completed in a maximum of 2 passes. The cleaned surface shall have a uniform surface appearance and be devoid of machine product streaks, ruts or overlapping grooves which will inhibit the free flow of water. It shall have a non-directional texture. Following the abrasive cleaning operation, the electromagnet shall pass over

the entire surface if deemed necessary by the Engineer.

The abrasion cleaning shall not encroach on the existing centerline stripes, lane stripes, traffic arrows, cross bar stripes, traffic buttons or other traffic markings unless approved by the Engineer. The distance from the edge of traffic markings to the texture shall be a maximum of 3 in. The longitudinal area between dashed lane markings need not be textured.

All surfacing materials removed during the abrasion cleaning process shall be collected and stored in the vacuum unit until it can be removed from the project and disposed of by the Contractor. No on-site transfer of, or storage of, the materials will be permitted. No loose material will be left on the roadway or swept off to the side of the roadway.

4. **Testing**. The Engineer will require the following testing procedure.

   ICRI Concrete Surface Profile (CSP) When cleaning first begins close visual inspection of cleaned surface should closely compare to the minimal texture of molded ICRI (International Concrete Repair Institute) coupons CSP1-3. This level of surface cleaning must remain similar throughout the cleaning of each milled slab, and each cleaned slab will be visually compared to the ICRI CSP coupons to the satisfaction of the inspector before an overlay is placed.

5. **Measurement.** This Item will be measured by the square yard of surface area. Square yard calculations will be based on the neat dimensions shown on the plans or as adjusted by the Engineer.

6. **Payment**. The work performed in accordance with this Item and measured as provided under “Measurement” will be paid for at the unit price bid for “Texturing Portland Cement Concrete Pavement.” This price shall be full compensation for texturing the pavement surface as well as vacuuming, hauling, unloading and satisfactory storing or disposing of the material, for all labor, equipment, supplies and incidentals necessary to complete the work.

SPECIAL SPECIFICATION

9999

Ultra-Thin, Rapid-Strength, Latex-Modified Bonded Concrete Overlay (LMCO)

1. **Description**. Construct an ultra thin, rapid-strength-gain, latex-modified, bonded concrete overlay (LMCO) of a portland cement concrete pavement surface in accordance with the details shown on the plans and the requirements of this Item.

2. **Materials.**

   a) **Latex-Modified Concrete**. Provide latex-modified hydraulic cement concrete in accordance with Item 439.4.C.3, "Latex-Modified Concrete." Unless otherwise shown on the plans or directed by the Engineer, design the concrete mix with a maximum water cement ratio of 0.40, Grade No.8 coarse aggregate, and a minimum average compressive strength of 3,000 psi at 24 hours (tested according to Tex-418-A, "Compressive Strength of Cylindrical Concrete Specimens.") and bond strengths of 120 psi (tested according to ASTM C 1583 Standard Test Method for Tensile Strength of Concrete Surfaces and the Bond Strength or Tensile Strength of Concrete Repair and Overlay Materials by Direct Tension (Pull-off Method)). (Instead of early compression tests, flexural strengths at 24 hours must reach a minimum of 580 psi when tested in accordance with Tex-427-A.).

   b) **Latex.** Provide latex emulsion admixture (ASTM C 1438, Type II polymer modifier) in accordance with Section 439.2.C

   c) **Joint Sealants and Fillers**. Provide joint sealants and fillers in accordance with Section 360.2.F, "Joint Sealants and Fillers."

   d) **Curing Materials**. Provide moist curing materials and procedures conforming to Section 439.4.E, "Curing."

   e) **Reinforcing Fibers**. When shown on the plans, provide Synthetic Fibers, ASTM C 1116-03 Type III, Polypropylene or Nylon, 3/4" to 1 1/2" in length. Mix 3 lb. synthetic fibers for each cubic yard concrete as per manufactures recommendation.

3. **Equipment**. Furnish equipment as per Section 439.3, "Equipment."

4. **Construction**. Submit a paving plan for approval before beginning pavement construction operations. Include details of all operations in the concrete paving process, including construction method and sequence of construction operation, construction and contraction joint layout, sawing plan and sequence, curing, other details and description of all equipment.

   a) Preparation of Surface.

      i) When shown on the plans, mill the pavement surface to the depth specified on the

plans, in accordance with Item 354, “Planing and Texturing Pavement.”

ii) Adjust the screed to provide an approved grade line and overlay thickness, as specified on the plans. To identify areas with deficient thickness prior to concrete placement, use the following or other approved methods. Attach a filler block having a thickness 1/4 in. less than the overlay thickness to the bottom of the screed and pass the screed over the area to be overlaid. Correct areas which have deficient thickness by adjustments of the screed and/or rail system or by chipping or scarifying of the milled concrete substrate prior to the latex-modified overlay as approved by the Engineer.

iii) Immediately prior to LMCO placement, prepare by shot blasting the pavement surface such that the surface is free of all contaminants and material detrimental to achieving an adequate bond between the original concrete substrate and the latex-modified overlay.

b) **Placing and Removing Forms**. When needed, place and remove forms in accordance with Section 360.4.E, “Placing and Removing Forms.”

c) **Concrete Proportioning, Mixing, and Delivery**. Batching, mixing, and delivering concrete will be done on site with a mobile continuous mixing facility in accordance with Section 439.3.B.4, “Proportioning and Mixing Equipment.”

d) **Temperature Restrictions for Concrete Placement**. Place LMCO at temperatures in accordance with Section 360.4.G.4, “Temperature Restrictions.”

e) **Spreading and Finishing**. Spread and finish concrete in accordance with Section 360.4.H, “Spreading and Finishing.”

f) **Construction Joints**. Saw and seal all construction joints using a Class 5 joint seal, in accordance with Section 360.2.F, “Joint Sealants and Fillers.” When placing of concrete is stopped, install a bulkhead of sufficient cross sectional area at a planned transverse contraction joint location and remove the excess of concrete. Place the bulkhead at right angles to the centerline of the pavement, perpendicular to the surface and at the required elevation. Saw and seal this joint.

g) **Curing**. Moist cure concrete in accordance with Section 439.4.E, “Curing.”

h) **Saw Cutting Contraction Joints**. Saw joints to the full depth of the overlay at existing contraction joints. Saw cuts in lines that are perpendicular and parallel to the centerline of the travel lanes. Saw cuts perpendicular to the surface of the overlay. Saw joints for radii as detailed in the plans. Use a chalk line, offset string line, sawing template or other approved methods to provide a true joint alignment. Remove all debris after sawing, and seal the saw cuts. The Contractor is fully responsible for the timing and order of the saw cutting to prevent uncontrolled cracking, spalling, or raveling. If excess spalling or raveling occurs at the top of the saw cuts or the intersection of saw cuts, or if uncontrolled cracking occurs before opening to traffic, remove and replace all damaged concrete panels without any additional compensation.

i) **Deficient Thickness**. The Engineer will determine the overlay thickness in accordance with Test Method Tex-423-A, "Determining Pavement Thickness by Direct Measurement," at selected locations. If the thickness of the overlay measured is deficient by more than 0.40 in. of the plan thickness, the Contractor may verify the thickness by cores taken in accordance with Test Method Tex-424-A, "Obtaining and Testing Drilled Cores of Concrete," at the locations selected by the Engineer. Remove and replace any concrete panel deficient by more than 0.40 in. of plan thickness without any additional compensation.

j) **Opening to Traffic**. The completed overlay may be opened to traffic after the concrete has been cured for 36 hours and has obtained a minimum compressive strength of 2,800 psi or as directed by the Engineer. Determine the compressive strength in accordance with Tex-418-A, "Compressive Strength of Cylindrical Concrete Specimens" using concrete cylinders cured at the job site under the same conditions as the pavement, or in accordance with Tex-426-A, "Estimating Concrete Strength by the Maturity Method".

k) **Ride Quality**. When shown on the plans, achieve ride quality in accordance with Item 585, "Ride Quality for Pavement Surfaces," Type A.

5. **Measurement**. This Item will be measured by the square yard of surface area in place.

6. **Payment**. The work performed and materials furnished in accordance with this Item and measured as provided under "Measurement" will be paid for at the unit price bid for "Latex-Modified Bonded Concrete Overlay" of the thickness specified. This price is full compensation for materials, equipment, labor, tools, and incidentals.

ACI 548.4-08

(Reapproved 2008)

Standard Specification for Latex-Modified Concrete (LMC) Overlays (ACI 548.4-08)

Reported by ACI Committee 548

This specification covers styrene-butadiene latex-modified concrete as an overlay on concrete bridge decks. It applies to both new construction and rehabilitation of existing decks. It includes certification requirements of the latex products, storage, handling, surface preparation, mixing, application, and limitations.

Keywords: bridge decks; latex-modified concrete; mixing; resurfacing.

FOREWORD

This foreword is included for explanatory purposes only; it does not form a part of Standard Specification ACI 548.4.

Standard Specification ACI 548.4 is a Reference Standard which the Engineer may cite in the Project Specifications for any building project, together with supplementary requirements for the specific project.

Each technical section of Standard Specification ACI 548.4 is written in the Three-Part Section Format of the Construction Specifications Institute, as adopted by ACI and modified to ACI requirements. The language is generally imperative and terse.

Checklists do not form a part of Standard Specification ACI 548.4. Checklists are to assist the Engineer improperly choosing and specifying any necessary requirements for the Project Specifications.

CONTENTS

SPECIFICATION GUIDE

SG1- Standard Specification ACI 548.4 is intended to be used in its entirety, by reference included in the project specification, to cover the requirements for constructing an LMC overlay on a bridge deck. Individual sections, parts, or articles should not be copied into project specifications since taking them out of context may change their meanings.

SG2 - Adjustments to the needs of a particular project shall be made by the Engineer/Specifier by reviewing each of the items indicated in this specification guide and checklist and then including their decisions on each as mandatory requirements in the project specification.

SG3 - These mandatory requirements may designate specific qualities, procedures, materials, and performance criteria for which alternatives are permitted or for which provision is not made in Standard Specification ACI 548.4. Exceptions shall be made to Standard Specification ACI 548.4, if required.

SG4 - A statement, such as the following, will serve to make Standard Specification ACI 548.4 an official part of the project specification:

> The latex-modified concrete overlay shall meet the requirements of "Standard Specification for Latex-Modified Concrete (LMC) Overlays (ACI 548.4)," published by the American Concrete Institute Detroit, MI, except as modified by the requirements of this project specification.

SG5 - The specification checklist that follows addresses each item of ACI 548.4 that requires the Engineer/Specifier to make a choice where alternatives are indicated, or to add provisions where they are not indicated in ACI 548.4, or to take exceptions to ACI 548.4. The checklist consists of one column identifying sections, parts, and articles of ACI 548.4, and a second column of notes to the Engineer/Specifier to indicate the action required of them.

SPECIFICATION CHECKLIST

Section/Part/Article of ACI 548.4	Notes to the Designer/Specifier
Part 1 - General	
1.1 Scope	Indicate specific scope.
1.5 Reference standards	Review applicability of cited references and take exceptions if required.
ASTM C 685, Specification for Concrete Made by Volumetric Batching and Continuous Mixing	Use ASTM C 685 for latex-modified concrete with the modifications listed in Part 3.1.2 of the specifications.
Part 2 - Products	There is no ASTM standard for these types of latex at this time. When such a standard becomes available, it shall govern.
2.1.1 Latex	

Part 3 - Execution	
3.1.2 Mixing	The slump of LMC produced from a mobile mixer should be measured 4 to 5 min after discharge.
3.2.1 Preparation	Surface preparation procedures apply to all surfaces to which the LMC is to bond, including the vertical surface of previously placed overlays. Repair or replacement of reinforcing steel shall be specified by the Engineer. Expansion joints in the overlay are to be located directly over those in the deck and are to be installed at the time of placement of the overlay. Casting across an expansion joint and sawing at a later date shall not be done.
3.2.2 Mix production	The minimum overlay thickness shall be 1 in.; if the overlay is to receive grooves, this dimension is from the bottom of the groove to the bottom of the overlay. The mix proportions that follow, based on years of field experience, have a demonstrated balance between cost and performance. They are also the only proportions that have been tested and approved by the FHWA. Use of a lower latex solids-cement ratio will increase the water requirement to achieve the same slump. Designer must fill in desired values at Paragraph 2.3. (Desired limits are given below:) Cement content, minimum 658 lb/yd^3 Latex polymer/Cement ratio 0.15 Maximum water/cement ratio* 0.40 Air content, maximum† 6.5 percent (ASTM C 231) of plastic concrete Slump, range‡ 3-8 in. Fine aggregate, range by weight, of total aggregate¥ 55-70 percent Weight ratio, typical§ cement: sand: coarse 1.0:2.8:1.7 (aggregate assumed saturated, surface dry; specific gravity = 2.65) € *The water-cement ratio shall not exceed 0.40. Water shall include the water in the polymer latex (typical polymer latex has 50% solids). Measure this ratio, and the resultant slump, by trial batches using the material approved for the project. †The desirable air content is less than 6.5 percent; if air content greater than 6.5 percent is obtained, steps should be taken to reduce it. Changing cement or latex may accomplish this. LMC with air content

3.2.4 Finishing	greater than 10 percent should not be installed as an overlay. ‡The slump will vary with temperature and the selection of cement and aggregates used. A trial mix will determine the relationship between water/cement and slump for the particular materials used. §This ratio may be adjusted to accommodate the allowable range of fine aggregate and variations in aggregate specific gravities. ¥ The fine aggregate specified above is a standard fine aggregate meeting ASTM C 33 € LMC mix proportioning can be identified similar to that of normal concrete. ACI mix proportioning methods (ACI 211) can be used to determine appropriate mix proportions of LMC. Previous knowledge of concrete mixes produced using local materials might be used to make trial batches. A number of trial batches using local materials will be necessary to meet the required performance criteria of fresh and hardened concrete. Surface finish shall be specified by the Engineer.
3.2.8 Limitations	Use the following graph* to determine evaporation rate for specific project conditions:

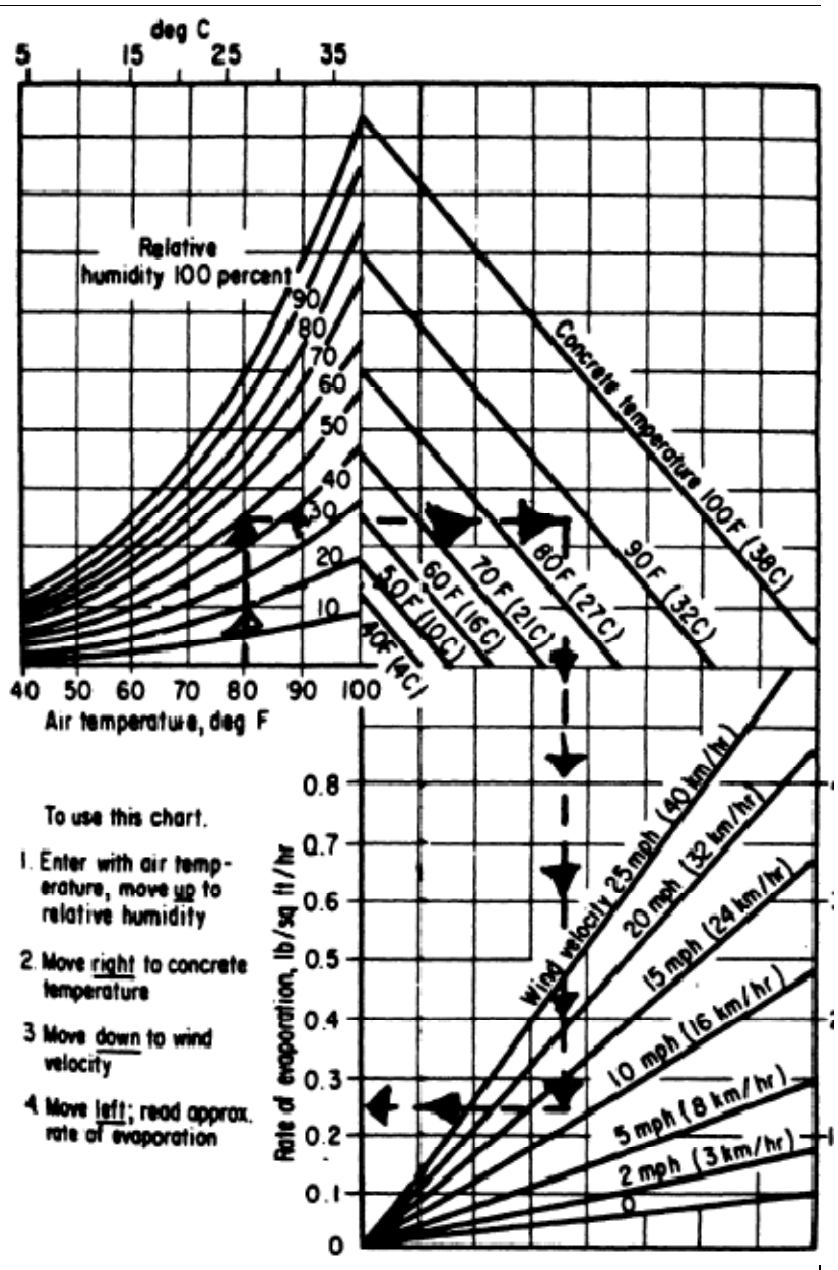

If evaporation rate exceeds 0.10 lb/ft^2/hr, contractor shall make provisions,

i.e., wind breaks, fogging, to reduce it.

---

*Ref. ACI 305R-91; Fig. 2.1.5.

PART 1 – GENERAL

1.1 - Scope

1.1.1 - This standard specification covers the materials and procedures for construction styrene-butadiene latex-modified concrete (LMC) overlays, for new construction as well as repair and rehabilitation, of bridge decks.

1.1.2 - The provisions of this Standard Specification shall govern unless otherwise specified in the contract documents. In case of conflicting requirements, the contract document shall govern.

1.2 - Definitions

LMC - Latex-modified concrete.

Accepted manufacturer - One whose latex complies with FHWA RD-78-35.

1.3 - Reference organizations

1.3.1 – ACI

American Concrete Institute
P.O. Box 9094
Farmington Hills, MI 48333-9094

1.3.2 – ASTM International

ASTM International
100 Barr Harbor Dr.
West Conshohocken, PA 19428-2959

1.3.3 - FHWA

Federal Highway Administration
Offices of Research and Development
Materials Division
HRS-20, Washington, DC 20590

1.4 - Specification wording

1.4.1 - The language of this standard Specification is generally imperative and terse, and may include in-complete sentences. Omission of phrases and/or words such as "the contractor shall," "in accordance with," "shall be," "as indicated," "a," "an," "the," "all," etc., are intentional. Omitted phrases and words are supplied by inference.

1.5 - Reference standards

1.5.1 - The standards referenced in this Standard Specification ACI 548.4 are listed in Articles 1.5.2 to 1.5.4 of this section, with their complete designation and title, including the year of adoption or revision, and are declared to be part of this Standard Specification ACI 548.4 as if fully set forth herein, unless otherwise indicated in the contract documents.

1.5.2 - ASTM standards

C 31-91 Standard Practice for Making and Curing Concrete Test Specimens in the Field
C 33-90 Standard Specification for Concrete Aggregates
C 150-92 Standard Specification for Portland Cement
C 231-91b Standard Test Method for Air Content of Freshly Mixed Concrete by the Pressure Method
C 380-89 Standard for Metric Practice
C 685-90 Standard Specification for Concrete Made by Volumetric Batching and

Continuous Mixing

1.5.3 -A CI standard
306.1-87 Specification for Cold Weather Concreting
1.5.4 - FH WA document
FHWA-RD-78-35 Styrene-Butadiene Latex-Modifiers for Bridge Deck Overlays

1.6 - Submittals
1.6.1 Submit a Certification of Compliance with FHWA RD-78-35 for each batch of latex to the Engineer.

1.7 - Quality assurance of latex
1.7.1 *Labeling* - Clearly mark containers with the following information:
Name of manufacturer.
Manufacturer's product identification.

1.8 - Storage and handling
1.8.1 *Storage of materials* - Store latex at temperatures between 40 to 85°F. Do not allow to freeze. Protect aggregate piles from precipitation.
1.8.2 *Handling of materials* - Handle materials properly to prevent spills and contamination of the environment.

PART 2 - PRODUCTS

2.1 Materials
2.1.1 Latex - Latex admixture conforming to the prequalification requirements specified in Report FHWA-RD-78-35.
2.1.2 Aggregate - ASTM C 33.
2.1.3 Cement - ASTM C 150, Types I, 11, or 111.
2.1.4 Water - ASTM C 685.

2.2 - Mixes (Default values are shown)

Cement content, minimum	658 1b/yd^3
Latex/cement ratio, minimum	0.15
Water*/cement ratio, maximum	0.40
Air content, maximum (ASTM C 231)	6.5 percent
Slump, range	3-8 in.
Overlay thickness, minimum	1 in.
Overlay thickness, maximum	4 in.
Coarse aggregate, maximum	No. 8
Fine aggregate, range by weight, of total aggregate	55-70 percent
Weight ratio, cement:sand:coarse (aggregate assumed saturated surface dry)	1.0:2.8:1.7

* Water including the water in the polymer latex typically (50%)

PART 3 - EXECUTION

3.1 Equipment

3.1.1 *Surface preparation* - Use surface preparation equipment capable of removing deleterious material which would inhibit bond of the overlay. This equipment includes:

- Scarifiers capable of removing up to ½ in. of concrete from the surface.
- Blasters (sand, water, and shot) capable of removing laitance, rust scale from reinforcing steel, and chips of partially loosened concrete.
- Jackhammers (30 lb or less) and chipping hammers (15 lb or less).
- Saws capable of sawing concrete to the specified depth.

3.1.2 *Mixing* - ASTM C 685, with the following modifications:

4.1.4 - Admixtures - This is not applicable to latex admixtures.
5.1.3 - The recommended air contents of (2.2) are not applicable; use the air content in Part 2 of this Specification.
6.8 - The admixture tolerance for latex shall be 0 to + 2 percent, by weight.
7.2 - Replace existing section with: "Each batching or mixing unit shall have affixed, in a prominent place, a metal plate or plates on which are plainly marked the gross volume of the unit in terms of mixed concrete, and discharge speed related to cement factor." Note 11 remains the same.
8.2 -Use the temperature limitations given in Part 3.2.8 of this Specification.
12.1.1 -The curing procedure for Compression Test Specimens shall be the same as the Overlay.

Make the following modifications to the mobile mixer:

- With capacity to deliver a minimum of 6 yd^3 of concrete per hr.
- Equipped with a cement meter that has a ticket printout.
- Equipped with a water hose for spraying the concrete surface.

3.1.3 *Placement* - Use street brooms for brushing mortar onto prepared surface; use shovels and hoes for spreading newly placed concrete in front of finishing machine.

3.1.4 *Finishing* - Use the following finishing equipment:

- A self-propelled rotating cylinder machine, either single or double roller, capable of forward and reverse movement under positive control. Equip the machine with devices that will automatically and continuously spread, consolidate, and finish the plastic concrete. Travel rails for the finishing machine shall be capable of providing support to maintain the finished grade of the LMC overlay.
- A work bridge capable of moving continuously with the finishing machine to facilitate final finishing operations.
- Metal trowels for hand-finishing and spud vibrators for areas the machine cannot reach.
- Tine rakes or brooms, to apply specified final finish.

3.1.5 *Curing* - Use the following:

- Burlap cloth that is clean and has been soaked by water immersion for at least 2 hr prior to use. Apply damp, not dripping.
- Polyethylene film, either white or clear; 6 mil minimum thickness.

3.2 - Construction procedure

3.2.1 *Preparation*

- Cure concrete to be overlaid a minimum of 48 hr or until specified strength has been achieved before beginning surface preparation procedures.
- Allow LMC to cure 48 hr before scarifying or chipping concrete deck within 6 ft of previously placed overlay.
- Repair or replace reinforcing steel as specified by the Engineer.
- Where the bond between existing concrete and reinforcing steel has been destroyed, or where more than half of the diameter of the bar is exposed, remove the concrete adjacent to the bar to a depth ¾ in. below bar to permit LMC to bond to the entire periphery of the bar.
- Install expansion joints in the overlay at the same locations as the expansion joints in the deck.
- Install screed rails so finishing machine will provide at least the minimum overlay thickness indicated on drawings and finish the surface to required profile. Anchor supporting rails to provide horizontal and vertical stability. Use polyethylene film or plastic coated tape if necessary to prevent LMC from bonding to wood and metal rails. Do not treat rails with release agents or parting compounds.
- Prepare all the concrete surface to which the LMC is to bond, vertical as well as horizontal, using specified surface preparation equipment so that loose and deteriorated concrete is removed; laitance, dust, dirt, oil, curing compound, polymer mortar and concrete, and any other material that could interfere with the bond of the overlay, is removed; aggregate is exposed.
- Blast clean the surface within 48 hr of placement of the overlay.
- Blast corroded reinforcing steel to grey metal.
- Wet the clean surface for a period of not less than 1 hr prior to placement of the LMC overlay. Remove standing water in depressions and areas of concrete removal.
- Maintain the surface in properly prepared condition by covering with polyethylene film.

3.2.2 *Mix production*

- Recalibrate each mixer for each new mix proportion, and for every 100 yd^3 of the same mix placed on the same project.
- Mix LMC at the site in accordance with the specified proportions for the project. Make concrete uniform in composition and consistency. Mixing capability shall be adequate to allow finishing operations to proceed continuously and be completed before the surface of the overlay dries.

3.2.3 *Placement*

- Discharge the LMC in front of the finishing machine and brush the concrete onto the deck surface. Insure that the prepared surfaces are evenly coated with the mortar and that the mortar does not dry before it is covered with concrete.
- Discard excess coarse aggregate.
- When placing LMC against LMC that has not achieved initial set but has formed a surface crust, remove the surface crust until plastic concrete is exposed, place the fresh LMC against this, and work the new into the old to prevent a construction joint crack.
- When placing LMC against LMC that has achieved initial set, wait until final set occurs; then blast the surface and treat like any other cured concrete surface being prepared for LMC.
- Install a construction dam or bulkhead in case of a delay longer than 60 min. During

delays between 5 and 60 min, protect the end of the placement with damp burlap.

- Protect freshly placed LMC from rain. Stop placing operations when rain begins. Remove material damaged by rainfall.

3.2.4 *Finishing*

- Consolidate and finish to final grade with finishing machine.
- Use spud vibrator to consolidate deep pockets, edges, and any other area where the finishing machine cannot reach.
- Use trowels to hand-finish areas the finishing machine cannot reach.
- Texture the surface with rake or broom, as specified.
- Complete finishing before the surface of the overlay dries.

3.2.5 *Curing*

- Apply a single layer of damp burlap (or damp polyethylene-backed burlap) on the surface immediately after the finishing operation. Exercise care to prevent damage to the surface texture. Insure that edges of adjacent strips of burlap overlap a minimum of 4 in.
- Apply a single layer of polyethylene film onto the burlap before the burlap begins to dry or apply a fog spray of water so that water does not run onto the surface of the overlay. (Not applicable if polyethylene-backed burlap is used.)
- Secure the edges of the polyethylene film to prevent wind from getting underneath.
- Maintain this cover system so that the overlay stays damp for 48 hr.
- Allow the overlay to be air cured (no water) until the required compressive strength (typically 3000 psi) is attained.

3.2.6 *Test specimens*

- Make compression cylinders according to ASTM C 31 and cure at the job site under the same conditions as the overlay. Test cylinders to determine when overlay has achieved specified strength for opening to traffic.
- Use 3000 psi as minimum compressive strength for opening overlay to traffic, unless otherwise specified.

3.2.7 *Cleanup*

- Use water to remove latex and LMC from equipment before it has hardened. After it has hardened, use mechanical abrasion.

3.2.8 *Limitations*

- Do not place LMC when the evaporation rate exceeds 0.10 lb/ft^2/hr, unless provisions are made to reduce the rate of evaporation. Wind breaks and fogging may be used. Complete finishing before the surface of the overlay dries.
- During cold weather, protect the freshly placed LMC from temperatures below 45 F during the first 72 hr of curing. Follow procedures in ACI 306.1.

3.3 - Very Early Strength Latex-Modified Concrete Overlays (LMC-VE)

Very early strength latex modified concrete overlays (LMC-VE) shall be constructed in accordance with the preceding requirements in this specification with the following exceptions:

- Hydraulic Cement: Cement shall be approximately 1/3 calcium sulfoaluminate (C_4A_3S) and 2/3 dicalcium silicate (C_2S) or other hydraulic cement that will provide a Latex-Modified Concrete that meets the physical requirements for LMC-VE as indicated in this special provision.
- Strength: The minimum compressive strength shall be 2500 psi at 3 hours and 3500 psi at 1 day.
- Curing: The overlay concrete shall be moist cured from the time it is placed until it is opened to traffic. The moist curing shall be initiated with the application of wet burlap and plastic to the surface of the overlay concrete as soon as practical and before the surface dries. The burlap shall be maintained in a wet condition during the curing period.

CONVERSION FACTORS

1 in. = 25.4 rnm

1 yd^3 = 0.765 m^3

1 lb/ft^2 = 47.9 Pa

1 gal. = 3.785 1

$t_c = (r_F - 32)/1.8$

Adopted as a standard of the American Concrete Institute in November 1993 in accordance with the Institute's standardization procedure.

RAPID SET LATEX MODIFIED CONCRETE

• Fast Setting
RSLMC sets in about one hour and is ready for traffic in 4 hours.
• Low Permeability
RSLMC is nearly impervious to the compounds that deteriorate standard concrete.
• Low Shrinkage
The low or "non" shrink characteristic of RSLMC results in better bonding and less cracking.
• Economical
An RSLMC overlay can be installed at a 25% - 35% cost savings over conventional concrete.

Materials and Mix Design
Rapid Set® Cement should be manufactured by CTS Cement Manufacturing Company, Cypress, CA (800)929-3030. Material should be of recent manufacture (Within 1 year) and free from lumps.

Sand should be clean and conform to the requirements of ASTM C 33 for concrete sand. Coarse aggregate should be clean, sound, crushed stone or gravel meeting the general requirements of AASHTO M 80. The maximum size particle should not be larger than 1/2 the depth of the section to be placed.

Latex emulsion should be DOW Modifier A as manufactured by DOW Chemical Company, Midland, MI (800)447-4369. Modifier A is a styrene butadiene polymeric emulsion. Stabilizers and an antifoam agent have been added at the point of manufacture. Emulsion should weigh approximately 8.5-lb per gallon.

Water used in the production of the Latex Modified Concrete should be clean and free from: salt, acid, oil, organic matter, or other substance injurious to the finished product.

Set Control® or Citric Acid (Food grade) can be used as a retarder to lengthen working time. Food grade Citric Acid should be dissolved into a solution with water. Solution should be added to the admixture tank, not containing latex emulsion, and dispensed as an admixture.

MIX DESIGN: (Typical formulation, consult your local CTS Cement Representative for correct proportions for job application.)

Mixing Equipment (Continuous Mixers)
Calibration of mobile mixers should be checked every 100 yards for proper proportioning. The yield will be required to be within tolerance of 1.0% according to the following tests:

1. With the cement meter set at zero, and all controls set for desired mix. Discharge mix material into a square container measuring 36" x 36" 9". When the container has been filled, and struck level, the cement meter should read an amount equal to the cement desired for 1/4 of a cubic yard.

2. They should have available fluid tanks to separate water and latex as well as any admixtures that will be used.

3. They should provide positive control of the flow of water, latex, and admixtures into the mixing chamber.

4. They should have provisions to prevent foreign matter or objects from entering the cement hopper during the loading process.

5. If citric acid is used in the Rapid Set® Latex Modified Concrete (RSLMC), it should be introduced to the auger through an on board admixture tank.

Surface Preparation
Surface should be sound, clean, and free of any laitance that will be detrimental to achieving proper bond. This is generally done with mechanized equipment such as scarifiers and shot blasters or with high pressure water from hydro-demolition equipment. This should be done within 24 hours to placing RSLMC. Immediately prior to placement of RSLMC the clean surface should be thoroughly wetted for a period of not less than 1 hour.

Concrete Batching
Accurate proportioning and thorough mixing are crucial requirements of a mixer of Rapid Set® Latex Modified Concrete (RSLMC). To assure the inspector and owner that the concrete being delivered to the deck is of proper and uniform composition, the following guidelines are suggested:

1. The capacity of the mixer and bulk materials handling system should be such that a minimum of 6 cubic yards per hour can be accurately proportioned, mixed, placed, and finished properly.

2. A cement meter, with ticket printout is a desirable feature to assure uniformity of composition. Alternate techniques may be available, but should be approved by the owner.

3. All ingredients should be accurately and positively proportioned by weight with an approved scale.

4. Mixing should be done with equipment that will not be aggravated by residual buildup of concrete. Ready mix trucks are not recommended.

5. Mixed material should be discharged on the deck in the sufficient time for the finishing operations to be completed. The working time of Rapid Set® Latex Modified Concrete (RSLMC) is largely dependent on temperature and as with regular Portland LMC it can be as short as 10 minutes in hot, windy, dry weather.

Placing and Finishing Equipment

1. Shovels and brooms are used for placing and brushing-in freshly mixed modified concrete and for distributing it to approximate correct level. Hand operated vibrators and screeds should be used to place and finish small areas.

2. A self propelled finishing machine, capable of forward and reverse movement should be used

for finishing large areas of work.

3. A suitable, portable, lightweight work bridge should be used behind the finishing operation for any brooming or tining.

Construction Method for Placing and Finishing:
Rapid Set® Latex Modified Concrete or slurry should be brushed into the moist substrate just ahead of the pour. Care should be exercised to cover all vertical surfaces as well as horizontal surfaces with an even coating. Stones that accumulate from the brushing operation should be discarded.

THE RSLMC should be placed as soon as possible over the brushed surface to prevent its drying out. The finishing machine should proceed over the pour as the material is placed. Deep sections should be vibrated with a spud vibrator. Edges will need to be finished by hand. Final finishing should be completed before the material has reached a final set. Water should not be applied to the surface to aid finishing. Working time can be extended by adding citric acid solution to an admixture tank. DO NOT ADD CITRIC ACID DIRECTLY TO DOW MODIFIER A.

Curing

The surface should be covered promptly after final finishing with a single, clean layer of wet burlap. Immediately following the covering of wet burlap, a layer of polyethylene (preferably white) film should be placed over the wet burlap. The coverings should remain until the RSLMC has reached a strength desired for initial traffic loading. Depending on temperatures, and specified strength, this will usually be within 1 - 6 hours after the pour. The surface of the RSLMC should remain wet for this time period. Additional water may need to be applied to the burlap during the curing, as the surface of the concrete will tend to dry out under the wet burlap.

Limitations:
Traffic Loading: No vehicular traffic should be permitted on the RSLMC until an early bearing strength has been achieved. This can be verified by making field cast test cylinders, and protecting them from adverse temperatures. An unheated foam curing box is recommended during a cold weather pour.

Cold Weather:
(Below 50° F): RSLMC should not be placed if temperatures will not be above 45° F for the duration of the pour and initial curing period. Provisions will have to be made to ensure that the RSLMC has an initial temperature above 60° F. During the curing phase, the covering of polyethylene should be replaced with an approved insulation blanket. All other aspects of the curing section should be followed. Also see ACI 306, “Recommended Practice for Cold Weather Concreting" for further guidance.

Hot Weather:
(Above 80° F): During periods of hot weather, RSLMC can be mixed with citric acid to extend working time. Consult your local CTS Representative for appropriate doses. When daytime conditions produce temperature in excess of 85° F, or when daytime conditions of temperature, wind, and humidity cause an evaporation rate greater than 0.15 lbs/sf/hour, consideration should

be given to night placement. Also see ACI 305, “Recommended Practices for Hot Weather Concreting" for further guidance.

Set Control™ Admix

The use of citric acid as a Set Control™ retarder when used in conjunction with Dow Modifier A Latex and Rapid Set® Cement in the production of RSLMC (Rapid Set® Latex Modified Concrete.) CTS Cement Mfg. Co. and Dow Chemical Co. recommend the use of citric acid (USP grade) as a Set Control™ Admixture in RSLMC when mix temperatures rise above 70° F to increase the time for workability.

The combination of Dow Latex, Rapid Set® Cement and citric acid as a Set Control™ retarder had been used on many projects in states that utilize RSLMC. The amount of retarder needed is dependent on the RSLMC mix temperature and should be adjusted according to jobsite conditions.

Guidelines for the Use of Rapid Set® Cement in Latex-Modified Concrete Overlays

Materials

Rapid Set® Cement should be manufactured by CTS Cement Manufacturing Company, Cypress, California, phone (800)929-3030. Material should be of recent manufacture (within 1 year) and free from lumps.

Sand should be clean and conform to the requirements of ASTM C 33 for concrete sand.

Coarse aggregate should be clean, sound, crushed stone or gravel meeting the general requirements of AASHTO M 80. The maximum size particle should not be larger than 1/2 the depth of the section to be placed.

Latex emulsion should be DOW Modifier A as manufactured by DOW Chemical Company, Midland, Michigan, (800)447-4369. Modifier A is a styrene butadiene polymeric emulsion in which the polymer comprises 47.05% - 49.0% of the total emulsion. Stabilizers and an antifoam agent have been added at the point of manufacture. Emulsion should weigh approximately 8.5 lb per gallon.

Water used in the production of the latex-modified concrete should be clean and free from: salt, acid, oil, organic matter, or other substance injurious to the finished product.

Citric acid (food grade) can be used as a retarder to lengthen working time. Food grade citric acid should be dissolved into a solution with water. Solution should be added to the admixture tank, not containing latex emulsion, and dispensed as an admixture.

Mix Design

(Typical formulation, consult your local CTS Representative for correct proportions for job application).

Material	*Quantity*
Rapid Set® Cement	658 lb
DOW Modifier A	208 lb
Fine Aggregate	1700 lb
Coarse Aggregate	1300 lb
Water	160 lb
Air Content	Max. 7%

Batching

Accurate proportioning and thorough mixing are crucial requirements of a mixer of Rapid Set® latex-modified concrete (RSLMC). To assure the inspector and owner that the concrete being delivered to the deck is of proper and uniform composition, the following guidelines are

suggested:

The capacity of the mixer and bulk materials handling system should be such that a minimum of 6 cubic yards per hour can be accurately proportioned, mixed, placed, and finished properly.

A cement meter with ticket printout is a desirable feature to assure uniformity of composition. Alternate techniques may be available but should be approved by the owner.

All ingredients should be accurately and positively proportioned by weight with an approved scale.

Mixing should be done with equipment that will not be aggravated by residual buildup of concrete. Ready mix trucks are not recommended.

Mixed material should be discharged on the deck in sufficient time for the finishing operations to be completed. The working time of RSLMC is largely dependent on temperature and as with regular portland LMC it can be as short as 10 minutes in hot, windy, dry weather.

Equipment
Continuous Mixers

1. Calibration of mobile mixers should be checked every 100 yards for proper proportioning. The yield will be required to be within tolerance of 1.0% according to the following tests: 2. With the cement meter set at zero, and all controls set for desired mix. Discharge mix material into a square container measuring 36" x 36" x 9". When the container has been filled, and struck level, the cement meter should read an amount equal to the cement desired for 1/4 of a cubic yard.

2. They should have available fluid tanks to separate water and latex as well as any admixtures that will be used.

3. They should provide positive control of the flow of water, latex, and admixtures into the mixing chamber.

4. They should have provisions to prevent foreign matter or objects from entering the cement hopper during the loading process.

5. If citric acid is used in the RSLMC, it should be introduced to the auger through an on board admixture tank.

Surface Preparation
Surface should be sound, clean, and free of any laitance. This is generally done with mechanized equipment such as scarifiers and shot blasters or with high-pressure water from hydrodemolition equipment. This should be done within 24 hours to placing the RSLMC. Immediately prior to placement, the clean surface should be thoroughly wetted for a period of not less than 1 hour.

Placing and Finishing

1. Shovels and brooms are used for placing and brushing-in freshly mixed modified concrete and for distributing it to approximate correct level. Hand operated vibrators and screeds

should be used to place and finish small areas.

2. A self propelled finishing machine, capable of forward and reverse movement should be used for finishing large areas of work.

3. A suitable, portable, lightweight work bridge should be used behind the finishing operation for any brooming or tining.

4. Metal trowels are recommended for any hand finishing required at scuppers, gutters, and along edges.

Construction Method

Placing and Finishing

RSLMC or slurry should be brushed into the moist substrate just ahead of the pour. Care should be exercised to cover all vertical surfaces as well as horizontal surfaces with an even coating. Stones that accumulate from the brushing operation should be discarded.

The RSLMC should be placed as soon as possible over the brushed surface to prevent its drying out. The finishing machine should proceed over the pour as the material is placed. Deep sections should be vibrated with a spud vibrator. Edges will need to be finished by hand. Final finishing should be completed before the material has reached a final set. Water should not be applied to the surface to aid finishing. Working time can be extended by adding citric acid solution to an admixture tank. *Do not add citric acid directly to Dow Modifier A.*

Curing

The surface should be covered promptly after final finishing with a single, clean layer of wet burlap. Immediately following the covering of wet burlap, a layer of polyethylene (preferably white) film should be placed over the wet burlap. The coverings should remain until the RSLMC has reached a strength desired for initial traffic loading. Depending on temperatures and specified strength this will usually be within 1 to 6 hours after the pour. The surface of the RSLMC should remain wet for this time period. Additional water may need to be applied to the burlap during the curing, as the surface of the concrete will tend to dry out under the wet burlap.

Limitations

Traffic Loading

No vehicular traffic should be permitted on the RSLMC until an early bearing strength has been achieved. This can be verified by making field cast test cylinders, and protecting them from adverse temperatures. An unheated foam curing box is recommended during a cold weather pour.

Cold Weather (Below 50 F Degrees)

RSLMC should not be placed if temperatures will not be above 45 F degrees for the duration of the pour and initial curing period. Provisions will have to be made to ensure that the RSLMC has an initial temperature above 60 F degrees. During the curing phase, the covering of polyethylene should be replaced with an approved insulation blanket. All other aspects of the curing section should be followed. Also see ACI 306, Recommended Practice for Cold Weather Concreting for further guidance.

Hot Weather (Above 80 degrees F)
During periods of hot weather, RSLMC can be mixed with citric acid to extend working time. Consult your local CTS Representative for appropriate doses. When daytime conditions produce temperature in excess of 85 degrees F, or when daytime conditions of temperature, wind, and humidity cause an evaporation rate greater than 0.15 lbs/sf/hour, consideration should be given to night placement. Also see ACI 305, Recommended Practices for Hot Weather Concreting for further guidance.

Health Hazard for Rapid Set 7 Cement
Rapid Set® Cement is a cementitious material. Cementitious materials can cause skin, eye, and respiratory irritation. Avoid contact with skin whenever possible. If cementitious material contacts eyes, rinse immediately and thoroughly with water and get prompt medical attention. See the MSDS SHEET for more detailed information.

Consult DOW Literature for information on Modifier A.

SHRP PRODUCT 2035A: Rapid Bridge Deck Rehabilitation Manual
Michael Sprinkel

Guidelines for the Use of Rapid Set® Cement in Latex-Modified Concrete Overlays

Materials

Rapid Set® Cement should be manufactured by CTS Cement Manufacturing Company, Cypress, California, phone (800)929-3030. Material should be of recent manufacture (within 1 year) and free from lumps.

Sand should be clean and conform to the requirements of ASTM C 33 for concrete sand.

Coarse aggregate should be clean, sound, crushed stone or gravel meeting the general requirements of AASHTO M 80. The maximum size particle should not be larger than 1/2 the depth of the section to be placed.

Latex emulsion should be DOW Modifier A as manufactured by DOW Chemical Company, Midland, Michigan, phone (800)447-4369. Modifier A is a styrene butadiene polymeric emulsion in which the polymer comprises 47.05% - 49.0% of the total emulsion. Stabilizers and an antifoam agent have been added at the point of manufacture. Emulsion should weigh approximately 8.5 lb per gallon.

Water used in the production of the latex-modified concrete should be clean and free from: salt, acid, oil, organic matter, or other substance injurious to the finished product.

Citric acid (food grade) can be used as a retarder to lengthen working time. Food grade citric acid should be dissolved into a solution with water. Solution should be added to the admixture tank, not containing latex emulsion, and dispensed as an admixture.

Mix Design

(Typical formulation, consult your local CTS Representative for correct proportions for job application).

Material	*Quantity*
Rapid Set® Cement	658 lb
DOW Modifier A	208 lb
Fine Aggregate	1700 lb
Coarse Aggregate	1300 lb
Water	160 lb

Air Content Max. 7%

Batching
Accurate proportioning and thorough mixing are crucial requirements of a mixer of Rapid Set® latex-modified concrete (RSLMC). To assure the inspector and owner that the concrete being delivered to the deck is of proper and uniform composition, the following guidelines are suggested:

1. The capacity of the mixer and bulk materials handling system should be such that a minimum of 6 cubic yards per hour can be accurately proportioned, mixed, placed, and finished properly.

2. A cement meter with ticket printout is a desirable feature to assure uniformity of composition. Alternate techniques may be available but should be approved by the owner.

3. All ingredients should be accurately and positively proportioned by weight with an approved scale.

4. Mixing should be done with equipment that will not be aggravated by residual buildup of concrete. Ready mix trucks are not recommended.

5. Mixed material should be discharged on the deck in sufficient time for the finishing operations to be completed. The working time of RSLMC is largely dependent on temperature and as with regular portland LMC it can be as short as 10 minutes in hot, windy, dry weather.

Equipment
Continuous Mixers

1. Calibration of mobile mixers should be checked every 100 yards for proper proportioning. The yield will be required to be within tolerance of 1.0% according to the following tests: 2. With the cement meter set at zero, and all controls set for desired mix. Discharge mix material into a square container measuring 36" x 36" x 9". When the container has been filled, and struck level, the cement meter should read an amount equal to the cement desired for 1/4 of a cubic yard.

2. They should have available fluid tanks to separate water and latex as well as any admixtures that will be used.

3. They should provide positive control of the flow of water, latex, and admixtures into the mixing chamber.

4. They should have provisions to prevent foreign matter or objects from entering the cement hopper during the loading process.

5. If citric acid is used in the RSLMC, it should be introduced to the auger through an on board admixture tank.

Surface Preparation

Surface should be sound, clean, and free of any laitance. This is generally done with mechanized equipment such as scarifiers and shot blasters or with high-pressure water from hydrodemolition equipment. This should be done within 24 hours to placing the RSLMC. Immediately prior to placement, the clean surface should be thoroughly wetted for a period of not less than 1 hour.

Placing and Finishing

1. Shovels and brooms are used for placing and brushing-in freshly mixed modified concrete and for distributing it to approximate correct level. Hand operated vibrators and screeds should be used to place and finish small areas.

2. A self propelled finishing machine, capable of forward and reverse movement should be used for finishing large areas of work.

3. A suitable, portable, lightweight work bridge should be used behind the finishing operation for any brooming or tining.

4. Metal trowels are recommended for any hand finishing required at scuppers, gutters, and along edges.

Construction Method

Placing and Finishing

RSLMC or slurry should be brushed into the moist substrate just ahead of the pour. Care should be exercised to cover all vertical surfaces as well as horizontal surfaces with an even coating. Stones that accumulate from the brushing operation should be discarded.

The RSLMC should be placed as soon as possible over the brushed surface to prevent its drying out. The finishing machine should proceed over the pour as the material is placed. Deep sections should be vibrated with a spud vibrator. Edges will need to be finished by hand. Final finishing should be completed before the material has reached a final set. Water should not be applied to the surface to aid finishing. Working time can be extended by adding citric acid solution to an admixture tank. *Do not add citric acid directly to Dow Modifier A.*

Curing

The surface should be covered promptly after final finishing with a single, clean layer of wet burlap. Immediately following the covering of wet burlap, a layer of polyethylene (preferably white) film should be placed over the wet burlap. The coverings should remain until the RSLMC has reached a strength desired for initial traffic loading. Depending on temperatures and specified strength this will usually be within 1 to 6 hours after the pour. The surface of the RSLMC should remain wet for this time period. Additional water may need to be applied to the burlap during the curing, as the surface of the concrete will tend to dry out under the wet burlap.

Limitations

Traffic Loading

No vehicular traffic should be permitted on the RSLMC until an early bearing strength has been achieved. This can be verified by making field cast test cylinders, and protecting them from adverse temperatures. An unheated foam curing box is recommended during a cold weather pour.

Cold Weather (Below 50 F Degrees)
RSLMC should not be placed if temperatures will not be above 45 F degrees for the duration of the pour and initial curing period. Provisions will have to be made to ensure that the RSLMC has an initial temperature above 60 F degrees. During the curing phase, the covering of polyethylene should be replaced with an approved insulation blanket. All other aspects of the curing section should be followed. Also see ACI 306, Recommended Practice for Cold Weather Concreting for further guidance.

Hot Weather (Above 80 degrees F)
During periods of hot weather, RSLMC can be mixed with citric acid to extend working time. Consult your local CTS Representative for appropriate doses. When daytime conditions produce temperature in excess of 85 degrees F, or when daytime conditions of temperature, wind, and humidity cause an evaporation rate greater than 0.15 lbs/sf/hour, consideration should be given to night placement. Also see ACI 305, Recommended Practices for Hot Weather Concreting for further guidance.

Health Hazard for Rapid Set 7 Cement
Rapid Set® Cement is a cementitious material. Cementitious materials can cause skin, eye, and respiratory irritation. Avoid contact with skin whenever possible. If cementitious material contacts eyes, rinse immediately and thoroughly with water and get prompt medical attention. See the MSDS SHEET for more detailed information.

Consult DOW Literature for information on Modifier A.

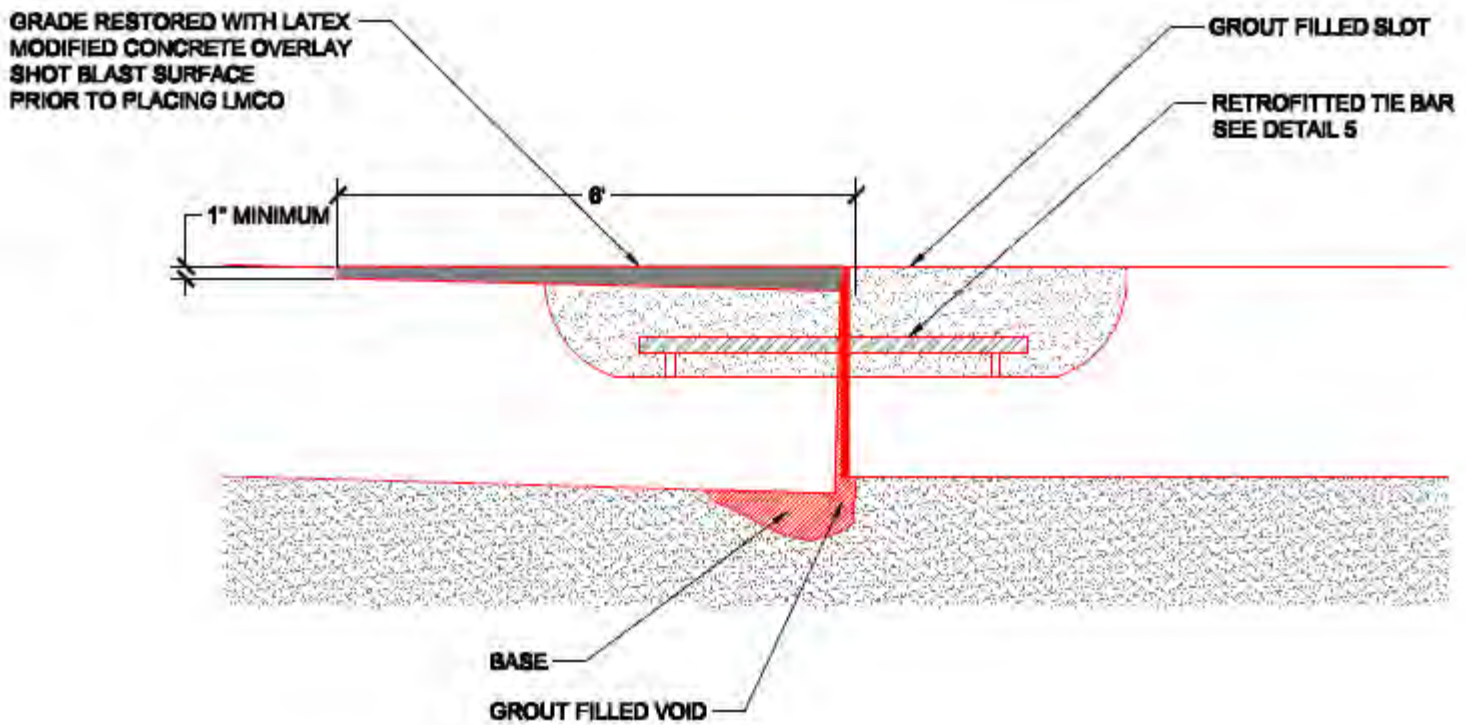

SLOT STITCHING DETAIL WITH LMCO

FOR FAULTED SLABS

Appendix N: Specifications for Construction of Longitudinal Joints

2004 Specifications

SPECIAL PROVISION
Chapter 4. 360---XXX

Concrete Pavement

For this project, Item 360, "Concrete Pavement," of the Standard Specifications, is hereby amended with respect to the clauses cited below, and no other clauses or requirements of this Item are waived or changed hereby.

Article 360.4. Construction, D. Joints is supplemented by the following:

3. Longitudinal Construction Joints. Install tie bars at depths and spacing specified in the governing design standards. When multi-piece tie bars are used, the ends of female tie bars shall be sufficiently close to the edge so that they are exposed and the male tie bars are securely connected to them. When the ends of female tie bars cannot be located, drill and epoxy grout tie bars. When single piece tie bars are used, insert tie bars into fresh concrete with minimal vibration so that no voids are created between tie bars and surrounding concrete and no edge slumps are formed.

Appendix O: Guidelines of Tie Bar Installations for New Construction

Multi-Piece Tie Bars

- The spacing for tie bars shall be in accordance with governing design standards.
- The precise locations of tie bars should be clearly marked, on top of the subbase, with brightly colored paint.
- Female tie bars should be placed as closely to the slip-form edge as possible, without protruding.
- The holes in the female tie bars should be covered with a plastic cover to prevent fresh concrete from entering.
- Once the slip form paver completes the pass, the excess concrete over the tips of female tie bars should be removed so that the plastic covers become clearly visible. Squirting water and subsequent removal of fresh concrete is acceptable as long as the water squirting does not cause too much concrete to be damaged.
- Clean the removed concrete from the subbase.
- Once the concrete has sufficiently hardened, install male pieces of tie bars by screwing them into the female pieces with sufficient force.
- Make sure that the other ends of male piece tie bars are within 1 inch vertically from mid-depth of the slab.

Single-Piece Tie Bars

- The spacing for tie bars shall be in accordance with governing design standards.
- The precise locations of tie bars should be clearly marked on top of the subbase with brightly colored paint.
- When the slip-form paving is utilized, insert the tie bars as soon as the slip-form paver completes the pass.
- While inserting tie bars, avoid excessive vibration or movements of the inserter to minimize the edge slump of the concrete.
- Cover the exposed tie bars with appropriate materials, such as plastic tubes, completely before the curing operation is applied.

Appendix P: Guidelines of Transverse Steel Installations for New Construction

- The spacing for transverse steel shall be in accordance with governing design standards.
- Transverse steel should be placed in chairs securely. The quality and placement of chairs should be in accordance with Item 360.
- The placement of transverse steel should be within the vertical and horizontal tolerance required in the governing design standards.
- Longitudinal steel should be placed on top of transverse steel and secured so that the force exerted from concrete paving operations do not move the reinforcement out of the tolerance.